STUDIES ON RUTHENIUM(II) AND OSMIUM(II) PARACYCLOPHANE COMPOUNDS.

A thesis presented to the University of London
in partial fulfilment of the requirements
for the degree of Doctor of Philosophy
in the Faculty of Science.

By

Mark Robert James Elsegood.

The Christopher Ingold Laboratories,
University College London,
June, 1991.

Declaration.

Except where specific reference is made to other sources, the work presented in this thesis is the original work of the author. It has not been admitted, in whole or in part, for any other degree. Certain of the results presented have already been published.

Mark R. J. Elsegood.

For my family.

ABSTRACT.

This thesis describes studies on ruthenium(II) and osmium(II) [2_2]paracyclophane compounds. Chapter 1 introduces the work, giving a historical background to the development of [2_2]paracyclophane chemistry. The properties of this compound and the syntheses of derived metal complexes are reviewed.

Chapter 2 describes the synthesis of $[Os(\eta^6\text{-}C_{16}H_{16})Cl_2]_2$. The reactions of $[M(\eta^6\text{-}C_{16}H_{16})Cl_2]_2$ (M=Ru,Os) with a variety of Lewis bases L (L=py, PR_3, etc.), in non-polar and polar solvents is reported. In non-polar solvents the compounds $[M(\eta^6\text{-}C_{16}H_{16})Cl_2L]$ are formed, while in polar solvents the reactions yield the compounds $[M(\eta^6\text{-}C_{16}H_{16})ClL_2][X]$ ($X=PF_6^-$, BPh_4^-). The crystal structures of $[Ru(\eta^6\text{-}C_{16}H_{16})Cl_2(PPh_3)].CHCl_3$, $[Ru(\eta^6\text{-}C_{16}H_{16})Cl_2(py)]$, $[Ru(\eta^6\text{-}C_{16}H_{16})Cl(py)_2][PF_6]$, and $[Ru(\eta^6\text{-}C_{16}H_{16})Cl(1,10\text{-phen})][PF_6]$ are presented.

Chapter 3 reports reactions of $[Ru(\eta^6\text{-}C_{16}H_{16})Cl_2]_2$ which lead to the formation of binuclear triply-bridged compounds of the type $[(\eta^6\text{-}C_{16}H_{16})Ru(\mu\text{-}Y)_3Ru(\eta^6\text{-}C_{16}H_{16})][X]$ ($Y=OMe^-$, OEt^-, OH^-, Cl^-). The crystal structures of the compounds $[(\eta^6\text{-}C_{16}H_{16})Ru(OMe)_3Ru(\eta^6\text{-}C_{16}H_{16})][BPh_4].C_{16}H_{16}$ and $[(\eta^6\text{-}C_{16}H_{16})Ru(OEt)_3Ru(\eta^6\text{-}C_{16}H_{16})][PF_6]$ are described. The reaction of $[(\eta^6\text{-}C_{16}H_{16})Ru(Cl)_3Ru(\eta^6\text{-}C_{16}H_{16})][PF_6]$ with pyridine leads to the formation of *trans*-$[Ru(py)_4Cl_2]$, which has been characterised by X-ray crystallography.

Chapter 4 presents studies on the compounds $[M(\eta^6\text{-arene})(\eta^6\text{-}C_{16}H_{16})][X]_2$. The synthesis and characterisation of new osmium compounds of this type is described, including the crystal structure of $[Os(\eta^6\text{-}C_6H_6)(\eta^6\text{-}C_{16}H_{16})[BF_4]_2$. The crystal structure of the previously reported compound $[Ru(\eta^6\text{-}p\text{-cymene})(\eta^6\text{-}C_{16}H_{16})][BF_4]_2$ is presented, together with that of the new complex $[Ru(\eta^6\text{-}p\text{-cymene})(\eta^6\text{-}C_{16}H_{16})][BPh_4]_2.\frac{1}{2}Me_2CO$. The reactions of $[Ru(\eta^6\text{-arene})(\eta^6\text{-}C_{16}H_{16})][BF_4]_2$ compounds with nucleophiles (H^-,CN^-) have been investigated. A new synthesis of $[Ru(\eta^5\text{-}C_5H_5)(\eta^6\text{-}C_{16}H_{16})][PF_6]$ is proposed.

Chapter 5 presents the syntheses of organometallic chain compounds containing [2_2]paracyclophane. Three classes of compound have been prepared and characterised, (i) bisruthenium hetero-arene compounds: $[(\eta^6\text{-arene}^1)Ru(\eta^6,\eta^6\text{-}C_{16}H_{16})Ru(\eta^6\text{-arene}^2)][BF_4]_4$, (ii) hetero-metallic binuclear compounds: $[(\eta^6\text{-arene})Ru(\eta^6,\eta^6\text{-}C_{16}H_{16})Os(\eta^6\text{-}C_6H_6)][BF_4]_4$, and (iii) hetero-metallic trinuclear compounds: $[(\eta^6\text{-arene})M^1(\eta^6,\eta^6\text{-}C_{16}H_{16})M^2(\eta^6,\eta^6\text{-}C_{16}H_{16})M^1(\eta^6\text{-arene})][BF_4]_6$ (M^1,M^2=Ru,Os).

Chapter 6 draws together structural and spectroscopic data on the coordinated [2_2]paracyclophane ligand.

TABLE OF CONTENTS.

Acknowledgements.

I would like to thank my supervisor, Dr Derek Tocher for his guidance, invaluable discussion, and infectious enthusiasm. Among the academic staff, I am most deeply indebted to Prof. Jackie Truter for assistance in solving some of the more taxing crystallographic problems, and Dr. Glyn Williams for his help with n.m.r. spectroscopy. I also thank the S.E.R.C. for financial support.

My thanks go also to many of the postgraduate and postdoctoral members of the department, who have given assistance or encouragement along the way. In this respect I thank Mr. Jonathan Steed especially, for valuable discussion on some of the n.m.r. spectra reported in Chapter 4, and for proof reading this thesis.

Finally, my warmest thanks go to my family for their love and moral support.

Abbreviations.

[2_2]paracyclophane = [2_2](1,4)cyclophane = $C_{16}H_{16}$

n.m.r.	nuclear magnetic resonance
i.r.	infrared
FAB	fast atom bombardment
HOMO	highest occupied molecular orbital
I_{pa}/I_{pc}	anodic current / cathodic current
$E_{\frac{1}{2}}$	half-wave potential
ΔE_p	peak to peak separation
Cp	cyclopentadienyl, $[\eta^5\text{-}C_5H_5]^-$
p-cymene	1-methyl-4-isopropylbenzene
acac	acetylacetone
bipy	2,2'-bipyridine
phen	1,10-phenanthroline
PPh_3	triphenylphosphine
PMe_2Ph	dimethylphenylphosphine
$PMePh_2$	methyldiphenylphosphine
THF	Tetrahydrofuran
$TBABF_4$	tetrabutylammonium tetrafluoroborate

py	pyridine	pyz	pyrazine
Me	methyl	Et	ethyl
^{i}Pr	isopropyl	^{t}Bu	tertiary butyl

Spectroscopic abbreviations.

n.m.r. spectroscopy:

s	singlet	m	multiplet
d	doublet	dd	doublet of doublets
t	triplet	dt	doublet of triplets
sept	septet	tt	triplet of triplets

Infrared spectroscopy:

s	strong	br	broad
m	medium	sh	shoulder
w	weak	v	very

CHAPTER 1.

INTRODUCTION.

1.1 Motivation.

The motivation behind the work presented in this thesis comes from two main areas of research. The first is the work of Boekelheide and his coworkers in the field of ruthenium-cyclophane chemistry. Evidence indicating that cyclophanes possess an overall π-electron system prompted Boekelheide to direct his research towards the synthesis of subunits of a potential transition metal-cyclophane polymer, the generalised structure of which is represented by Fig. 1.1.

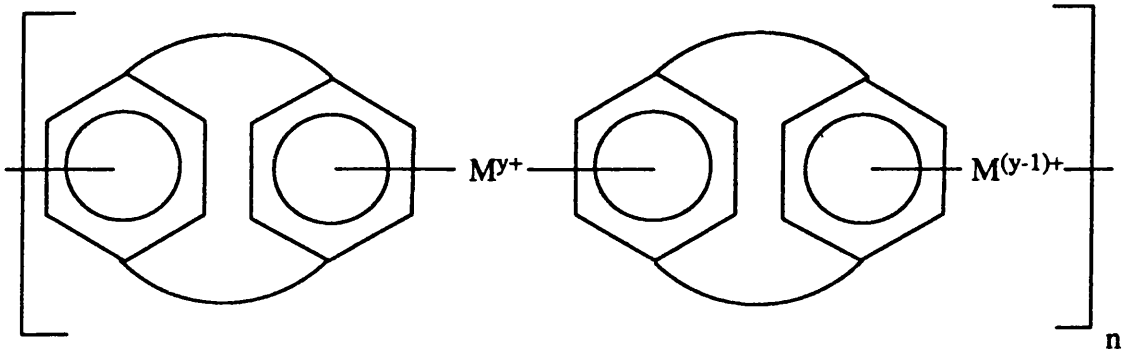

Fig. 1.1 The generalised structure of a transition metal-cyclophane polymer.

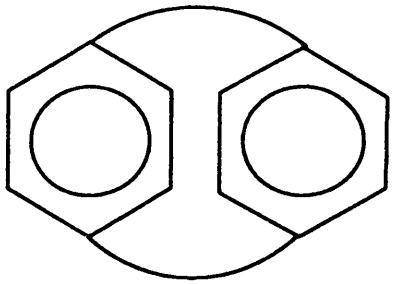

Is a generalised structure representing any of the $[2_n]$cyclophanes.

Such a polymer might possess interesting electronic properties or even electrical conductivity. For this to be possible the model subunits would also need to possess delocalised mixed-valence character. The model subunits of polymeric compounds which have been prepared thus far, have contained only one type of metal atom. The availability of mixed-metal subunits would provide a possible enhancement of the anisotropic electronic properties of these systems. Such electronic characteristics would be important if polymers of this type were to have applications in solid state devices. Therefore the extension of Boekelheide's work to mixed-metal ruthenium/osmium systems seemed a worthwhile endeavour.

Included in the development of synthetic pathways to such model subunits was the synthesis of the compound $[Ru(\eta^6\text{-}[2_2]paracyclophane)Cl_2]_2$ (1). The chemistry of this compound was not investigated by Boekelheide beyond its use as a precursor to the tris-solvate complex $[Ru(\eta^6\text{-}[2_2]paracyclophane)(acetone)_3][BF_4]_2$ (2). (2) was used in capping reactions, which will be described in more detail later. Compound (1) is a member of the family of $[M(\eta^6\text{-arene})Cl_2]_2$ compounds, and this provides the link to the second part of the motivation for this work. That is the large and still expanding field of η^6-arene transition metal chemistry, more specifically that involving ruthenium and osmium in the divalent oxidation state. Much of this chemistry uses $[M(\eta^6\text{-arene})Cl_2]_2$ (M=Ru,Os) compounds as starting materials. The availability of a new $[Ru(\eta^6\text{-arene})Cl_2]_2$ compound with an arene possessing novel aromatic properties suggested a comparison of its reactivity with that of simpler $[M(\eta^6\text{-arene})Cl_2]_2$ (M=Ru,Os; arene = benzene, *p*-cymene, hexamethylbenzene, etc) compounds would be worthwhile.

1.2 A GENERAL INTRODUCTION TO $[2_2]$PARACYCLOPHANE.

$[2_2]$Paracyclophane (3) is a novel aromatic hydrocarbon with the empirical formula $C_{16}H_{16}$. It comprises of two benzene rings stacked face to face, and linked by two ethylenic bridges in the *para* positions as shown in Fig. 1.2.

The $[2_n]$cyclophanes are compounds having two benzene decks linked by between two and six bridges. $[2_2]$Paracyclophane is the simplest of such compounds and, due to its simplicity and high symmetry, enjoys a similar position in cyclophane folklore to that held by benzene among simple aromatic compounds.

Although the compound was first named di-p-xylylene by Brown and Farthing[1], who discovered it, the two generally accepted[2] names are $[2_2]$paracyclophane[3] and $[2_2]$(1,4)cyclophane. Both names are widely used and equally valid. The generally adopted numbering scheme[2] for the carbon skeleton is shown in Fig. 1.2.

$[2_2]$Paracyclophane is a white, air stable solid at room temperature with a melting point of 458 K. It is only sparingly soluble in most common organic solvents, but dissolves best in pyridine, glacial acetic acid, trifluoroacetic acid, hexane and toluene. It can be sublimed under reduced pressure at *ca.* 373 K and, at the time of writing, is the only commercially available simple hydrocarbon cyclophane.

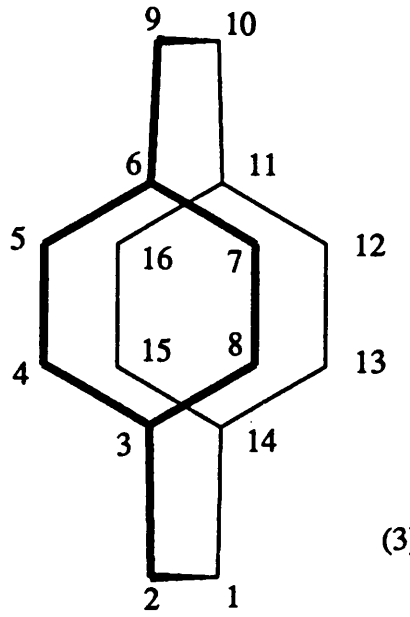

(3)

Fig. 1.2 The molecular structure of [2_2]paracyclophane (3) showing the atom numbering scheme.

1.2.1 The Discovery and Characterisation of [2_2]Paracyclophane.

The synthetic challenge of bringing two benzene rings into close face to face proximity was addressed as long ago as 1933[4]. It was not until 1949 however that, in the laboratories of I.C.I., "di-p-xylylene" was first isolated and characterised by Brown and Farthing[1]. The compound was crystallised from an acetone insoluble mixture of low molecular weight products obtained from the low temperature pyrolysis of p-xylene. Despite a very low yield, recrystallisation from pyridine gave pure crystals with a sharp melting point, which were suitable for an X-ray structural analysis[5]. The compound crystallises in the tetragonal space group $P4_2/mnm$ with a = 7.82 and c = 9.33 Å. There are two molecules per unit cell. Three mutually perpendicular mirror planes intersect in the centre of the cyclophane cavity, which results in just five atoms being crystallographically unique. One carbon atom (C3, Fig. 1.3) and the two hydrogen atoms (H1 and H3) are in general positions, while the two remaining carbon atoms (C1 and C2) are located in one of the crystallographic mirror planes (Fig. 1.3).

The aromatic rings are distorted into a shallow boat conformation, with the bridgehead carbon atoms (C2) displaced out of the plane of the other four aromatic carbons, towards the cyclophane cavity[5]. The interdeck spacing between the four planar atoms in each deck is 3.09 Å, and the bridgehead carbon atoms of the two decks are 2.78 Å apart. The intermolecular distance between the stacked aromatic rings in graphite is

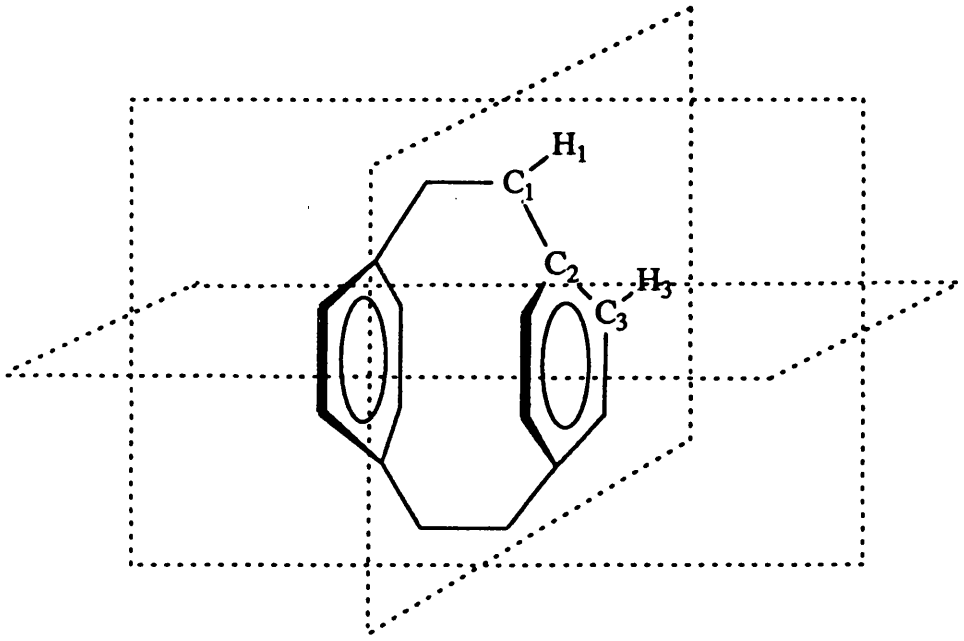

Fig. 1.3 The unique atoms in the solid state structure of [2$_2$]paracyclophane.

significantly larger at *ca.* 3.35 Å. The bond angles of the ethylenic bridges vary considerably from the ideal values of 109.5 and 120° for sp^3 and sp^2 hybridised carbon atoms respectively. The aliphatic C-C bond lengths in the ethylenic bridges were also significantly elongated compared with examples in unstrained molecules.

Brown's determination[5] of the structure identified the geometry of the carbon skeleton, and revealed the highly strained nature of the molecule, but was lacking in precision. The advent of computers and the development of programmes to perform diagonal least-squares calculations for structure refinements aided Lonsdale *et al*[6] in their redetermination of the structure at 291 and 93 K in 1959. This work[6] showed primarily that, as the temperature is lowered, the benzene rings move slightly towards each other, accompanied by a significant shortening of the bond length between the two atoms in each bridge. The possibility of one ring twisting with respect to the other was also identified[6].

The most accurate structure determination carried out on this compound to date is that performed by Hope, Bernstein, and Trueblood[7]. New, more precise data were collected on a four-circle diffractometer which, combined with more powerful computing facilities, allowed an extremely detailed analysis of the structure. The unit cell parameters were redetermined as a = 7.781(1) and c = 9.290(2) Å. Unusually large thermal ellipsoids were associated with all of the hydrogen atoms, especially those bound to the bridging atoms, which were elongated in a direction normal to the CH_2-CH_2 bond. This phenomenon was explained[7] in terms of a disorder that occurs by the benzene rings

twisting in opposite directions and causing an estimated 3.2° torsion angle in the interdeck linkages (Fig. 1.4). A refinement employing a statistically disordered model with two

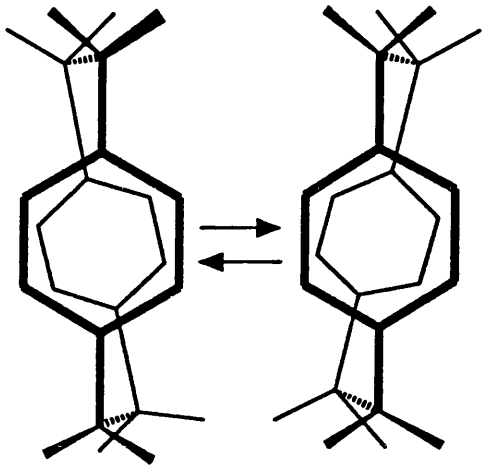

Fig. 1.4 Dynamic disorder in the solid state structure of [2_2]paracyclophane.

equally occupied sets of atomic positions at the two extremes of the twisting motion, gave a residual of 0.029. This compared with a value of 0.039 when no disorder was modelled. Although the crystal data does not facilitate differentiation between statistical and dynamic disorder in this case, there is evidence from temperature dependant heat capacity measurements[8] supporting a dynamic disorder above *ca.* 50 K. At around this temperature it is argued[8] that most of the molecules have acquired sufficient energy for the twisting motion to have become an active vibrational mode, which results in the observed irregularity in the plot of heat capacity against temperature.

Potential energy calculations[7] show that the interdeck repulsions are at a maximum when the two rings are exactly eclipsed, but are relieved if the rings are mutually twisted by a few degrees. However, such a deformation leads to the two rings being pulled closer together and/or the elongation of C-C bonds of the bridging functions. These latter effects are unfavourable and act as restoring forces.

The important geometrical parameters derived from Trueblood's structure determination[7] are shown in Fig. 1.5. The bridgehead carbon atoms of the benzene rings are bent *ca.* 12° out of the plane of the other four aromatic carbon atoms. These sp^2 hybridised atoms are also distorted from planarity by *ca.* 11°, while the sp^3 hybridised CH_2-CH_2 groups show a distortion to *ca.* 113° in the angle made with the aromatic decks. Thus the steric strain is accommodated by small distortions in several parts of the molecule.

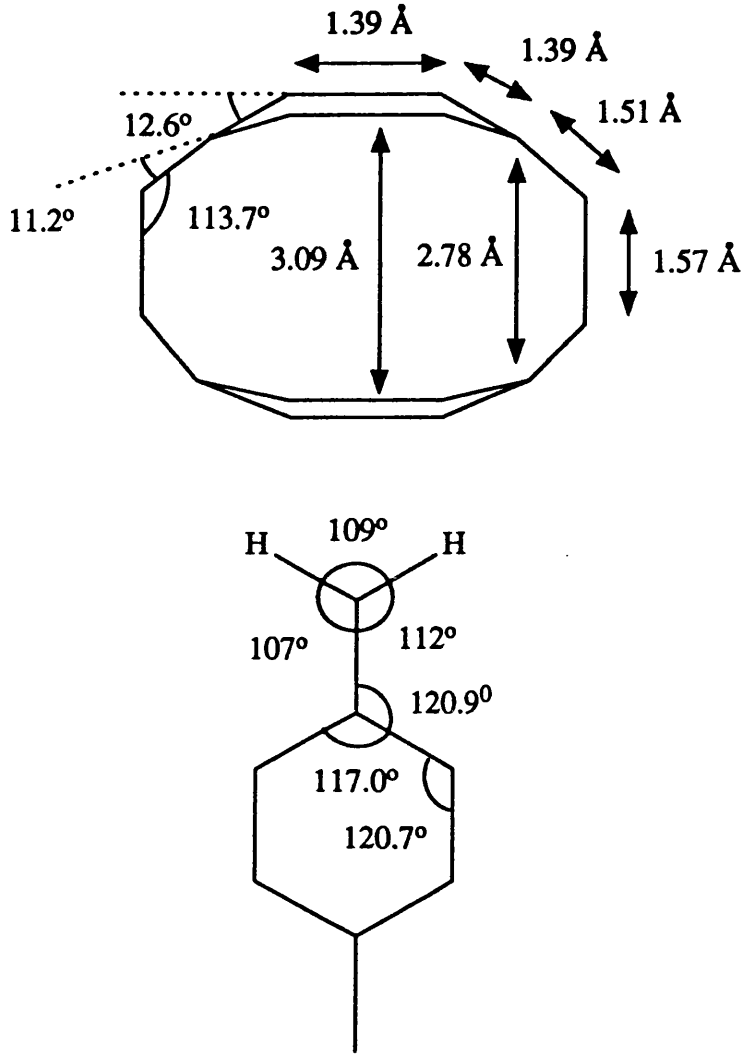

Fig. 1.5 Important geometrical parameters for [2_2]paracyclophane in the solid state.

1.2.2 The Syntheses of [2_2]Paracyclophane.

Brown and Farthing's first, essentially accidental, isolation of [2_2]paracyclophane came at the same time as Cram and Steinberg were investigating the properties of rigid, geometrically strained molecules. In 1951 Cram and Steinberg published[3] a designed synthesis of (3) employing an intramolecular Wurtz coupling (Scheme 1.1). Their yield was only 2.1%, but more recent studies[2] have shown that care with reaction conditions can give yields around 20%. Several alternative synthetic methods have since been published[2]. The extrusion of sulphur from dithiaparacyclophane can be achieved by pyrolytic or irradiation procedures to give good yields[2] (Scheme 1.2). Hoffmann type 1,6 eliminations

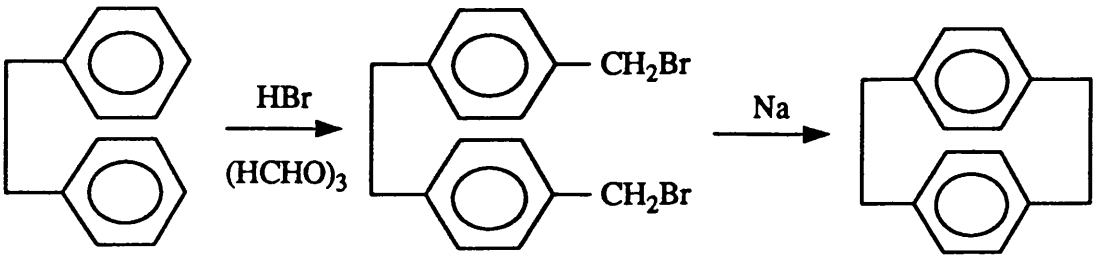

Scheme 1.1 The synthesis of [2$_2$]paracyclophane by the Wurtz coupling reaction.

provide another route. A popular laboratory synthesis[9] involves decomposition of *p*-methylbenzyltrimethylammonium halides in hot alkali to produce *p*-xylylene, a highly

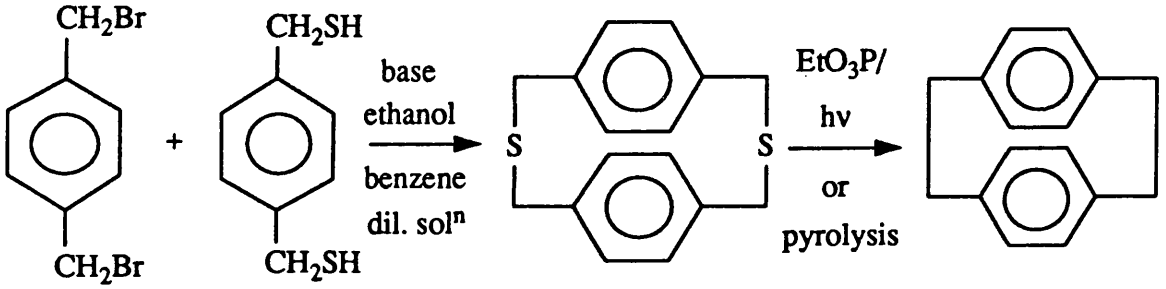

Scheme 1.2 The synthesis of [2$_2$]paracyclophane by sulphur extrusion of dithiaparacyclophane.

unstable intermediate, which then undergoes an intermolecular 1,6 to 1,6 cycloaddition in dilute solution to give the desired product (Scheme 1.3). Industrially[10] *p*-xylene is converted to [2$_2$]paracyclophane by pyrolysis in steam at 1173 K.

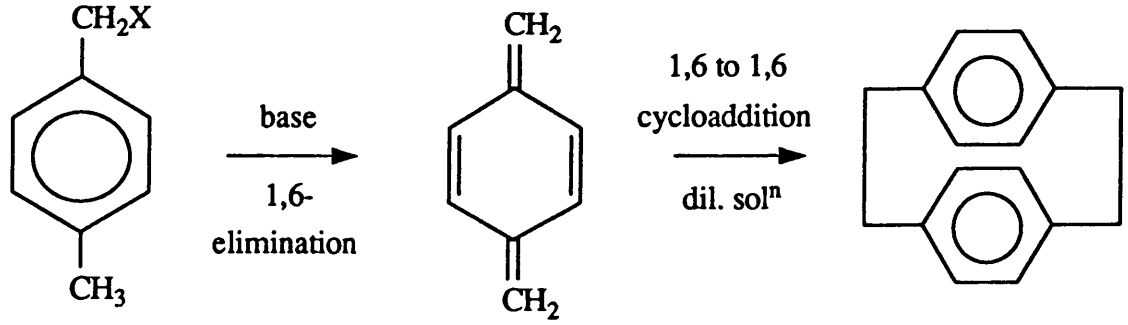

Scheme 1.3 The synthesis of [2$_2$]paracyclophane via Hoffmann degradation.

1.2.3 Transannular Interactions in [2_2]Paracyclophane: Spectroscopic Evidence.

Evidence for the transannular interaction of the two π-systems in [m.n]cyclophanes is provided by a variety of spectroscopic measurements.

Highly resolved e.s.r. spectra of the radical cation of [2_2]paracyclophane have been recorded[11,12] in a variety of solvents at low temperatures (*ca.* 180 K), using an alkali metal as the reductant. The spectra show coupling of the free electron to all sixteen of the protons in the molecule, with the frequency of electron exchange between the two aromatic decks reported[11] as being very rapid on the e.s.r. timescale.

The photoelectron spectra of a range of cyclophanes have been recorded[13,14]. The spectrum[14] of [2_2]paracyclophane itself exhibits bands at the following ionisation potentials: 8.1 (two overlapping bands), 8.4, 9.6, and 10.3 eV. The first and second ionisation potentials of 1,4-dimethylbenzene occur at 8.6 and 9.1 eV in comparison.

Two series of cyclophanes have been studied[13]. In the first series[13], the number of methyl substituents on the aromatic rings of [2_2]paracyclophane was increased from zero to eight. Increasing the degree of methylation results in a steady decrease in ionisation potentials, with octamethylparacyclophane having the lowest first ionisation potential of 7.1 eV.

In the second series,[13] the number of ethylenic bridges between the two benzene decks was successively increased from two to six. Increasing the number of bridges decreases the inter-ring separation and leads to a general decrease in the ionisation energies. Two factors play a role in this observation:

(i) "through space" π-π interaction increases linearly with a decrease in interdeck separation, facilitating easier ionisation, but

(ii) "through bond" interactions are severely limited by orbital symmetry restrictions.

These factors result in a much shallower fall-off in ionisation potentials for this second series of compounds than might be predicted purely on the grounds of increasing the number of alkyl substituents alone.

Thus, interaction between the two cyclophane decks, as explained[13] by molecular orbital models[15], gives rise to the more facile ionisation when compared with para-di-alkylated arenes.

Ultraviolet absorption spectra are also consistent with a strong interaction between the two cyclophane decks. A series of [m.n]cyclophanes and related compounds have been studied[3,16,17] to gain an insight into the important factors governing the observed differences between the spectra of compounds with stacked decks and those of linear

analogues. The length of the interdeck connectivity was varied[16,17] systematically from m=n=2 up to m=n=6 (Fig. 1.6a). For compounds with m,n > 4 the spectra resemble those

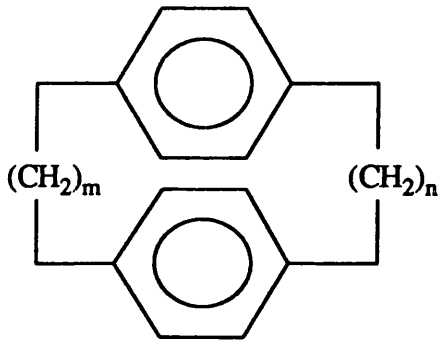

Fig. 1.6a [m.n]Paracylophanes with varying bridgelengths.

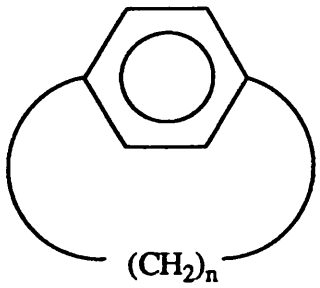

Fig. 1.6b [n]Cyclophanes with varying chainlengths.

of the linear compounds, consisting of intense bands in the 230 nm region and weaker bands with resolved fine structure around 265 nm. As the bridges are shortened the bands shift progressively to higher wavelengths, decrease somewhat in intensity, and exhibit no fine structure[16]. The spectrum of [2_2]paracyclophane exhibits bands at 225, 244, 286 and 302 nm[2,16], the latter arising from an electronic transition much lower in energy than any observed for the linear complexes. A recent paper[18] has provided a detailed theoretical interpretation of the absorption and ionisation spectra of the [m.m]paracyclophanes, assigning many of the observed electronic transitions.

There remained the task of distinguishing between the effects arising from the distortions in the aromatic rings and the effects due to the enforced close proximity of the rings. Single decked cyclophanes were prepared[19] with one benzene ring and alkyl chains of varying lengths attached in the 1 and 4 positions (Fig. 1.6b). The compound with n = 8 proved difficult to prepare, and was initially calculated[19] to have its bridgehead carbon atoms distorted by *ca.* 20° out of the plane of the remaining atoms of the aromatic ring. This compares with just 12.6° for [2_2]paracyclophane. The later structure determination[20] of a carboxylate derivative, 3-carboxy[8]paracyclophane, showed that the distortion was only of the order of *ca.* 9°. However, the u.v. spectrum[19] of the single decked compound, [8]paracyclophane deviated considerably less from those of the linear compounds than did that of [2_2]paracyclophane, the bands being shifted to only slightly longer wavelengths.

The important conclusion to be drawn from these studies is that the close packing of the aromatic rings is principally responsible for the observed behaviour of (3), although distortions from planarity of the aromatic decks contribute to a small degree.

1.3 EXTENDING THE ELECTRONIC DELOCALISATION: POLYMERS AND POLYMER SUBUNITS.

1.3.1 Options for Polymerisation.

There have been two main approaches to extending the π-electron delocalisation in cyclophane compounds. The first approach is simply to increase the number of stacked aromatic decks to form an infinite cyclophane column. Misumi and co-workers have addressed[21,22] this problem but thus far the largest column synthesised is one with just six decks (Fig. 1.7). Unfortunately, the synthesis proceeds by adding only one deck at a time,

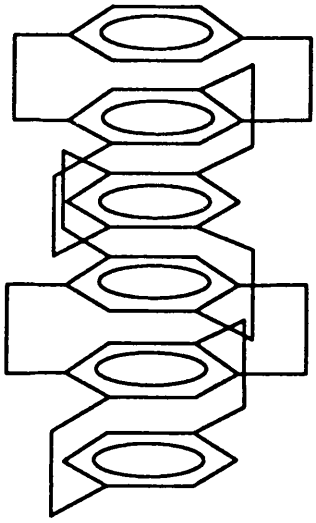

Fig. 1.7 "Hexadecked paracyclophane".

so yields of the multidecked compounds are excruciatingly low. Indeed the task of synthesising such polymers has been described[2] as being "exceedingly formidable, if not impossible".

The second approach employs metal-cyclophane complexation. The ability of cyclophanes to coordinate metals to both external aromatic faces gives the possibility of forming infinite chains with alternate transition metal atoms and cyclophanes as shown in Fig. 1.1. Such systems offer advantages as they can use the more economically synthesised smaller cyclophanes. A number of transition metals, including Cr, Mo, W, Fe and Ru, have been coordinated to cyclophanes. The following sections aim to provide a survey both of the cyclophane compounds that have been prepared and the synthetic techniques employed. The emphasis will be on the success and further potential of the synthetic strategy to produce stable, characterisable subunits of polymeric species.

1.3.2 CHROMIUM, MOLYBDENUM, AND TUNGSTEN COMPLEXES OF CYCLOPHANES.

The first transition metal-cyclophane compounds were made by Cram and Wilkinson in 1960[22]. Chromium hexacarbonyl was refluxed with a series of [m.n]paracyclophanes (Fig. 1.6a) at *ca.* 440 K. For m,n ≤ 4 only mononuclear complexes were formed (Fig. 1.8), but for [m.n] = [4.5] or [6.6] binuclear species (Fig. 1.9) were also

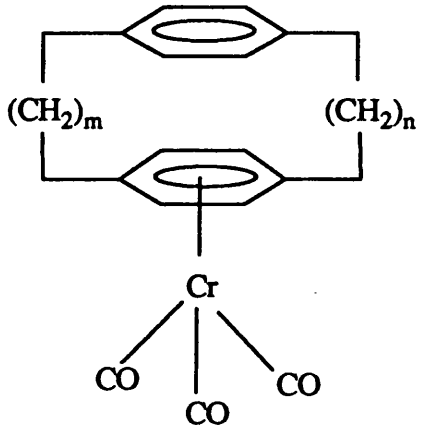

Fig. 1.8 [Cr(η⁶-[m.n]paracyclophane)(CO)₃].

isolated. Cram concluded[23] that when the chain was short the rings were close enough to interact, such that the electron withdrawing carbonyl groups deactivated the uncomplexed cyclophane face towards further attack. However, when the chainlength exceeded a critical value, the decks were far enough apart to be electronically independent allowing the bis-complexes to form.

Misumi *et al* used the multidecked paracyclophane compounds they had prepared previously[19] in reactions[22,23] with [Cr(CO)$_6$]. Paracyclophanes with two, three, and four decks were treated[23] with [Cr(CO)$_6$] in various stoichiometric ratios. Low yields of the binuclear complexes (Fig. 1.9, m=n=2) were achieved under forcing conditions. When the number of layers was increased it became easier to form the binuclear complexes, and higher yields were possible. The electronic deactivation of the outer deck can therefore be decreased by increasing the number of layers.

The crystal structure of [Cr(η⁶-[2$_2$]paracyclophane)(CO)$_3$] (4) has been determined[24] at low temperature (123 K). This study shows that on complexation to the transition metal, the geometry of the cyclophane changes markedly. The interdeck spacing decreases from 3.09 to 3.02 Å, allowing a relaxation in the angular distortions observed in the pure hydrocarbon. The rings flatten slightly, the complexed face more so than the

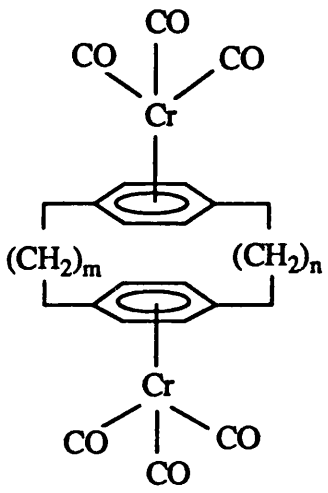

Fig 1.9 [(Cr(CO)$_3$)$_2$(η^6,η^6-[m.n]paracyclophane)].

non-complexed one, and the angles at the bridging carbon atoms become closer to the ideal value of 109.5°. The CH_2-CH_2 bond length increases to 1.59 Å, which is significantly longer than is normally observed for such a bond (1.54 Å). As in the case of [Cr(η^6-C_6H_6)(CO)$_3$] (5)[25] the bondlengths of the coordinated deck are alternately long (average 1.417 Å) and short (average 1.398 Å), with the longer bonds being *trans* to the carbonyl ligands.

An improved synthesis[26], irradiating a refluxing solution of (3) and [M(CO)$_6$] in ligroin at the lower temperature of 373 K, allowed the thermally less stable Mo(0) and W(0) tricarbonyl complexes to be isolated. The ^{1}H n.m.r. spectra[26] of these complexes exhibit two peaks due to the aromatic protons, and two multiplets due to the aliphatic protons. Compared with the spectrum of the free ligand[19] (3), one aromatic resonance is shifted to lower frequency by *ca.* 1.75 ppm, while the other moves to slightly higher frequency in the metal complexes. The resonance of the benzene protons in (5) also exhibits[27] a strong shift to lower frequency, and therefore the signals at *ca.* 5 and 7 ppm in the spectrum of the cyclophane compounds are assigned to the protons of the coordinated and non-coordinated decks respectively. Misumi has suggested[23] that the large shielding effect observed on complexation of an aromatic ring is principally due to a decrease in the ring current and, to a lesser extent, to the additional magnetic anisotropy of the metal. ^{1}H n.m.r. studies[28] on a range of [η^6-meta-, [η^6-para-, and [(η^6-metaparacyclophane)Cr(CO)$_3$] complexes has provided additional support for the ring current disruption hypothesis. Each of these cyclophanes remain essentially geometrically unchanged on complexation to a metal and have protons situated directly above the ring plane of the coordinated deck (Fig. 1.10). Monitoring the chemical shifts of these protons allows changes in the ring current of

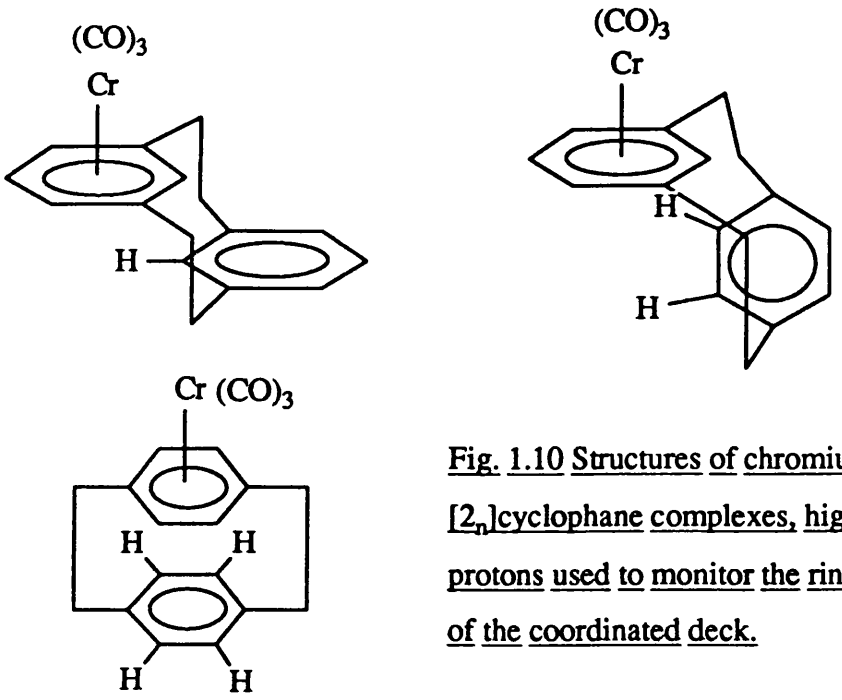

Fig. 1.10 Structures of chromiumtricarbonyl [2_n]cyclophane complexes, highlighting the protons used to monitor the ring current of the coordinated deck.

the coordinated deck to be detected when the ligand binds to a metal atom. A full assignment of the ^{13}C n.m.r. spectrum of [(η^6-[2_2]paracyclophane)Mo(CO)$_3$] has also been reported[29] (Fig. 1.11).

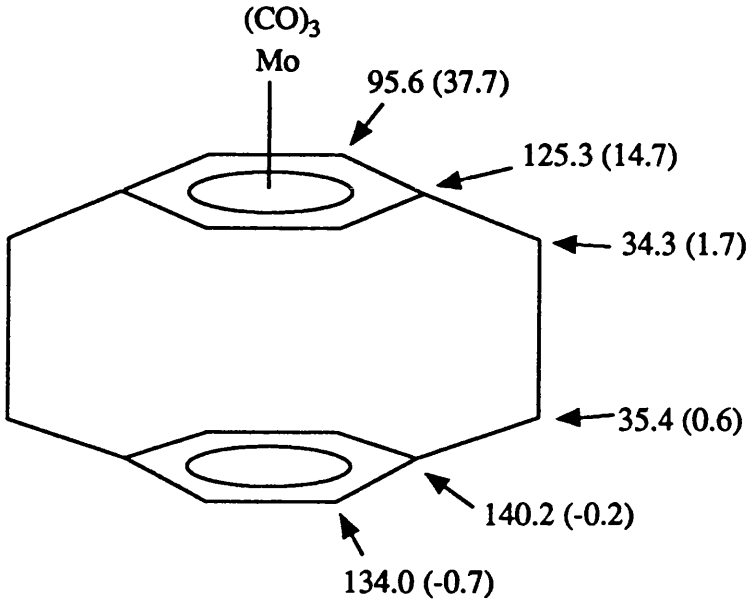

Fig. 1.11 ^{13}C n.m.r. chemical shift assignment for [Mo(η^6-[2_2]paracyclophane)(CO)$_3$]. () ≡ shifts on complexation; δ hydrocarbon-δ complex.

Metal and ligand vapour co-condensation techniques have been used to insert a metal atom into the cyclophane cavity (Fig. 1.12). Chromium has been inserted into the

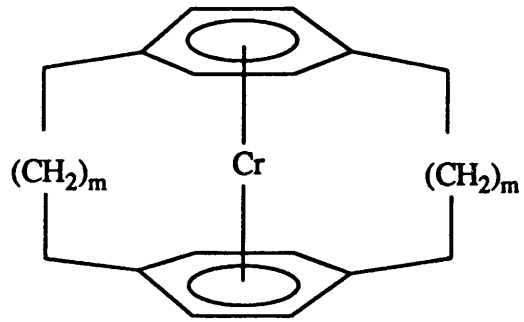

Fig. 1.12 A chromium atom inserted into the paracyclophane cavity; m = 2 or 3.

cavity of $[2_2]$-[30] and $[3_3]$paracyclophane[31,32,33]. The [Cr(η^{12}-$[2_2]$paracyclophane)] complex (Fig. 1.12, m=2) is chemically inert and stable[30] in solution, even in the presence of acid over a period of weeks, whereas complexes where the ligand is externally coordinated to the metal decompose rapidly under similar conditions. Exposure of a solution of [Cr(η^{12}-$[3_3]$paracyclophane)] (Fig. 1.12 m=3) to the air[32] leads to the formation of the radical cation which has been isolated and structurally characterisd[31,33]. As observed for the externally coordinated complex, (4), the aromatic rings flatten slightly on complexation, but the Cr-C distances remain comparable to those in dibenzenechromium[34] (*ca.* 2.14 Å).

The metal vapour technique has yielded[30] a third class of metal complexes where a chromium atom is sandwiched between two $[2_2]$paracyclophane ligands (Fig. 1.13). The complex is unstable in solution, and its formation has only been demonstrated by the detection of its radical cation using e.s.r. and mass spectroscopic techniques. The instability is unfortunate in that this complex represents just the sort of building block required for the formation of polymers, where further complexation could, in theory, be achieved at the two free cyclophane faces.

None of the above techniques lend themselves particularly to the controlled synthesis of oligomeric or polymeric species, nor have they succeeded in generating any suitably stable building blocks for electrochemical study. As a result chemists have turned to other metals and developed new methods which give greater control over the products formed.

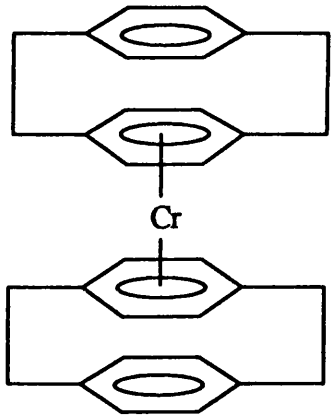

Fig. 1.13 [Cr(η^6-[2$_2$]paracyclophane)$_2$].

1.3.3 Arene-Cyclopentadienyl Compounds of Iron.

In 1957 Coffield *et al*[35] prepared the first transition metal compound containing both an η^6-arene and a η^5-cyclopentadienyl ligand. The compound [FeCp(η^6-1,3,5-$C_6H_3Me_3$)]I was prepared from [FeCp(CO)$_2$Cl] and mesitylene in the presence of a Lewis acid catalyst, $AlCl_3$, under reflux conditions. Nesmeyanov *et al*[36] also used $AlCl_3$ as a catalyst in their reaction to exchange one of the cyclopentadienyl ligands of ferrocene for an arene. The Nesmeyanov synthesis also works for substituted ferrocenes. Electron withdrawing substituents hinder the reaction while electron donating groups facilitate it. The products obtained then contain one substituted cyclopentadienyl ligand in addition to the arene. The reaction conditions have been fine tuned to give excellent yields for a wide range of arenes. The reaction is carried out in the neat arene

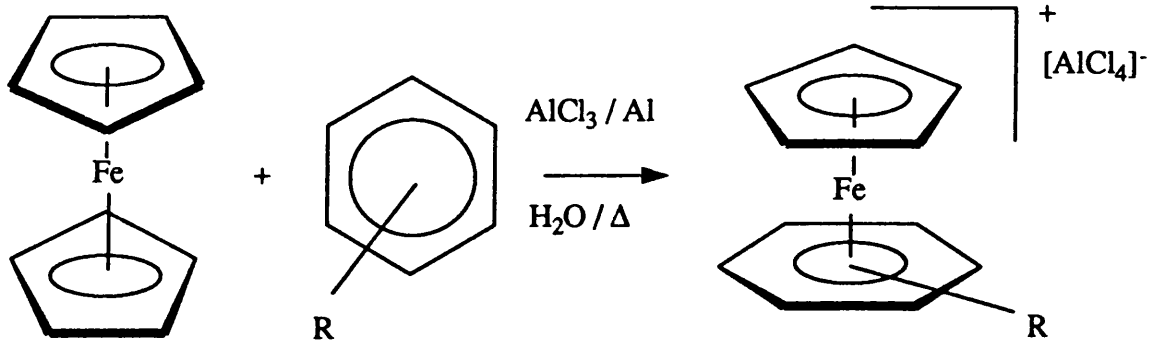

Scheme 1.4 The synthesis of [Fe(η^5-C_5H_5)(η^6-arene)][$AlCl_4$].

whenever possible, or in refluxing nonane or decane for those arenes with higher melting points. Trace amounts of water have been shown to assist the reaction. One equivalent of aluminium powder per mole of the ferrocene is added to the reaction mixture to prevent the ferrocene being oxidised to the ferricinium cation. The optimum reagent ratios of ferrocene:$AlCl_3$:Al:arene:H_2O are 1:2-4:1:excess:trace (Scheme 1.4).

Both mono- and binuclear [2_2]paracyclophane ironcyclopentadienyl compounds have been prepared[37] in excellent yield by the Nesmeyanov method. Reaction of equimolar quantities of ferrocene and (3) yields the mononuclear product (6), while reaction with an excess of ferrocene gives the binuclear compound (7) (Scheme 1.5). Both

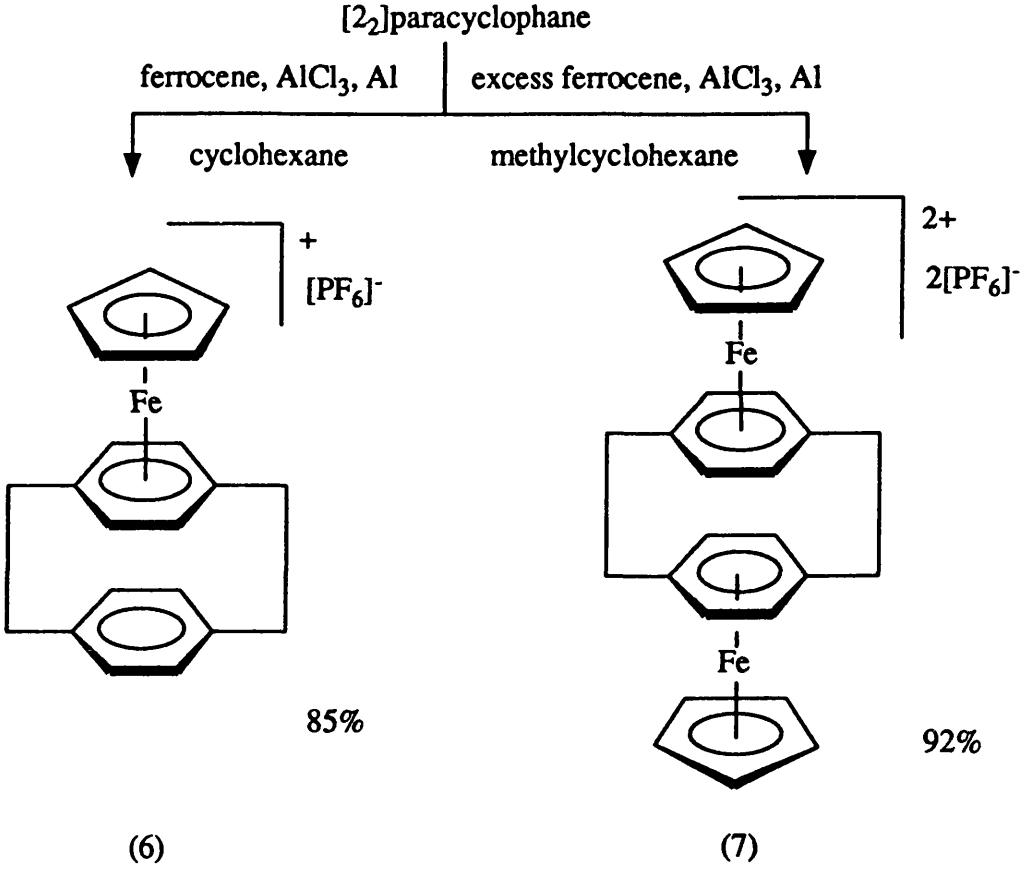

Scheme 1.5 The synthesis of mono- and binuclear [2_2]paracyclophane ironcyclopentadienyl compounds.

of these compounds have been characterised[37] by ^1H and ^{13}C n.m.r. spectroscopy, and elemental analysis. In solution the complexes are stable under an inert atmosphere, but decompose over a period of hours when exposed to the air. The solids are reported[2] to be air stable indefinitely. (6) has been studied[2] by cyclic voltammetry and exhibits a reversible one electron reduction.

The final, high yield route[2,38] to [2_2]paracyclophane ironcyclopentadienyl compounds, is via arene exchange of (3) for *p*-xylene in [Fe(η^5-C_5H_5)(η^6-*p*-xylene)]$^+$ (8) under photolytic conditions (Scheme 1.6). This general method works well for the exchange of any of the more basic arenes. Complex (6) has been prepared[38] in 88% yield via this route.

These complexes of iron(II) therefore represent a considerable improvement in stability when compared with the chromium complexes described previously. The reversible electrochemical behaviour is particularly encouraging in view of the potential applications of any polymer that might be produced.

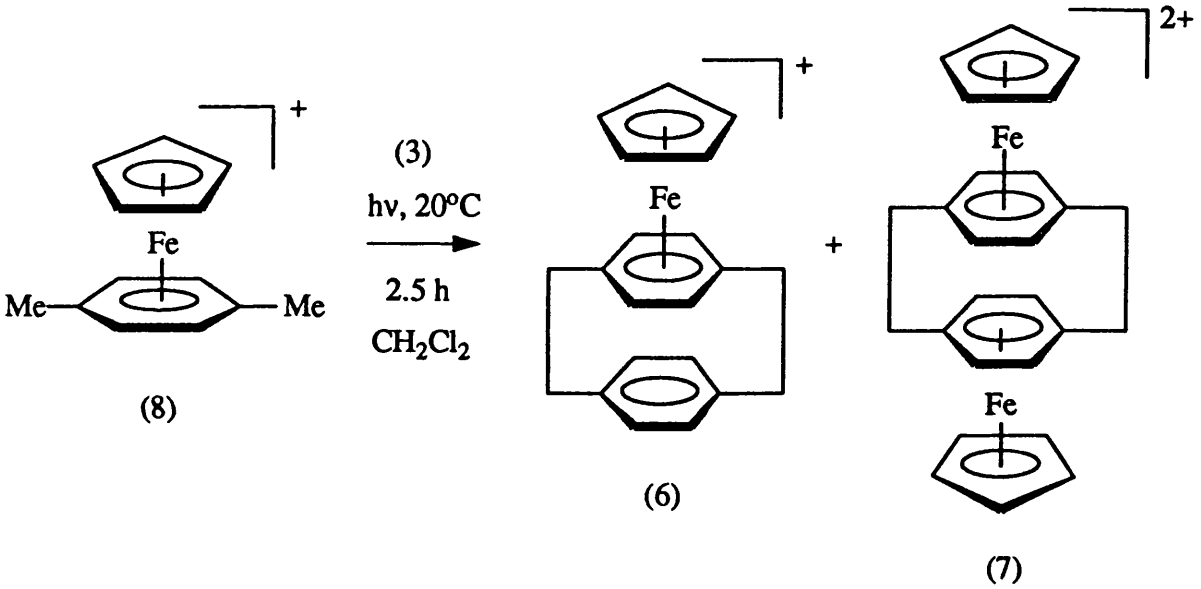

Scheme 1.6 The photolytic preparation of [2_2]paracyclophane ironcyclopentadienyl complexes.

1.3.4 Bis-Arene Compounds of Iron.

Bis-arene complexes of iron are generally fairly unstable, unless the arenes are extensively alkylated. For example, [Fe(η^6-C_6Me_6)$_2$] is thermally stable at room temperature but the benzene analogue is only stable below 200 K and actually explodes[39] at 223 K! Nevertheless, there is a brief report[40] of a third type of iron(II)cyclophane compound having been prepared[40] by the synthetic route shown in the following equation:

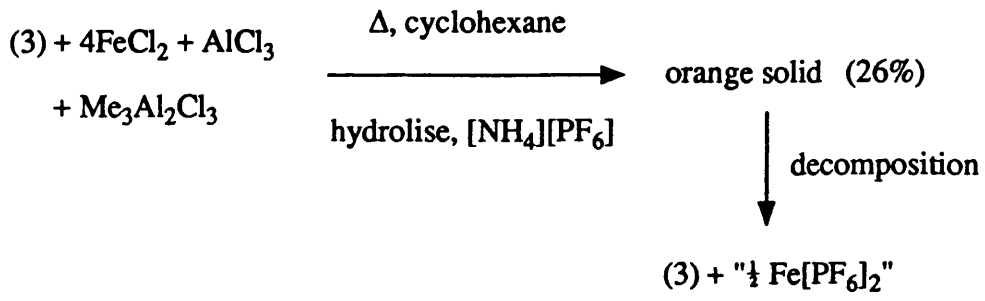

To prevent the known[41] rearrangement of (3) to the *metapara* isomer, which is catalysed by $H[AlCl_4]$, a proton scavenger, $Me_3Al_2Cl_3$, is required. The orange solid, though not characterised directly has been shown by a quantitative analysis of its decomposition products to contain two moles of (3) per mole of iron(II). The orange solid is thought to be[40] $[Fe(\eta^6\text{-}[2_2]paracyclophane)_2][PF_6]_2$ (Fig. 1.14). The complex is unstable both in solution and in the solid state at ambient temperatures. A cyclophane with a greater degree of alkylation, 4,7,13,16-tetramethyl-$[2_2]$paracyclophane, was used in an analogous reaction[40] and produced an air stable metal complex. The complex was moderately stable in nitromethane solution below 273 K, so characterisation by ^1H n.m.r. spectroscopy was possible. The spectrum recorded was consistent with the proposed structure.

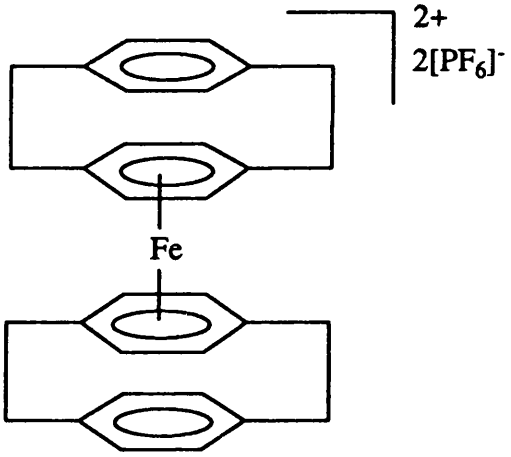

Fig. 1.14 $[Fe(\eta^6\text{-}[2_2]paracyclophane)_2][PF_6]_2$

1.3.5 Arene-Cyclopentadienyl Compounds of Ruthenium and Osmium.

Several of the synthetic procedures developed for preparation of arene-ironcyclopentadienyl compounds have been used, often with minor modifications, for the preparation of similar ruthenium and osmium compounds.

The Lewis acid catalysed exchange of one cyclopentadienyl ring of ruthenocene[42] for an arene[43,44] requires more forcing conditions than in the case if iron, and gives lower yields. Higher temperatures (440-465 K) are required and yields of only *ca.* 10% were achieved at best[44]. The addition of one mole of water per mole of ruthenocene has a dramatic effect, increasing yields up to sixfold. Thus a typical reaction would require reagents in the following stoichiometries: ruthenocene:$AlCl_3$:Al:H_2O:arene = 1:3:1:1:excess. One problem encountered with the syntheses[44] incorporating water, is the extensive dealkylation of some peralkylated arenes. For example, in the reaction designed to produce $[Ru(\eta^5\text{-}C_5H_5)(\eta^6\text{-}C_6Me_6)]^+$, a statistical mixture of products results in which the arene ligand has had one or more of its methyl groups substituted by hydrogen atoms. Strangely, with mesitylene, no demethylation is observed[44] and a 30% yield of $[Ru(\eta^5\text{-}C_5H_5)(\eta^6\text{-}1,3,5\text{-}C_6H_3Me_3)]^+$ is obtained. The generally observed lower yields compared with the related iron compounds are attributed[43] to the Ru-C bonds being more difficult to break than the Fe-C bonds. More recently an improved synthesis has been reported[45]. If the reaction is carried out in an autoclave at higher pressures with just a few drops of water, at temperatures of 375-425 K, yields are generally increased (up to 66%), and demethylation is less of a problem. There are no reports of cyclophane complexes being prepared by this method to date.

The photolysis[46] of $[RuCp(\eta^6\text{-}C_6H_6)][PF_6]$ in acetonitrile leads to the synthetically useful tris-solvate complex $[RuCp(MeCN)_3][PF_6]$ (9) in quantitative yield. The three acetonitrile ligands can be substituted for a variety of arenes or successively by 1, 2, or 3 monodentate ligands by thermal reaction, giving excellent yields. Use of (3) as the incoming arene leads to the formation[46] of $[RuCp(\eta^6\text{-}[2_2]$paracyclophane$)][PF_6]$ (10), which is isolated in 85% yield (Scheme 1.7). The dicationic complex $[(\eta^5\text{-}C_5H_5)Ru(\eta^6,\eta^6\text{-}C_{16}H_{16})Ru(\eta^5\text{-}C_5H_5)]^{2+}$ has also been prepared by this method, presumably by decreasing the stoichiometric amount of the cyclophane added in the second step of the reaction, but the precise details have not been published[2].

A final method of preparing arene-Ru/Oscyclopentadienyl cationic compounds is to treat[47,48] $[M(\eta^6\text{-arene})Cl_2]_2$ compounds with two equivalents of $Tl[C_5H_5]$[49-51]. Yields are in the range 40-85%.

^{1}H n.m.r. spectra have been recorded for the three complexes $[MCp(\eta^6\text{-}C_6H_6)]^+$ of

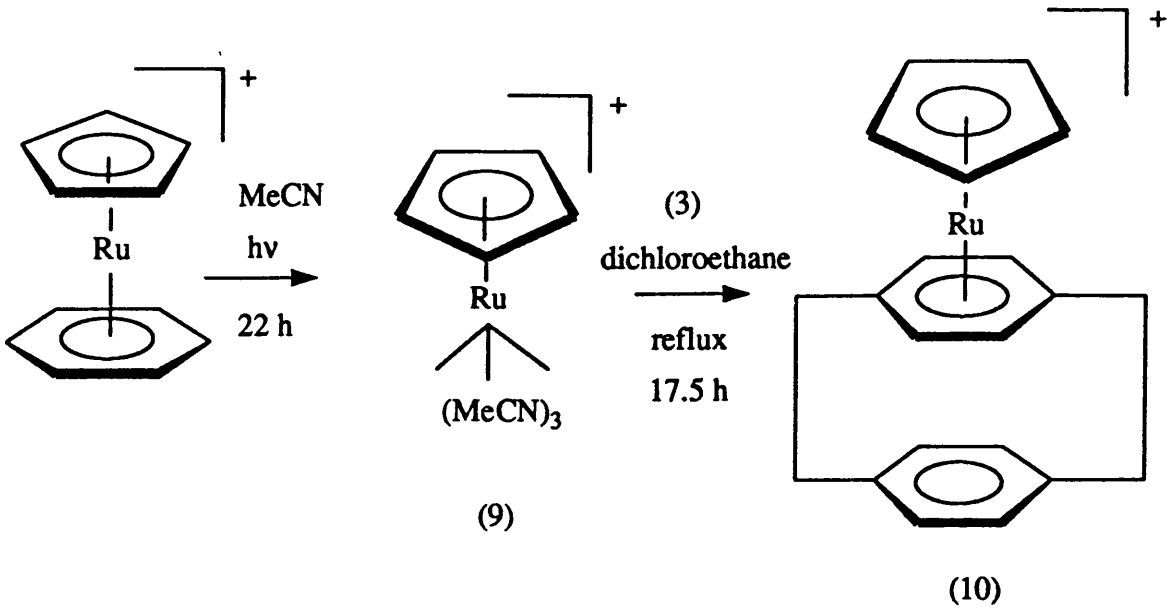

(9)

(10)

Scheme 1.7 The synthesis of $[RuCp(\eta^6\text{-}[2_2]paracyclophane)]^+$ from $[RuCp(\eta^6\text{-}C_6H_6)]^+$ via $[RuCp(MeCN)_3]^+$.

the iron triad. The chemical shift (δ) of the Cp protons moves to higher frequency on descending the triad: M=Fe, 5.23[43]; M=Ru, 5.43[48]; M=Os, 5.67[48] ppm, while the chemical shift (δ) of the benzene protons moves to lower frequency: M=Fe, 6.44[43]; M=Ru, 6.20[48]; M=Os, 6.14[48] ppm. This suggests that the positive charge of the cations is delocalised onto the arene ligand increasingly in the order Fe > Ru > Os. This hypothesis is supported by the observation that the iron complexes react readily with a variety of nucleophiles giving stable exo-substituted η^5-cyclohexadienyl products[52,53,91], whereas the Ru and Os analogues show very little reactivity towards them, or decompose with the probable loss of both the Cp and arene rings[48].

1.3.6 Bis-Arene Compounds of Ruthenium and Osmium.

There are a number of synthetic routes to bis-arene Ru and Os compounds. These have been well described in reviews[54,55] and, apart from one of these methods, only warrant the briefest of comment here.

The Fischer synthesis[56,57] yields $[Ru(II)(\eta^6\text{-arene})_2]^{2+}$ compounds, with the corresponding Ru(0) derivatives obtained[58,59] on reduction with sodium-mercury amalgam (Scheme 1.8).

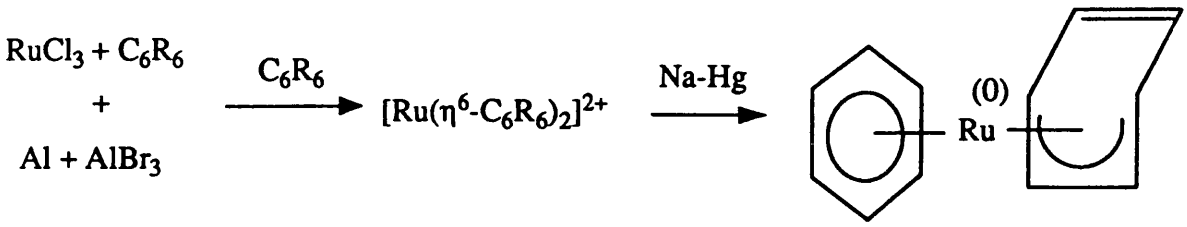

Scheme 1.8 The Fischer synthesis of bis-arene ruthenium compounds.

The metal atom reaction[54] with benzene affords the complex $[Ru(\eta^6\text{-}C_6H_6)_2]$. The complexes $[M(\eta^4\text{-}C_6H_8)(\eta^6\text{-}C_6H_6)]^{2+}$ (M = Ru,Os) are prepared by the reaction of MCl_3 with 1,3-cyclohexadiene in the presence of ^{i}PrMgBr in ether. None of these syntheses have found applications in the preparation of cyclophane complexes to date.

It was Bennett's high yield method of preparing bis-arene ruthenium complexes containing either two identical, or different arenes, that laid the foundation for Boekelheide's work. Boekelheide *et al* have prepared and studied in detail the electrochemical and other physical properties of a wide range of ruthenium-cyclophane complexes. These complexes represent the first air and solution stable subunits of a possible conducting transition metal-cyclophane polymer (Fig. 1.1).

The general reaction scheme for Bennett's synthesis[60] of bis-arene ruthenium complexes, is shown in Scheme 1.9. Yields range from 20% to 100%, depending on the arenes used, with decreasing yields obtained in the order C_6Me_6 > 1,3,5-$C_6H_3Me_3$ > C_6H_6. The addition of acid allows shorter reaction times and results in higher yields of the products. Trifluoroacetic acid was found to be the most effective. The function of the acid is to protonate and thereby labilise the solvato ligands.

Although Bennett and Matheson[60] used only three different arenes as arene^1 (Scheme 1.9), the choice is not limited to these. The availability of $[Ru(\eta^6\text{-arene})Cl_2]_2$ compounds is limited only by the availability of a suitable 1,3- or 1,4-cyclohexadiene,

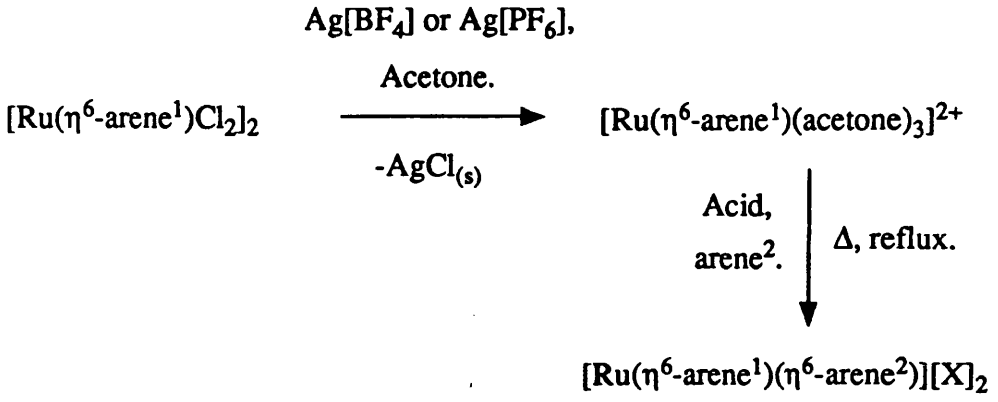

arene^1 = benzene, mesitylene or hexamethylbenzene.
arene^2 = a wide range of arenes.
$[X]^-$ = $[BF_4]^-$ or $[PF_6]^-$.
Acid = CF_3CO_2H, $H[BF_4]$ or $H[PF_6]$.

Scheme 1.9 The Bennett synthesis of bis-arene ruthenium(II) complexes.

which is required for the synthesis of the dimer. The hexamethylbenzene[61] and durene derivatives of the dimer are prepared by exchange reactions with $[Ru(\eta^6\text{-}p\text{-cymene})Cl_2]_2$[61] at elevated temperatures (450 K). The dimeric nature of these $[Ru(\eta^6\text{-arene})Cl_2]_2$ compounds has been confirmed by the crystal structure determination[62] of $[Ru(\eta^6\text{-}C_6Me_6)Cl_2]_2$.

The compounds $[Os(\eta^6\text{-arene})Cl_2]_2$ (Fig. 1.14) are generally prepared[63] from $Na_2[OsCl_6]$ by dehydrogenation of an appropriate 1,3- or 1,4-cyclohexadiene in a small volume of commercial ethanol under reflux conditions for *ca.* 4 h. The yields (*ca.* 33%) are considerably less than for the ruthenium compounds (80%-almost quantitative). A high yield (80%) synthesis of $[Os(\eta^6\text{-}p\text{-cymene})Cl_2]_2$ has now been reported[64]. The dimeric nature of the $[Os(\eta^6\text{-arene})Cl_2]_2$ complexes has been confirmed by the single crystal structure determination[65] of the representative compound $[Os(\eta^6\text{-}p\text{-cymene})Cl_2]_2$.

Boekelheide's aim[48,66,73,74] was to synthesise and study model subunits of the polymer shown in Fig. 1.1. The subunits should exhibit class (II) or class (III) mixed valence character. Iron was rejected[66] as a candidate for the metal atom due to the subtle and unpredictable way structural changes influence the electronic properties of the compounds[67-71]. In addition, iron forms fairly weak bonds[40] with $[2_n]$cyclophanes.

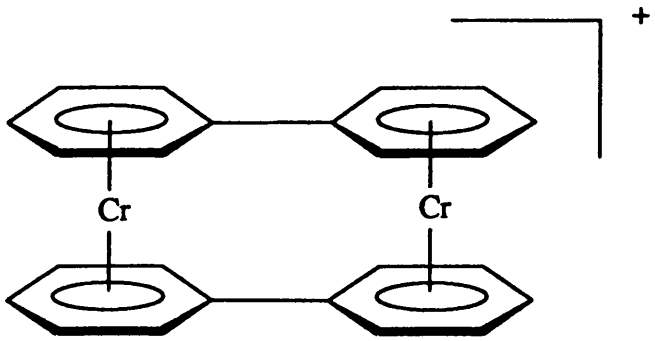

Fig. 1.15 [Bis(η^6,η^6-biphenyl)dichromium]$^+$, a class (I) mixed-valence complex.

Chromium was also rejected[66] since there was a known example[72] of a cationic compound, [bis(η^6,η^6-biphenyl)dichromium]$^+$ (Fig. 1.15), which is similar in nature to those desired, where the unpaired electron was localised on one of the metal atoms. Ruthenium was chosen since it forms strong metal-arene bonds and there were established high yield syntheses[60] for bis-arene ruthenium complexes that could readily be extended to facilitate the coordination of cyclophanes to the metal. Ruthenium complexes have been prepared for a wide range of [m.n]cyclophanes[66,73,74,76,77].

Both mono- and binuclear cyclophane-ruthenium complexes have been prepared[66,73,74,76] by the Bennett synthesis[60]. In these complexes either one or both of the cyclophane faces are capped by an "Ru(η^6-arene)" fragment. The cyclophane is introduced in the second step of the synthesis (Scheme 1.9). Trifluoroacetic acid is used as the solvato-ligand protonating agent. The synthesis is outlined in Scheme 1.10. When equivalent stoichiometric quantities of the solvate complex and the cyclophane are used the mononuclear dications are formed, but when the solvate complex is in a five-fold excess, both faces of the cyclophane are capped, and binuclear complexes result. This reaction has afforded arene-ruthenium(II) complexes of a range of [2_n]cyclophanes.

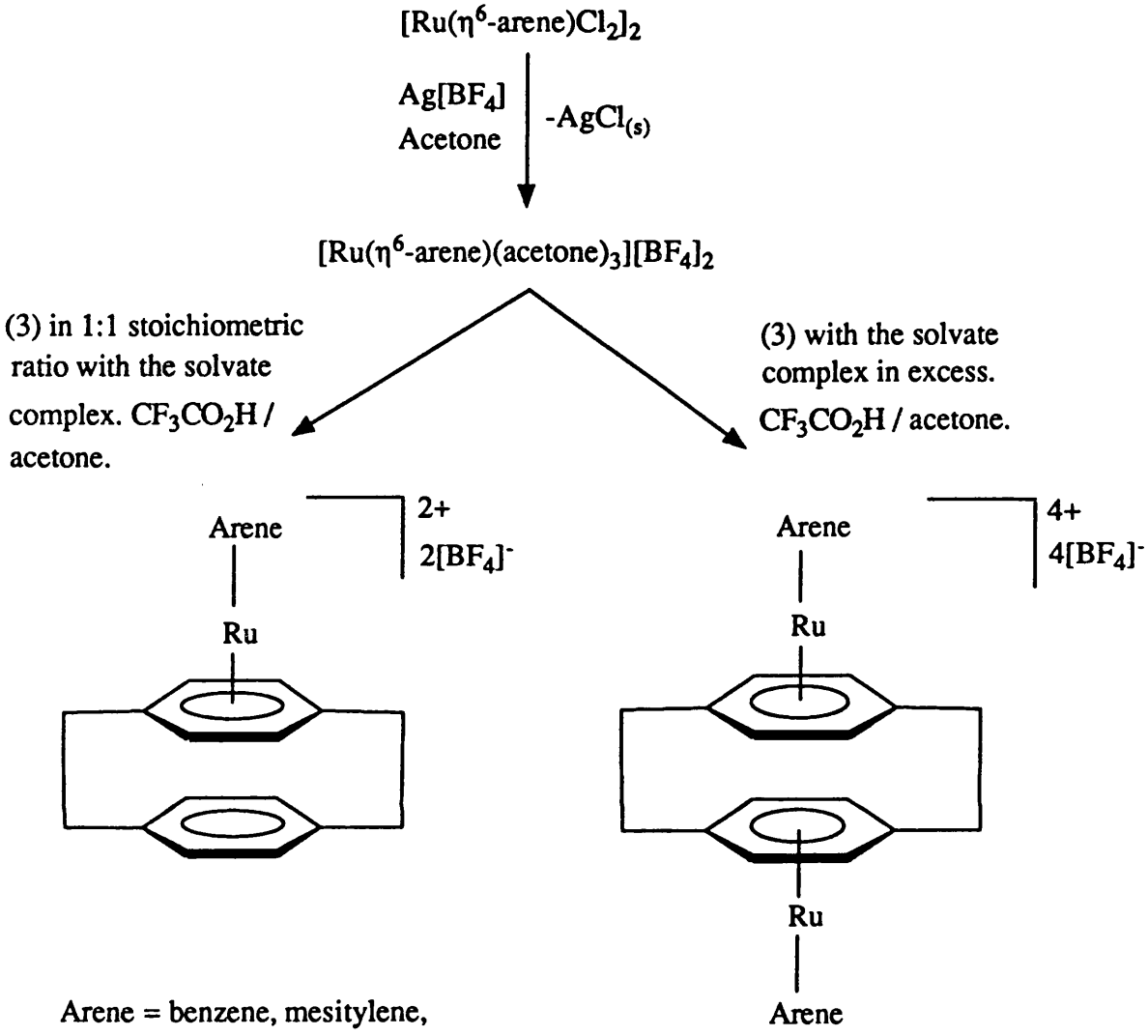

Scheme 1.10 The synthesis of mono- and binuclear arene-ruthenium [2$_2$]paracyclophane complexes.

A synthesis of bis-cyclophane ruthenium(II) complexes has also been developed[66,75] by Boekelheide and his coworkers (Scheme 1.11). Treatment of [Ru(η^6-C_6H_6)(η^6-[2$_2$]paracyclophane)][BF_4]$_2$ (11) with a reducing agent (Red-Al: sodium bis(methoxyethoxy)aluminium hydride in toluene) in THF results in the formation of the ruthenium(0) complex [Ru(η^4-C_6H_8)(η^6-[2$_2$]paracyclophane)] (12). The diene ligand of

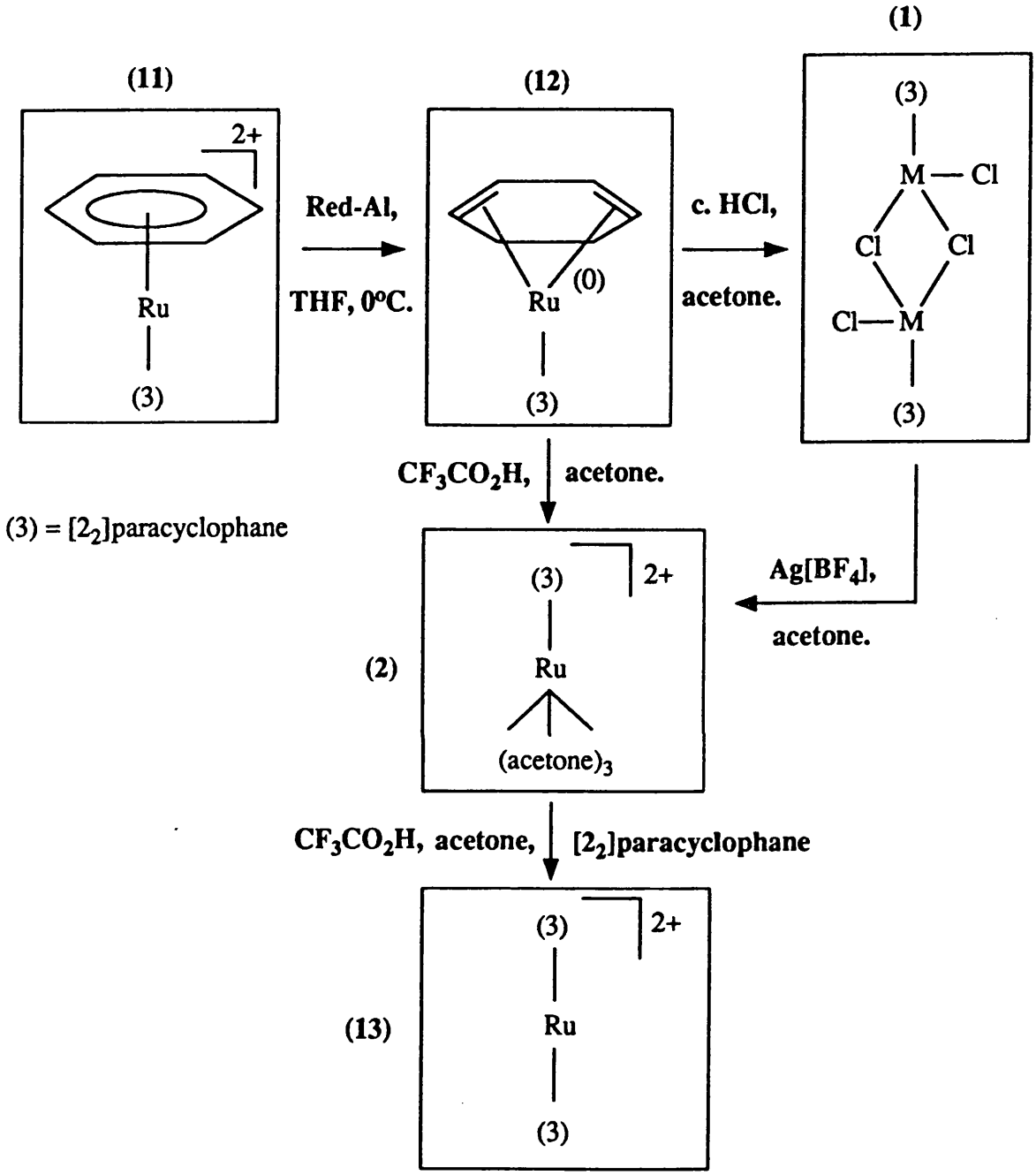

Scheme 1.11 The synthesis of $[Ru(\eta^6\text{-}[2_2]paracyclophane)_2]^{2+}$, (13).

(12) is easily removed by the addition of H^+, allowing chloride ions to fill the vacant coordination sites, and forming the dimeric compound $[Ru(\eta^6\text{-}[2_2]paracyclophane)Cl_2]_2$ (1), which is air stable. Removal of the chloride ions from (1) with silver salts in acetone solution affords the tris-solvate complex $[Ru(\eta^6\text{-}[2_2]paracyclophane)(acetone)_3][BF_4]_2$ (2).

The action of trifluoroacetic acid in acetone solution on the diene complex (12) affords the tris-solvate species (2) directly. Compound (2) may then be capped by a second $[2_2]$paracyclophane ligand to give the bis(η^6-$[2_2]$paracyclophane)ruthenium(II) compound (13). (2) may alternatively be capped by a different $[2_n]$cyclophane to give a mixed-cyclophane ruthenium(II) compound.

The air stable complex $[Ru(\eta^6\text{-}[2_2]paracyclophane)_2][BF_4]_2$ (13) has been capped[66] at each external cyclophane face with an "$Ru(\eta^6\text{-}C_6Me_6)$" fragment, resulting in the formation of the trinuclear complex (14), shown in Fig. 1.16. The capping is achieved via the Bennett method[60] using $[Ru(\eta^6\text{-}C_6Me_6)(acetone)_3]^{2+}$.

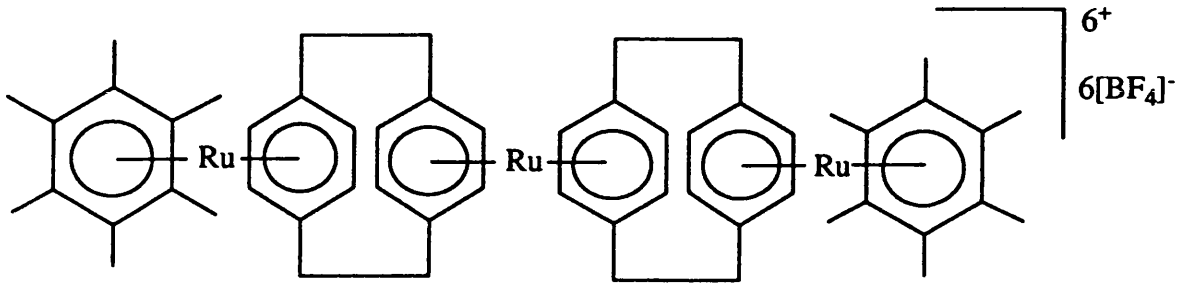

(14)

Fig. 1.16 $[(\eta^6\text{-}C_6Me_6)Ru(\eta^6,\eta^6\text{-}C_{16}H_{16})Ru(\eta^6,\eta^6\text{-}C_{16}H_{16})Ru(\eta^6\text{-}C_6Me_6)][BF_4]_6$.

The synthesis[66] of multilayered subunits containing only ruthenium and $[2_2]$paracyclophane is achieved with greater difficulty. This is due to the highly reactive nature of (2) which, on heating in acetone, self condenses to give a mixture of oligomers which are not easily separated and characterised. Nevertheless, such a compound has been

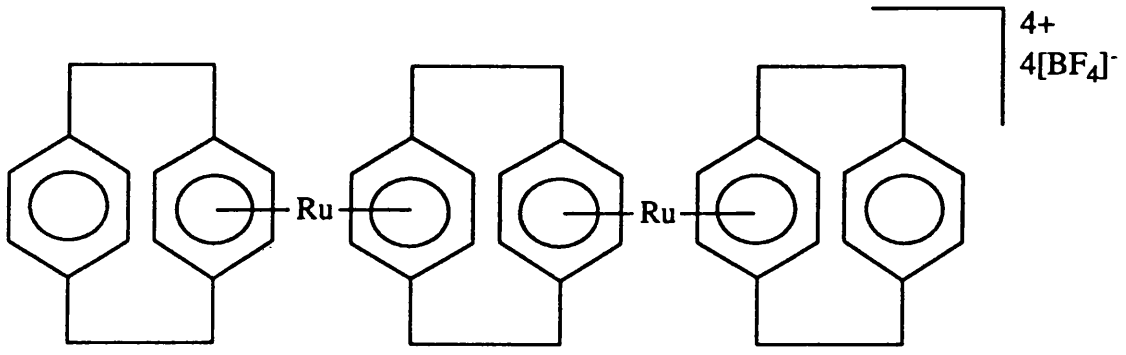

(15)

Fig. 1.17 $[(\eta^6\text{-}C_{16}H_{16})Ru(\eta^6,\eta^6\text{-}C_{16}H_{16})Ru(\eta^6\text{-}C_{16}H_{16})][BF_4]_4$.

formed by treating (13) with (2) in neat trifluoroacetic acid. An extensive work-up procedure, involving fractional crystallisation and selective precipitation, affords the compound $[(\eta^6\text{-}C_{16}H_{16})Ru(\eta^6,\eta^6\text{-}C_{16}H_{16})Ru(\eta^6\text{-}C_{16}H_{16})][BF_4]_4$ (15) (Fig. 1.17) in 12% yield.

1.3.7 The Characterisation of Cyclophane-Ruthenium Compounds.

In contrast to the iron complexes discussed earlier, most of the cyclophane-ruthenium complexes are stable as solids and in solution, and full characterisation has therefore been possible. Elemental analyses, n.m.r. spectroscopy[66,73,74] and, in a few instances, X-ray crystallography[66,77,78], have been employed in the analysis. Detailed electrochemical studies[66,73,79,80] have also been performed on a number of complexes.

To allow dicussion[73] of the ^1H n.m.r. spectra of the ruthenium [2$_2$]paracyclophane complexes the spectrum of the free ligand (3) needs to be mentioned first. The spectrum[66] exhibits singlet resonances at δ 6.47 (the eight aromatic protons) and 3.05 ppm (the eight methylenic protons of the bridges). In comparison the aromatic protons of *p*-xylene resonate at δ 7.05 ppm. The shift to lower frequency for the cyclophane aromatic protons is due to the cumulative ring current effect.

The ^1H n.m.r. spectrum of (11) exhibits[73] resonances as follows: δ 2.99-3.49 (8H, m, $C\underline{H}_2\text{-}C\underline{H}_2$); 6.08 (4H, s, coordinated cyclophane ring protons); 6.56 (6H, s, $C_6\underline{H}_6$); 7.00 ppm (4H, s, non-coordinated cyclophane ring protons). When compared with the free ligand the resonance for the protons of the coordinated ring is shifted to lower frequency by *ca.* 0.4 ppm. This shift is considered[73] to be due to rehybridisation of the ring carbon atoms, a loss of ring current, and to the direct magnetic anisotropy of the metal atom. The resonance of the unbound deck shifts to higher frequency by *ca.* 0.5 ppm. This is due to electron withdrawal from the bound deck by the metal ion, and therefore a decrease in its ring current, causing a decrease in the shielding of the non-coordinated ring. The direct magnetic anisotropy of the metal on the unbound deck is small due to the considerable distance from the metal ion. Any geometric changes between the coordinated and free ligand have only a minor effect. A full assignment of the ^{13}C n.m.r. spectrum of (11) has been published[81].

The synthesis of the symmetrical binuclear complex $[(\eta^6\text{-}C_6H_6)Ru(\eta^6,\eta^6\text{-}C_{16}H_{16})Ru(\eta^6\text{-}C_6H_6)][BF_4]_4$ has not been reported. The ^1H n.m.r. spectra of analogous binuclear complexes employing other arenes exhibit[73] one singlet

resonance between δ 6.2 and 6.6 ppm for the eight aromatic cyclophane protons. The complexes with the more heavily alkylated arenes exhibit cyclophane aromatic resonances at the lower end of this range. The cyclophane bridge protons also give rise to singlet resonances in the range δ 3.36-3.46 ppm.

The number of reported crystal structure determinations of ruthenium [2_n]cyclophane compounds is rather small. Indeed prior to this work there were no published structures of compounds containing a ruthenium(II) ion bound by [2_2]paracyclophane. The ruthenium(0) compound [Ru(η^4-*exo*-3',6'-dihydridohexamethyl-1,4-cyclohexadiene)(η^6-$C_{16}H_{16}$)], which is formed by the chemical reduction of [Ru(η^6-C_6Me_6)(η^6-$C_{16}H_{16}$)][BF_4]$_2$, has been structurally characterised[66] (Fig. 1.18). The reduction introduces hydrogen atoms in the 3'

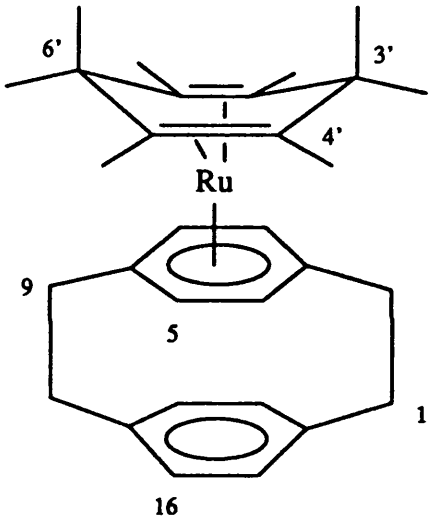

Fig. 1.18 The molecular structure of [Ru(η^4-*exo*-3',6'-$C_6H_2Me_6$)(η^6-$C_{16}H_{16}$)].

and 6' positions and the diene adopts a boat conformation. The Ru-C bonds vary greatly in length, with the longest being Ru-C(3) and Ru-C(6) at *ca.* 2.36 Å while the others are closer to the normally observed ruthenium to arene-carbon distance of *ca.* 2.14 Å. The remaining structural parameters were not published[66].

The only other published structures are those of [Ru(η^6-C_6Me_6)(η^6-4,12-Me_2-7,15-$(OMe)_2$-[2_2]metacyclophane)][BF_4]$_2$[66,78], and of [Ru(0)(η^6-C_6Me_6)(η^5-3-H-[2_2]paracyclophane)][HCl_2][66,77]. At the time of writing there are no reports of any osmium-cyclophane complexes in the chemical literature, other than those resulting from this work.

Electrochemical measurements have been made on several ruthenium-cyclophane

compounds. Bis(arene)ruthenium(II) complexes are known[57] to undergo two-electron reductions to give ruthenium(0) complexes in which one of the arenes has changed its bonding mode[58,59] from η^6 to η^4 coordination, hence retaining an 18 e^- count for the metal. For the arene-ruthenium cyclophane compounds, the ease and reversibility of reduction is predominantly influenced by the geometry of the cyclophane[66]. Cyclophanes with boat shaped decks most easily undergo the η^6 to η^4 conversion. Thus (11) ($E_{\frac{1}{2}}$ (vs SCE) = -0.50V, I_{pa}/I_{pc} = 0.81) and $[Ru(\eta^6\text{-}C_6H_6)(\eta^6\text{-}[2_4](1,2,4,5)cyclophane][BF_4]_2$ ($E_{\frac{1}{2}}$ = -0.31V, I_{pa}/I_{pc} = 0.85) are most easily and reversibly reduced. Superphane ($[2_6](1,2,3,4,5,6)$cyclophane) has rigidly held flat decks and $[Ru(\eta^6\text{-}C_6H_6)(\eta^6\text{-}[2_6](1,2,3,4,5,6)cyclophane)][BF_4]_2$ is less easily and less reversibly reduced[66,73,80] ($E_{\frac{1}{2}}$ = -0.95V, I_{pa}/I_{pc} = 0.27). The two-electron nature of the reductions was demonstrated by coulometric measurements. For some compounds[73] the cyclic voltammograms exhibited two closely spaced one-electron reductions, e.g. $[Ru(\eta^6\text{-}C_6Me_6)(\eta^6\text{-}[2_4](1,2,3,4)cyclophane)][BF_4]_2$ ($E_{\frac{1}{2}}$ = -0.82 and -0.93V).

The ease of reduction is also influenced[66] by the ability of the cyclophane to accept negative charge. When one hexamethylbenzene ligand in $[Ru(\eta^6\text{-}C_6Me_6)_2]^{2+}$ is exchanged for a more rigid $[2_3](1,3,5)$cyclophane ligand, an easier reduction is observed! The cyclophane would have a higher energy barrier to deformation for η^4 bonding than the hexamethylbenzene ligand, and therefore, the greater ease of reduction is attributed to the better electron accepting properties of the cyclophane.

Complex (13) exhibits a reversible two-electron reduction at -0.62V. The binuclear complex (15) (Fig. 1.17) exhibits two, widely spaced irreversible reduction waves ($E_{\frac{1}{2}}$ = -0.294 and -1.615V). The first of these occurs considerably more readily than that for (11) ($E_{\frac{1}{2}}$ = -0.50V). This large difference in the potentials of the two waves for (15) cannot be adequately explained solely on the basis of the coulombic effects of the two metal ions. An electronic interaction between the two ruthenium atoms in the reduced species is strongly suggested by this observation. Due to the irreversibility of the reductions no mixed-valence complex could be isolated. The trinuclear complex (14) (Fig. 1.16) exhibits[66] three reduction waves, the first two of which are largely reversible. The difference between the potentials of the three waves is less pronounced than for the trinuclear complex (15). Again no mixed-valence products were isolated.

One binuclear complex, $[Ru_2(\eta^6\text{-}C_6Me_6)_2(\eta^6,\eta^6\text{-}[2_4](1,2,4,5)cyclophane][BF_4]_4$, has been studied[79] in-depth, both electrochemically, and structurally by n.m.r. spectroscopy. This complex undergoes two reversible, two-electron reductions to give sequentially, the "ruthenium(II,0)", and ruthenium(0,0) species, both of which have been isolated (Scheme 1.12). The reduction potentials are -0.06 and -0.59V. At room

temperature the n.m.r. spectroscopic evidence points to a symmetrical molecule for the "ruthenium(II,0)" complex, indicating a Ru(I)-Ru(I) system. At lower temperatures the evidence suggests a Ru(0)-Ru(II) model being appropriate. The hexamethylbenzene ligand remains η^6-coordinated throughout, with the cyclophane undergoing conformational changes.

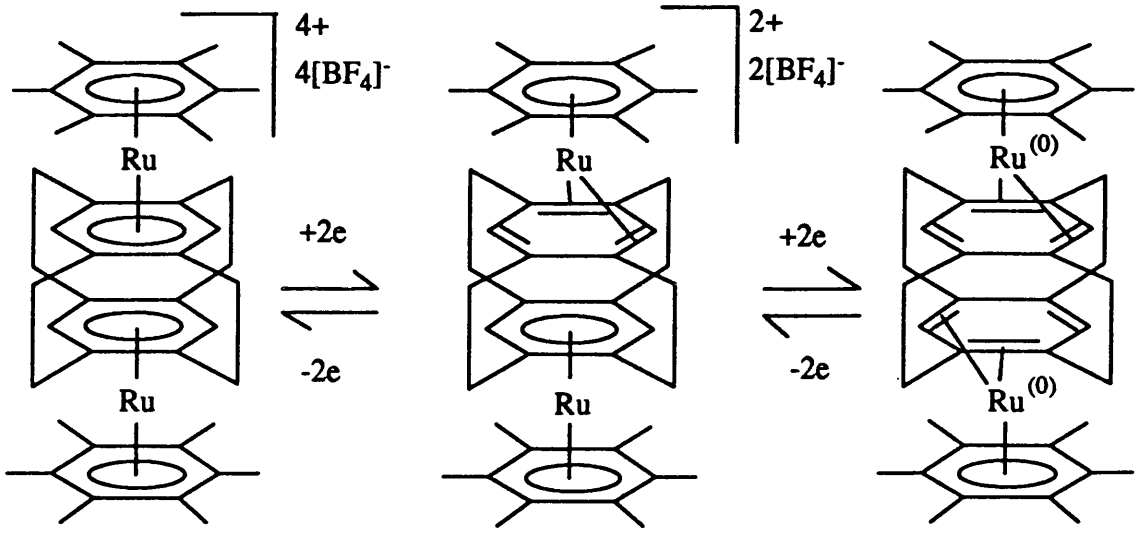

Scheme 1.12 The reversible electrochemical behaviour of $[Ru_2(\eta^6\text{-}C_6Me_6)_2(\eta^6,\eta^6\text{-}[2_4](1,2,4,5)cyclophane)]$.

1.4 A GENERAL SURVEY OF THE REACTIVITY OF THE DIMERIC COMPOUNDS $[M(\eta^6\text{-ARENE})Cl_2]_2$ {M=Ru(II),Os(II)}.

The previous section considered arene transition metal chemistry with particular relevance to cyclophane complexes. In this section the aim is to provide a brief general background of ruthenium and osmium arene chemistry. This area of chemistry is now fairly extensive and has been the subject of a number of reviews[54,55,82-84], most recently by Le Bozec, Touchard, and Dixneuf[85]. In addition, a broad overview of the work published is provided by an annual review in "Organometallic Chemistry". Therefore the topics covered will be limited to those of direct relevance to the work presented in this thesis. More detailed discussion will be presented at the appropriate time.

A wide range of ruthenium and osmium complexes are known in which the π-accepting arenes stabilise the lower oxidation states. The M(II) (d^6) (M=Ru,Os) compounds are of direct interest here, although many M(0) (d^8) compounds are also known. The starting materials used as an entry into this field of chemistry are the dimeric complexes $[M(\eta^6\text{-arene})Cl_2)]_2$. In the complexes under consideration the arene can be considered as a terdentate ligand occupying three adjacent coordination sites about the octahedral metal centre.

The chemistry of the $[M(\eta^6\text{-arene})Cl_2)]_2$ complexes and their derivatives can be divided into four main sections:

(i) Monomeric complexes which are neutral, mono- or dicationic, and are formed by reaction of $[M(\eta^6\text{-arene})Cl_2)]_2$ with Lewis bases;

(ii) Reactions to give binuclear halide bridged complexes;

(iii) Reactions with alkoxides, hydroxide and sodium carbonate to give binuclear and tetranuclear cationic compounds and;

(iv) Reactions with nucleophiles.

1.4.1 Monomeric Complexes of Ruthenium(II) and Osmium(II).

Neutral complexes of the type $[M(\eta^6\text{-arene})Cl_2L]$ (Fig. 1.19) are formed by reaction[64,86-89] of neutral Lewis bases, L (L = py, PR_3, AsR_3, $P(OR)_3$, etc.), with $[M(\eta^6\text{-arene})Cl_2)]_2$ in non-polar solvents at room temperature. In these reactions the chloride bridges of the dimer are broken and the ligand, L, inserts into the vacant

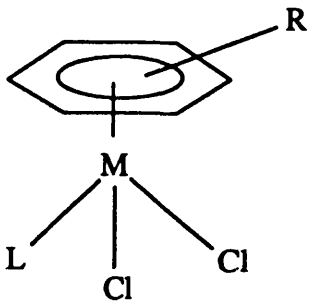

Fig. 1.19 Neutral half-sandwich complexes, $[M(\eta\text{-}^6\text{arene})Cl_2L]$.

coordination site. The monodentate nature of these complexes has been confirmed by structural analyses of a number of examples[86,90].

Reaction of Lewis bases with $[M(\eta^6\text{-arene})Cl_2)]_2$ in polar solvents gives monocationic complexes[63,88], $[M(\eta^6\text{-arene})ClL_2]^+$ (Fig. 1.20) which can be isolated by

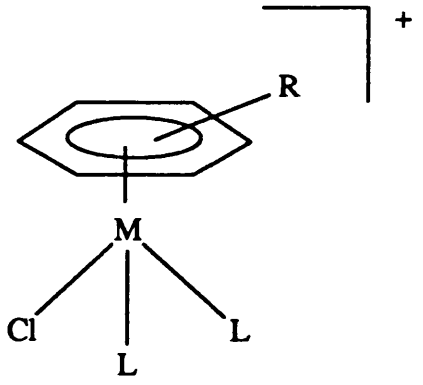

Fig. 1.20 Monocationic half-sandwich complexes, $[M(\eta^6\text{-arene})Cl_2L]^+$.

addition of an appropriate anion to the reaction solution. The chloride bridges of the dimeric starting material are cleaved and one of the chloride ions is displaced. Two molecules of the incoming ligand coordinate to the metal ion. Treatment[91,92] of $[M(\eta^6\text{-arene})Cl_2)]_2$ with neutral bidentate ligands L-L (L-L = 2,2'-bipyridyl, 1,10-phenanthroline, etc.) under similar conditions, yields the monocations $[M(\eta^6\text{-arene})Cl(L\text{-}L)]^+$.

When the complexes $[M(\eta^6\text{-arene})Cl(L\text{-}L)]^+$ are treated[91] with tertiary phosphines the dicationic products $[M(\eta^6\text{-arene})PR_3(L\text{-}L)]^{2+}$ are formed (Fig. 1.21). Dicationic complexes, $[M(\eta^6\text{-arene})L_3]^{2+}$, where three identical ligands are coordinated to the metal are also known[93,94].

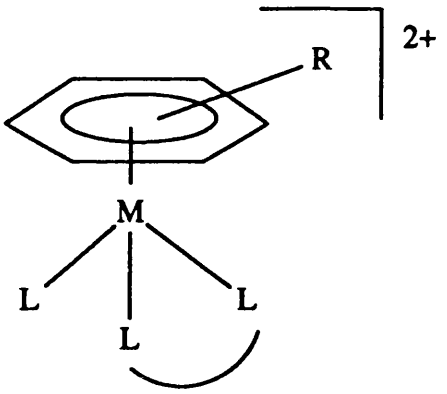

Fig. 1.21 Dicationic half-sandwich complexes containing one bidentate and one monodentate ligand, $[M(\eta^6\text{-arene})L(L\text{-}L)]^{2+}$.

The reactions[95,96] of $[M(\eta^6\text{-arene})Cl_2]_2$ with bidentate mono-anionic ligands gives the neutral $[M(\eta^6\text{-arene})Cl(L\text{-}L)]$ (L-L = acac$^-$, O_2CR^-, etc.) compounds. The acetate and trifluoroacetate compounds have proved useful precursors to complexes which are not available by direct reaction of the dimer[95,96].

The ^1H and ^{13}C solution n.m.r. spectroscopic studies on these compounds suggest a rapid rotation of the arene ligand with respect to the other ligands. Recently however in a related area there has been strong evidence put forward[97] for slowed rotation and even a static conformation for a severely sterically crowded chromiumtricarbonyl complex, $[Cr(\eta^6\text{-}C_6Et_5COCH_3)(CO)_3]$, at low temperatures (173 K).

1.4.2 Binuclear Halide-Bridged Complexes of Ruthenium(II) and Osmium(II).

Binuclear triply halide-bridged cations, $[(\eta^6\text{-arene})MCl_3M(\eta^6\text{-arene})][X]$ (Fig. 1.22), are formed[98,99] on stirring $[M(\eta^6\text{-arene})Cl_2)]_2$ with a suitable anion ([X] = $[PF_6]^-$ or $[BPh_4]^-$) in methanol. Such cations are also formed when an equimolar solution of $[M(\eta^6\text{-arene})Cl_2(py)]$ and $[M(\eta^6\text{-arene})Cl(py)_2]^+$ in methanol, is treated[63,100] with $H[BF_4]$. The structure determination[101] of the representative compound $[Ru_2(\eta^6\text{-}p\text{-cymene})_2Cl_3][BPh_4]$.MeOH has confirmed the proposed geometry.

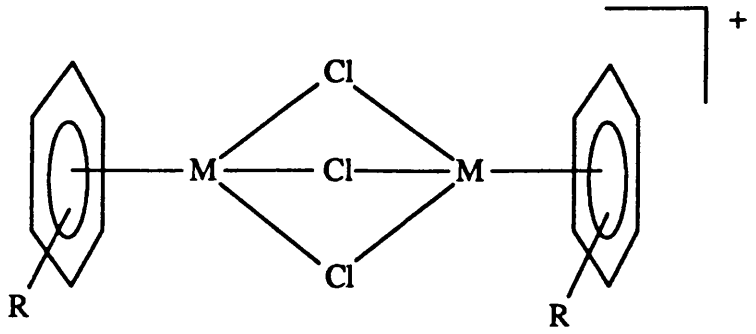

Fig. 1.22 Binuclear triply chloro-bridged complexes, $[(\eta^6\text{-arene})RuCl_3Ru(\eta^6\text{-arene})]^+$.

1.4.3 Reactions with Alkoxides, Hydroxide and Sodium Carbonate.

Reaction[102] of $[M(\eta^6\text{-arene})Cl_2)]_2$ with alkoxide ions $[OR]^-$ (R = Me, Et, Ph) in alcoholic solution results in the formation of binuclear, triply alkoxide-bridged, monocations $[(\eta^6\text{-arene})M(OR)_3M(\eta^6\text{-arene})]^+$ (Fig. 1.23). The binuclear nature of these

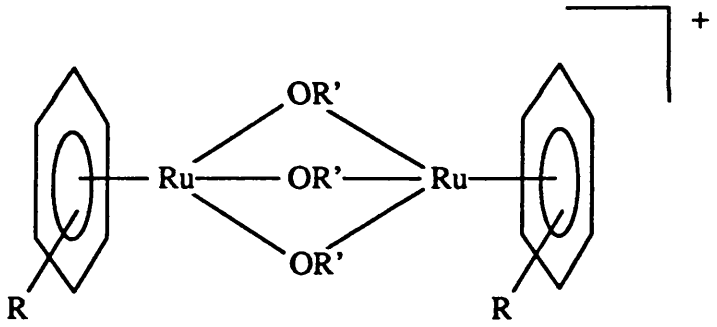

Fig. 1.23 Binuclear triply hydroxide- or alkoxide-bridged complexes, $[(\eta^6\text{-arene})Ru(OR)_3Ru(\eta^6\text{-arene})]^+$.

complexes has been confirmed by a structural analysis[103] of the representative compound $[Ru_2(\eta^6\text{-}C_6H_6)_2(OMe)_3][BPh_4]$. The corresponding reaction[98,102] with aqueous hydroxide ion or sodium carbonate yields analogous triply hydroxide-bridged binuclear monocations if the arene is alkyl-substituted. A crystallographic analysis[104] of the complex $[Ru_2(\eta^6\text{-}1,3,5\text{-}C_6H_3Me_3)_2(OH)_3]Cl.3H_2O$ verified the proposed structure.

When the arene is benzene, novel tetranuclear complexes are formed, whose structures have been confirmed[105,106] by single crystal X-ray analysis. Reaction of $[M(\eta^6\text{-}C_6H_6)Cl_2)]_2$ with aqueous sodium carbonate in the presence of excess sulphate ion yields the complex $[\{Ru(\eta^6\text{-}C_6H_6)(OH)\}_4][SO_4]_2.12H_2O$ (Fig. 1.24), which has a distorted

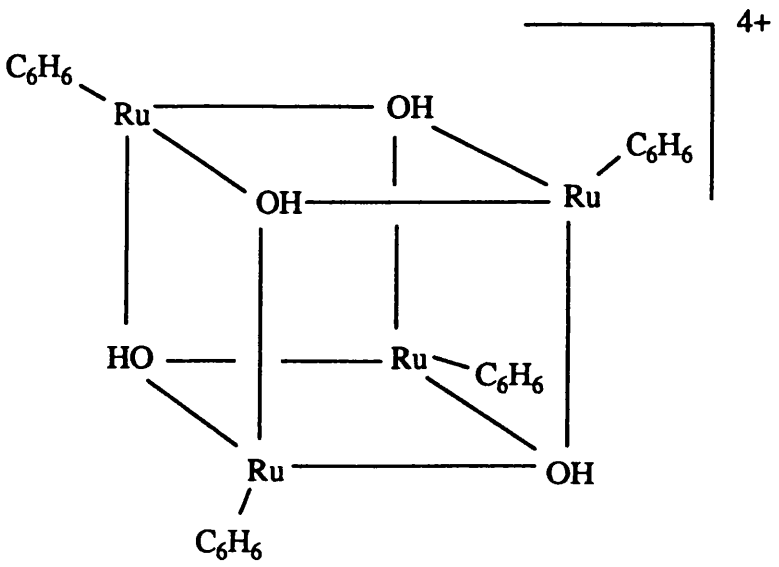

Fig. 1.24 The cubane cation $[\{(\eta^6\text{-}C_6H_6)Ru(OH)\}_4]^{4+}$.

cubane structure. Reaction[104] of $[M(\eta^6\text{-}C_6H_6)Cl_2)]_2$ with aqueous hydroxide ion or sodium carbonate yields $[(\eta^6\text{-}C_6H_6)(OH)Ru(\mu\text{-}OH)_2Ru(OH_2)(\eta^6\text{-}C_6H_6)]^+$ which, on recrystallisation from acetone, gives an alternative tetranuclear complex $[M_4(\eta^6\text{-}C_6H_6)_4(\mu_2\text{-}OH)_4(\mu_4\text{-}O)][BPh_4]_2.2Me_2CO$ (Fig. 1.25), containing a tetrahedrally coordinated O^{2-} ion.

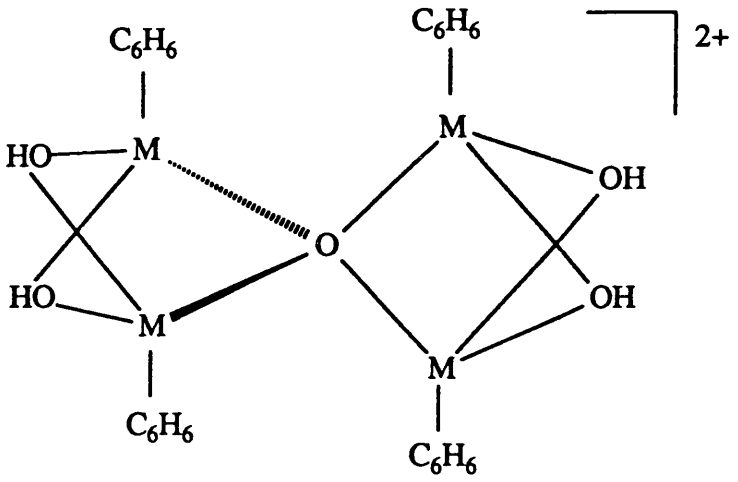

Fig. 1.25 The tetranuclear cation $[M_4(\eta^6\text{-}C_6H_6)(\mu_2\text{-}OH)_4(\mu_4\text{-}O)]^{2+}$.

1.4.4 Reactions with Nucleophiles.

The aromatic rings in the complexes described above are frequently inert towards electrophilic attack, but are susceptible to attack by nucleophiles (Y^- = H^-, CN^-, OH^-, etc.)[87,89,91,107]. The nucleophile has been shown to add *exo* to the aromatic ring giving η^5-cyclohexadienyl complexes (Fig. 1.26). For the neutral and monocationic complexes

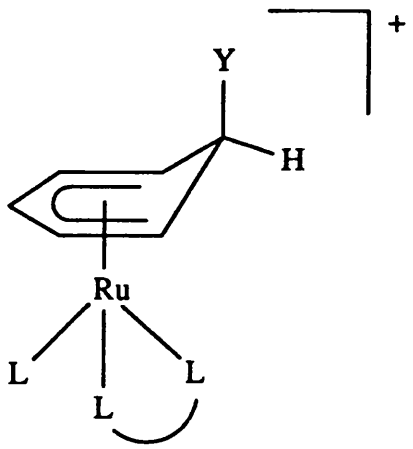

Fig. 1.26 [Ru(η^5-*exo*-Y-cyclohexadienyl)L(L-L)]$^+$ complexes.

these reactions have been monitored by n.m.r. spectroscopy, but the products were too unstable to be isolated[87,89]. However, for dications containing only good π-acceptor ligands (e.g. PR_3, bipy, phen, etc) the possibility of the reaction following a pathway other than the desired one, (e.g. the facile decomposition of unstable metal hydrides), is minimised, and the arene is made more prone to nucleophillic attack. The π-acceptor ligands help to stabilise the products which can be isolated as pale-coloured powders[91,107].

CHAPTER 2.

THE REACTIONS OF [M(η^6-[2$_2$]PARACYCLOPHANE)Cl$_2$]$_2$ (M=Ru,Os) COMPOUNDS WITH LEWIS BASES.

2.1 INTRODUCTION.

During studies on a range of ruthenium [2_2]paracyclophane complexes[66] Boekelheide *et al* prepared the complex [Ru(η^6-[2_2]paracyclophane)Cl_2]$_2$ (1). Complex (1) was used subsequently only in the rather limited capacity as the precursor to the complex [Ru(η^6-[2_2]paracyclophane)(acetone)$_3$][BF_4]$_2$ (2), which was employed in the cyclophane capping reactions discussed in the previous chapter. Although (1) was not prepared by the classical method of dehydrogenating a 1,3- or 1,4- cyclohexadiene in the presence of $RuCl_3$, the complex is clearly closely related to the [Ru(η^6-arene)Cl_2]$_2$ compounds which have previously been extensively studied[54,55,82-84]. The unusual properties of [2_2]paracyclophane meant this new compound warranted further investigation. In this chapter the reactions of (1) with a range of Lewis bases in polar and non-polar solvents are discussed. The chemistry has also been extended to osmium via the previously unknown complex [Os(η^6-[2_2]paracyclophane)Cl_2]$_2$ (16).

2.2 RESULTS AND DISCUSSION.

2.2.1 The Synthesis and Characterisation of the Compounds [M(η^6-[2_2]Paracyclophane)Cl_2]$_2$ (M=Ru,Os).

(i) [Ru(η^6-[2_2]paracyclophane)Cl_2]$_2$ (1).

The compound [Ru(η^6-[2_2]paracyclophane)Cl_2]$_2$ (1) was prepared by Boekelheide's method[66] which is described in detail in the experimental section and illustrated in Scheme 1.11. The yields obtained in this synthesis (*ca.* 35-50%) are comparable to those reported by Boekelheide *et al*[66]. Extreme care was taken to dry the THF used as the solvent in the reduction step, and to maintain an oxygen and moisture free environment. The extraction of the Ru(0) intermediate, the removal of the solvent, and the subsequent treatment with HCl in acetone were carried out as rapidly as possible to minimise decomposition, which involves loss of the cyclophane ligand. Even when all of these precautions were rigorously employed the product (1) was often contaminated with the free cyclophane ligand. This was sublimed off under vacuum to give pure starting material for subsequent reactions.

Complex (1) exhibits two ν(Ru-Cl) stretching bands in the infrared spectrum at 295 and 254 cm^{-1} (Section 2.3.3), similar to those reported for other [Ru(η^6-arene)Cl_2]$_2$

complexes[61,87,108]. In the ^{1}H n.m.r. spectrum (Table 2.1), recorded in d_6-DMSO, four signals are observed: δ 5.19 (s, coordinated $C_6\underline{H}_4$), 6.84 (s, non-coordinated $C_6\underline{H}_4$), and the two multiplets of an AA'XX' coupling pattern (see Section 2.2.2) at 2.75 and 3.13 ppm (-$C\underline{H}_2C\underline{H}_2$-), each comprising six well resolved lines. These figures correspond to those observed by Boekelheide *et al*[66], although the signals arising from the methylenic protons were reported simply as "multiplets". In common with other [Ru(η^6-arene)Cl$_2$]$_2$ complexes it is likely that the dimer is cleaved[87,89,108] by dissolving it in a strongly coordinating solvent such as d_6-DMSO, and that the observed species in solution is actually [Ru(η^6-$C_{16}H_{16}$)Cl$_2$(d_6-DMSO)]. ^{13}C-{^{1}H} n.m.r. data were not reported by Boekelheide *et al* and are presented here (Table 2.2). That spectrum, recorded in

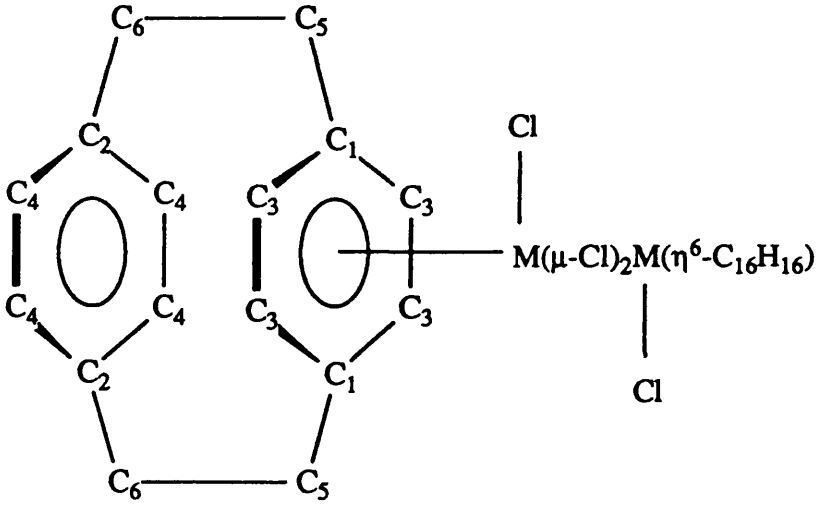

Fig. 2.1 The carbon atom numbering scheme for the ^{13}C-{^{1}H} n.m.r. spectra of (1), (M=Ru) and (16), (M=Os).

d_6-DMSO, exhibits six singlet resonances, which are assigned to the unique carbon atoms C_1-C_6 (Fig. 2.1) as follows: δ C_1:121.7; C_2:139.3; C_3:83.4; C_4:133.2; C_5:31.3; C_6:32.8$_6$:32.8 ppm. Compared with the spectrum of the free ligand, the resonances due to the aromatic carbon atoms of the non-coordinated ring (C_2 and C_4) move to slightly higher frequency when the cyclophane coordinates, while those of the coordinated deck (C_1 and C_3) show a large shift to lower frequency. This large shift to lower frequency on complexation of an arene to a metal ion is frequently observed[63,91,93,95,99,100,102,103,109]. The resonances of the aliphatic carbon atoms (C_5 and C_6) are shifted *ca.* 2 ppm to lower frequency and appear *ca.* 1.5 ppm apart.

(ii) [Os(η^6-[2$_2$]paracyclophane)Cl$_2$]$_2$ (16).

The synthetic method for [Os(η^6-[2$_2$]paracyclophane)Cl$_2$]$_2$ (16) was based on that for (1)[66], but fortunately proved less tedious and, surprisingly, gave higher yields than for the ruthenium analogue. The reverse observation is more frequently made[61,63,89]. The synthesis employs [Os(η^6-C$_6$H$_6$)(η^6-[2$_2$]paracyclophane)][BF$_4$]$_2$ (17), the preparation and characterisation of which is more appropriately discussed in Chapter 4.

In the first stage of the synthesis, complex (17) is reduced using the same procedure as for the ruthenium analogue (11). However, after water is added to destroy the excess reducing agent, the sticky black residue which forms, first coagulates, and then falls to the bottom of the reaction vessel, leaving a clear yellow solution of [Os(0)(η^4-C$_6$H$_8$)(η^6-C$_{16}$H$_{16}$)]. The yellow solution is then filtered off and transferred to a clean Schlenk tube, without the need for the tedious extraction procedure required for (1). The solution is pumped to dryness and the resulting yellow solid is treated with a solution of *conc.* HCl in acetone. The tan coloured product (16) is readily precipitated. Typical yields of (16) were *ca.* 75%, which is considerably greater than those obtained for (1), while contamination with the free cyclophane ligand was rather less severe.

In the infrared spectrum two ν(Os-Cl) bands are observed at 313 and 263 cm^{-1} (Section 2.3.3). The ^{1}H n.m.r. spectrum of (16), recorded in d_6-DMSO, exhibits singlet resonances at δ 5.49 and 6.86 ppm, arising from the protons of the coordinated and noncoordinated aromatic rings respectively, and an AA'XX' coupling pattern with two six-line multiplets at δ 2.70 and 3.17 ppm (Table 2.1). Thus the spectrum of (16) mirrors that of the ruthenium analogue (1), with the only major difference being that the signal due to the coordinated ring protons appears 0.3 ppm to higher frequency in the osmium complex. This chemical shift difference is comparable in magnitude to that observed for the benzene proton resonances in the complexes [M(η^6-C$_6$H$_6$)Cl$_2$]$_2$ (M=Ru: δ 5.98; M=Os: 6.15 ppm). As discussed above for complex (1), it is probable that the species actually observed in solution is [Os(η^6-C$_{16}$H$_{16}$)Cl$_2$(d_6-DMSO)]. The ^{13}C-{^{1}H} n.m.r. spectrum, recorded in d_6-DMSO (Table 2.2), is closely similar to that recorded for the ruthenium analogue. The only noteworthy difference is the additional shift to lower frequencies of the resonances associated with the metal-coordinated carbon atoms. Once again similar observations have been made for the complexes [M(η^6-C$_6$H$_6$)Cl$_2$]$_2$ (Table 2.2).

2.2.2 The reactions of $[M(\eta^6\text{-}[2_2]Paracyclophane)Cl_2]_2$ (M=Ru,Os) with Various Lewis Bases in Non-Polar Solvents.

(i) The reaction of (1) with PPh_3 in toluene.

Complex (1) was stirred in toluene with an excess of PPh_3 at room temperature. The reaction mixture first became yellow and then an orange powder was deposited. The orange powder was isolated by filtration. Microanalytical data (Table 2.3) closely fitted that expected for $[Ru(\eta^6\text{-}C_{16}H_{16})Cl_2(PPh_3)]$ (18) (Fig. 2.2). In the FAB mass spectrum the molecular ion was observed at 642 mass units, as would be predicted for the given formulation based on the isotopes ^{102}Ru and ^{35}Cl. A computer simulation of the isotopic pattern matched that observed experimentally. Fragmentation peaks were observed at 607 and 572 mass units, and correspond to the successive loss of the two chloride ligands from $[Ru(\eta^6\text{-}C_{16}H_{16})Cl_2(PPh_3)]^+$.

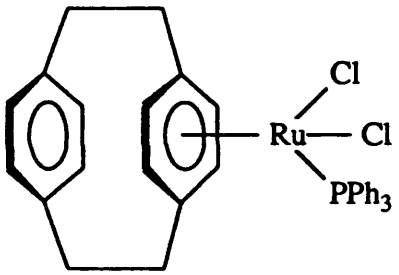

Fig. 2.2 $[Ru(\eta^6\text{-}C_{16}H_{16})Cl_2(PPh_3)]$ (18).

The infrared spectrum exhibits two terminal ν(Ru-Cl) stretching bands at 281 and 303 cm^{-1}, together with bands characteristic of coordinated triphenylphosphine at 500, 513, 529, 695, 722, 733, 744 and 754 cm^{-1} (Section 2.3.4).

The ^1H n.m.r. spectrum, recorded in $CDCl_3$ (Fig. 2.3, Table 2.4), exhibits four resonances due to the coordinated cyclophane ligand: a singlet resonance at δ 6.69 (4H) arising from the non-coordinated aromatic ring protons, a doublet at δ 4.70 (4H, $^3J_{P\text{-}H}$ = 1.1 Hz), due to the coordinated aromatic ring protons, and two six-line multiplets at δ 2.31 and 3.01 ppm (each 4H) arising from the methylenic protons. The phenyl protons of the tertiary phosphine ligand give rise to two multiplets at δ 7.32 (9H) and 7.54 (6H) ppm. Small (*ca.* 1 Hz) three-bond couplings between the protons of coordinated aromatic ligands and the phosphorus-31 nuclei of coordinated tertiary phosphines has been observed previously[88]. Integration of the spectrum supports the proposed 1:1 ratio of

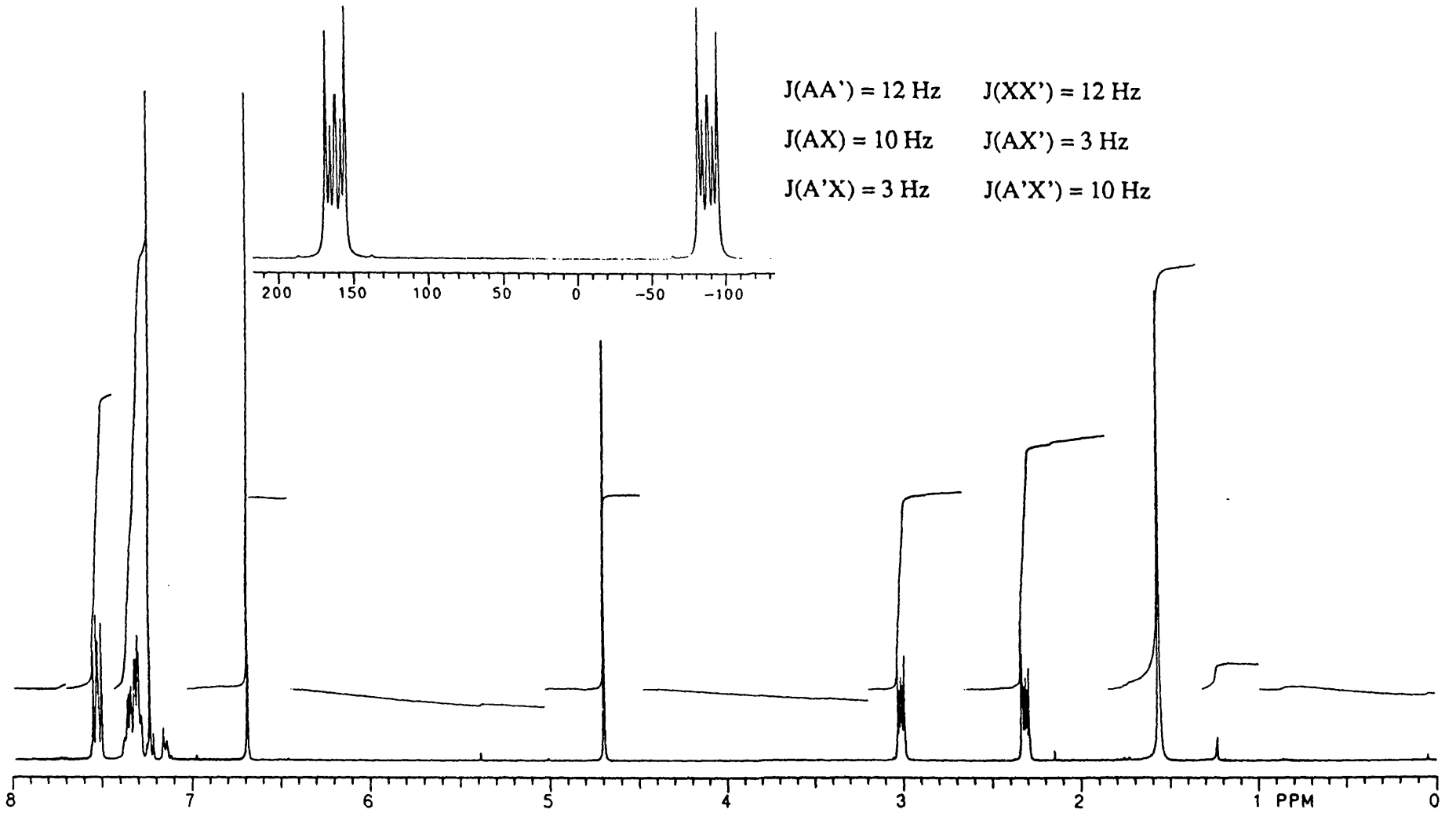

Fig. 2.3 The ^1H n.m.r. spectrum of $[Ru(\eta^6\text{-}C_{16}H_{16})Cl_2(PPh_3)]$ (18) at 298 K, recorded in $CDCl_3$.

The inset shows the computer simulated AA'XX' coupling pattern and derived coupling constants for the $\text{-}CH_2CH_2\text{-}$ resonances.

cyclophane:triphenylphosphine ligands. A computer aided spin simulation of the multiplet resonances arising from the $-CH_2CH_2-$ protons of the cyclophane has confirmed the coupling pattern as being of the AA'XX' type (Fig. 2.3). The pattern is observed for two reasons. Firstly, because of the chemical inequivalence of the protons closer to the metal atom (H_A and $H_{A'}$, Fig. 2.4) compared with those closer to the non-coordinated deck (H_X and $H_{X'}$), and secondly, due to the torsion in the bridging functions. The precise appearance of the coupling pattern is governed by the magnitude of the chemical shift difference between the two resonances, and by the torsion angle. The simulated coupling

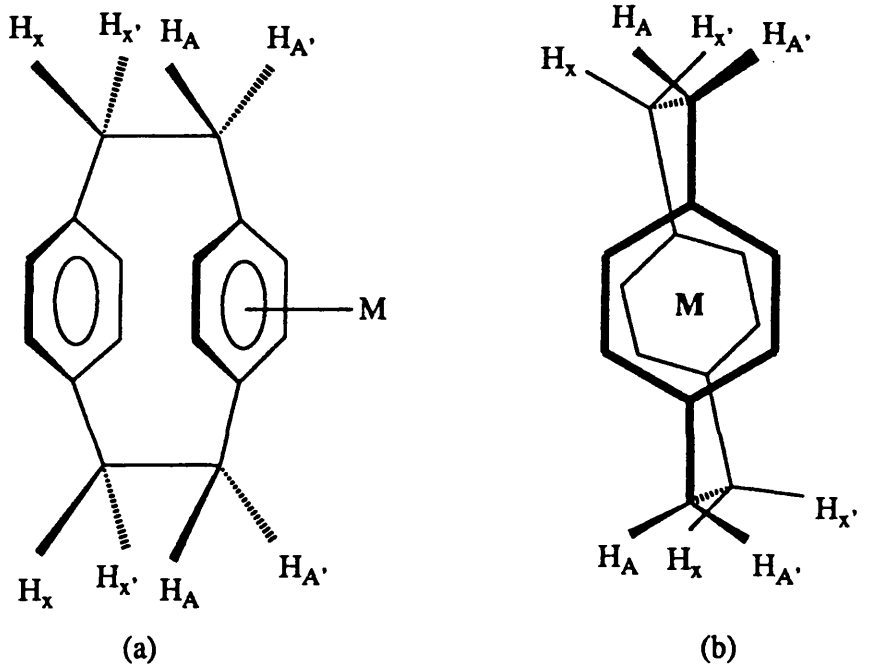

Fig. 2.4 (a) Chemical inequivalence gives rise to an AA'XX' coupling pattern for the methylenic protons in the ^1H n.m.r. spectrum. The twist in (b) modifies the coupling constants.

pattern and derived coupling constants are presented in the inset to Fig. 2.3. These resonances had previously been reported[46,66] only as "multiplets", at a mean chemical shift, which is a considerable oversimplification, and belies the true complexity of the factors governing their appearance.

The $^{31}P-\{^1H\}$ n.m.r. spectrum exhibits a singlet resonance at δ 37.3 ppm arising from the single phosphorus atom of the PPh_3 ligand (Table 2.10). A comparable chemical shift, δ 31.6 ppm, was reported for the resonance observed in the $^{31}P-\{^1H\}$ n.m.r. spectrum of $[Ru_2(\eta^6-C_6H_6)_2(\mu-Cl)_2(PPh_3)_2][PF_6]_2$[88].

The structure of (18) has been unequivocally confirmed by a single crystal X-ray diffraction experiment. The crystal used for the experiment was obtained by the slow

evaporation of a chloroform solution of the complex. In the crystal lattice there is one molecule of chloroform per molecule of the metal complex, but there are no short contacts between them. A thermal ellipsoid plot of the metal complex and some important bond lengths and bond angles are presented in Fig. 2.5. Tables of crystal data, fractional coordinates, bond lengths, and bond angles (Tables 2.11-2.14 respectively), and details of the data collection and structure refinement (Sections 2.3.5 and 2.3.6) are given in the experimental section.

The geometry at the metal ion is that of a distorted tetrahedron, with the cyclophane and the other ligands adopting a "piano-stool" configuration. The arene adopts a staggered conformation with respect to the three other ligands (Fig. 2.6). It is therefore, in general terms, similar to the structures of the complexes $[Ru(\eta^6\text{-}p\text{-cymene})Cl_2(PMePh_2)]$ and $[Ru(\eta^6\text{-}C_6H_6)Cl_2(PMePh_2)]$[86]. The L-Ru-L (L=Cl1, Cl2, P1) angles are all close to 90°, and are typical for structures of this type[24,86,95]. The C-P-C angles about the phosphorus atom fall in the range 101-106°, while the Ru-P-C angles are in the range 108-122°. Thus the geometry at the phosphorus atom is distorted from being an ideal tetrahedron by the phenyl rings being forced away from the metal centre. Reported structures also exhibit this distortion[110,111]. The phenyl rings of the PPh_3 ligand show no significant distortions from planarity. The Ru-Cl distances are 2.383(2) and 2.392(2) Å, and are therefore slightly shorter than those typically observed, which lie in the range 2.394-2.415 Å[62,86,95,109,111-115]. The Ru-P bond length of 2.292(2) Å is typical among similar reported distances, which fall in the range 2.261-2.353 Å[86,110-112,114,116,117].

A notable feature of the structure of the cyclophane complex is the variation in Ru-C bond lengths. In the case of (η^6-arene)ruthenium(II) compounds the metal-carbon distances typically fall in the narrow range 2.14-2.21 Å[86,95,96,101,103,104,106], while in this complex the Ru-C distances fall in the range 2.13-2.38(1) Å. This large variation in M-C distances has been observed previously in the structures of the complexes (4)[24] and $[Ru(\eta^4\text{-}exo\text{-}3',6'\text{-}C_6H_2Me_6)(\eta^6\text{-}C_{16}H_{16})]$[66]. This feature arises because of the non-planarity of the aromatic decks of the cyclophane ligand. Thus the bonds from the ruthenium ion to the bridgehead carbon atoms of the cyclophane (Ru1-C1 and Ru1-C4) are significantly longer than those to the other four atoms of the aromatic ring. There is another distortion present in the molecule whereby the Ru-C bonds *trans* to the phosphorus atom are elongated relative to those which are *trans* to the chloride ions. For example Ru1-C4(*trans* to P)=2.38(1) Å, while Ru1-C1(*trans* to Cl)=2.30(1) Å; and Ru1-C5(*trans* to P)=2.28(1) Å, while Ru1-C2,3,6(*trans* to Cl) *ca.* 2.16(1) Å. A similar observation was made for the complexes $[Ru(\eta^6\text{-}p\text{-cymene})Cl_2(PMePh_2)]$ and $[Ru(\eta^6\text{-}C_6H_6)Cl_2(PMePh_2)]$[86], where there was a significant lengthening of the two Ru-C

Lengths, Å.	
Ru-Cl1	2.383(2)
Ru-Cl2	2.392(2)
Ru-P	2.292(2)
Ru-C1	2.297(6)
Ru-C4	2.380(6)
Ru-C2,3,6	*av.* 2.160(6)
Ru-C5	2.277(6)
Inter-ring sep.	2.99
Angles °	
Cl1-Ru-Cl2	89.0(1)
Cl1-Ru-P	87.8(1)
Cl2-Ru-P	98.1(1)
Torsion	10.8, 10.1

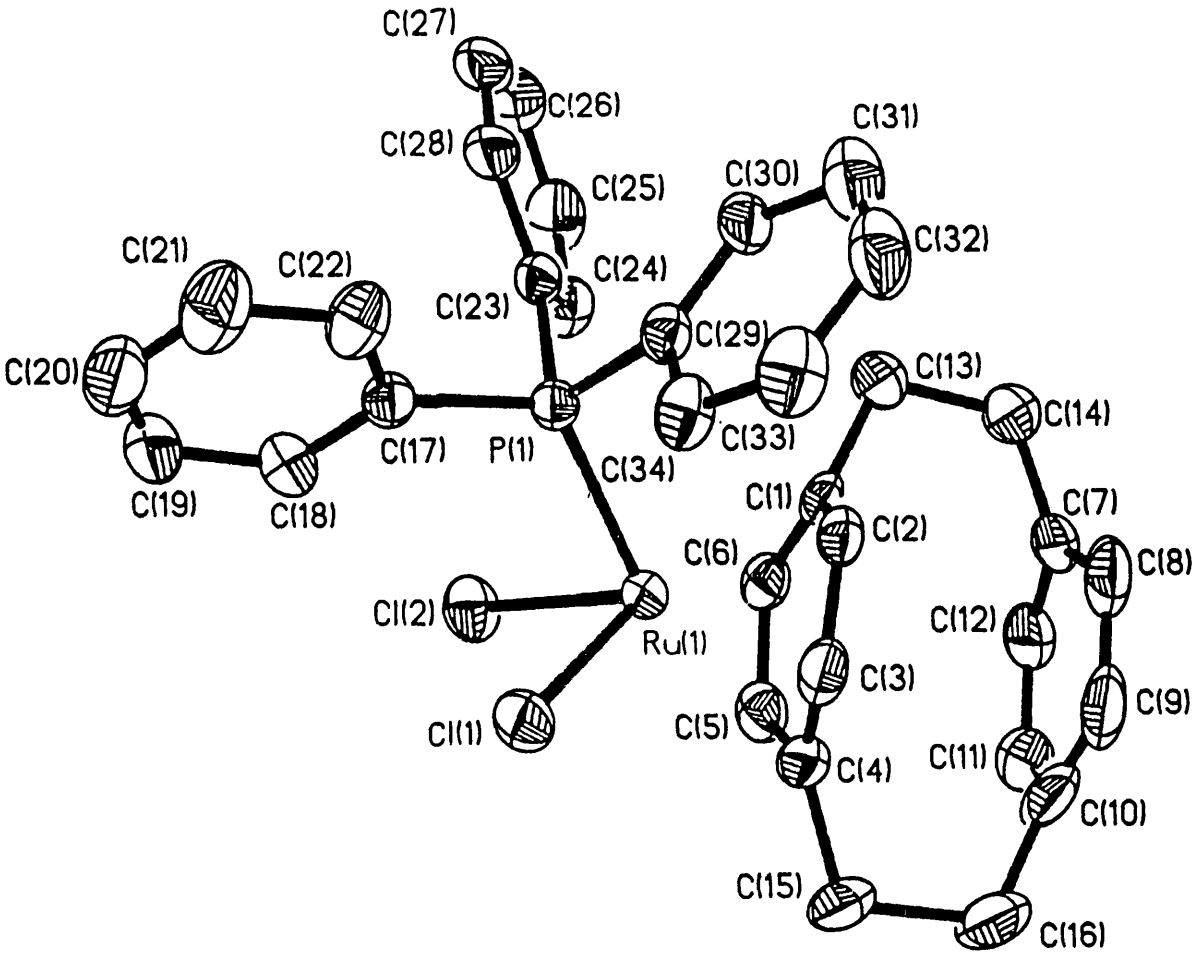

Fig. 2.5 A themal ellipsoid plot of $[Ru(\eta^6\text{-}C_{16}H_{16})Cl_2(PPh_3)]$ (18), with some important structural parameters.

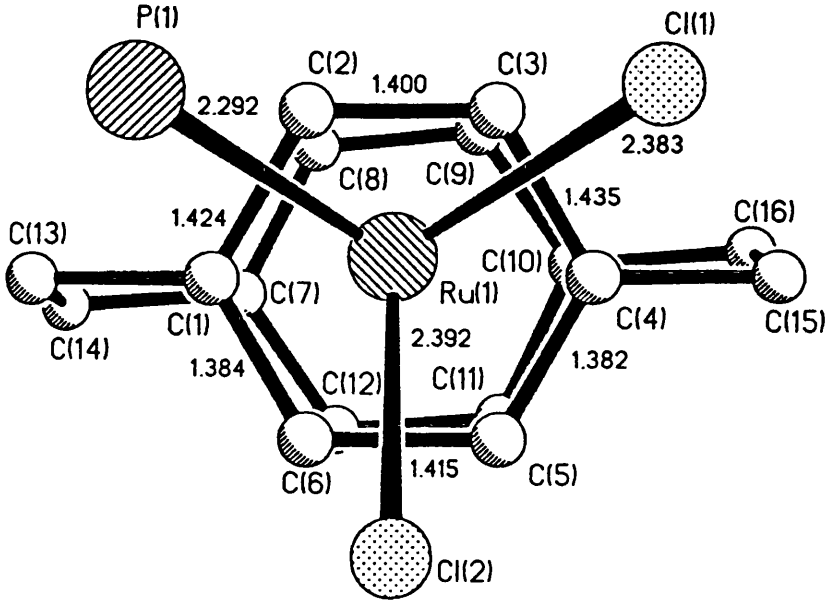

Fig. 2.6 The staggered geometry, and alternately long and short bond lengths of the coordinated ring, in the structure of (18).

bonds (Ru-C5 and Ru-C6, Fig. 2.7) *trans* to the tertiary phosphine ligand. These observations were attributed[86] to the *trans* bond-weakening effect of the tertiary phosphine ligand. In these complexes the arene rings were actually bent about C1-Ru-C4, rather than simply tilted. Bennett *et al*[86] argue that this effect would only be possible if there was a significant localising of the π-electrons in the rings, although no bond length alternation was reported for the coordinated aromatic rings. There is substantial evidence for the localisation of π-electron density in the coordinated ring in the structure of the cyclophane complex (18). As observed for the chromium complexes (4)[24] and (5)[25], and also for the ruthenium complex [Ru(η^6-*p*-cymene)Cl(2-hydroxypyridine)][109], there is a clear alternation of long (average 1.42(1) Å) and short (average 1.39(1) Å) C-C bond lengths in the coordinated ring (Fig. 2.6). No such alternation is observed in the non-coordinated deck. The distance from the ruthenium ion to the centroid of the non-bridgehead carbon atoms of the coordinated ring (C2,C3,C5,C6) is 1.69 Å. This value is comparable to similar reported Ru-Ar distances, which lie in the range 1.64-1.79 Å[62,96,101,103,104,110,112,113,115,118].

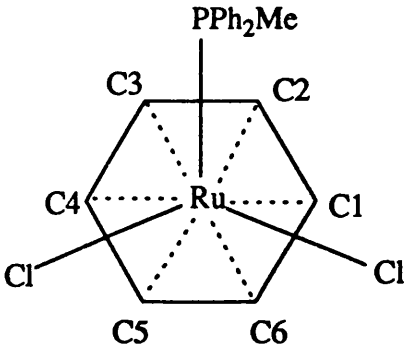

Fig. 2.7 The structure of $[Ru(\eta^6\text{-}C_6H_6)Cl_2(PPh_2Me)]$[86].

Ru-C1,2,3,4 *ca.* 2.19 Å, Ru-C5,6 = 2.27 Å.

The cyclophane inter-ring separation of 2.99 Å shows a decrease of 0.10 Å when compared with the free ligand[7]. The effect is larger in this complex of ruthenium(II) than in the chromium(0) complex, (4), where a 0.07 Å shortening was observed[24]. As a result of this contraction the geometry of the rings and the ring to bridge linkages flattens slightly, the coordinated face more so than the non-coordinated one, and the angular

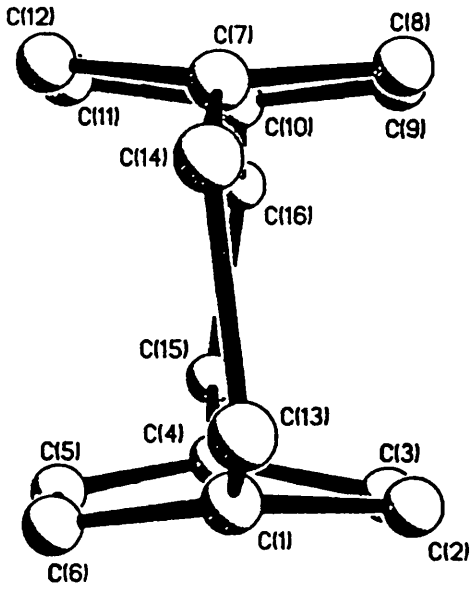

Fig. 2.8 Torsion in the $-CH_2CH_2-$ bridges of (18).

distortions from the ideal values of 109.5 and 120.0°, for sp^3 and sp^2 hybridised carbon atoms respectively, become less severe. The two decks of the cyclophane are not exactly eclipsed (Fig. 2.8). The torsion angles in the ethylenic bridges are 10.8 and 10.1°. The torsion angle in the ethylenic bridges of the free ligand was calculated[7] to be much smaller, of the order of 3.2°. This value was obtained[7] by a detailed analysis of the crystallographic data on the disordered structure of the free ligand. A similarly small torsion angle (3.8°) was observed in the structure of complex (4)[24].

Complex (18) has also been studied electrochemically in dichloromethane solution by cyclic voltammetry. Unusually, a fully reversible one electron oxidation is observed at +1.15 V (relative to Ag/AgCl). The peak to peak separation ΔE_p=60 mV (at v=100 mVs^{-1}), is characteristic of a one electron process, while $I_{pa}/I_{pc} \approx 1$, which is the requirement for a fully reversible process. ΔE_p did not change with scan rate in the range 50-500 mVs^{-1}. The cyclic voltammograms at varying scan rates are shown in Fig. 2.9. There is also evidence of an irreversible reduction at *ca.* -1.35 V. In general (η^6-arene)ruthenium(II) compounds exhibit only irreversible electrochemical behaviour, often resulting in loss of the arene ligand[48,109].

(ii) [Ru(η^6-$C_{16}H_{16}$)Cl_2(PMe_2Ph)] (19).

The complex [Ru(η^6-$C_{16}H_{16}$)Cl_2(PMe_2Ph)] (19) was prepared in an analogous manner to (18), and has been similarly characterised. The details are given in the experimental section.

Complex (19) has also been the subject of a cyclic voltammetric study, and undergoes a reversible one electron oxidation at +1.08 V, (ΔE_p=65 mV and was constant with the scan rate, $^ip_a/^ip_c \approx 1$). The oxidation of (19) occurs at a slightly less positive potential than that for (18), due to the better electron releasing properties of the substituent groups on the tertiary phosphine ligand.

(iii) [Ru(η^6-$C_{16}H_{16}$)Cl_2(NC_5H_5)] (20).

The complex [Ru(η^6-$C_{16}H_{16}$)Cl_2(NC_5H_5)] (20) was prepared and characterised in a similar fashion to (18). The details are given in the experimental section.

The structure of the monocationic complex [Ru(η^6-$C_{16}H_{16}$)Cl(NC_5H_5)$_2$][PF_6] (23) was determined at an early stage of the project and is discussed in Section 2.2.3. Therefore, when crystals of (20) were obtained, an X-ray structural analysis was

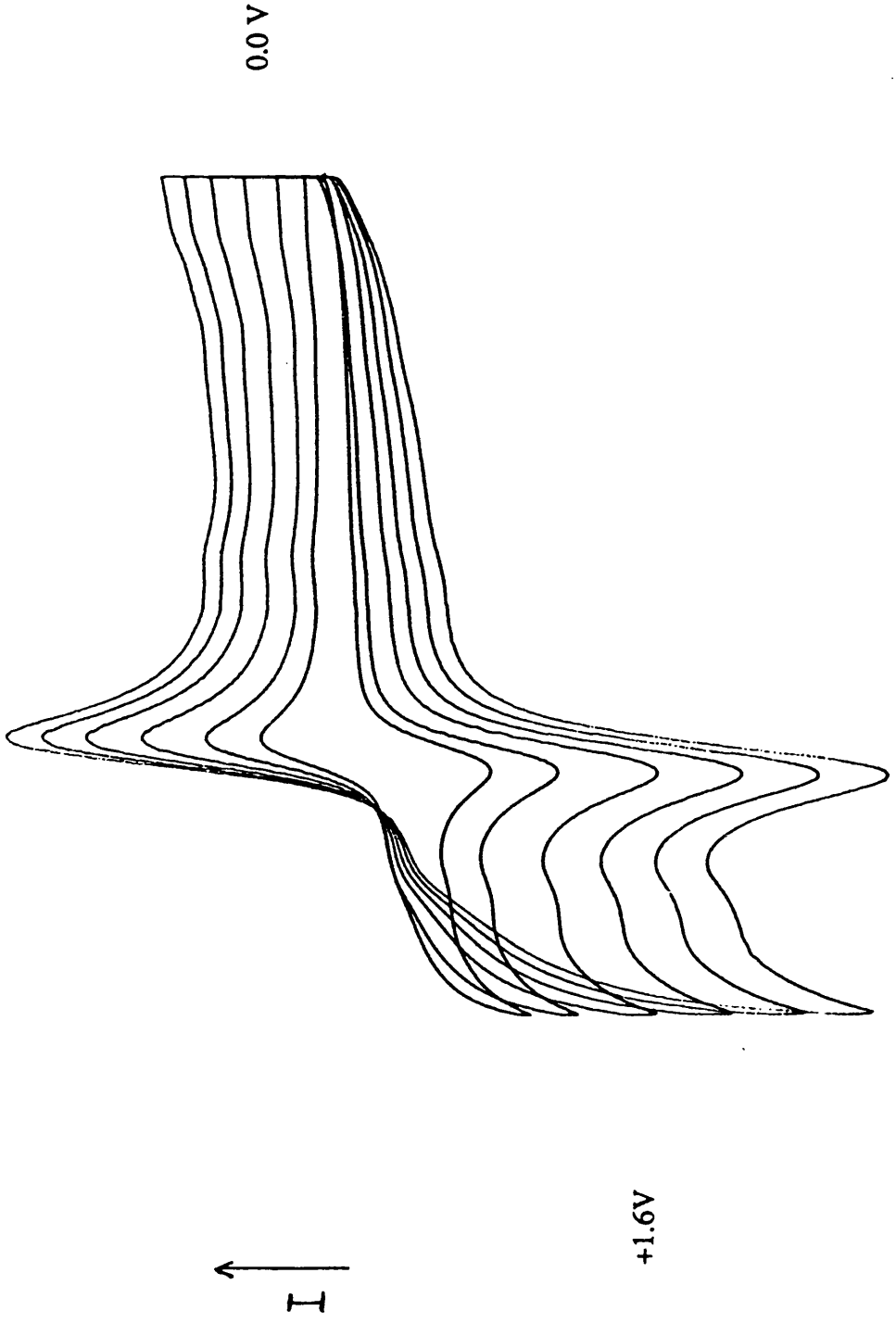

Fig 2.9 Cyclic voltammograms recorded in CD_2Cl_2 at scan rates from 50-500 mVs^{-1} for compound (18).

performed for purposes of comparison, despite the fact that the solid state structure of this class of compounds had already been established for complex (18). A thermal ellipsoid plot of (20) with some important bond lengths and angles is presented in Fig. 2.10. Tables of crystal data, fractional coordinates, bond lengths, and bond angles (Tables 2.15-2.18), and details of the data collection and structure refinement (Sections 2.3.5 and 2.3.6) are given in the experimental section.

The geometry of (20) is of the "piano-stool" type and is broadly similar to that of (18). In contrast to the structures containing a tertiary phosphine ligand, the structure of (20) has three of the carbon atoms of the arene ring eclipsing those of Cl1, Cl2 and N1 (Fig. 2.11). The L-Ru-L (L=Cl1,Cl2,N1) angles are close to 90°, as was the case for the similar complexes (4)[24] and (18). The Ru-Cl distances are 2.398(7) and 2.405(7) Å, and are comparable to those observed for (18), and those previously reported[62,86,95,109,111-115]. The Ru-N bond length is 2.10(2) Å, and therefore lies in the middle of the range of typical Ru-N values (2.04-2.18 Å) reported elsewhere[95,96,109,117-120]. There is no significant deviation from planarity of the pyridyl ring, and the internal angles are all close to 120°. The substantial e.s.d.'s associated with the C-C bond lengths prevent any comment on bond length alternation for this structure. The inter-ring separation between the cyclophane decks is 2.99 Å, which represents a 0.10 Å shortening compared with the free ligand[7] as discussed previously. As observed for the structure of (18), there is a significant lengthening of the Ru-C bonds *trans* to the Group 15 atom, nitrogen in this case, compared with those *trans* to the chloride ions {i.e. Ru-C1(*trans* to N)=2.35(2) Å, while Ru-C4(*trans* to Cl)=2.29(2) Å, and Ru-C2(*trans* to N)=2.21(2) Å, while Ru-C3,5,6(*trans* to Cl)=2.14-2.16(2) Å}.

The ^{1}H n.m.r. spectrum was recorded in $CDCl_3$ at room temperature (Table 2.4) and in CD_2Cl_2 at 188 K. The spectrum was recorded at low temperature in an attempt to investigate the chemical inequivalence of different parts of the bound deck of the cyclophane. However, the spectrum at 188 K was essentially unchanged from that observed at room temperature. Bennett *et al*[86] also found no evidence for ring asymmetry in solution for the complexes [Ru(η^6-*p*-cymene)Cl_2(PMe_2Ph)] and [Ru(η^6-C_6H_6)Cl_2(PMe_2Ph)] using low temperature ^{1}H n.m.r. spectroscopy. The crystal structures of these complexes had been determined[86], and clearly showed that such asymmetry was present in the solid state.

The ^{13}C-{^{1}H} n.m.r. spectrum was recorded over a range of temperatures in CD_2Cl_2. A proton coupled ^{13}C n.m.r. spectrum was recorded at 188 K in CD_2Cl_2 and allowed a full assignment of the observed resonances. The ^{13}C n.m.r. data for (20) are presented in Table 2.5. The spectra were essentially identical at all accessible

Lengths, Å.	
Ru-Cl1	2.398(7)
Ru-Cl2	2.405(7)
Ru-N	2.10(2)
Ru-C1	2.35(2)
Ru-C4	2.29(2)
Ru-C2	2.21(2)
Ru-C3,5,6	*av.* 2.15(2)
Inter-ring sep.	2.99
Angles, °.	
Cl1-Ru-Cl2	88.0(2)
Cl1-Ru-N	85.6(6)
Cl2-Ru-N	87.1(6)
Torsion	*av.* 12.2

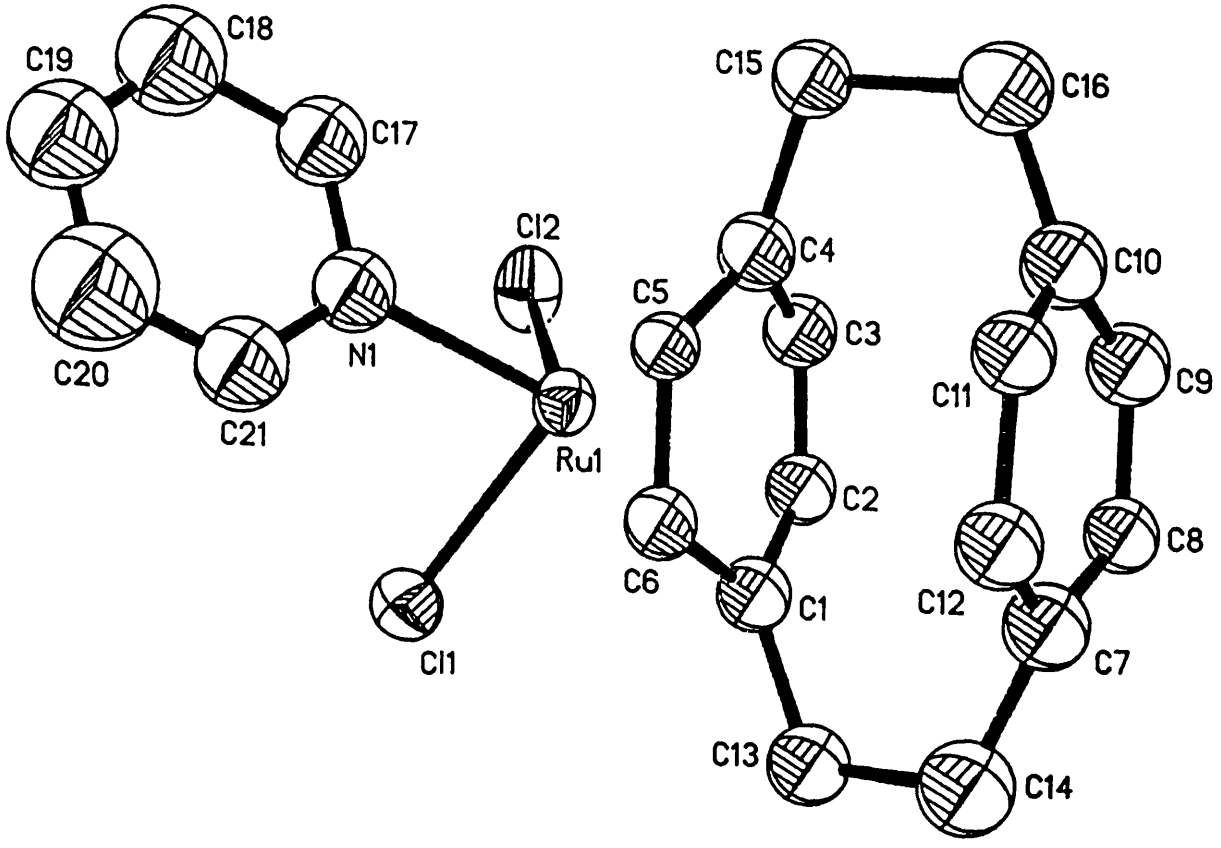

Fig. 2.10 A themal ellipsoid plot of $[Ru(\eta^6\text{-}C_{16}H_{16})Cl_2(py)]$ (20) with some important structural parameters.

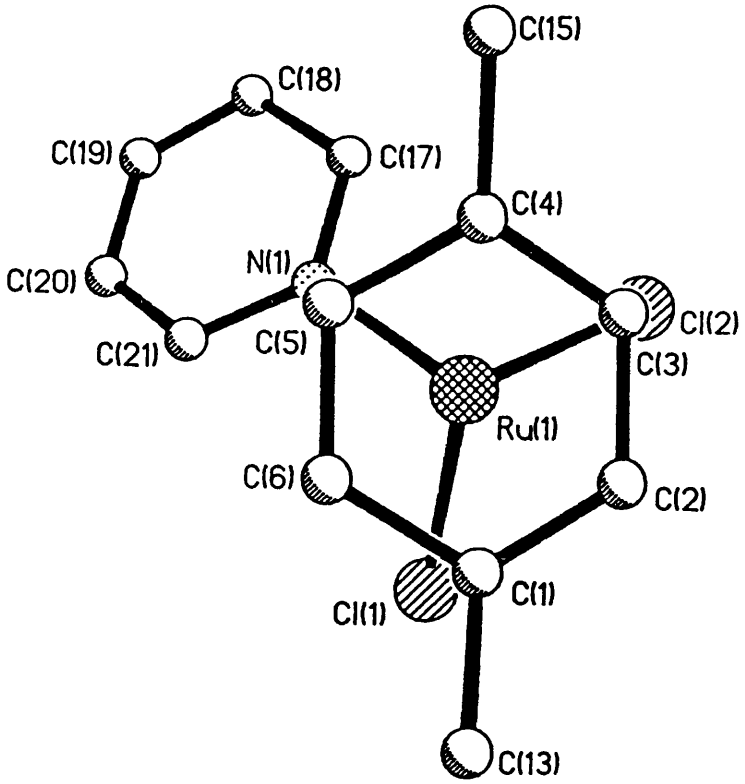

Fig. 2.11 The eclipsed conformation of (20) in the solid state.

temperatures. The four metallated non-bridgehead aromatic carbon atoms gave rise to just one doublet resonance in the proton coupled spectrum, even at 188 K, indicating chemical equivalence in solution on the n.m.r. timescale. The one-bond C-H coupling constants for the resonances of the coordinated and non-coordinated aromatic carbon atoms (C_3: $^1J_{C\text{-}H}$=175 Hz, C_4:$^1J_{C\text{-}H}$=158 Hz, Table 2.5) are closely similar to those observed for (11) (C_3:$^1J_{C\text{-}H}$=186 Hz, C_4: $^1J_{C\text{-}H}$=158 Hz)[81].

(iv) [Os(η^6-$C_{16}H_{16}$)Cl_2(PMe_2Ph)] (21) and [Os(η^6-$C_{16}H_{16}$)Cl_2(NC_5H_5)] (22).

Compounds (21) and (22) were prepared and characterised in a similar fashion to (18). The full details are given in the experimental section. The ^1H n.m.r. spectra (Table 2.4) are closely similar to those of the ruthenium analogues, the only significant difference being that the resonances due to the protons of the coordinated cyclophane ring appear to higher frequency in the spectra of the osmium compounds.

(v) The reaction of (1) with 2,6-dimethylpyridine in toluene.

Complex (1) was stirred with an excess of 2,6-dimethylpyridine in toluene for 5 h at room temperature. The toluene remained colourless throughout and a ^1H n.m.r. spectrum of the brown solid isolated showed only the starting material. It is possible that steric hindrance, due to the two methyl groups adjacent to the pyridyl nitrogen atom, prevents coordination of the ligand.

(vi) The reaction of (1) with pyrazine in toluene.

When (1) was stirred with an excess of pyrazine in toluene under similar conditions to those described for the preparation of (18), the major product formed was shown by its ^1H n.m.r. spectrum (Table 2.4) to be the monomeric complex $[Ru(\eta^6\text{-}C_{16}H_{16})Cl_2(N_2C_4H_4)]$ (23). In that spectrum, recorded in CD_2Cl_2, resonances due to this complex are observed as follows: δ 4.87 (s,4H), coordinated cyclophane ring; 6.78 (s,4H), non-coordinated cyclophane ring; 2.75 and 3.19 (each 4H, AA'XX'), $-CH_2CH_2-$; 8.45 and 8.89 ppm (each 2H, A_2B_2), $N_2C_4H_4$. The spectrum also indicated that a small quantity (*ca.* 10%) of a second complex, containing a coordinated cyclophane ligand and a different type of coordinated pyrazine ligand, had been formed. For this second compound a sharp singlet resonance was observed at δ 8.77 ppm due to the protons of the pyrazine ligand, while the resonances due to the cyclophane ligand appear to slightly lower frequency than those of the mononuclear complex. This suggests that the second compound is the symmetrical dimeric complex $[\{Ru(\eta^6\text{-}C_{16}H_{16})Cl_2\}_2(pyz)]$ (24) shown in Fig. 2.12 . When (1) was stirred with one equivalent of pyrazine under similar conditions

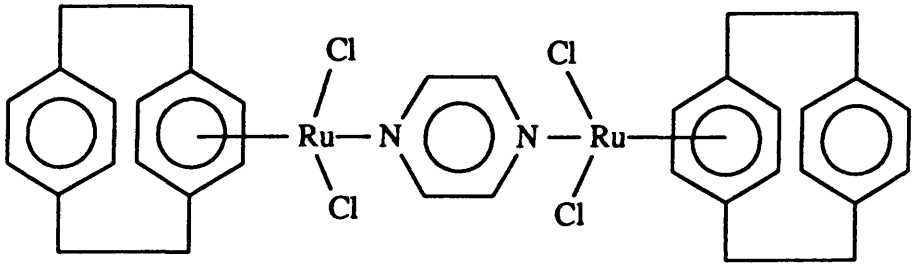

Fig. 2.12 A possible binuclear complex (24) formed in the reaction of (1) with pyrazine.

only (24) was formed. A broad ν(Ru-Cl) band, centred at 287 cm^{-1}, is observed in the

infrared spectrum. A previously reported[95] analogous compound, $[\{Ru(\eta^6\text{-}p\text{-cymene})Cl_2\}_2(pyz)]$, also exhibited a sharp singlet resonance in the ^1H n.m.r. spectrum, at δ 9.10 ppm, due to the protons of the symmetrically coordinated pyrazine ligand, and a broad ν(Ru-Cl) band at 290 cm^{-1} in its infrared spectrum.

2.2.3 The Reactions of $[M(\eta^6\text{-}[2_2]Paracyclophane)Cl_2]_2$ (M=Ru,Os) Compounds with Various Lewis Bases in Polar Solvents.

(i) The reaction of $[Ru(\eta^6\text{-}C_{16}H_{16})Cl_2]_2$(1) with pyridine in methanol.

The complex (1) was stirred in methanol with an excess of pyridine at room temperature. A deep red solution resulted, which was filtered to remove any unreacted starting material. A red solid was precipitated by the addition of a methanolic ammonium hexafluorophosphate solution. The red solid analysed (Table 2.6) closely for $[Ru(\eta^6\text{-}C_{16}H_{16})Cl(NC_5H_5)_2][PF_6]$ (25) (Fig. 2.13).

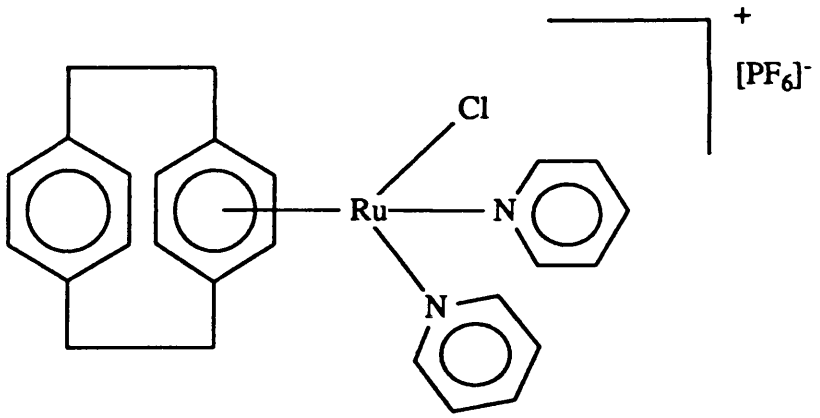

Fig. 2.13 $[Ru(\eta^6\text{-}C_{16}H_{16})Cl(py)_2][PF_6]$ (25).

In the FAB mass spectrum the highest mass peak was observed at 503 mass units which corresponds to the cationic fragment of the complex, $[Ru(\eta^6\text{-}C_{16}H_{16})Cl(NC_5H_5)_2]^+$. A computer simulation matched the spectrum observed experimentally. Fragmentation peaks were observed as noted below:

m/e	Fragment
468	$[Ru(\eta^6\text{-}C_{16}H_{16})(NC_5H_5)_2]^+$
424	$[Ru(\eta^6\text{-}C_{16}H_{16})Cl(NC_5H_5)]^+$
389	$[Ru(\eta^6\text{-}C_{16}H_{16})(NC_5H_5)]^+$
345	$[Ru(\eta^6\text{-}C_{16}H_{16})Cl]^+$
310	$[Ru(\eta^6\text{-}C_{16}H_{16})]^+$

The infrared spectrum exhibits two ν(Ru-Cl) bands at 288 and 310 cm^{-1}, a band at 841 cm^{-1} characteristic of the $[PF_6]^-$ anion, and bands at 1604 and 1586 cm^{-1} arising from the aromatic pyridyl ligands.

The ^1H n.m.r. spectrum, recorded in CD_2Cl_2, exhibits four resonances characteristic of the coordinated cyclophane ligand at: δ 6.88 (s, 4H), non-coordinated aromatic ring; 5.15 (s, 4H), coordinated aromatic ring; 2.79 and 3.26 ppm (AA'XX', each 4H), $-CH_2CH_2-$. The resonances due to the pyridyl protons are observed at δ 7.31 (m, 4H); 7.77 (tt, 2H); and 8.53 ppm (dt, 4H) (Table 2.7). Integration of the spectrum supports the proposed 1:2 ratio of [2$_2$]paracyclophane:pyridine ligands.

The structure of complex (25) has been confirmed by a single crystal X-ray diffraction experiment. The crystal used for the experiment was grown by the slow evaporation of a chloroform solution of the compound. There are two anions and two cations in the asymmetric unit. To maintain an acceptable ratio of data to parameters an isotropic rather than an anisotropic model was adopted to describe the carbon atoms of the cyclophane ligands. In addition, one of the $[PF_6]^-$ anions was substantially disordered. As a result the overall precision of the parameters describing the structure is poorer than is generally desirable. A detailed description of the data collection and the structure refinement (Sections 2.3.5 and 2.3.6), and tables of crystal data, fractional coordinates, bond lengths, and bond angles (Tables 2.19-2.22 respectively) are given in the experimental section. The structure of one of the cations of (25) and some important structural parameters are shown in Fig. 2.14.

The geometry of the cation is similar to that of the complexes (18) and (20), being distorted tetrahedral about the ruthenium ion, with the paracyclophane and the other ligands adopting a "piano stool" configuration. In this respect it is also closely similar to the complex $[Ru(\eta^6\text{-}p\text{-cymene})Cl(C_4H_4N_2)_2][PF_6]$[95]. It was not immediately clear why there were two unique cations in the asymmetric unit, since there are no significant differences between the bond lengths or bond angles in each cation. However, plots of the two molecules viewed along the Ru to ring centroid axes reveals that they are enantiomers in the solid state (Fig. 2.15). Each enantiomer has one pyridine ligand quasi-parallel to the

Lengths, Å.	
Ru-Cl	2.389(6)
Ru-N	2.15(2)
Ru-C1	2.36(2)
Ru-C4	2.30(2)
Ru-C2	2.22(2)
Ru-C3,5,6	2.18(2)
Inter-ring sep.	3.01
Angles, °.	
Cl-Ru-N1	88.6(6)
N1-Ru-N2	84.3(7)
Torsion	*av.* 8

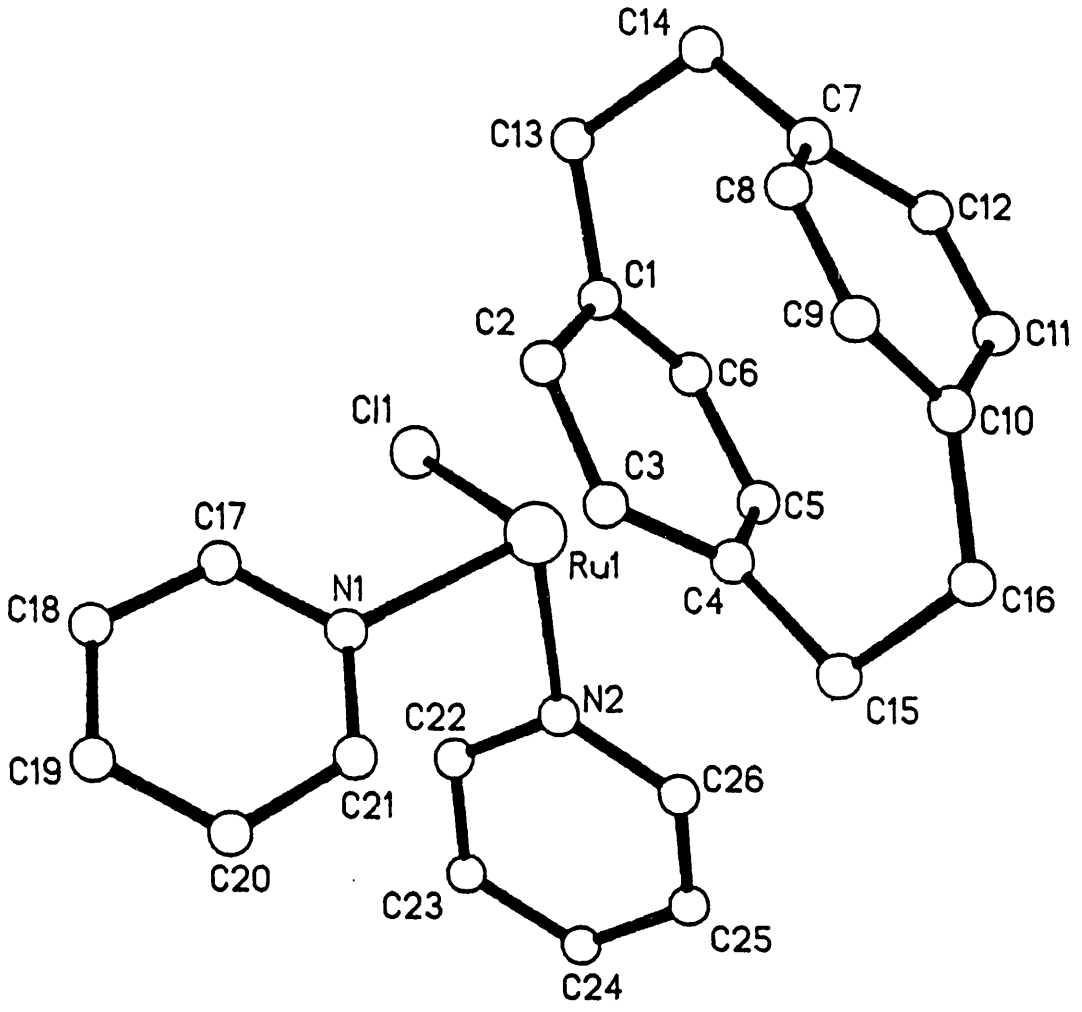

Fig. 2.14 The structure of one of the cations of $[Ru(\eta^6\text{-}C_{16}H_{16})Cl(py)_2][PF_6]$ (25) with some important structural parameters (averaged over the two cations).

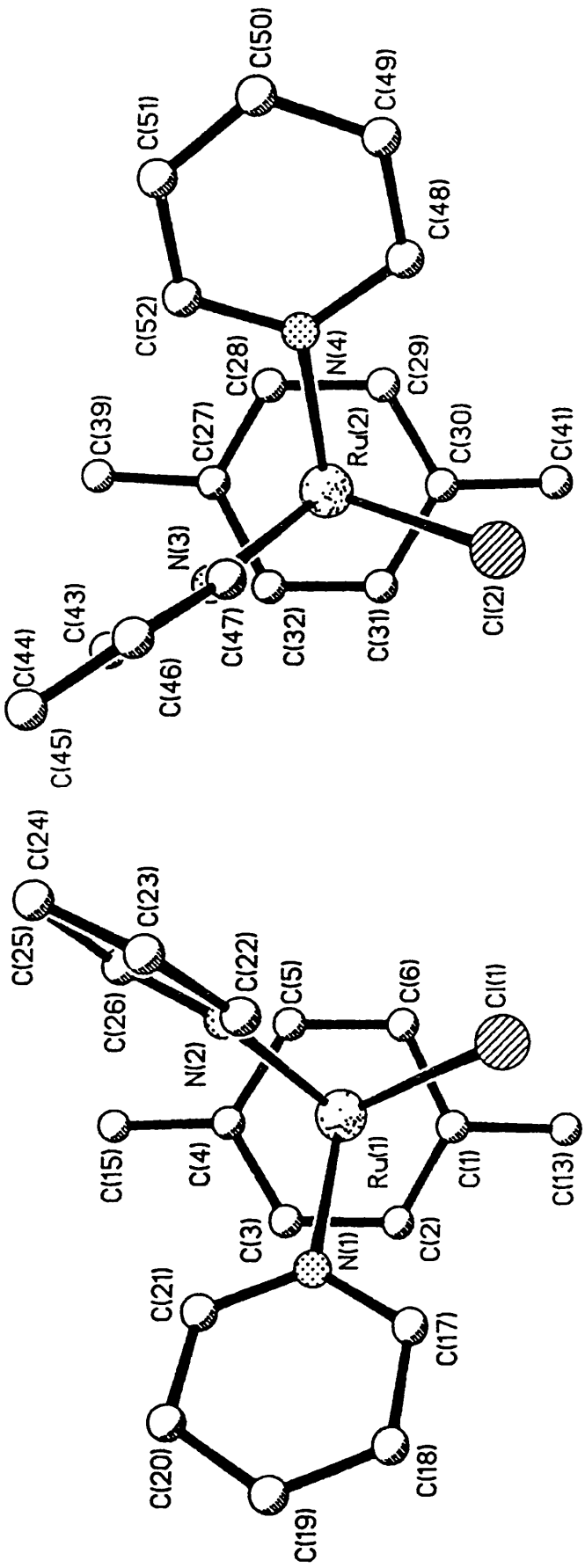

Fig. 2.15 The two enantiomers in the solid state structure of (25).

coordinated arene deck, and one perpendicular to it. The ruthenium ion is a chiral centre with the four different groups being the cyclophane, a chloride ion, and two differently oriented pyridyl ligands.

As was the case for complexes (18) and (20) there is a significant variation in the Ru-C bond lengths, due to the non-planarity of the cyclophane rings. The Ru to bridgehead carbon atom distances are in the range 2.31-2.37(2) Å, while the Ru to non-bridgehead carbon atom distances are significantly shorter at 2.16-2.25(2) Å. The Ru-C bonds *trans* to the nitrogen atoms are slightly longer than those *trans* to the chloride ions, indicating a similar lengthening effect to that observed for (18) and (20). The lack of precision in the bond lengths prevents any definite comment on bond length alternation in the coordinated aromatic rings in this case. The Cl-Ru-N angles are approximately 90°, but the N-Ru-N angles are closer to 85°. There is no significant deviation from planarity in any of the pyridyl ligands. In the complex $[Ru(\eta^6\text{-}p\text{-cymene})Cl(C_4H_4N_2)_2][PF_6]$[95] the chloride and pyrazine ligands are twisted a few degrees away from exactly eclipsing three of the carbon atoms of the *p*-cymene ligand. This is also true of both cations in the structure of (25).

The averaged interdeck separation is 3.01 Å, the distance from the centroid of the non-bridgehead atoms of the coordinated cyclophane deck to the metal ion is *ca.* 1.67 Å, and the averaged torsion angle in the ethylenic bridges is *ca.* 8°. These values are very similar to those observed in the structures of (18) and (20). The Ru-N distances are in the range 2.13-2.17(2) Å, which is rather longer than that observed for (20), 2.10(2) Å, but comparable to those reported [95] for the cation $[Ru(\eta^6\text{-}p\text{-cymene})Cl(pyz)_2]^+$, 2.15,2.18(≤2) Å. The Ru-Cl distance, 2.404(6) Å, is indistinguishable from that reported[95] for $[Ru(\eta^6\text{-}p\text{-cymene})Cl(pyz)_2][PF_6]$, 2.41(≤2) Å.

(ii) $[Ru(\eta^6\text{-}C_{16}H_{16})Cl(NC_5H_5)_2][BPh_4]$ (26).

The compound $[Ru(\eta^6\text{-}C_{16}H_{16})Cl(NC_5H_5)_2][BPh_4]$ (26) was prepared and characterised spectroscopically similarly to (25). The details are presented in the experimental section.

(iii) [Ru(η^6-$C_{16}H_{16}$)Cl(PPh_3)$_2$][PF_6] (27).

The compound [Ru(η^6-$C_{16}H_{16}$)Cl(PPh_3)$_2$][PF_6] (27) was prepared and characterised in a similar fashion to (25). The details of the synthesis, and the data used in characterisation are presented in the experimental section.

There are two noteworthy features of the ^{1}H n.m.r. spectrum of (27) (Table 2.7). Firstly, the resonance due to the coordinated ring protons of the cyclophane was broadened, but not resolved into a triplet. This is in contrast to the observation made for (18) where the corresponding resonance was split into a doublet by coupling to a single phosphorus atom. Secondly, the two branches of the AA'XX' coupling pattern arising from the -CH_2CH_2- bridge protons occur at very different chemical shifts (*ca.* 1.3 ppm apart). Indeed, the separation is the largest of this kind measured for any compound in this study and is due to the presence of two tertiary phosphine ligands in the cation. For the compounds [Ru(η^6-$C_{16}H_{16}$)Cl_2L] the largest such separations (*ca.* 0.7 ppm) were observed for those compounds containing a tertiary phosphine ligand. The ^{31}P-{^{1}H} n.m.r. spectrum (Table 2.10) was recorded in CD_2Cl_2 and exhibits a singlet resonance at δ 26.8 ppm.

(iv) [Ru(η^6-$C_{16}H_{16}$)Cl(PMe_2Ph)$_2$][PF_6] (28).

The compound [Ru(η^6-$C_{16}H_{16}$)Cl(PMe_2Ph)$_2$][PF_6] (28) was prepared and characterised similarly to (27). The full details are presented in the experimental section.

(v) [Ru(η^6-$C_{16}H_{16}$)Cl(PMe_2Ph)$_2$][BPh_4] (29).

The compound [Ru(η^6-$C_{16}H_{16}$)Cl(PMe_2Ph)$_2$][BPh_4] (29) was prepared and characterised in a similar fashion to (28). The details are presented in the experimental section. In the ^{1}H n.m.r. spectrum (Table 2.7) the resonance due to the protons of the coordinated aromatic ring was not only broadened, as was the case for (27) and (28), but also showed triplet character ($^3J_{P\text{-}H}$ *ca.* 0.7 Hz).

(vi) $[Os(\eta^6\text{-}C_{16}H_{16})Cl(NC_5H_5)_2][BPh_4]$ (30).

One monocationic osmium(II) complex has been prepared, namely $[Os(\eta^6\text{-}C_{16}H_{16})Cl(NC_5H_5)_2][BPh_4]$ (30). Using compound (16) as the starting material, the new complex (30) was prepared and characterised similarly to (26). Full details are given in the experimental section. The ^1H n.m.r. spectra of the two complexes (26) and (30) are almost identical, except that the resonance for the protons of the coordinated aromatic ring in the osmium compound appears *ca.* 0.4 ppm to higher frequency.

2.2.4 The Reactions of $[Ru(\eta^6\text{-}[2_2]Paracyclophane)Cl_2]_2$ with Bidentate Ligands in Polar Solvents.

(i) The reaction of $[Ru(\eta^6\text{-}C_{16}H_{16})Cl_2]_2$ (1) with 1,10-phenanthroline in methanol.

When complex (1) is stirred in methanol with an excess of 1,10-phenanthroline at room temperature a deep red solution is formed rapidly. From this solution a red solid can be precipitated by the addition of methanolic $K[PF_6]$. Although the main product formed is $[Ru(\eta^6\text{-}C_{16}H_{16})Cl(1,10\text{-Phen})][PF_6]$ (31), the ^1H n.m.r. spectrum reveals that some of the known[91] compound $[Ru(1,10\text{-phen})_3][PF_6]_2$ is also formed. A reduction in the reaction time leads to a purer product, as does the use of a single equivalent of the 1,10-phen ligand. However, overall yields are extremely poor under these circumstances.

A different synthetic approach gives better yields, and eliminates the contamination problem. If complex (1) is first treated with two equivalents of $Ag[BF_4]$ in methanol, the monocationic bis-solvato complex $[Ru(\eta^6\text{-}C_{16}H_{16})Cl(MeOH)_2]^+$ is generated in situ. After removal of the solid AgCl by filtration, the solvato complex was treated with a methanolic solution containing one equivalent of 1,10-phenanthroline, while being stirred vigorously. The reaction is essentially complete in the time of mixing and complex (31) is isolated by the addition of $K[PF_6]$ as before. The ^1H n.m.r. spectrum (Table 2.8) indicated that only the desired product was obtained by this method.

The problem encountered with the first route is that complex (1) is rather insoluble in methanol and is in suspension rather than solution. Therefore only small quantities of (1) are available for reaction when the ligand is added. However, the new complex (31) is susceptible to further attack and, since 1,10-phen is an excellent chelating ligand, further reaction occurs, resulting in the displacement of both the remaining chloride ion and the cyclophane ligand.

The second approach places all of the ruthenium complex in solution before the ligand is added, with the additional benefit that the methanol ligands which are to be displaced are extremely labile. Thus when the 1,10-phenanthroline ligand is added, replacement of the coordinated solvent molecules is extremely rapid. The new complex has little chance to react further, since the 1,10-phenanthroline ligand is rapidly consumed.

The complex was characterised by infrared and ^{1}H n.m.r. spectroscopy, and by elemental analysis. The data are given in the experimental section. The assignment of the resonances due to the protons of the 1,10-phenanthroline ligand in the ^{1}H n.m.r. spectrum was confirmed by a series of decoupling experiments.

The structure of complex (31) has been confirmed by a single crystal X-ray diffraction experiment. A detailed description of the data collection and the structure refinement (Sections 2.3.5 and 2.3.6), and tables of crystal data, fractional coordinates, bond lengths, and bond angles (Tables 2.23-2.26 respectively) are presented in the experimental section. A thermal ellipsoid plot of the cation is shown in Fig. 2.16 together with some important structural parameters.

The asymmetric unit contains one cation and one disordered $[PF_6]^-$ anion. The geometry at the ruthenium ion is that of a distorted tetrahedron with the arene and the other ligands adopting a "piano stool" conformation as described previously. The coordinated chloride ion and nitrogen atoms adopt an eclipsed conformation with respect to the carbon atoms of cyclophane (Fig. 2.17). The Cl1-Ru1-N bond angles average 85.2°, and the N1-Ru-N2 bite angle is 78.6(2)°. A similar N-M-N bite angle has been reported for 1,10-phen complexes of iridium[121]: 79.1(5)°, rhodium[122]: 77.5(1)°, and ruthenium[117]: 77.5(2), 77.2(2)°. The cyclophane ligand is once again non-planar, with the two Ru to bridgehead carbon atom bond lengths (2.34(1) and 2.31(1) Å) being significantly longer than the other Ru-C bond lengths (2.17-2.19(1) Å). There is no evidence for longer Ru-C bonds *trans* to the Group 15 atoms, in contrast to the structures of (18), (20) and (25). As observed in the tertiary phosphine complex (18), the C-C bond lengths of the coordinated cyclophane ring are alternately long (average 1.42(1) Å) and short (average 1.39(1) Å), indicating a degree of "bond-fixing". No such bond length alternation is observed in the non-coordinated deck.

The cyclophane inter-ring separation of 2.97 Å is the shortest measured in this study. The distance from the ruthenium atom to the ring centroid of the non-bridgehead atoms of the coordinated deck is 1.68 Å, which is typical for this type of compound[62,96,101,103,104,110,112,113,115,118]. The Ru-N {2.064, 2.083(6) Å} and Ru-Cl {2.394(2) Å} bond lengths, are also comparable to those previously reported[62,86,95,96,109,111-115,117-120] or observed elsewhere in this study. The torsion angles

Lengths, Å.	
Ru-Cl	2.394(2)
Ru-N1	2.064(6)
Ru-N2	2.083(6)
Ru-C1	2.314(8)
Ru-C4	2.337(7)
Ru-C2,3,5,6	*av.* 2.179(8)
Inter-ring sep.	2.97
Angles, °.	
Cl-Ru-N1	85.0(2)
Cl-Ru-N2	85.4(2)
N1-Ru-N2	78.6(2)
Torsion	3.8, 5.1

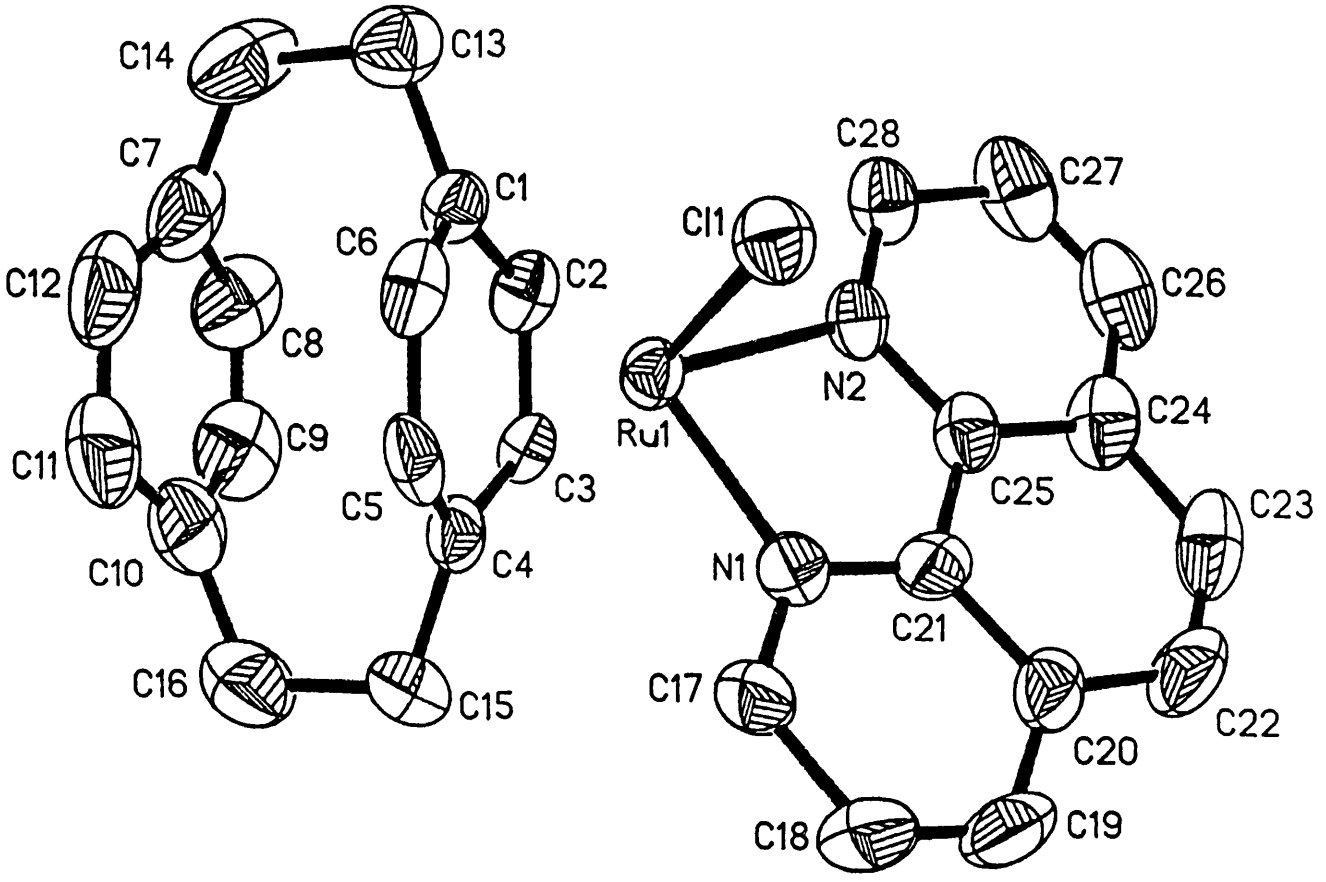

Fig. 2.16 A themal ellipsoid plot of $[Ru(\eta^6\text{-}C_{16}H_{16})Cl(1,10\text{-phen})]^+$ (31) with some important structural parameters.

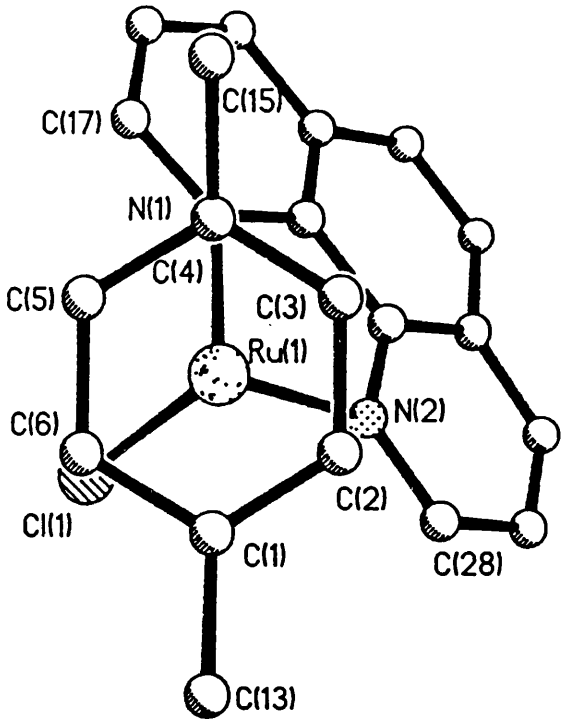

Fig. 2.17 The eclipsed conformation adopted by (31) in the solid state.

in the cyclophane bridges are 3.8 and 5.1°, and are rather smaller than observed for some of the other complexes for which measurements have been made {i.e. (18) and (20)}, but are similar to those observed in the chromium complex (4). The phenanthroline ligand shows no significant distortion from planarity, and its geometry, in terms of the pattern of long and short C-C and C-N bonds, bears a striking resemblance to that of the 1,10-phen ligands in structures reported previously[117,122,123].

(ii) [Ru(η^6-$C_{16}H_{16}$)Cl(2,2'-bipy)][BPh_4] (32).

The compound [Ru(η^6-$C_{16}H_{16}$)Cl(2,2'-bipy)][BPh_4] (32) was prepared by stirring (1) with an excess of 2,2'-bipyridyl for 10 min. in methanol and then isolating the orange product by addition of methanolic Na[BPh_4]. The ^{1}H n.m.r. spectrum (Table 2.8) revealed that the product was contaminated with a small quantity of the known[119] compound [Ru(2,2'-bipy)$_3$][BPh_4]$_2$, i.e. a similar problem was encountered as with the preparation of (31) (see above). Prolonged exposure of (1) to an excess of the ligand led exclusively to the formation of [Ru(2,2'-bipy)$_3$][BPh_4]$_2$.

(iii) [Ru(η^6-$C_{16}H_{16}$)Cl(2,2'-bipy)][PF_6] (33).

To obtain a pure salt of [Ru(η^6-$C_{16}H_{16}$)Cl(2,2'-bipy)]$^+$ a similar procedure was adopted to that which gave a pure sample of (31) (see above). The data used in the characterisation of (33) are presented in the experimental section. The assignment of the 2,2'-bipyridyl resonances in the ^{1}H n.m.r. spectrum (Table 2.8) was verified by a series of decoupling experiments.

2.2.5 The Reactions of [Ru(η^6-$C_{16}H_{16}$)Cl_2(PPh_3)] (18) and [Ru(η^6-$C_{16}H_{16}$)Cl_2(PMe_2Ph)] (19) with Pyridine in Methanol.

(i) The reaction of [Ru(η^6-$C_{16}H_{16}$)Cl_2(PPh_3)] (18) with pyridine in methanol.

If [Ru(η^6-$C_{16}H_{16}$)Cl_2(PPh_3)] (18) is stirred with an excess of pyridine in methanol a yellow/orange product can be isolated by the addition of methanolic Na[BPh_4] or K[PF_6]. Integration of the ^{1}H n.m.r. spectra of the products thus obtained indicate that the pyridine had displaced just one of the remaining chloride ligands producing the cation, [Ru(η^6-$C_{16}H_{16}$)Cl(PPh_3)(py)]$^+$. Although the solids isolated were not pure, the major products formed were salts of this cation.

The ^{1}H n.m.r. spectrum (Table 2.9) of [Ru(η^6-$C_{16}H_{16}$)Cl(PPh_3)(py)][PF_6] (34) exhibits resonances at δ 8.65 (d, 2H), 7.51 (dd, 1H) and 7.01 (t, 2H) ppm due to the pyridyl ligand, and resonances at δ 7.39 (t, 3H), 7.31 (t, 6H) and 7.10 (dd, 6H) ppm due to the PPh_3 ligand. The resonances due to the cyclophane ligand are considerably more complex than for the compounds described thus far, due to the chirality of the molecule. Despite the rapid rotation of the coordinated cyclophane ligand, the protons within each aromatic deck are always in different magnetic environments. Similarly, the protons of the bridging functions adjacent to a given deck of the ligand are also inequivalent. Thus the resonance due to the protons of the coordinated aromatic ring appears with a four line A_2B_2 coupling pattern at δ 5.03 ppm, while that for the protons of the non-coordinated ring appears with an eight line pattern at δ 6.81 ppm. The resonances of the -CH_2CH_2- protons appear as two complex multiplets at δ 2.38 and 3.09 ppm.

The full ^{1}H n.m.r. data for [Ru(η^6-$C_{16}H_{16}$)Cl(PPh_3)(py)][BPh_4] (35) are presented in Table 2.9. For this salt the resonance due to the protons of the non-coordinated ring of the cyclophane appears as a singlet, while that due to the coordinated ring protons appears with a four line A_2B_2 coupling pattern. Although one complex multiplet due to the

$-CH_2CH_2-$ protons appears at *ca.* δ 3.0 ppm with an intensity of 4H, as was observed for (34), the other is split into two multiplets at δ 2.12 and 2.28 ppm, each with an integral corresponding to 2H. Similar compounds, $[Ru(\eta^6\text{-}C_6H_6)Cl(PR_3)L][PF_6]$ (PR_3=PPh_3, PMe_2Ph, $P(OMe)_3$; L=PMe_3, PMe_2Ph, $PMePh_2$) have been prepared and characterised previously by Werner and Werner[88].

(ii) The reaction of $[Ru(\eta^6\text{-}C_{16}H_{16})Cl_2(PMe_2Ph)]$ (19) with pyridine in methanol.

If (19) is treated with pyridine in methanol, a yellow solution is obtained, from which a yellow solid can be precipitated by addition of methanolic $Na[BPh_4]$. An analysis of the ^1H n.m.r. spectrum of this solid clearly suggests that the product formed is $[Ru(\eta^6\text{-}C_{16}H_{16})Cl(PMe_2Ph)(py)][BPh_4]$ (36). The full ^1H n.m.r. data are presented in Table 2.9. As for (35), which is also a $[BPh_4]^-$ salt, the protons of the non-coordinated ring give rise to a singlet resonance, while those of the coordinated ring give rise to a resonance with a four line A_2B_2 coupling pattern (Fig. 2.18). The resonances due to the protons of the $-CH_2CH_2-$ bridging functions also appear with an analogous pattern (Fig. 2.18) to those observed for (35).

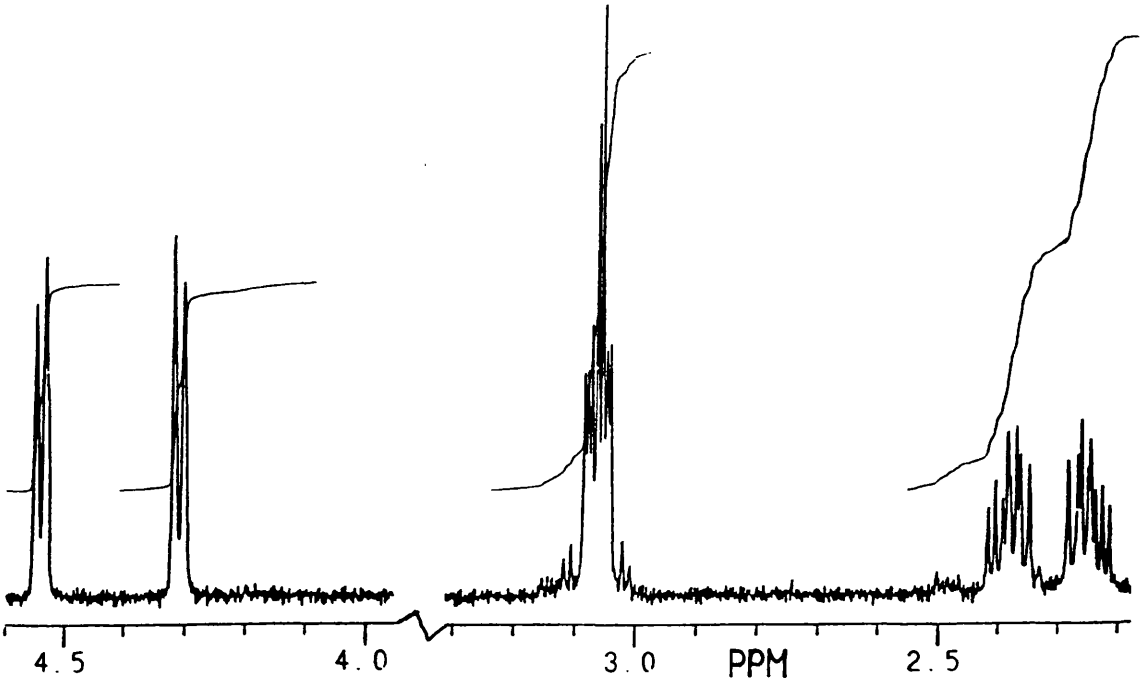

Fig. 2.18 The ^1H n.m.r. resonances of the coordinated ring and $-CH_2CH_2-$ protons of $[Ru(\eta^6\text{-}C_{16}H_{16})Cl(PMe_2Ph)(py)][BPh_4]$ (35).

2.2.6 Some Attempted Reactions to form Complexes of the type $Ru(\eta^6\text{-}[2_2]Paracyclophane)L(L\text{-}L)][X]_2$.

After the complex $[Ru(\eta^6\text{-}C_{16}H_{16})Cl(1,10\text{-phen})][PF_6]$ (31) was stirred with an excess of $PMePh_2$ in methanol at 293 K, a red solid was isolated by addition of methanolic $K[PF_6]$ to the reaction solution. The ^1H n.m.r. spectrum of this solid indicated that it was a mixture of two products comprising the starting compound and a species which did not contain a coordinated cyclophane ligand. Integration of the resonances due to this second compound strongly suggest a 2:1 ratio of $PMePh_2$:1,10-phenanthroline and a non-symmetrical magnetic environment for the phenanthroline ligand. When the reaction was repeated at elevated temperatures (*ca.* 325 K) the cyclophane ligand was displaced completely from the metal ion so only the latter compound was isolated. The infrared spectrum exhibits a band at 292 cm^{-1}, which is readily assigned to ν(Ru-Cl), and an intense, broad band at 835 cm^{-1} due to the P-F stretch of $[PF_6]^-$. Bands are also observed which arise from vibrations in the 1,10-phenanthroline and $PMePh_2$ ligands. Therefore one might tentatively suggest the formulation $[RuCl(phen)(PMePh_2)_2(MeOH)][PF_6]$.

2.3 EXPERIMENTAL.

2.3.1 Instrumentation and Physical Measurements.

Elemental analyses were performed by the microanalytical service of the Chemistry Department, University College London. Infrared spectra were recorded in the region 4000-250 cm^{-1} on a Perkin-Elmer 983 grating specrophotometer using Nujol mulls on caesium iodide plates. Hydrogen-1-n.m.r. spectra were recorded on Varian XL-200 and VXR-400 spectrometers, operating at 200.1 and 400.0 MHz respectively, and were referenced internally to TMS. Carbon-13-n.m.r. spectra were recorded on a Varian VXR-400 spectrometer operating at 100.6 MHz, and were referenced internally to TMS. Phosphorus-31-n.m.r. spectra were recorded on a Varian XL-200 spectrometer operating at 81.0 MHz, ($^{31}P-\{^{1}H\}$ n.m.r. chemical shifts quoted in ppm to trimethyl phosphite at 141.0 ppm, referenced internally, with the reference solution in a sealed capillary). Cyclic voltammetric studies were performed using a Metrohm potentiostat and VA scanner, linked to a cell stand having a three electrode geometry. The working electrode was a platinum wire. The reference electrode was a non-aqueous $Ag/AgCl/Cl^-$, CH_2Cl_2 electrode, and the auxiliary electrode was a large platinum wire. All potentials are reported relative to the Ag/AgCl reference electrode, against which ferrocene is oxidised at a potential of +0.60 V. The dichloromethane solutions contained tetra-*n*-butyl ammonium tetrafluoroborate ($TBABF_4$, 0.2 mol dm^{-3}) as a supporting electrolyte. These solutions were degassed in the electrochemical cell by bubbling solvent saturated dinitrogen for *ca.* 20 min., and a stream of solvent saturated dinitrogen was passed over the solution throughout the experiment. Mass spectra were recorded by the University of London Mass Spectrometry Service at the School of Pharmacy, using the fast atom bombardment (FAB) technique. Masses are reported based on the the following isotopes: ^{192}Os, ^{102}Ru, and ^{35}Cl. Computer simulations were used to verify assignments.

2.3.2 Materials.

Ruthenium trichloride trihydrate was obtained on loan from Johnson Matthy plc., and was activated before use by repeated evaporation of its aqueous solution[26]. All reactions were carried out under an atmosphere of dinitrogen in degassed solvents, although the final products were air stable. Tetrahydrofuran and *n*-hexane were dried before use by distilling from sodium wire. Dichloromethane used for electrochemical studies was distilled from P_2O_5. All other reagents and solvents were used as obtained

from commercial suppliers.

2.3.3 The Synthesis of the Compounds $[M(\eta^6\text{-}C_{16}H_{16})Cl_2]_2$ (M=Ru,Os).

The synthesis of $[Ru(\eta^6\text{-}C_{16}H_{16})Cl_2]_2$ (1)[66].

The complex $[Ru(\eta^6\text{-}C_6H_6)(\eta^6\text{-}C_{16}H_{16})][BF_4]_2$ (11)[73] (1.56 g; 2.79 mmol) was suspended in degassed THF (50 cm^3) under a dinitrogen atmosphere at 0°C in a Schlenk tube. A solution of sodium bis(methoxyethoxy)aluminium hydride (3.4 M) in toluene (3.10 cm^3; 10.5 mmol) was added dropwise with stirring. The solution became a dark amber colour within a few minutes, and was subsequently stirred for 3 h. After that time degassed water (1.00 cm^3) was added dropwise to destroy the excess reducing agent. The solvent was removed from the black solution *in vacuo*, leaving a light-grey solid. This solid was extracted with degassed *n*-hexane (9 x 20 cm^3), which was subsequently filtered, then pumped to dryness, to give a yellow air sensitive solid, $[(\eta^4\text{-}C_6H_8)Ru(0)(\eta^6\text{-}C_{16}H_{16})]$. The solid was dissolved in degassed acetone (50 cm^3), and concentrated hydrochloric acid (2.00 cm^3) was added dropwise with stirring, to precipitate the red/brown product. After 30 min. the product was filtered off, washed with acetone (10 cm^3) and diethyl ether (10 cm^3), and air dried. Yield: 0.50 g; 0.65 mmol; 47%.

Infrared Spectrum: ν(Ru-Cl): 298 (s), 258 (s) cm^{-1}.

The synthesis of $[Os(\eta^6\text{-}C_{16}H_{16})Cl_2]_2$ (16).

A solution of sodium bis(methoxyethoxy)aluminium hydride (3.4M) in toluene (1.50 cm^3; 5.10 mmol) was added to a suspension of $[Os(\eta^6\text{-}C_6H_6)(\eta^6\text{-}C_{16}H_{16})][BF_4]_2$ (17) (0.86 g; 1.33 mmol) in degassed THF (50 cm^3) at 0°C. After stirring for a few minutes the solution became a clear, dark amber colour. The solution was stirred for 2.5 h. Water (1.00 cm^3) was added dropwise to destroy the excess reducing agent. The solution which darkened and formed a sticky dark residue was stirred for 45 min. During this time the dark residue coagulated and fell to the bottom of the Schlenk tube. The clear, deep yellow solution of $[(\eta^4\text{-}C_6H_8)Os(0)(\eta^6\text{-}C_{16}H_{16})]$ was decanted off, filtered, and pumped to dryness. The resulting yellow solid was treated with a solution of concentrated hydrochloric acid (2.00 cm^3) in acetone (30 cm^3), and a yellow/tan precipitate formed. The product was filtered off and washed with acetone (10 cm^3), then air dried. Yield: 0.48g; 0.51 mmol; 77%.

Infrared Spectrum: ν(Os-Cl): 313 (s), 263 (m) cm^{-1}.

2.3.4 The Synthesis of Adducts of $[M(\eta^6\text{-}C_{16}H_{16})Cl_2]_2$.

(i) Neutral Complexes.

The synthesis of $[Ru(\eta^6\text{-}C_{16}H_{16})Cl_2(PPh_3)]$ (18).

$[Ru(\eta^6\text{-}C_{16}H_{16})Cl_2]_2$ (0.07g; 0.10 mmol) was added to a solution of triphenylphosphine (0.12 g; 0.48 mmol) in toluene (7 cm^3). The mixture was stirred for 2.5 h. at room temperature during which time an orange precipitate formed. The product was filtered off, washed with toluene (5 cm^3) and diethyl ether (5 cm^3), and then air dried. Yield: 0.10 g; 0.15 mmol; 79%.

Infrared Spectrum: ν(Ru-Cl): 303 (m), 281 (m); PPh_3: 754 (s), 744 (s), 733 (s), 722 (s), 695 (s), 529 (s), 513 (s), 500 (s) cm^{-1}.

Mass Spectrum:

m/e	Fragment
642	$[Ru(\eta^6\text{-}C_{16}H_{16})Cl_2(PPh_3)]^+$
607	$[Ru(\eta^6\text{-}C_{16}H_{16})Cl(PPh_3)]^+$
572	$[Ru(\eta^6\text{-}C_{16}H_{16})(PPh_3)]^+$

The synthesis of $[Ru(\eta^6\text{-}C_{16}H_{16})Cl_2(PMe_2Ph)]$ (19).

This compound was prepared by an analogous method to that for (18). $[Ru(\eta^6\text{-}C_{16}H_{16})Cl_2]_2$ (0.06 g; 0.08 mmol), dimethylphenylphosphine (0.05 cm^3, 0.35 mmol), reaction time 1.75 h. Yield of orange/brown product: 0.05 g; 0.11 mmol; 65%.

Infrared Spectrum: ν(Ru-Cl): 307 (m), 283 (m); PMe_2Ph: 945 (s), 916 (s), 742 (s) cm^{-1}.

Mass Spectrum:

m/e	Fragment
518	$[Ru(\eta^6\text{-}C_{16}H_{16})Cl_2(PMe_2Ph)]^+$
483	$[Ru(\eta^6\text{-}C_{16}H_{16})Cl(PMe_2Ph)]^+$
448	$[Ru(\eta^6\text{-}C_{16}H_{16})(PMe_2Ph)]^+$
346	$[Ru(\eta^6\text{-}C_{16}H_{16})Cl]^+$
310	$[Ru(\eta^6\text{-}C_{16}H_{16})]^+$.

The synthesis of $[Ru(\eta^6\text{-}C_{16}H_{16})Cl_2(NC_5H_5)]$ (20).

Pyridine (0.05 cm^3, 0.62 mmol) was added to a suspension of $[Ru(\eta^6\text{-}C_{16}H_{16})Cl_2]_2$ (0.07 g; 0.09 mmol) in toluene (7 cm^3). The mixture was stirred for 3.25 h. at room temperature. A red/brown precipitate formed, which was filtered off, washed with toluene (5 cm^3) and diethyl ether (5 cm^3), and then air dried. Yield: 0.06 g; 0.13 mmol; 72%.

Infrared Spectrum: ν(Ru-Cl): 300 (m), 284 (m); py: 1601 (s), 1583 (m) cm^{-1}.

Mass Spectrum:

m/e	Fragment
459	$[Ru(\eta^6\text{-}C_{16}H_{16})Cl_2(NC_5H_5)]^+$
424	$[Ru(\eta^6\text{-}C_{16}H_{16})Cl(NC_5H_5)]^+$
380	$[Ru(\eta^6\text{-}C_{16}H_{16})Cl_2]^+$
345	$[Ru(\eta^6\text{-}C_{16}H_{16})Cl]^+$
310	$[Ru(\eta^6\text{-}C_{16}H_{16})]^+$

The synthesis of $[Os(\eta^6\text{-}C_{16}H_{16})Cl_2(PMe_2Ph)]$ (21).

This compound was prepared by the method given for (18). $[Os(\eta^6\text{-}C_{16}H_{16})Cl_2]_2$ (0.06 g; 0.06 mmol), dimethylphenylphosphine (0.05 cm^3, 0.35 mmol), reaction time 2.5 h. Yield of tan product: 0.03 g; 0.06 mmol; 86%.

Infrared Spectrum: ν(Os-Cl): 302 (s), 278 (m); PMe_2Ph: 944 (s), 915 (s), 741 (s) cm^{-1}.

The synthesis of $[Os(\eta^6\text{-}C_{16}H_{16})Cl_2(NC_5H_5)]$ (22).

This compound was prepared by the method given for (20). $[Os(\eta^6\text{-}C_{16}H_{16})Cl_2]_2$ (0.06 g; 0.06 mmol), pyridine (0.05 cm^3, 0.62 mmol), reaction time 2.5 h. Yield of tan product: 0.05 g; 0.10 mmol; 83%.

Infrared Spectrum: ν(Ru-Cl): 294 (s, br); py: 1601 (s), 1582 (w, sh) cm^{-1}.

The synthesis of $[Ru(\eta^6\text{-}C_{16}H_{16})Cl_2(N_2C_4H_4)]$ (23).

This compound was prepared by the method given for (20). $[Ru(\eta^6\text{-}C_{16}H_{16})Cl_2]_2$ (0.06 g; 0.08 mmol), pyrazine (0.07 g, 0.82 mmol), reaction time 3.5 h. Yield of tan product based on the formulation of (23): 0.06 g; 0.13 mmol; 76%. The ^1H n.m.r. spectrum showed that the solid isolated contained a small quantity of $[\{Ru(\eta^6\text{-}C_{16}H_{16})Cl_2\}_2(pyz)]$ (24) in addition to the desired product.

Infrared spectrum: ν(Ru-Cl): 285 (s, br); pyz: 1584 (s), 1157 (s), 823 (s), 806 (s), cm^{-1}.

The synthesis of $[\{Ru(\eta^6\text{-}C_{16}H_{16})Cl_2\}_2(pyz)]$ (24)

This compound was prepared by the method given for (23), but using one equivalent of pyz per mole of the dimer (1). $[Ru(\eta^6\text{-}C_{16}H_{16})Cl_2]_2$ (0.05 g; 0.06 mmol), pyrazine (0.005 g, 0.05 mmol), reaction time 3.5 h. Yield of tan product based on the formulation of (24): 0.04 g; 0.05 mmol; 78%.

Infrared spectrum: ν(Ru-Cl): 287 (s, br); pyz: 810 (m), 820 (s), 1166 (m), 1530 (m), 1585 (m) cm^{-1}.

(ii) Monocationic Complexes.

The synthesis of $[Ru(\eta^6\text{-}C_{16}H_{16})Cl(NC_5H_5)_2][PF_6]$ (25).

Pyridine (0.05 cm^3, 0.62 mmol) was added to a suspension of $[Ru(\eta^6\text{-}C_{16}H_{16})Cl_2]_2$ (0.07 g; 0.09 mmol) in methanol (10 cm^3). The solution, which was stirred at room temperature for 1.75 h, became deep red. The solution was filtered to remove any unreacted starting material. The filtrate was then treated with a filtered solution of

ammonium hexafluorophosphate in methanol, and a red/brown microcrystalline precipitate formed. The solid product was filtered off, washed with methanol (2 cm^3) and diethyl ether (5 cm^3), and then air dried. Yield: 0.07 g; 0.10 mmol; 54%.

Infrared Spectrum: ν(Ru-Cl): 310 (m), 288 (w); py: 1604 (m), 1586 (w); $[PF_6]^-$: 841 (s, br) cm^{-1}.

Mass Spectrum:

m/e	Fragment
503	$[Ru(\eta^6\text{-}C_{16}H_{16})Cl(NC_5H_5)_2]^+$
468	$[Ru(\eta^6\text{-}C_{16}H_{16})(NC_5H_5)_2]^+$
424	$[Ru(\eta^6\text{-}C_{16}H_{16})Cl(NC_5H_5)]^+$
389	$[Ru(\eta^6\text{-}C_{16}H_{16})(NC_5H_5)]^+$
345	$[Ru(\eta^6\text{-}C_{16}H_{16})Cl]^+$
310	$[Ru(\eta^6\text{-}C_{16}H_{16})]^+$

The synthesis of $[Ru(\eta^6\text{-}C_{16}H_{16})Cl(NC_5H_5)_2][BPh_4]$ (26).

This complex was prepared similarly to (23). $[Ru(\eta^6\text{-}C_{16}H_{16})Cl_2]_2$ (0.12 g; 0.16 mmol), pyridine (0.05 cm^3, 0.62 mmol), reaction time 70 min. Tetraphenylboron sodium (0.22 g; 0.64 mmol) in methanol (5 cm^3) was added to precipitate the pale orange product. Yield: 0.17 g; 0.20 mmol; 64%.

Infrared Spectrum: ν(Ru-Cl): 294 (m); py: 1599 (m), 1575 (m); $[BPh_4]^-$: 760 (s), 743 (s), 724 (s), 707 (s), 690 (s) cm^{-1}.

The synthesis of $[Ru(\eta^6\text{-}C_{16}H_{16})Cl(PPh_3)_2][PF_6]$ (27).

$[Ru(\eta^6\text{-}C_{16}H_{16})Cl_2]_2$ (0.08 g; 0.10 mmol) was added to a solution of triphenylphosphine (0.25 g; 0.95 mmol) in methanol (5 cm^3). The mixture was stirred at room temperature for 3 h., giving an orange solution. This was filtered to remove any unreacted starting material and a filtered solution of ammonium hexafluorophosphate in methanol was added to the orange filtrate. This resulted in the rapid precipitation of the yellow microcrystalline product. This was recovered by filtration. Concentration of the filtrate caused further precipitation. The combined precipitates were washed with

methanol (5 cm^3), diethyl ether (5 cm^3), and then air dried. Yield: 0.04 g; 0.04 mmol; 19%.

Infrared Spectrum: ν(Ru-Cl): 295 (w); PPh_3: 760 (s), 743 (s), 723 (s), 703 (s), 692 (s), 534 (s), 521 (s), 511 (s), 494 (s); $[PF_6]^-$: 848 (s, br) cm^{-1}.

Mass Spectrum:

m/e	Fragment
869	$[Ru(\eta^6\text{-}C_{16}H_{16})Cl(PPh_3)_2]^+$
834	$[Ru(\eta^6\text{-}C_{16}H_{16})(PPh_3)_2]^+$
661	$[RuCl(PPh_3)_2]^+$
626	$[Ru(PPh_3)_2]^+$
607	$[Ru(\eta^6\text{-}C_{16}H_{16})Cl(PPh_3)]^+$
572	$[Ru(\eta^6\text{-}C_{16}H_{16})(PPh_3)]^+$

The synthesis of $[Ru(\eta^6\text{-}C_{16}H_{16})Cl(PMe_2Ph)_2][PF_6]$ (28).

This complex was prepared similarly to (25). $[Ru(\eta^6\text{-}C_{16}H_{16})Cl_2]_2$ (0.05 g; 0.07 mmol), dimethylphenylphosphine (0.10 cm^3, 0.70 mmol), reaction time 3 h. A clear yellow solution formed, to which a filtered solution of ammonium hexafluorophosphate in methanol was added. The solution was kept at *ca.* 258 K for 3 days during which time the orange product precipitated. Yield: 0.05 g; 0.06 mmol; 47%.

Infrared Spectrum: ν(Ru-Cl): 289 (w); PMe_2Ph: 944 (s), 909 (s), 901 (s), 750 (s), 744 (s); $[PF_6]^-$: 840 (s, br) cm^{-1}.

The synthesis of $[Ru(\eta^6\text{-}C_{16}H_{16})Cl(PMe_2Ph)_2][BPh_4]$ (29).

This complex was prepared similarly to (25). $[Ru(\eta^6\text{-}C_{16}H_{16})Cl_2]_2$ (0.08 g; 0.10 mmol), dimethylphenylphosphine (0.25 cm^3, 1.75 mmol), reaction time 3.5 h. After this time an orange solid was isolated by filtration. The ^1H n.m.r. spectrum of this solid revealed it to be (19). Yield of (19): 0.04 g; 0.08 mmol; 39%. A solution of tetraphenylboron sodium in methanol was added to the yellow filtrate. A yellow precipitate formed immediately. Yield of (29): 0.06 g; 0.06 mmol; 32%.

Infrared Spectrum: ν(Ru-Cl): 290 (w); PMe_2Ph: 937 (s), 902 (s), 748 (s); $[BPh_4]^-$: 732 (s), 721 (s), 706 (s) cm^{-1}.

Mass Spectrum:

m/e	Fragment
621	$[Ru(\eta^6\text{-}C_{16}H_{16})Cl(PMe_2Ph)_2]^+$
586	$[Ru(\eta^6\text{-}C_{16}H_{16})(PMe_2Ph)_2]^+$
483	$[Ru(\eta^6\text{-}C_{16}H_{16})Cl(PMe_2Ph)]^+$
448	$[Ru(\eta^6\text{-}C_{16}H_{16})(PMe_2Ph)]^+$
413	$[RuCl(PMe_2Ph)]^+$
378	$[Ru(PMe_2Ph)_2]^+$

The synthesis of $[Os(\eta^6\text{-}C_{16}H_{16})Cl(NC_5H_5)_2][BPh_4]$ (30).

This complex was prepared similarly to complex (25). $[Os(\eta^6\text{-}C_{16}H_{16})Cl_2]_2$ (0.03 g; 0.03 mmol), pyridine (0.05 cm^3, 0.62 mmol), reaction time 2 h. The solution was treated with a filtered solution of tetraphenylboron sodium in methanol. After standing overnight, microcrystalline yellow needles had formed. Concentration of the solution to *ca.* half volume led to the formation of more of the solid product. Yield: 0.005 g; 0.006 mmol; 9%.

Infrared Spectrum: ν(Os-Cl): 289 (m); py: 1601 (w), 1574 (w); $[BPh_4]^-$: 761 (m), 742 (s), 722 (s), 708 (s), 689 (m) cm^{-1}.

The synthesis of $[Ru(\eta^6\text{-}C_{16}H_{16})Cl(1,10\text{-phen})][PF_6]$ (31).

Silver tetrafluoroborate (0.04 g; 0.22 mmol) was added to a suspension of $[Ru(\eta^6\text{-}C_{16}H_{16})Cl_2]_2$ (0.10 g; 0.13 mmol) in methanol (10 cm^3). The mixture was stirred for 75 min. at room temperature, and then filtered through celite to remove the precipitated silver chloride . The red solution was treated with 1,10-phenanthroline (0.04 g; 0.22 mmol). The solution darkened to a deep amber colour after a few seconds. After 5 min. a solution of potassium hexafluorophosphate in methanol (3 cm^3) was added. A pale orange solid precipitated immediately. The solution was cooled to *ca.* 258 K for 30 min. causing more of the solid to form. The product was filtered off, washed with methanol (2 cm^3), and diethyl ether (10 cm^3), and then air dried. Yield: 0.05 g; 0.08 mmol; 30%.

Infrared Spectrum: ν(Ru-Cl): 293 (m); phen: 1575 (m), 1587 (m); $[PF_6]^-$: 838 (s, br) cm^{-1} .

The synthesis of $[Ru(\eta^6\text{-}C_{16}H_{16})Cl(2,2'\text{-bipy})][BPh_4]$ (32).

To a suspension of $[Ru(\eta^6\text{-}C_{16}H_{16})Cl_2]_2$ (0.10 g; 0.13 mmol) in methanol (5 cm^3), a solution of 2,2'-bipyridyl (0.32 g; 2.07 mmol) in methanol (5 cm^3) was added. The solution was stirred for 10 min. at room temperature, and filtered to remove any unreacted starting material. The deep red solution was treated with a filtered solution of tetraphenylboron sodium in methanol, resulting in the immediate precipitation of the red/brown product. The solid was filtered off, washed with methanol (10 cm^3), and diethyl ether (10 cm^3), and then air dried. Yield: 0.06 g; 0.07 mmol; 28%.

Infrared Spectrum: ν(Ru-Cl): 290 (w); bipy: 1602 (m), 1576 (m); $[BPh_4]^-$: 743 (s), 723 (s), 709 (s) cm^{-1}.

Mass Spectrum:

m/e	Fragment
501	$[Ru(\eta^6\text{-}C_{16}H_{16})Cl(bipy)]^+$
466	$[Ru(\eta^6\text{-}C_{16}H_{16})(bipy)]^+$

The synthesis of $[Ru(\eta^6\text{-}C_{16}H_{16})Cl(2,2'\text{-bipy})][PF_6]$ (33).

This complex was prepared similarly to complex (30). $[Ru(\eta^6\text{-}C_{16}H_{16})Cl_2]_2$ (0.06 g; 0.08 mmol), $Ag[BF_4]$ (0.03 g; 0.16 mmol), 2,2'-bipy (0.03 g; 0.16 mmol). Yield of bright orange product: 0.03 g; 0.04 mmol; 25%.

Infrared Spectrum: ν(Ru-Cl): 292 (m, br), bipy: 1604 (m), 1583 (w, sh); $[PF_6]^-$: 835 (s, br) cm^{-1}.

2.3.5 General Experimental Method for Crystal Structure Determinations.

In the following paragraphs a general description of the experimental procedures employed during each of the crystal structure determinations reported in this thesis is given. Any variation from these procedures is detailed in the experimental section for the particular structure determination concerned, as are the details of the refinement of the individual crystal structures.

Crystals of maximum dimensions 0.8 x 0.8 x 0.8 mm were mounted on a glass fibre, using a fast-setting epoxy resin as an adhesive. All geometric and intensity data were collected from this crystal using a Nicolet R3m/V automated four-circle diffractometer, equipped with graphite monochromated Mo-K_α radiation (λ=0.71073 Å).

Initially the lattice vectors were identified by application of the automatic indexing routine of the diffractometer to the positions of at least 20 orientation reflections (typically in the range $10° \leq 2\Theta \leq 30°$) taken from a rotation photograph, and located and centred by the diffractometer. Axial photography was used to verify Laué class and unit cell dimensions. Precise cell dimensions and the crystal orientation matrix were obtained by a least squares fit to the goniometer positions of these orientation reflections.

Data sets were collected in the range $5° \leq 2\Theta \leq 50°$ (or $5° \leq 2\Theta \leq 55°$, if the crystal was very strongly diffracting). Three standard reflections were remeasured every 97 scans to monitor any long term crystal decay. The data sets were corrected for intensity variation, and for Lorentz and polarisation effects. Empirical absorption corrections were based on azimuthal scans of between 6 and 10 reflections with $\chi = 270 \pm 20°$ or $90 \pm 20°$. The space groups were determined from an analysis of the systematically absent data where possible. Cases where systematic absences result in space group ambiguities are discussed in the experimental sections of the relevant compounds. Hydrogen atoms were not included in models unless stated explicitly.

2.3.6 Details of Crystal Structure Determinations.

(i) Details of the crystal structure determination of $[Ru(\eta^6\text{-}C_{16}H_{16})Cl_2(PPh_3)].CHCl_3$ (18).

A red crystal was grown by slow evaporation of a chloroform solution of the compound. Initially the lattice vectors were identified by application of the automatic indexing routine of the diffractometer to the positions of 22 reflections ($15° \leq 2\Theta \leq 27°$) taken from a rotation photograph and located and centred by the diffractometer. A

preliminary primitive data set was collected in the range $20° \leq 2\Theta \leq 35°$. The crystal was recentred on 49 high angle data. Analysis of the data indicated that C centring was present and the full data set was collected in the range $5° \leq 2\Theta \leq 55°$ omitting the reflections where h+k=(2n+1). From the systematically absent data the space group was either C2/c or Cc. The refinement of the structure proceeded most smoothly in the higher symmetry space group, C2/c, which can thus be regarded as established.

The positions of most of the non-hydrogen atoms were found by direct methods. Iterative application of least-squares refinement and difference-Fourier synthesis led to the development of the entire structure. The asymmetric unit contains one molecule of the metal complex and one chloroform of crystallisation. No attempt was made to locate the hydrogen atoms. All non-hydrogen atoms were refined anisotropically. The final difference-Fourier was featureless, the highest peak being 0.84 $eÅ^{-3}$. The crystal data are presented in Table 2.11. Tables 2.12-2.14 give fractional coordinates, bond lengths, and bond angles, respectively.

(ii) Details of the crystal structure determination of $[Ru(\eta^6\text{-}C_{16}H_{16})Cl_2(NC_5H_5)]$ (20).

An orange crystal was grown by slow evaporation of a chloroform solution of the compound. Initially the lattice vectors were identified by application of the automatic indexing routine of the diffractometer to the positions of 8 reflections ($6° \leq 2\Theta \leq 13°$) taken from a rotation photograph and located and centred by the diffractometer. A preliminary data set was collected in the range $15° \leq 2\Theta \leq 30°$. The crystal was recentred on 32 of these high-angle data. The full data set was collected as described in the general description. From the systematically absent data the space group was uniquely defined as $P2_12_12_1$.

The position of the ruthenium ion was found using a three-dimensional Patterson function. Iterative application of least-squares refinement and difference-Fourier synthesis led to the development of the entire structure. The asymmetric unit contains one complete molecule of the metal complex. The ruthenium and chloride ions were refined anisotropically, while the light atoms were refined using an isotropic model. Hydrogen atoms were included in a riding model only, with a common, fixed temperature factor ($U=0.08$ $Å^2$). The highest peak in the final electron density map was 1.66 $eÅ^{-3}$, and was close to the ruthenium ion. All other peaks in the final map were less than 1 $eÅ^{-3}$. The relatively high final residuals can be attributed to the poor quality of the data set. The

crystal data are presented in Table 2.15. Tables 2.16-2.18 give fractional coordinates, bond lengths, and bond angles, respectively.

(iii) Details of the crystal structure determination of $[Ru(\eta^6\text{-}C_{16}H_{16})Cl(NC_5H_5)_2][PF_6]$ (25).

An orange crystal was grown by slow evaporation of a dichloromethane solution. Initially the lattice vectors were identified by application of the automatic indexing routine of the diffractometer to the positions of 25 reflections ($15° \leq 2\Theta \leq 25°$) taken from a rotation photograph and located and centred by the diffractometer. A preliminary data set was then collected in the range $20° \leq 2\Theta \leq 35°$. The crystal was recentred on 31 of these data, and the full data set was collected as described in the general description. From the systematic absences the space group was uniquely defined as $P2_12_12_1$. No absorption correction was applied.

The asymmetric unit contains two cations and two $[PF_6]^-$ anions, one of which is substantially disordered. The positions of the two ruthenium atoms were found by direct methods. Iterative application of least-squares refinement and difference-Fourier synthesis led to the development of the entire structure.

In the two cations the ruthenium and chloride ions, and the nitrogen and pyridyl carbon atoms were refined anisotropically.

One of the $[PF_6]^-$ anions was modelled with two sets of positions for the fluorine atoms. The occupancy ratio for the two sets refined to 70:30. The fluorine atoms in the major set of positions were given a common freely refining isotropic temperature factor during the early stages of the structure refinement. The temperature factors of the fluorine atoms having the minor occupancy were similarly constrained initially. The temperature factors of all atoms in both sets of positions were allowed to refine freely in the latter cycles. The fluorine atoms in the major set of positions and the phosphorus atom were refined anisotropically.

The second $[PF_6]^-$ anion was refined with the fluorine atoms having a common isotropic temperature factor initially and, in the latter stages of refinement, with freely refining anisotropic parameters . An insufficient number of data prevented the anisotropic refinement of the cyclophane ligands. The crystal data are presented in Table 2.19. Tables 2.20-2.22 give fractional coordinates, bond lengths, and bond angles, respectively.

(iv) Details of the crystal structure determination of $[Ru(\eta^6\text{-}C_{16}H_{16})Cl(1,10\text{-phen})][PF_6]$ (31).

An orange crystal was grown by the slow evaporation of an acetone solution of the compound. The data collection was carried out routinely. An initial analysis of the systematic absences suggested that the space group was either Pmba (non-centrosymmetric) or $P2_1ab$ (centrosymmetric). No satisfactory solution could be obtained in the higher symmetry space group, while the solution in the lower symmetry one led to the two crystallographically unique molecules being heavily correlated. The addition of a centre of symmetry at $\frac{1}{4},0,\frac{1}{4}$, gives a further 4 equivalent positions at:

$\frac{1}{2}$-x,-y,$\frac{1}{2}$-z	$(\bar{1})$
-x,$\frac{1}{2}$+y,$\frac{1}{2}$+z	(2_1)(b)
$\frac{1}{2}$-x,$\frac{1}{2}$-y,$\frac{1}{2}$+z	(2_1)(c)
-x,y,$\frac{1}{2}$-z	(glide along c perpendicular to a).

From the last line one would expect the reflections of the type 0kl ($l \neq 2n$) to be absent. These reflections were in fact observed, but were very weak. The addition of the centre of symmetry implies the space group is Pcab. A more satisfactory solution was obtained in this space group, albeit with the $[PF_6]^-$ anion requiring a disordered model.

The positions of the ruthenium and phosphorus atoms were obtained from a three-dimensional Patterson function. Iterative application of least-squares refinement and difference-Fourier synthesis led to the development of the entire structure. The asymmetric unit contains one cation and one anion. The $[PF_6]^-$ anion was rotationally disordered about one F-P-F axis. The model used in refinement employed two sets of four equally occupied fluorine atom positions in the equatorial plane of the anion. All of the non-hydrogen atoms were refined anisotropically. The hydrogen atoms were included in a riding model only, with a common, fixed, isotropic temperature factor ($U=0.08$ Å^2). The crystal data are presented in Table 2.23. Tables 2.24-2.26 give fractional coordinates, bond lengths, and bond angles, respectively.

TABLE 2.1 ^{1}H n.m.r. Data for the Compounds $[M(\eta^6\text{-arene})Cl_2]_2$ and $[M(\eta^6\text{-}C_6H_6)(\eta^6\text{-}C_{16}H_{16})][BF_4]_2$ at 298 K.

Compound.		Solvent.	^{1}H n.m.r. data. δ,ppm.				
			Cyclophane resonances.			Other resonances.	
			non-coord. C_6H_4	coord. C_6H_4	$-CH_2CH_2-$ (AA'XX')		
$[Ru(\eta^6\text{-}C_6H_6)Cl_2]_2$		d_6-DMSO[a]	-	-	-	5.98 (s)	C_6H_6
$[Os(\eta^6\text{-}C_6H_6)Cl_2]_2$		d_6-DMSO[b]	-	-	-	6.54 (s), 6.15 (s)	C_6H_6[c]
$[Ru(\eta^6\text{-}C_6H_6)(\eta^6\text{-}C_{16}H_{16})][BF_4]_2$	(11)	CD_3NO_2[b]	7.04 (s)	6.25 (s)	3.22 and 3.46	6.71 (s)	C_6H_6
$[Os(\eta^6\text{-}C_6H_6)(\eta^6\text{-}C_{16}H_{16})][BF_4]_2$	(17)	CD_3NO_2[b]	7.11 (s)	6.54 (s)	3.21 and 3.51	6.91 (s)	C_6H_6
$[Ru(\eta^6\text{-}C_{16}H_{16})Cl_2]_2$	(1)	d_6-DMSO[b]	6.84 (s)	5.19 (s)	2.75 and 3.13	-	
$[Os(\eta^6\text{-}C_{16}H_{16})Cl_2]_2$	(16)	d_6-DMSO[b]	6.90 (s)	5.57 (s)	2.74 and 3.16	-	

a) Operating frequency: 200 MHz.

b) Operating frequency: 400 MHz.

c) Two resonances due to the presence of two species in solution:-
(i) $[(\eta^6\text{-}C_6H_6)OsCl_2(DMSO)]$ (δ 6.54 ppm) and (ii) $[(\eta^6\text{-}C_6H_6)OsCl(DMSO)_2]^+$.

TABLE 2.2 ^{13}C-{^1H} n.m.r. Data for the Compounds [2.2](1,4)$C_{16}H_{16}$, [M(η^6-arene)Cl_2]$_2$ and [M(η^6-C_6H_6)(η^6-$C_{16}H_{16}$)][BF_4]$_2$ at 298 K.

Compound.		Solvent.	^{13}C-{^1H} n.m.r. data. δ, ppm.							
			Cyclophane resonances[a].						Other resonances.	
			C_1	C_2	C_3	C_4	C_5	C_6		
[2.2](1,4)$C_{16}H_{16}$	(3)	d_6-DMSO	139.1	139.1	132.8	132.8	35.0	35.0	-	
[Ru(η^6-C_6H_6)Cl_2]$_2$		d_6-DMSO	-	-	-	-	-	-	87.6	C_6H_6
[Os(η^6-C_6H_6)Cl_2]$_2$		d_6-DMSO	-	-	-	-	-	-	79.4, 88.0	C_6H_6[b]
[Ru(η^6-C_6H_6)(η^6-$C_{16}H_{16}$)][BF_4]$_2$	(11)	CD_3NO_2	134.9	141.1	90.0	135.8	33.5	35.2	94.0	C_6H_6
[Os(η^6-C_6H_6)(η^6-$C_{16}H_{16}$)][BF_4]$_2$	(17)	CD_3NO_2	133.0	141.2	83.4	135.8	33.8	34.9	87.2	C_6H_6
[Ru(η^6-$C_{16}H_{16}$)Cl_2]$_2$	(1)	d_6-DMSO	121.7	139.3	83.4	133.2	31.3	32.8	-	
[Os(η^6-$C_{16}H_{16}$)Cl_2]$_2$	(16)	d_6-DMSO	119.7	139.3	74.6	132.8	31.5	32.8	-	

a) The carbon atom numbering scheme is shown in the figure.

b) Two resonances due to two species in solution:-

(i) [(η^6-C_6H_6)$OsCl_2$(DMSO)] (δ 88.0 ppm) and (ii) [(η^6(C_6H_6)OsCl(DMSO)$_2$]$^+$.

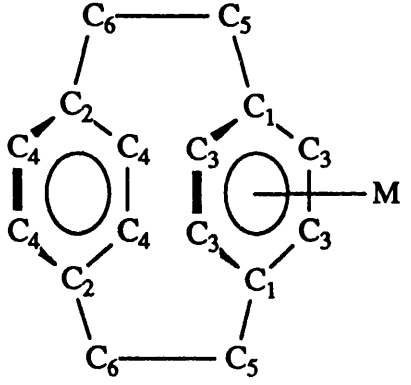

TABLE 2.3 Microanalytical Data for the Compounds $[M(\eta^6\text{-}C_{16}H_{16})Cl_2L]$.

Compound.		Microanalytical data.							
		%C		%H		%N		%Cl	
		found	calc.	found	calc.	found	calc.	found	calc.
$[Ru(\eta^6\text{-}C_{16}H_{16})Cl_2(PPh_3)]$	(18)	63.0	63.3	4.9	5.3	-	-	10.9	11.0
$[Ru(\eta^6\text{-}C_{16}H_{16})Cl_2(PMe_2Ph)]$	(19)	54.4	55.5	4.5	5.4	-	-	-	-
$[Ru(\eta^6\text{-}C_{16}H_{16})Cl_2(py)]$	(20)	54.0	54.9	4.6	4.6	3.1	3.1	15.9	15.4
$[Os(\eta^6\text{-}C_{16}H_{16})Cl_2(PMe_2Ph)]$	(21)	46.2	47.5	4.5	4.5	-	-	-	-
$[Os(\eta^6\text{-}C_{16}H_{16})Cl_2(py)]$	(22)	44.0	46.0	3.6	3.9	2.3	2.6	-	-
$[Ru(\eta^6\text{-}C_{16}H_{16})Cl_2(pyz)]$	(23)	51.3	52.2	4.2	4.4	5.8	6.1	-	-

TABLE 2.4 ^{1}H n.m.r. Data for the Compounds [M(η^6-$C_{16}H_{16}$)Cl_2L] and [{Ru(η^6-$C_{16}H_{16}$)Cl_2}$_2$(pyz)] at 298 K.

Compound.		Solvent.	^{1}H n.m.r. data. δ, ppm.			
			Cyclophane resonances.			Other resonances.
			non-coord. C_6H_4	coord. C_6H_4	-CH_2CH_2- (AA'XX')	
[Ru(η^6-$C_{16}H_{16}$)Cl_2(PPh_3)]	(18)	$CDCl_3$[a]	6.69 (s)	4.70 (d)[c]	2.31, 3.01	7.32 (m, 9H), 7.54 (m,6H): P-Ph_3.
[Ru(η^6-$C_{16}H_{16}$)Cl_2(PMe_2Ph)]	(19)	$CDCl_3$[a]	6.68 (s)	4.52 (d)[d]	2.38, 3.03	1.68 (d[e], 6H): P-(CH_3)$_2$; 7.44 (m, 3H), 7.70 (m, 2H): P-Ph.
[Ru(η^6-$C_{16}H_{16}$)Cl_2(py)]	(20)	$CDCl_3$[b]	6.77 (s)	4.90 (s)	2.76, 3.18	7.20 (m, 2H), 7.64 (tt, 1H) 8.90 (dt, 2H): py.
[Os(η^6-$C_{16}H_{16}$)Cl_2(PMe_2Ph)]	(21)	$CDCl_3$[b]	6.75 (s)	4.88 (s)[f]	2.36, 3.05	1.71 (d[g], 6H): P-(CH_3)$_2$; 7.42 (m, 3H), 7.60 (m, 2H): P-Ph.
[Os(η^6-($C_{16}H_{16}$)Cl_2(py)]	(22)	$CDCl_3$[b]	6.81 (s)	5.43 (s)	2.70, 3.18	7.15 (t, 2H), 7.58 (t, 1H), 8.82 (d, 2H): py.
[Ru(η^6-$C_{16}H_{16}$)Cl_2(pyz)]	(23)	CD_2Cl_2[a]	6.78 (s)	4.87 (s)	2.75, 3.19	8.45 and 8.89 (AB, both d[h], 2H): pyz.
[{Ru(η^6-$C_{16}H_{16}$)Cl_2}$_2$(pyz)]	(24)	CD_2Cl_2[a]	6.75 (s)	4.83 (s)	2.72, 3.15	8.77 (s, 4H): pyz.

a) Operating frequency: 400 MHz. c) $^3J_{P-H}$ = 1.1 Hz. e) $^2J_{P-H}$ = 11.7 Hz. g) $^2J_{P-H}$ = 11.4 Hz.

b) Operating frequency: 200 MHz. d) $^3J_{P-H}$ = 1.6 Hz. f) $^3J_{P-H}$ = 1.2 Hz. h) $^3J_{H-H}$ = 2.6 Hz.

TABLE 2.5 Variable Temperature ^{13}C n.m.r. Data for $[Ru(\eta^6\text{-}C_{16}H_{16})Cl_2(NC_5H_5)]$ (20) in CD_2Cl_2.

Atom.	^{13}C n.m.r. data. δ, ppm.				Carbon atom labelling scheme.
	298 K[a]	228 K[a]	188 K[b]	$^1J_{C\text{-}H}$ (Hz)	
C_1	115.5	114.8	114.3 (s)	-	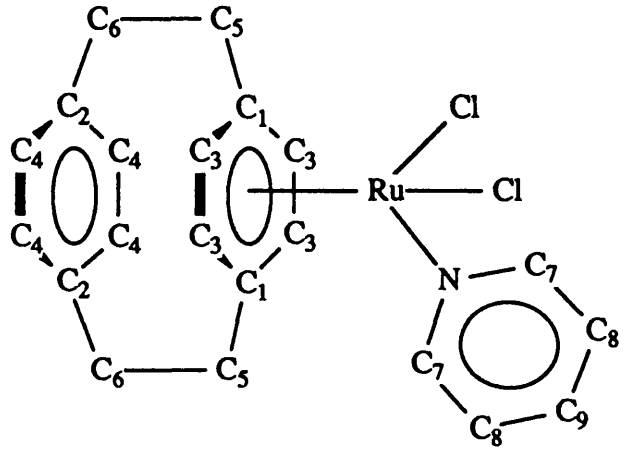
C_2	139.9	139.5	139.1 (s)	-	
C_3	79.6	78.7	78.2 (d)	175.2	
C_4	133.6	133.1	132.7 (d)	157.8	
C_5	31.9	31.1	30.5 (t)	133.2	
C_6	33.7	33.0	32.5 (t)	133.4	
C_7	156.4	155.4	155.0 (d)	188.6	
C_8	124.6	124.3	124.1 (d)	167.4	
C_9	137.7	137.4	137.2 (d)	165.4	

a) All singlets, proton decoupled spectrum.

b) Proton coupled spectrum.

TABLE 2.6 Microanalytical Data for the Compounds

$[M(\eta^6\text{-}C_{16}H_{16})Cl(L)_2][X]$ and $[Ru(\eta^6\text{-}C_{16}H_{16})Cl(L\text{-}L)][X]$.

Compound.		Microanalytical data.							
		%C		%H		%N		%Cl	
		found	calc.	found	calc.	found	calc.	found	calc.
$[Ru(\eta^6\text{-}C_{16}H_{16})Cl(py)_2][PF_6]$	(25)	48.3	48.2	4.1	4.0	4.3	4.3	5.8	5.5
$[Ru(\eta^6\text{-}C_{16}H_{16})Cl(py)_2][BPh_4]$	(26)	72.4	73.0	5.7	5.6	3.3	3.4	4.7	4.3
$[Ru(\eta^6\text{-}C_{16}H_{16})Cl(PPh_3)_2][PF_6].1.5(MeOH)$	(27)	60.3	60.5	4.9	4.9	-	-	3.4	3.3
$[Ru(\eta^6\text{-}C_{16}H_{16})Cl(PMe_2Ph)_2][PF_6]$	(28)	48.5	50.2	4.8	5.0	-	-	4.4	4.6
$[Ru(\eta^6\text{-}C_{16}H_{16})Cl(PMe_2Ph)_2][BPh_4]$	(29)	70.4	71.5	6.1	6.2	-	-	-	-
$[Os(\eta^6\text{-}C_{16}H_{16})Cl(py)_2][BPh_4]$	(30)	66.7	65.9	4.9	5.1	2.8	3.1	-	-
$[Ru(\eta^6\text{-}C_{16}H_{16})Cl(phen)][PF_6]$	(31)	48.4	50.2	3.4	3.6	4.3	4.2	-	-
$[Ru(\eta^6\text{-}C_{16}H_{16})Cl(bipy)][BPh_4]$	(32)	71.5	73.2	5.2	5.4	3.8	3.4	4.1	4.3
$[Ru(\eta^6\text{-}C_{16}H_{16})Cl(bipy)][PF_6]$	(33)	48.9	48.3	3.5	3.7	4.6	4.3	-	-

TABLE 2.7 ^{1}H n.m.r. Data for the Compounds [M(η^6-$C_{16}H_{16}$)ClL$_2$][X] at 298 K.

Compound.		Solvent.	^{1}H n.m.r data. δ, ppm			
			Cyclophane resonances.			
			non-coord. C_6H_4	coord. C_6H_4	-CH_2CH_2- (AA'XX')	Other resonances.
[Ru(η^6-$C_{16}H_{16}$)Cl(py)$_2$][PF_6]	(25)	CD_2Cl_2[a]	6.88 (s)	5.15 (s)	2.79, 3.26	7.31 (m, 4H), 7.77 (tt, 2H), 8.53 (dt, 4H): NC_5H_5.
[Ru(η^6-$C_{16}H_{16}$)Cl(py)$_2$][BPh_4]	(26)	CD_2Cl_2[b]	6.80 (s)	4.81 (s)	2.67, 3.22	7.21 (m, 4H), 7.78 (tt, 2H), 8.25 (dt, 4H): NC_5H_5; [e].
[Ru(η^6-$C_{16}H_{16}$)Cl(PPh_3)][PF_6]	(27)	$CDCl_3$[a]	6.82 (s)	5.18 (s, br)	1.60, 2.86	7.28 (m, 30H): P-Ph_3.
[Ru(η^6-$C_{16}H_{16}$)Cl(PMe_2Ph)$_2$][PF_6]	(28)	$CDCl_3$[b]	6.78 (s)	4.95 (s, br)	2.00, 2.98	1.39 (vt[c], 6H), 1.79 (vt[c], 6H): PPh(CH_3)$_2$; 7.44 (m, 6H), 7.61 (m, 4H): PMe_2(Ph).
[Ru(η^6-$C_{16}H_{16}$)Cl(PMe_2Ph)$_2$][BPh_4]	(29)	CD_2Cl_2[b]	6.71 (s)	4.67 (t[d])	2.06, 3.01	1.37 (vt[c], 6H), 1.61 (vt[c], 6H): PPh(CH_3)$_2$; 7.50 (m, 10 H): PMe_2(Ph); [e].
[Os(η^6-$C_{16}H_{16}$)Cl(py)$_2$][BPh_4]	(30)	CD_2Cl_2[b]	6.87 (s)	5.26 (s)	2.68, 3.25	7.18 (m, 4H), 7.76 (tt,2H), 8.29 (dt, 4H): NC_5H_5; [e].

a) Operating frequency 200 MHz.

b) Operating frequency 400 MHz.

c) vt = virtual triplet.

d) $^3J_{P\text{-}H}$ *ca.* 0.7 Hz.

e) The usual [BPh_4]$^-$ resonances were observed at *ca.* δ 6.91 (t, 4H), 7.05 (t, 8H) and 7.35 (m, 8H) ppm.

TABLE 2.8 ^{1}H n.m.r. Data for the Compounds [Ru(η^6-$C_{16}H_{16}$)Cl(L-L)][X] at 298 K.

Compound.	Solvent.	^{1}H n.m.r. data. δ, ppm.			
		Cyclophane resonances..			Other resonances[b].
		non-coord. C_6H_4	coord. C_6H_4	-CH_2CH_2- (AA'XX')	
[Ru(η^6-$C_{16}H_{16}$)Cl(1,10-phen)][PF_6]	(31) CD_3NO_2[a]	7.01 (s)	5.42 (s)	3.11, 3.37	7.96 (dd, H_B), 8.11 (s, H_D), 8.67 (dd, H_D), 9.49 (dd, H_A): phen. $^4J_{A\text{-}C}$ = 1.3 Hz, $^3J_{A\text{-}B}$ = 5.3 Hz, $^3J_{C\text{-}B}$ = 8.3 Hz.
[Ru(η^6-$C_{16}H_{16}$)Cl(bipy)][BPh_4]	(32) CD_2Cl_2[a]	6.82 (s)	4.92 (s)	2.86, 3.26	7.39 (m), 7.90 (m), 8.80 (m): bipy. 6.87 (t), 7.00 (t), 7.32 (m): B[Ph_4]$^-$.
[Ru(η^6-$C_{16}H_{16}$)Cl(bipy)][PF_6]	(33) CD_3CN[a]	6.89 (s)	5.23 (s)	2.96, 3.26	7.54 (ddd, H_B), 8.05 (ddd, H_C), 8.20 (dd, H_D), 9.04 (dd, H_A); $^3J_{A\text{-}B}$ = 5.5 Hz, $^4J_{A\text{-}C}$ =1.5 Hz, $^3J_{B\text{-}C}$ = 7.5 Hz, $^4J_{B\text{-}D}$ = 1.5 Hz, $^3J_{C\text{-}D}$ = 8.0 Hz.

a) Operating frequency 400 MHz.

b) The hydrogen atom labeling schemes are shown in the figures.

1,10-phen

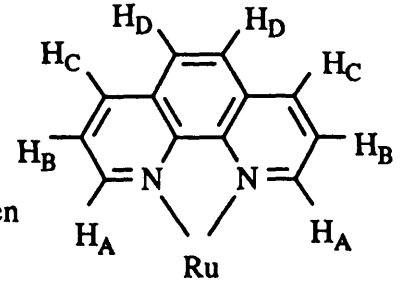

bipy

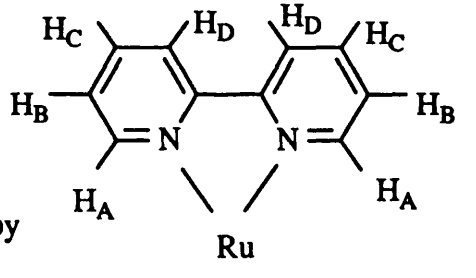

TABLE 2.9 ^{1}H n.m.r. Data for the Compounds [Ru(η^6-$C_{16}H_{16}$)Cl(PR_3)(Py)][X] in $CDCl_3$ at 298 K.

Compound.	^{1}H n.m.r. data. δ, ppm.			
	Cyclophane resonances.			Other resonances.
	non-coord. C_6H_4	coord. C_6H_4	-CH_2CH_2-	
[Ru(η^6-$C_{16}H_{16}$)Cl(PPh_3)(py)][PF_6] (34)[a]	6.81 (4H,A_2B_2)	5.03 (4H,A_2B_2)	3.09, 2.38 (each 4H, m)	7.01 (t, 2H), 7.51 (m, 1H), 8.65 (d, 2H): py; 7.10 (dd, 6H), 7.31 (t, 6H), 7.39 (t, 3H):P-Ph_3.
[Ru(η^6-$C_{16}H_{16}$)Cl(PPh_3)(py)][BPh_4] (35)[a]	6.65 (4H,s)	4.56 (4H,A_2B_2)	3.00 (4H, m), 2.28, 2.12 (each 2H, m)	6.74 (t, 2H), *ca.*7.4 (1H), 8.33 (d, 2H): py; 7.00 (m, 6H), 7.23 (m, 6H), 7.39 (t, 3H): P-Ph_3;[b].
[Ru(η^6-$C_{16}H_{16}$)Cl(PMe_2Ph)(py)][BPh_4] (36)[a]	6.67 (4H,s)	4.40 (4H,A_2B_2)	3.05 (4H, m) 2.24, 2.37 (each 2H, m)	7.00 (m, 2H), 7.60 (tt, 1H), 8.31 (d, 2H): py; 7.37 (m, 4H), 7.42 (m, 1H): PMe_2Ph; 1.32 (dd, 6H): $PPh(CH_3)_2$;[b].

a) Operating frequency 400 MHz. b) The usual [BPh_4]$^-$ resonances were observed at *ca.* δ 6.95 (t, 4H), 7.05 (t, 8H), and 7.46 (m, 8H) ppm.

TABLE 2.10 ^{31}P-{^{1}H} n.m.r. Data for Selected Mononuclear Compounds.

Compound.		Solvent.	δ, ppm[a].
$[Ru(\eta^6\text{-}C_{16}H_{16})Cl_2(PPh_3)]$	(18)	$CDCl_3$	37.3 (s)
$[Ru(\eta^6\text{-}C_{16}H_{16})Cl_2(PMe_2Ph)]$	(19)	$CDCl_3$	19.6 (s)
$[Ru(\eta^6\text{-}C_{16}H_{16})Cl(PPh_3)_2][PF_6]$	(27)	CD_2Cl_2	26.8 (s)
$[Ru(\eta^6\text{-}C_{16}H_{16})Cl(PMe_2Ph)_2][PF_6]$	(28)	$CDCl_3$	12.7 (s)
$[Ru(\eta^6\text{-}C_{16}H_{16})Cl(PMe_2Ph)_2][BPh_4]$	(29)	$CDCl_3$	12.1 (s)

a) Referenced to Trimethylphosphite (141.0 ppm).

Table 2.11 **Crystallographic Data for $[Ru(\eta^6\text{-}C_{16}H_{16})Cl_2PPh_3].CHCl_3$ (18).**

Formula	$Ru_1P_1Cl_5C_{35}H_{32}$
fw, g	761.9
Space group	C2/c
a, Å	40.325(24)
b, Å	8.341(2)
c, Å	22.646(7)
α, deg	90.0
β, deg	120.12(3)
γ, deg	90.0
V, $Å^3$	6587(4)
Z	8
F(000)	3088
d_{calc}, g/cm^3	1.54
Crystal size, mm	0.5 x 0.2 x 0.1
Scan technique	ω
$\mu(Mo\text{-}K_\alpha)$, cm^{-1}	8.92
Orientation reflections, no.; range (2Θ)	49; ($25° \leq 2\Theta \leq 35°$)
Temperature, °C	20
Total No. of reflections measured	6331
No. of unique data	5804
Total with $I \geq 2\sigma(I)$	4413
No. of parameters	379
R[a]	0.0568
R'[b]	0.0532
Weighting scheme	$w = 1.000/(\sigma^2F + 0.000264F^2)$
Largest shift/esd, final cycle	0.026
Largest peak, $e/Å^3$	0.84

a) $R = \Sigma[|F_o|-|F_c|]/\Sigma|F_o|$

b) $R' = \Sigma[(|F_o|-|F_c|) \cdot w^{\frac{1}{2}}]/\Sigma[|F_o| \cdot w^{\frac{1}{2}}]$

TABLE 2.12 **Atomic Coordinates (x10^4) and Equivalent Isotropic Displacement Parameters (Å^{2}x10^3) for [Ru(η^6-$C_{16}H_{16}$)Cl_2(PPh_3)].$CHCl_3$ (18).**

Atom	x		y		z		U(eq)[a]	
Ru1	935	(1)	117	(1)	766	(1)	26	(1)
P1	1278	(1)	800	(2)	1898	(1)	27	(1)
Cl1	1356	(1)	-2111	(2)	1026	(1)	46	(1)
Cl2	529	(1)	-1515	(2)	1007	(1)	43	(1)
C1	732	(2)	2678	(7)	380	(3)	32	(3)
C2	1097	(2)	2303	(7)	460	(3)	35	(3)
C3	1131	(2)	991	(8)	108	(3)	40	(3)
C4	793	(2)	165	(8)	-389	(3)	43	(3)
C5	465	(2)	344	(8)	-347	(3)	41	(3)
C6	441	(2)	1560	(7)	65	(3)	33	(3)
C7	506	(2)	4603	(7)	-697	(3)	43	(3)
C8	855	(2)	4503	(9)	-689	(4)	54	(4)
C9	921	(3)	3283	(11)	-1035	(5)	66	(5)
C10	632	(4)	2192	(11)	-1411	(4)	75	(6)
C11	253	(3)	2490	(10)	-1541	(4)	72	(5)
C12	196	(2)	3720	(8)	-1182	(4)	51	(4)
C13	663	(2)	4347	(8)	549	(4)	49	(4)
C14	489	(2)	5411	(8)	-124	(4)	55	(4)
C15	787	(3)	-715	(10)	-976	(4)	67	(5)
C16	732	(4)	528	(11)	-1546	(5)	112	(8)
C17	1525	(2)	-708	(7)	2561	(3)	33	(3)
C18	1328	(2)	-2082	(8)	2548	(4)	47	(4)
C19	1507	(3)	-3149	(9)	3102	(4)	58	(5)
C20	1870	(3)	-2903	(10)	3616	(4)	60	(4)
C21	2062	(2)	-1568	(11)	3632	(4)	63	(4)
C22	1892	(2)	-443	(9)	3098	(3)	48	(3)
C23	1010	(2)	1861	(7)	2217	(3)	32	(3)
C24	621	(2)	2088	(8)	1806	(3)	39	(3)
C25	418	(2)	2942	(9)	2059	(4)	56	(4)
C26	607	(3)	3531	(9)	2717	(4)	54	(4)
C27	997	(2)	3277	(8)	3130	(4)	48	(4)

C28	1198	(2)	2436	(8)	2892	(3)	41 (3)
C29	1660	(2)	2159	(7)	2017	(3)	31 (3)
C30	1648	(2)	3770	(8)	2128	(3)	40 (3)
C31	1921	(2)	4794	(9)	2113	(4)	51 (3)
C32	2196	(2)	4163	(10)	1993	(4)	55 (4)
C33	2213	(2)	2532	(10)	1893	(4)	52 (4)
C34	1939	(2)	1525	(8)	1895	(3)	39 (3)
Cl4	2575	(1)	6798	(5)	-1182	(2)	124 (2)
Cl5	3067	(1)	5781	(6)	188	(2)	162 (3)
Cl6	3024	(1)	9088	(6)	-163	(2)	171 (3)
C35	3008	(3)	7090	(14)	-438	(5)	90 (5)

a) Equivalent isotropic U defined as $\frac{1}{3}$ of the trace of the orthoganalised U_{ij} tensor.

TABLE 2.13 Selected Bond Lengths (Å) for $[Ru(\eta^6\text{-}C_{16}H_{16})Cl_2(PPh_3)].CHCl_3$ (18).

Ru1-P1	2.292	(2)	Ru1-Cl1	2.383	(2)
Ru1-Cl2	2.392	(2)	Ru1-C1	2.297	(6)
Ru1-C2	2.164	(6)	Ru1-C3	2.133	(6)
Ru1-C4	2.380	(6)	Ru1-C5	2.277	(6)
Ru1-C6	2.182	(6)	P1-C17	1.823	(6)
P1-C23	1.806	(6)	P1-C29	1.820	(6)
C1-C2	1.424	(8)	C1-C6	1.384	(8)
C1-C13	1.506	(9)	C2-C3	1.400	(9)
C3-C4	1.435	(9)	C4-C5	1.382	(9)
C4-C15	1.507	(9)	C5-C6	1.415	(9)
C7-C8	1.398	(10)	C7-C12	1.390	(10)
C7-C14	1.496	(10)	C8-C9	1.390	(11)
C9-C10	1.383	(13)	C10-C11	1.426	(13)
C10-C16	1.519	(12)	C11-C12	1.197	(11)
C13-C14	1.589	(10)	C15-C16	1.581	(11)
C17-C18	1.386	(9)	C17-C22	1.384	(9)
C18-C19	1.408	(10)	C19-C20	1.351	(11)
C20-C21	1.346	(12)	C21-C22	1.407	(10)
C23-C24	1.378	(9)	C23-C28	1.407	(9)
C24-C25	1.405	(9)	C25-C26	1.381	(11)
C26-C27	1.384	(11)	C27-C28	1.370	(9)
C29-C30	1.372	(9)	C29-C34	1.390	(9)
C30-C31	1.409	(9)	C31-C32	1.373	(11)
C32-C33	1.386	(11)	C33-C34	1.389	(9)

TABLE 2.14 Selected Bond Angles (°) for [Ru(η^6-$C_{16}H_{16}$)Cl_2(PPh_3)].$CHCl_3$ (18).

Cl1-Ru1-P1	87.8	(1)	Cl2-Ru1-P1	89.1	(1)
Cl2-Ru1-Cl1	89.0	(1)	C1-Ru1-P1	95.4	(1)
C1-Ru1-Cl1	153.2	(2)	C1-Ru1-Cl2	117.5	(2)
C17-P1-Ru1	121.6	(2)	C23-P1-Ru1	115.0	(2)
C23-P1-C17	101.4	(3)	C29-P1-Ru1	108.2	(2)
C29-P1-C17	103.7	(3)	C29-P1-C23	105.5	(3)
C6-C1-C2	118.3	(6)	C13-C1-Ru1	147.1	(4)
C13-C1-C2	118.8	(6)	C13-C1-C6	122.3	(6)
C3-C2-C1	119.2	(6)	C4-C3-C2	119.8	(6)
C5-C4-C3	117.3	(6)	C15-C4-Ru1	148.1	(5)
C15-C4-C3	121.0	(7)	C15-C4-C5	121.3	(7)
C6-C5-C4	120.5	(6)	C5-C6-C1	120.1	(6)
C12-C7-C8	118.6	(7)	C14-C7-C8	120.0	(7)
C14-C7-C12	120.6	(7)	C9-C8-C7	120.8	(8)
C10-C9-C8	119.3	(8)	C11-C10-C9	119.8	(8)
C16-C10-C9	119.9	(9)	C16-C10-C11	118.8	(11)
C12-C11-C10	118.6	(8)	C11-C12-C7	120.3	(8)
C14-C13-C1	108.8	(5)	C13-C14-C7	112.9	(5)
C16-C15-C4	109.5	(6)	C15-C16-C10	112.2	(6)
C18-C17-P1	118.9	(5)	C22-C17-P1	120.9	(5)
C24-C23-P1	120.4	(5)	C28-C23-P1	119.8	(5)
C30-C29-P1	122.1	(5)	C34-C29-P1	116.2	(5)

The angles within the phenyl rings of the PPh_3 ligands lie in the range 118-122° with e.s.d.s of less than 1°.

Table 2.15 **Crystallographic Data for [Ru(η^6-$C_{16}H_{16}$)Cl_2(NC_5H_5)] (20).**

Formula	$Ru_1Cl_2N_1C_{21}H_{21}$
fw, g	459.4
Space group	$P2_12_12_1$
a, Å	7.744(2)
b, Å	12.935(4)
c, Å	19.455(5)
α, deg	90.0
β, deg	90.0
γ, deg	90.0
V, Å^3	1949(1)
Z	4
F(000)	928
d_{calc}, g/cm^3	1.57
Crystal size, mm	0.45 x 0.17 x 0.02
Scan technique	ω-2Θ
μ(Mo-K_α), cm^{-1}	10.68
Orientation reflections, no.; range (2Θ)	32; ($6° \leq 2\Theta \leq 23°$)
Temperature, °C	20
Total No. of reflections measured	1937
No. of unique data	1916
Total with $I \geq 2.5\sigma(I)$	989
No. of parameters	116
R[a]	0.0713
R'[b]	0.0686
Weighting scheme	$w = 1.000/(\sigma^2F + 0.000411F^2)$
Largest shift/esd, final cycle	0.001
Largest peak, e/Å^3	1.66

a) $R = \Sigma[|F_o|-|F_c|]/\Sigma|F_o|$

b) $R' = \Sigma[(|F_o|-|F_c|) \cdot w^{\frac{1}{2}}]/\Sigma[|F_o| \cdot w^{\frac{1}{2}}]$

TABLE 2.16 **Atomic Coordinates ($x10^4$) and Equivalent Isotropic Displacement Parameters ($Å^2x10^3$) for $[Ru(\eta^6\text{-}C_{16}H_{16})Cl_2(NC_5H_5)]$ (20).**

Atom	x		y		z		U(eq)[a]	
Ru1	-152	(3)	7992	(2)	2123	(1)	33	(1)
Cl1	2363	(7)	6926	(6)	1998	(3)	47	(2)
Cl2	1452	(9)	9374	(5)	1598	(3)	51	(2)
C1	-397	(35)	7471	(19)	3275	(12)	40	(7)
C2	-113	(38)	8532	(17)	3203	(11)	39	(6)
C3	-1207	(28)	9135	(18)	2809	(12)	42	(6)
C4	-2689	(32)	8719	(20)	2484	(13)	42	(7)
C5	-2768	(29)	7625	(17)	2416	(11)	31	(6)
C6	-1594	(25)	7006	(22)	2793	(10)	36	(5)
C7	-2771	(37)	7478	(22)	4305	(13)	49	(8)
C8	-2587	(34)	8511	(20)	4400	(13)	39	(7)
C9	-3544	(34)	9225	(20)	4034	(12)	48	(7)
C10	-4811	(38)	8888	(17)	3561	(11)	47	(6)
C11	-5221	(33)	7848	(17)	3570	(17)	41	(6)
C12	-4202	(28)	7095	(23)	3928	(11)	44	(6)
C13	211	(34)	6832	(19)	3873	(10)	50	(6)
C14	-1232	(39)	6768	(24)	4426	(13)	64	(9)
C15	-4234	(29)	9382	(20)	2290	(11)	44	(7)
C16	-5305	(34)	9595	(18)	2976	(12)	59	(7)
N1	-758	(29)	7506	(17)	1125	(11)	52	(7)
C17	-1156	(35)	8201	(24)	619	(13)	62	(8)
C18	-1619	(46)	7845	(29)	-63	(18)	90	(11)
C19	-1632	(44)	6850	(30)	-165	(17)	84	(10)
C20	-1273	(49)	6187	(33)	338	(18)	108	(13)
C21	-878	(37)	6493	(25)	971	(16)	62	(9)

a) Equivalent isotropic U defined as $\frac{1}{3}$ of the trace of the orthoganalised U_{ij} tensor.

TABLE 2.17 Selected Bond Lengths (Å) for [Ru(η^6-$C_{16}H_{16}$)Cl_2(NC_5H_5)] (20).

Ru1-Cl1	2.398	(7)	Ru1-Cl2	2.405	(7)
Ru1-C1	2.35	(2)	Ru1-C2	2.21	(2)
Ru1-C3	2.15	(2)	Ru1-C4	2.29	(2)
Ru1-C5	2.16	(2)	Ru1-C6	2.14	(2)
Ru1-N1	2.10	(2)	C1-C2	1.40	(3)
C1-C6	1.45	(3)	C1-C13	1.50	(3)
C2-C3	1.38	(3)	C3-C4	1.42	(3)
C4-C5	1.42	(3)	C4-C15	1.52	(3)
C5-C6	1.42	(3)	C7-C8	1.36	(4)
C7-C12	1.42	(4)	C7-C14	1.52	(4)
C8-C9	1.38	(4)	C9-C10	1.41	(4)
C10-C11	1.38	(3)	C10-C16	1.51	(3)
C11-C12	1.43	(3)	C13-C14	1.55	(4)
C15-C16	1.60	(3)	N1-C17	1.36	(4)
N1-C21	1.35	(4)	C17-C18	1.45	(4)
C18-C19	1.30	(5)	C19-C20	1.33	(5)
C20-C21	1.33	(5)			

TABLE 2.18 **Selected Bond Angles (°) for [Ru(η^6-$C_{16}H_{16}$)Cl_2(NC_5H_5)] (20).**

Cl1-Ru1-Cl2	88.0	(2)	Cl1-Ru1-C1	89.9	(7)
Cl2-Ru1-C1	131.3	(6)	Cl1-Ru1-N1	85.6	(6)
Cl2-Ru1-N1	87.1	(6)	C1-Ru1-N1	141.2	(9)
C2-C1-C6	116	(2)	Ru1-C1-C13	151	(2)
C2-C1-C13	125	(2)	C6-C1-C13	118	(2)
C1-C2-C3	121	(2)	C2-C3-C4	122	(2)
C3-C4-C5	117	(2)	Ru1-C4-C15	146	(2)
C3-C4-C15	122	(2)	C5-C4-C15	120	(2)
C4-C5-C6	119	(2)	C1-C6-C5	121	(2)
C8-C7-C12	120	(3)	C8-C7-C14	119	(2)
C12-C7-C14	119	(2)	C7-C8-C9	122	(2)
C8-C9-C10	120	(2)	C9-C10-C11	117	(2)
C9-C10-C16	119	(2)	C11-C10-C16	123	(2)
C10-C11-C12	123	(2)	C7-C12-C11	116	(2)
C1-C13-C14	110	(2)	C7-C14-C13	115	(2)
C4-C15-C16	107	(2)	C10-C16-C15	113	(2)
Ru1-N1-C17	121	(2)	Ru1-N1-C21	121	(2)
C17-N1-C21	118	(2)	N1-C17-C18	120	(3)
C17-C18-C19	117	(3)	C18-C19-C20	122	(3)
C19-C20-C21	123	(4)	N1-C21-C20	121	(3)

Table 2.19 **Crystallographic Data for $[Ru(\eta^6\text{-}C_{16}H_{16})Cl(NC_5H_5)_2][PF_6]$ (25).**

Formula	$Ru_1C_{26}H_{26}N_2P_1F_6Cl_1$
fw, g	648.0
Space group	$P2_12_12_1$
a, Å	7.814(1)
b, Å	20.251(3)
c, Å	32.785(5)
α, deg	90.0
β, deg	90.0
γ, deg	90.0
V, Å^3	5187(1)
Z	8
F(000)	2608
d_{calc}, g/cm^3	1.66
Crystal size, mm	0.40 x 0.15 x 0.10
Scan technique	ω
μ(Mo-K_α), cm^{-1}	7.74
Orientation reflections, no.; range (2Θ)	32; ($20^\circ \leq 2\Theta \leq 30^\circ$)
Temperature, °C	20
Total No. of reflections measured	6684
No. of unique data	6648
Total with $I \geq 2.5\sigma(I)$	3399
No. of parameters	531
R[a]	0.0921
R'[b]	0.0752
Weighting scheme	$w = 1.000/(\sigma^2F + 0.000024F^2)$
Largest shift/esd, final cycle	0.011
Largest peak, e/Å^3	0.94

a) $R = \Sigma[|F_o|-|F_c|] / \Sigma|F_o|$

b) $R' = \Sigma[(|F_o|-|F_c|) \cdot w^{\frac{1}{2}}] / \Sigma[|F_o| \cdot w^{\frac{1}{2}}]$

TABLE 2.20 Atomic Coordinates (x10^4) and Equivalent Isotropic Displacement Parameters (Å^{2}x10^3) for [Ru(η^6-$C_{16}H_{16}$)Cl(NC_5H_5)$_2$][PF_6] (25).

Atom	x		y		z		U(eq)[a]	
Ru1	5187	(2)	4233	(1)	2207	(1)	36	(1)
Cl1	2943	(9)	4222	(3)	1705	(2)	70	(3)
N1	5764	(22)	5249	(8)	2054	(5)	40	(6)
N2	3343	(25)	4650	(9)	2611	(6)	51	(7)
C1	6572	(30)	3341	(10)	1877	(6)	42	(6)
C2	7670	(28)	3865	(10)	1945	(6)	41	(6)
C3	7870	(27)	4119	(10)	2349	(6)	38	(5)
C4	7049	(27)	3808	(10)	2688	(6)	38	(5)
C5	5635	(25)	3385	(9)	2594	(5)	30	(5)
C6	5341	(27)	3161	(8)	2184	(6)	37	(4)
C7	8828	(30)	2364	(11)	2020	(7)	48	(6)
C8	10222	(30)	2773	(10)	2119	(6)	45	(5)
C9	10474	(35)	3022	(11)	2505	(7)	61	(7)
C10	9379	(32)	2870	(11)	2831	(7)	62	(7)
C11	8188	(29)	2318	(11)	2748	(7)	51	(6)
C12	7944	(31)	2082	(11)	2370	(7)	51	(6)
C13	6783	(36)	2905	(13)	1485	(8)	69	(8)
C14	8008	(32)	2312	(12)	1597	(7)	52	(6)
C15	7738	(35)	3900	(13)	1324	(7)	61	(7)
C16	9080	(33)	3310	(12)	3190	(7)	61	(7)
C17	5605	(35)	5451	(11)	1654	(6)	61	(9)
C18	6132	(37)	6105	(13)	1561	(7)	66	(10)
C19	6677	(42)	6526	(12)	1863	(9)	74	(12)
C20	6723	(40)	6310	(11)	2274	(9)	76	(12)
C21	6296	(38)	5647	(10)	2345	(7)	66	(11)
C22	2196	(31)	5121	(13)	2467	(9)	71	(11)
C23	1091	(33)	5438	(13)	2741	(10)	72	(11)
C24	1174	(38)	5275	(14)	3158	(11)	83	(13)
C25	2195	(32)	4780	(13)	3299	(8)	66	(10)
C26	3360	(37)	4496	(13)	3034	(8)	65	(11)
Ru2	9599	(2)	4859	(1)	331	(1)	37	(1)

Cl2	7445	(9)	4688	(3)	830	(2)	72	(3)
N3	7801	(27)	5455	(10)	4	(7)	64	(9)
N4	10276	(26)	5776	(9)	614	(6)	56	(7)
C27	11545	(29)	4595	(10)	-168	(6)	41	(6)
C28	12329	(28)	4762	(11)	189	(6)	42	(6)
C29	11962	(32)	4406	(11)	544	(7)	54	(7)
C30	10794	(27)	3854	(10)	538	(6)	40	(5)
C31	7935	(28)	3811	(8)	181	(5)	33	(5)
C32	10080	(27)	4162	(9)	-167	(5)	39	(5)
C33	13930	(33)	3706	(12)	-387	(8)	65	(7)
C34	14981	(34)	3803	(10)	-36	(7)	57	(6)
C35	14639	(36)	3463	(11)	329	(7)	65	(7)
C36	13291	(34)	3014	(12)	359	(8)	65	(7)
C37	12478	(32)	2789	(11)	-26	(7)	52	(6)
C38	12791	(30)	3147	(11)	-382	(7)	51	(6)
C39	12434	(33)	4812	(13)	-574	(7)	62	(7)
C40	13728	(34)	4235	(14)	-706	(8)	70	(7)
C41	10820	(33)	3321	(12)	870	(7)	65	(7)
C42	12463	(41)	2888	(14)	774	(9)	87	(10)
C43	7770	(32)	5412	(11)	-432	(9)	67	(11)
C44	6626	(41)	5831	(17)	-626	(10)	94	(14)
C45	5627	(49)	6272	(18)	-428	(17)	125	(22)
C46	5721	(41)	6312	(19)	-13	(15)	118	(19)
C47	6774	(29)	5881	(13)	195	(12)	99	(15)
C48	10359	(36)	5796	(14)	1040	(8)	82	(11)
C49	10992	(49)	6387	(22)	1203	(11)	131	(19)
C50	11496	(53)	6893	(20)	952	(20)	174	(31)
C51	11374	(45)	6835	(13)	542	(14)	105	(17)
C52	10700	(36)	6278	(12)	369	(10)	84	(12)
P1	3503	(10)	1149	(4)	1439	(2)	57	(3)
P2	6095	(13)	8082	(6)	961	(4)	95	(4)
F1A	4469	(36)	1579	(11)	1106	(7)	93	(11)
F2A	4985	(42)	1171	(19)	1778	(7)	136	(16)
F3A	1752	(45)	1325	(23)	1222	(14)	151	(19)
F4A	2702	(59)	629	(17)	1739	(10)	157	(20)
F5A	3441	(34)	1863	(11)	1646	(8)	101	(11)

F6A	3306	(73)	494	(18)	1223	(19)	222	(31)
F1B	4970	(55)	1323	(19)	1147	(12)	30	(10)
F2B	5145	(78)	880	(24)	1562	(17)	62	(14)
F3B	2683	(118)	945	(46)	1052	(26)	105	(29)
F4B	2400	(61)	1001	(23)	1831	(15)	40	(12)
F5B	1922	(114)	1417	(40)	1550	(28)	124	(26)
F6B	4704	(110)	554	(39)	1245	(23)	120	(26)
F7	6101	(52)	7305	(11)	924	(9)	232	(21)
F8	4468	(41)	8001	(15)	740	(16)	320	(29)
F9	5933	(60)	8741	(11)	1048	(8)	271	(26)
F10	5668	(61)	7948	(15)	1413	(10)	335	(28)
F11	6781	(40)	8150	(18)	558	(6)	222	(19)
F12	7769	(30)	7956	(24)	1126	(9)	245	(23)

a) Equivalent isotropic U defined as $\frac{1}{3}$ of the trace of the orthoganalised U_{ij} tensor.

TABLE 2.21 **Selected Bond Lengths (Å) for $[Ru(\eta^6\text{-}C_{16}H_{16})Cl(NC_5H_5)_2][PF_6]$ (25).**

Ru1-Cl1	2.404	(6)	Ru1-N1	2.17	(2)
Ru1-N2	2.13	(2)	Ru1-C1	2.37	(2)
Ru1-C2	2.25	(2)	Ru1-C3	2.16	(2)
Ru1-C4	2.31	(2)	Ru1-C5	2.16	(2)
Ru1-C6	2.18	(2)	N1-C17	1.38	(2)
N1-C21	1.32	(3)	N2-C22	1.39	(3)
N2-C26	1.42	(3)	C1-C2	1.38	(3)
C1-C6	1.44	(3)	C1-C13	1.57	(3)
C2-C3	1.43	(3)	C3-C4	1.43	(3)
C4-C5	1.43	(3)	C4-C15	1.54	(3)
C5-C6	1.44	(2)	C7-C8	1.41	(3)
C7-C12	1.46	(3)	C7-C14	1.53	(3)
C8-C9	1.38	(3)	C9-C10	1.43	(3)
C10-C11	1.48	(3)	C10-C16	1.50	(3)
C11-C12	1.34	(3)	C13-C14	1.58	(3)
C15-C16	1.60	(3)	C17-C18	1.42	(3)
C18-C19	1.38	(4)	C19-C20	1.42	(4)
C20-C21	1.40	(3)	C22-C23	1.40	(3)
C23-C24	1.41	(4)	C24-C25	1.36	(4)
C25-C26	1.39	(3)	Ru2-Cl2	2.373	(6)
Ru2-N3	2.14	(2)	Ru2-N4	2.14	(2)
Ru2-C27	2.30	(2)	Ru2-C28	2.19	(2)
Ru2-C29	2.18	(2)	Ru2-C30	2.34	(2)
Ru2-C31	2.18	(2)	Ru2-C32	2.19	(2)
N3-C43	1.44	(3)	N3-C47	1.33	(3)
N4-C48	1.40	(3)	N4-C52	1.34	(3)
C27-C28	1.37	(3)	C27-C32	1.44	(3)
C27-C39	1.56	(3)	C28-C29	1.40	(3)
C29-C30	1.44	(3)	C30-C31	1.44	(3)
C30-C41	1.53	(3)	C31-C32	1.37	(2)
C33-C34	1.43	(3)	C33-C38	1.44	(3)
C33-C40	1.51	(3)	C34-C35	1.41	(3)
C35-C36	1.39	(3)	C36-C37	1.48	(3)
C36-C42	1.53	(4)	C37-C38	1.39	(3)

C39-C40	1.61	(3)	C41-C42	1.59	(4)
C43-C44	1.39	(4)	C44-C45	1.35	(5)
C45-C46	1.37	(5)	C46-C47	1.38	(5)
C48-C49	1.40	(4)	C49-C50	1.37	(6)
C50-C51	1.35	(6)	C51-C52	1.36	(4)

TABLE 2.22 Selected Bond Angles (°) for $[Ru(\eta^6\text{-}C_{16}H_{16})Cl(NC_5H_5)_2][PF_6]$ (25).

N1-Ru1-Cl1	90.1	(5)	N2-Ru1-Cl1	86.4	(6)
N2-Ru1-N1	84.8	(6)	C1-Ru1-Cl1	90.8	(6)
C1-Ru1-N1	121.6	(7)	C1-Ru1-N2	153.5	(7)
N3-Ru2-Cl2	87.8	(7)	N4-Ru2-Cl2	90.2	(6)
N4-Ru2-N3	83.7	(7)	C27-Ru2-Cl2	157.9	(5)
C27-Ru2-N3	102.2	(8)	C27-Ru2-N4	110.3	(7)
C17-N1-Ru1	119	(2)	C21-N1-Ru1	119	(1)
C21-N1-C17	123	(2)	C22-N2-Ru1	120	(2)
C26-N2-Ru1	121	(2)	C26-N2-C22	119	(2)
C43-N3-Ru2	118	(2)	C47-N3-Ru2	121	(2)
C47-N3-C43	120	(3)	C48-N4-Ru2	118	(2)
C52-N4-Ru2	117	(2)	C52-N4-C48	124	(2)
C6-C1-C2	120	(2)	C13-C1-Ru1	148	(2)
C13-C1-C2	120	(2)	C13-C1-C6	120	(2)
C3-C2-C1	119	(2)	C4-C3-C2	121	(2)
C5-C4-C3	116	(2)	C15-C4-Ru1	144	(2)
C15-C4-C3	121	(2)	C15-C4-C5	123	(2)
C6-C5-C4	121	(2)	C5-C6-C1	118	(2)
C12-C7-C8	115	(2)	C14-C7-C8	125	(2)
C14-C7-C12	119	(2)	C9-C8-C7	123	(2)
C10-C9-C8	122	(2)	C11-C10-C9	114	(2)
C16-C10-C9	124	(2)	C16-C10-C11	120	(2)
C12-C11-C10	122	(2)	C11-C12-C7	121	(2)
C14-C13-C1	108	(2)	C13-C14-C7	114	(2)
C16-C15-C4	105	(2)	C15-C16-C10	116	(2)
C18-C17-N1	117	(2)	C19-C18-C17	121	(2)
C20-C19-C18	120	(2)	C21-C20-C19	117	(3)
C20-C21-N1	123	(2)	C23-C22-N2	120	(3)
C24-C23-C22	119	(3)	C25-C24-C23	122	(3)
C26-C25-C24	119	(3)	C25-C26-N2	121	(3)
C32-C27-C28	120	(2)	C39-C27-Ru2	147	(2)
C39-C37-C28	118	(2)	C39-C27-C32	122	(2)
C29-C28-C27	120	(2)	C30-C29-C28	121	(2)
C31-C30-C29	115	(2)	C41-C30-Ru2	146	(2)

C41-C30-C29	122	(2)	C41-C30-C31	123	(2)
C32-C31-C30	122	(2)	C31-C32-C27	118	(2)
C38-C33-C34	117	(2)	C40-C33-C34	121	(2)
C40-C33-C38	120	(2)	C35-C34-C33	121	(2)
C36-C35-C34	122	(2)	C37-C36-C35	117	(2)
C42-C36-C35	119	(2)	C42-C36-C37	122	(2)
C38-C37-C36	119	(2)	C37-C38-C33	122	(2)
C40-C39-C27	108	(2)	C39-C40-C33	113	(2)
C42-C41-C30	105	(2)	C41-C42-C36	115	(2)
C44-C43-N3	115	(3)	C45-C44-C43	124	(4)
C46-C45-C44	119	(4)	C47-C46-C45	119	(4)
C46-C47-N3	123	(4)	C49-C48-N4	115	(3)
C50-C49-C48	121	(4)	C51-C50-C49	120	(3)
C52-C51-C50	121	(4)	C51-C52-N4	118	(3)

Table 2.23 Crystallographic Data for [Ru(η^6-$C_{16}H_{16}$)Cl(1,10-phen)][PF_6] (31).

Formula	$Ru_1C_{28}N_2H_{24}P_1F_6$
fw, g	670.0
Space group	Pcab
a, Å	11.588(3)
b, Å	11.844(3)
c, Å	37.998(9)
α, deg	90.0
β, deg	90.0
γ, deg	90.0
V, Å^3	5217(2)
Z	8
F(000)	2688
d_{calc}, g/cm^3	1.71
Crystal size, mm	0.60 x 0.40 x 0.05
Scan technique	ω
μ(Mo-K_α), cm^{-1}	8.16
Orientation reflections, no.; range (2Θ)	25; (13° ≤ 2Θ ≤ 25°)
Temperature, °C	20
Total No. of reflections measured	5064
No. of unique data	4503
Total with I ≥ 2σ(I)	2778
No. of parameters	388
R[a]	0.0513
R'[b]	0.0598
Weighting scheme	$w = 1.000/(\sigma^2F + 0.005003F^2)$
Largest shift/esd, final cycle	0.029
Largest peak, e/Å^3	0.48

a) $R = \Sigma[|F_o|-|F_c|]/\Sigma|F_o|$

b) $R' = \Sigma[(|F_o|-|F_c|) \cdot w^{\frac{1}{2}}]/\Sigma[|F_o| \cdot w^{\frac{1}{2}}]$

TABLE 2.24 **Atomic Coordinates ($x10^4$) and Equivalent Isptropic Displacement Parameters ($Å^2x10^3$) for $[Ru(\eta^6\text{-}C_{16}H_{16})Cl(1,10\text{-phen})][PF_6]$ (31).**

Atom	x		y		z		U(eq)[a]	
Ru1	2283	(1)	148	(1)	1042	(1)	35	(1)
Cl1	3352	(2)	-99	(2)	508	(1)	45	(1)
N1	1078	(6)	-896	(5)	809	(2)	44	(2)
N2	1307	(5)	1305	(5)	756	(2)	37	(2)
C1	3558	(7)	1019	(7)	1424	(2)	40	(3)
C2	2408	(7)	1282	(7)	1490	(2)	43	(3)
C3	1599	(7)	438	(7)	1568	(2)	38	(2)
C4	1930	(7)	-686	(7)	1588	(2)	40	(3)
C5	3009	(8)	-977	(7)	1442	(2)	48	(3)
C6	3820	(8)	-141	(7)	1355	(2)	48	(3)
C7	4182	(9)	1065	(11)	2108	(2)	69	(4)
C8	3091	(9)	1271	(10)	2242	(2)	70	(4)
C9	2329	(10)	407	(11)	2310	(2)	75	(4)
C10	2630	(10)	-705	(11)	2247	(2)	70	(4)
C11	3768	(11)	-942	(11)	2187	(2)	74	(4)
C12	4520	(10)	-61	(12)	2117	(3)	78	(5)
C13	4511	(8)	1860	(8)	1479	(2)	60	(3)
C14	4795	(9)	1889	(11)	1887	(3)	83	(4)
C15	1250	(8)	-1528	(8)	1787	(3)	63	(3)
C16	1690	(11)	-1576	(10)	2172	(3)	82	(4)
C17	1045	(8)	-2023	(6)	827	(2)	51	(3)
C18	155	(9)	-2616	(8)	664	(3)	67	(4)
C19	-674	(9)	-2083	(9)	491	(3)	65	(4)
C20	-645	(7)	-918	(8)	445	(2)	53	(3)
C21	276	(7)	-349	(7)	622	(2)	43	(3)
C22	-1440	(8)	-262	(9)	249	(3)	63	(4)
C23	-1324	(8)	862	(10)	221	(2)	64	(4)
C24	-408	(7)	1468	(8)	387	(2)	54	(3)
C25	379	(7)	846	(7)	589	(2)	42	(3)
C26	-205	(9)	2614	(9)	369	(3)	65	(4)
C27	710	(10)	3070	(8)	527	(2)	68	(4)

C28	1470	(8)	2398	(7)	727	(2)	50	(3)
P1	2784	(2)	5183	(2)	1410	(1)	58	(1)
F1	2215	(9)	4110	(7)	1555	(4)	171	(6)
F2	3321	(10)	6260	(7)	1249	(3)	162	(5)
F3	3627	(23)	4856	(23)	1719	(5)	137	(11)
F4	3531	(26)	4431	(15)	1155	(6)	101	(8)
F5	1975	(26)	5487	(24)	1114	(9)	176	(14)
F6	2088	(26)	5881	(21)	1668	(9)	140	(13)
F3A	3111	(29)	5945	(27)	1728	(6)	158	(13)
F4A	4004	(15)	4788	(21)	1374	(12)	165	(17)
F5A	2423	(41)	4563	(29)	1084	(8)	215	(20)
F6A	1548	(18)	5732	(20)	1468	(11)	135	(14)

a) Equivalent isotropic U defined as $\frac{1}{3}$ of the trace of the orthoganalised U_{ij} tensor.

TABLE 2.25 **Selected Bond Lengths (Å) for [Ru(η^6-$C_{16}H_{16}$)Cl(1,10-phen)][PF_6] (31).**

Ru1-Cl1	2.394	(2)	Ru1-N1	2.064	(6)
Ru1-N2	2.083	(6)	Ru1-C1	2.314	(8)
Ru1-C2	2.174	(8)	Ru1-C3	2.178	(8)
Ru1-C4	2.337	(7)	Ru1-C5	2.192	(8)
Ru1-C6	2.170	(9)	N1-C17	1.338	(10)
N1-C21	1.338	(10)	N2-C25	1.362	(10)
N2-C28	1.313	(10)	C1-C2	1.392	(11)
C1-C13	1.502	(12)	C2-C3	1.402	(11)
C3-C4	1.389	(11)	C4-C5	1.411	(12)
C4-C15	1.478	(12)	C5-C6	1.404	(12)
C7-C8	1.386	(15)	C7-C12	1.390	(18)
C7-C14	1.470	(16)	C8-C9	1.376	(17)
C9-C10	1.384	(18)	C10-C11	1.367	(17)
C10-C16	1.527	(17)	C11-C12	1.385	(18)
C13-C14	1.587	(13)	C15-C16	1.550	(14)
C17-C18	1.394	(13)	C18-C19	1.323	(14)
C19-C20	1.392	(14)	C20-C21	1.430	(12)
C20-C22	1.416	(13)	C21-C25	1.426	(11)
C22-C23	1.343	(16)	C23-C24	1.428	(13)
C24-C25	1.401	(12)	C24-C26	1.379	(14)
C26-C27	1.333	(15)	C27-C28	1.409	(13)

TABLE 2.26 Selected Bond Angles (°) for [Ru(η^6-$C_{16}H_{16}$)Cl(1,10-phen)][PF_6] (31).

Cl1-Ru1-N1	85.0	(2)	Cl1-Ru1-N2	85.4	(2)
N1-Ru1-N2	78.6	(2)	Cl1-Ru1-C1	104.8	(2)
N1-Ru1-C1	165.4	(3)	N2-Ru1-C1	112.4	(3)
Ru1-N1-C17	126.5	(6)	Ru1-N1-C21	114.1	(5)
C17-N1-C21	119.4	(7)	Ru1-N2-C25	114.2	(5)
Ru1-N2-C28	127.9	(5)	C25-N2-C28	117.9	(7)
C2-C1-C6	116.8	(7)	Ru1-C1-C13	148.5	(6)
C2-C1-C13	122.0	(7)	C6-C1-C13	120.4	(7)
C1-C2-C3	121.3	(7)	C2-C3-C4	120.7	(7)
C3-C4-C5	117.2	(7)	Ru1-C4-C15	146.4	(6)
C3-C4-C15	121.9	(7)	C5-C4-C15	120.6	(8)
C4-C5-C6	120.9	(8)	C1-C6-C5	119.5	(8)
C8-C7-C12	114.6	(11)	C8-C7-C14	122.3	(11)
C12-C7-C14	121.0	(10)	C7-C8-C9	121.6	(11)
C8-C9-C10	120.9	(11)	C9-C10-C11	117.9	(11)
C9-C10-C16	119.7	(11)	C11-C10-C16	121.3	(11)
C10-C11-C12	119.0	(12)	C7-C12-C11	123.4	(11)
C1-C13-C14	107.6	(7)	C7-C14-C13	116.3	(9)
C4-C15-C16	109.4	(8)	C10-C16-C15	112.7	(8)
N1-C17-C18	120.0	(8)	C17-C18-C19	121.2	(9)
C18-C19-C20	121.2	(9)	C19-C20-C21	115.2	(8)
C19-C20-C22	126.5	(9)	C21-C20-C22	118.3	(9)
N1-C21-C20	122.7	(8)	N1-C21-C25	118.0	(7)
C20-C21-C25	119.3	(7)	C20-C22-C23	121.4	(9)
C22-C23-C24	122.5	(9)	C23-C24-C25	117.5	(9)
C23-C24-C26	126.9	(9)	C25-C24-C26	115.7	(8)
N2-C25-C21	114.9	(7)	N2-C25-C24	124.0	(7)
C21-C25-C24	121.0	(7)	C24-C26-C27	120.0	(9)
C26-C27-C28	120.7	(9)	N2-C28-C27	120.8	(8)

CHAPTER 3.

REACTIONS OF [Ru(η^6-[2$_2$]PARACYCLOPHANE)Cl$_2$]$_2$ LEADING TO BINUCLEAR TRIPLY-BRIDGED CATIONS.

3.1 INTRODUCTION.

In Sections 1.4.2 and 1.4.3 some reactions of $[M(\eta^6\text{-arene})Cl_2]_2$ compounds were outlined, which result in the formation of binuclear or tetranuclear cations. Binuclear triply chloro-bridged compounds $[(\eta^6\text{-arene})M(\mu\text{-}Cl)_3M(\eta^6\text{-arene})][X]$ can be prepared by a variety of synthetic methods for a number of arenes[63,98-101,108]. Triply hydroxide- or alkoxide-bridged compounds $[(\eta^6\text{-arene})M(\mu\text{-}OR)_3M(\eta^6\text{-arene})][X]$ (R=H,Me,Et,Ph) are prepared by reaction of $[M(\eta^6\text{-arene})Cl_2]_2$ with sodium carbonate or hydroxide ions, or alkoxide ions $[OR]^-$ respectively[98,102,103]. However, under particular reaction conditions, and when the arene is benzene, novel tetranuclear compounds (Figs. 1.24 and 1.25) are formed. The work presented in this Chapter is an investigation into the reactivity of $[Ru(\eta^6\text{-}C_{16}H_{16})Cl_2]_2$ (1) under analogous reaction conditions to those described above, and describes some subsequent reactions of the compounds thus obtained.

3.2 RESULTS AND DISCUSSION.

3.2.1 The Reactions of $[Ru(\eta^6\text{-}C_{16}H_{16})Cl_2]_2$ (1) with Alkoxide Ions, $[OR]^-$, in Alcohols, ROH.

(i) The reaction of $[Ru(\eta^6\text{-}C_{16}H_{16})Cl_2]_2$ (1) with sodium methoxide in methanol.

The reaction of $[Ru(\eta^6\text{-}C_{16}H_{16})Cl_2]_2$ (1) with Na[OMe] in methanol at *ca.* 315 K gives a yellow/orange solution from which an orange solid can be precipitated by addition of $Na[BPh_4]$. The ^1H n.m.r. spectrum (Table 3.4), recorded in CD_2Cl_2, exhibits resonances due to the cyclophane at δ 6.62 (s, 4H): noncoordinated ring; 4.55 (s, 4H): coordinated ring; 2.65 and 3.09 ppm (AA'XX', each 4H): $-C\underline{H}_2C\underline{H}_2-$. The methoxide protons give rise to a singlet resonance at δ 4.22 (9H), while the protons of the $[BPh_4]^-$ anion give rise to resonances at 6.91 (t, 4H), 7.06 (t, 8H), and 7.34 ppm (m, 8H). Integration of the spectrum is consistent with a $C_{16}H_{16}$:$[OMe]^-$:$[BPh_4]^-$ ratio of 2:3:1, suggesting the formulation $[Ru_2(\eta^6\text{-}C_{16}H_{16})_2(OMe)_3][BPh_4]$ (37) (Fig. 3.1). The infrared spectrum exhibits no bands near 300 cm^{-1} attributable to ν(Ru-Cl), but does contain a strong ν(C-O) band at 1046 cm^{-1}. The bands at 708, 722 and 734 cm^{-1} confirm the presence of the $[BPh_4]^-$ counter-ion.

A reaction solution stored at *ca.* 258 K for several weeks yielded crystals suitable for crystallographic investigation. The structure is remarkable in that the cation and anion

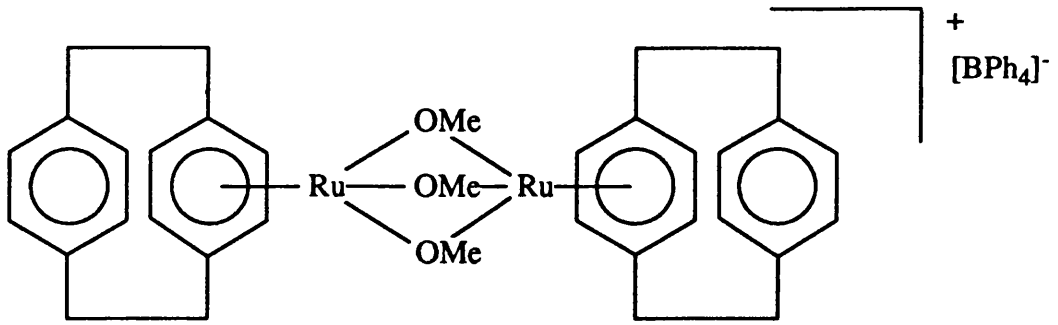

Fig. 3.1 The compound $[(\eta^6\text{-}C_{16}H_{16})Ru(OMe)_3Ru(\eta^6\text{-}C_{16}H_{16})][BPh_4]$ (37).

have co-crystallised with one equivalent of [2$_2$]paracyclophane. Integration of the ^{1}H n.m.r. spectrum of the crystalline material confirmed the 1:1:1 ratio of $[Ru_2(\eta^6\text{-}C_{16}H_{16})(OMe)_3]^+$:$[BPh_4]^-$:$C_{16}H_{16}$. The cyclophane was present in the reaction solution either as an impurity in the starting material (1), or as a result of partial decomposition of the product during the reaction. Due to problems of disorder in the "$Ru_2(OMe)_3$" subunit and in one of the crystallographically unique half-cyclophane molecules, the structure is presented only in outline. Although the best mathematical model for refinement of the structure was one with only one set of atomic positions for the methoxide ligands, there was evidence for a second, minor set of positions. The structure of the cation is presented in Fig. 3.2 with some important structural parameters for the well defined parts of the cation. The $[BPh_4]^-$ anion is well-defined and is generally unremarkable.

The cation has confacial-bioctahedral geometry with a Ru-Ru distance of 2.993(1) Å, which is similar to that found for the related cations $[Ru_2(\eta^6\text{-}C_6H_6)_2(OMe)_3]^+$, 3.005(1) Å[103], and $[Ru_2(\eta^6\text{-}C_6H_3Me_3)_2(OH)_3]^+$, 2.989(3) Å[104]. The Ru-C distances fall into two groups, firstly the Ru to bridgehead carbon atom distances, which lie in the range 2.27-2.31(1) Å, and secondly the Ru to non-bridgehead carbon atom distances, which lie in the range 2.14-2.17(1) Å. In contrast to the structures of the mononuclear compounds (18), (20), and (25) described in Chapter 2, there is no significant variation in bond length within these two groups, since the three coordination sites *trans* to the arene are occupied by identical groups. The inter-ring separations of the coordinated cyclophane ligands are *ca.* 3.00 Å, while the torsion angles in the ethylenic bridges are *ca.* 2°. The inter-ring separation is similar to that observed in the structures presented in Chapter 2, while the torsion angles are rather smaller. The smaller torsion angles may also be due to the uniform electronic influence of the three *trans* ligands. The geometry of the well-*d*efined

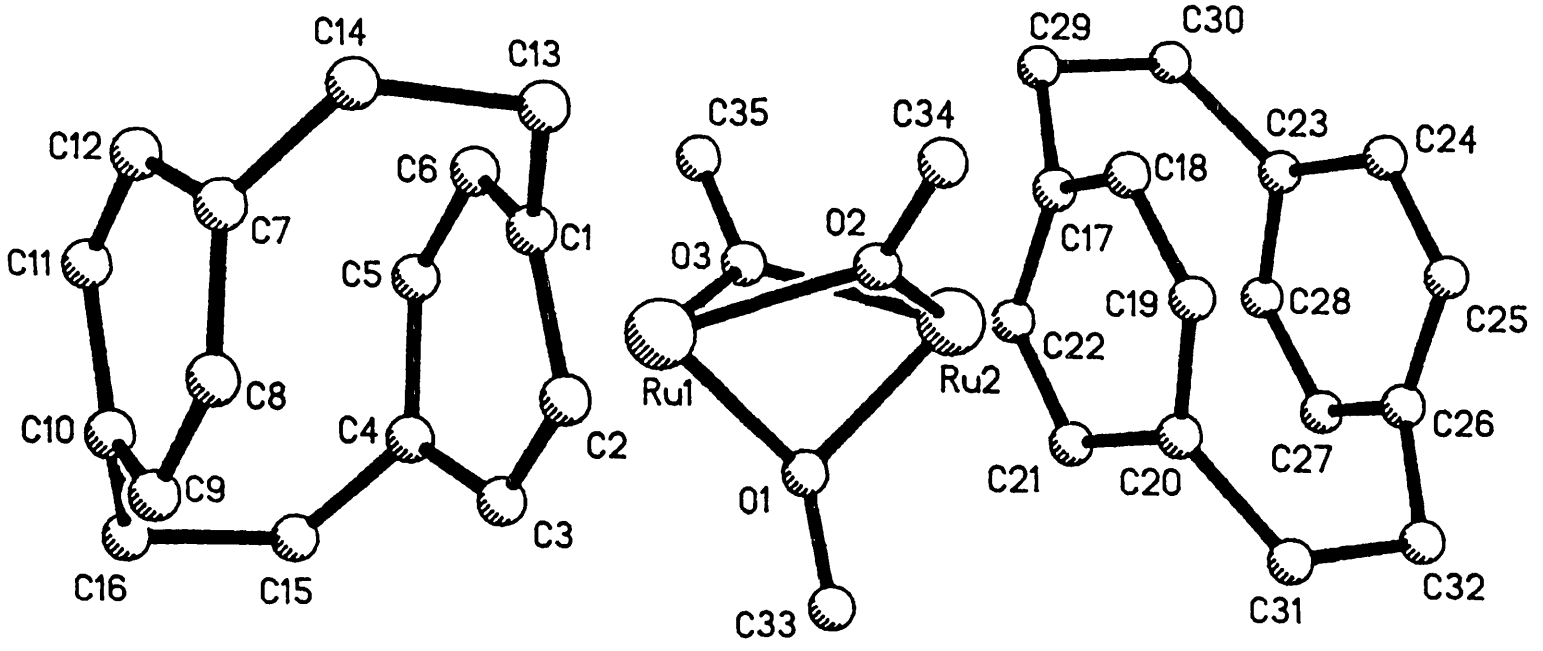

Lengths, Å.

Ru1-Ru2	2.993(1)
Inter-ring sep.	*av.* 3.00
Ru-C(bridgehead)	2.27-2.31(1)
Ru-C(non-bridgehead)	2.14-21.7(1)

Angles, °.

Torsion *av.* 2

Fig. 3.2 The stucture of the cation $[Ru_2(\eta^6\text{-}C_{16}H_{16})_2(OMe)_3]^+$ (37), with some important structural parameters.

cyclophane of crystallisation is similar to that found by Trueblood *et al*[7].

(ii) $[Ru_2(\eta^6\text{-}C_{16}H_{16})_2(OMe)_3][PF_6]$ (38).

Compound (38) was prepared and characterised similarly to (37). The details are given in the experimental section.

If the reaction solution is not warmed, or if the reaction time is too short, a mixture of products is isolated. The ^1H n.m.r. spectrum of such a mixture clearly indicates the presence of each of the binuclear cations $[Ru_2(\eta^6\text{-}C_{16}H_{16})_2Cl_3]^+$, $[Ru_2(\eta^6\text{-}C_{16}H_{16})_2Cl_2(OMe)]^+$ and $[Ru_2(\eta^6\text{-}C_{16}H_{16})_2Cl(OMe)_2]^+$ in addition to the desired product, $[Ru_2(\eta^6\text{-}C_{16}H_{16})_2(OMe)_3]^+$.

(iii) The Reaction of $[Ru(\eta^6\text{-}C_{16}H_{16})Cl_2]_2$ (1) with sodium ethoxide in ethanol.

The reaction of $[Ru(\eta^6\text{-}C_{16}H_{16})Cl_2]_2$ with sodium ethoxide in ethanol at *ca.* 315 K gives an orange solution from which an orange solid can be precipitated by addition of $K[PF_6]$. This solid, $[Ru_2(\eta^6\text{-}C_{16}H_{16})_2(OEt)_3][PF_6]$, (39) was characterised similarly to (37). The full details are given in the experimental section.

The crystal structure of this compound has been determined and represents a considerable improvement on that obtained for (37). The crystals used for the experiment were obtained from a reaction solution which had been stored at *ca.* 253 K. The full details of the structure determination and refinement are given in Section 3.3.4, while the crystal data, fractional coordinates, bond lengths, and bond angles are presented in Tables 3.6-3.9. A thermal ellipsoid plot of the cation is presented in Fig. 3.3 with some important structural parameters.

The cation has a confacial-bioctahedral geometry with a non-bonded Ru-Ru distance of 3.015(1) Å. This distance is very similar to the corresponding distances observed in the related cations (37): 2.993(1) Å, $[Ru_2(\eta^6\text{-}C_6H_6)_2(OMe)_3]^+$ (40): 3.005(2) Å[103], and $[Ru_2(\eta^6\text{-}C_6H_3Me_3)_2(OH)_3]^+$: 2.989(3) Å[104]. The Ru-O distances lie in the range 2.055-2.084(5) Å and have an average value of 2.068(5) Å, which is indistinguishable from that of 2.060(8) Å observed in compound (40)[103]. The averaged distance from the ruthenium ions to the centroids of the non-bridgehead carbon atoms of the coordinated cyclophane rings is 1.65 Å, and is identical to the metal to benzene ring centroid distances observed for (40)[103]. The Ru-O-Ru angles lie in the range 93.4-94.4(2)° and have an

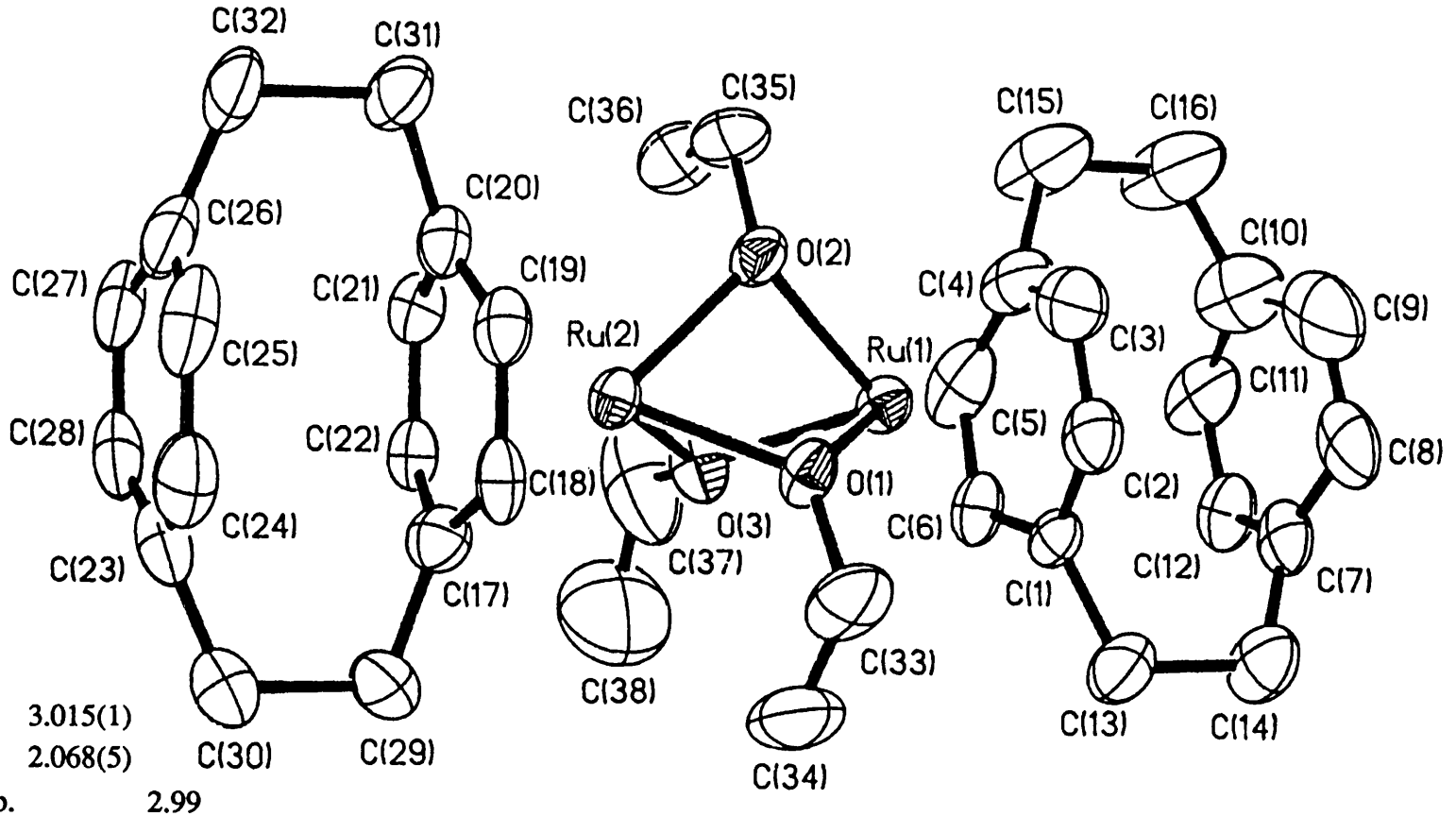

Lengths, Å.	
Ru1-Ru2	3.015(1)
Ru-O	2.068(5)
Inter-ring sep.	2.99
Ru-C(bridgehead)	2.27-2.33(1)
Ru-C(non-bridgehead)	2.16-2.22(1)

Angles, °.	
O-Ru-O	69.8-74.4(2)
Ru-O-Ru	93.4-94.4(2)
Torsion	*av.* 2.9

Fig. 3.3 A thermal ellipsoid plot of $[Ru_2(\eta^6\text{-}C_{16}H_{16})_2(OEt)_3][PF_6]$ (38), with some important structural parameters.

average value of 93.6(2)°. The corresponding angles in (40)[103] average 93.7(3)°. The O-Ru-O angles lie in the range 69.8-74.4(2)° with an average value of 72.7(2)° (c.f. 72.6(3)° for (40)[103]). Thus the parameters defining the "Ru_2O_3" subunits of (39) and (40)[103] are remarkably similar.

As observed for (37) the Ru-C distances fall into two distinct groups. The Ru to bridgehead carbon atom distances lie in the range 2.269-2.332(8) Å, while the Ru to non-bridgehead carbon atom distances fall in the range 2.155-2.215(8) Å. These figures are broadly similar to those observed for (37). The inter-ring separations in the cyclophane ligands show a 0.10 Å decrease to 2.99 Å when compared with the free ligand[7]. The torsion angles in the cyclophane bridging functions fall in the range 1.0-5.7 Å and have an average value of 2.9°. A comparably small average of *ca.* 2° value was observed in the structure of (37). There is no statistically significant evidence for C-C bond length alternation in either of the coordinated cyclophane rings.

In complex (40) each of the benzene rings was disordered over two sets of atomic positions. The major sites were twisted 26° with respect to each other, giving an approximately staggered conformation[103]. Figure 3.4 presents views along the Ru-Ru axes for compounds (37) and (39). In complex (39), as observed for (40), the oxygen atoms of the alkoxide ligands are eclipsed with respect to one aromatic ring and staggered with respect to the other. However, the orientation of the cyclophane ligands in complexes (37) and (39) is radically different. In complex (39) the ethylenic bridging functions of one cyclophane ligand are twisted *ca.* 23° with respect to those of the other, yet in (37) they are almost perpendicular, having a twist angle of 87°. It is also worth noting that the ethoxide ligands of (39) have not adopted the three-fold symmetry which might have been expected.

(iv) $[Ru_2(\eta^6\text{-}C_{16}H_{16})_2(OEt)_3][BPh_4]$ (41).

The compound $[Ru_2(\eta^6\text{-}C_{16}H_{16})_2(OEt)_3][BPh_4]$ (41) was prepared and characterised similarly to (39). The details are given in the experimental section.

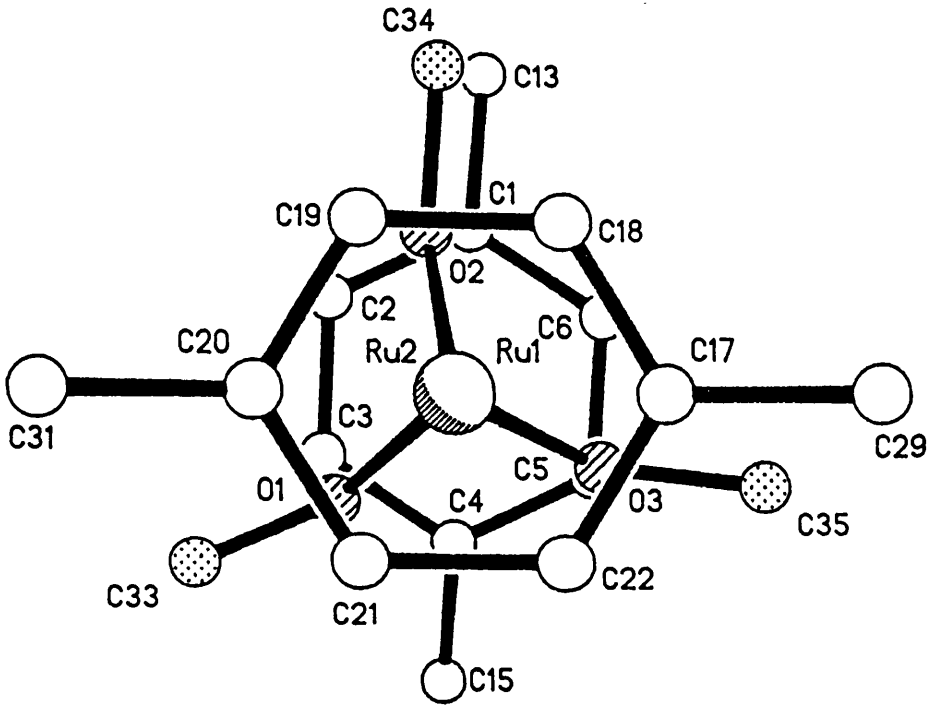

$[Ru_2(\eta^6\text{-}C_{16}H_{16})_2(OMe)_3]^+$ (37).

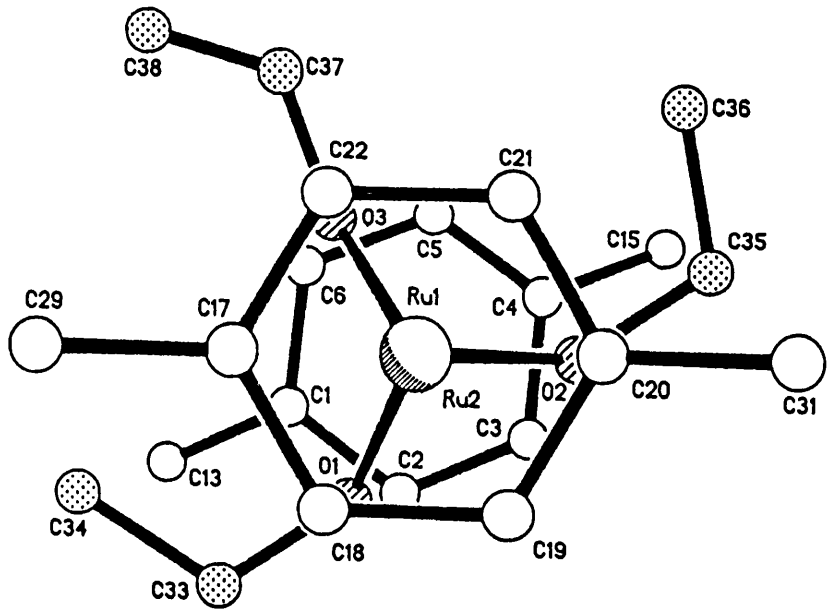

$[Ru_2(\eta^6\text{-}C_{16}H_{16})_2(OEt)_3]^+$ (39).

Fig. 3.4 Views along the Ru-Ru axes of (37) and (39).

(v) The reactions of $[Ru(\eta^6\text{-}C_{16}H_{16})Cl_2]_2$ (1) with Na[OR] in ROH (R=^{i}Pr,^{t}Bu).

Attempts to prepare analogues of the compounds $[Ru_2(\eta^6\text{-}C_{16}H_{16})_2(OR)_3][X]$ (R=Me,Et) with longer alkyl chains by the Na[OR] in ROH route for $[OR]^-$= isopropoxide and *t*-butoxide proved unsuccessful. Extensive decomposition occurred and no ruthenium-cyclophane products were isolated. Similar attempts by Stephenson *et al*[102] to prepare longer chain compounds of this type from $[Ru(\eta^6\text{-}C_6H_6)Cl_2]_2$ also resulted in decomposition.

3.2.2 The Reactions of $[Ru(\eta^6\text{-}C_{16}H_{16})Cl_2]_2$ (1) with Sodium Hydroxide or Sodium Carbonate, and of $[Ru_2(\eta^6\text{-}C_{16}H_{16})_2(OMe)_3][PF_6]$ (38) with Water.

(i) The reactions of $[Ru(\eta^6\text{-}C_{16}H_{16})Cl_2]_2$ (1) with sodium carbonate or sodium hydroxide in water.

When $[Ru(\eta^6\text{-}C_{16}H_{16})Cl_2]_2$ (1) was treated with an excess of aqueous Na_2CO_3 a yellow solution was obtained on warming, from which an orange/yellow precipitate was obtained on addition of $Na[BPh_4]$. The infrared spectrum of this solid exhibits a band at 3523 cm^{-1}, which is similar to that observed previously for $[Ru_2(\eta^6\text{-arene})_2(OH)_3]^+$ compounds[102]. However, the ^1H n.m.r. spectrum, recorded in $CDCl_3$, indicates that the precipitate is a mixture of three products, one major and two minor. Integration of the peaks of the principle product strongly suggest a 1:1 ratio of $C_{16}H_{16}$:$[BPh_4]^-$. No resonance was observed that might be attributed to OH^-. The data presented above were recorded on the "purest" solid obtained from a number such reactions. In general, some decomposition always occurred, and mixtures of ruthenium-cyclophane compounds were isolated on each occasion. Even for the data presented above it is by no means clear what the major product might be.

Reactions of $[Ru(\eta^6\text{-}C_{16}H_{16})Cl_2]_2$ (1) with aqueous NaOH under various conditions yielded mixtures of ruthenium-cyclophane products at best, and resulted in extensive decomposition in the worst cases.

(ii) The reaction of $[Ru_2(\eta^6\text{-}C_{16}H_{16})_2(OMe)_3][PF_6]$ (38) with water.

It has been reported that for a variety of $[Ru_2(\eta^6\text{-arene})_2(OH)_3][X]$ compounds the triply alkoxide-bridged species $[Ru_2(\eta^6\text{-arene})_2(OR)_3][X]$ can be prepared by refluxing in alcohol, ROH. The weakly acidic alcohol is thought to protonate the hydroxide ligand which can then easily be displaced by $[OR]^-$ ligands. There seemed to be no apparent reason for this reaction not to work in reverse. Since the compound $[Ru_2(\eta^6\text{-}C_{16}H_{16})_2(OMe)_3][PF_6]$ (38) was available, this reverse reaction was attempted. Initially (38) was warmed in water to *ca.* 323 K for four hours. No darkening of the solution occurred to suggest decomposition, and therefore the solution was heated more strongly to 348 K for a further two hours. A solid was recovered by cooling the solution in an ice bath. In the ^1H n.m.r. spectrum of this solid the integral for the methoxide protons was much reduced compared with that in the spectrum of (38), indicating that some of the methoxide ligands had been displaced by hydroxide. In addition, a second set of cyclophane resonances was observed. Finally, the solid was refluxed in aqueous solution for *ca.* 2 h. At this elevated temperature a little decomposition occurred, and a small amount of dark solid was removed from the reaction solution before the product was recovered by cooling the solution and adding $K[PF_6]$. The solid recovered analysed closely for $[Ru_2(\eta^6\text{-}C_{16}H_{16})_2(OH)_3][PF_6].2H_2O$ (42). The ^1H n.m.r. spectrum (Table 3.4), recorded in CD_3NO_2, exhibited no resonance at δ 4.12 ppm due to methoxide protons. No resonance was observed for the hydroxide protons. In the infrared spectrum the μ-OH ligands exhibit a ν(OH) band at 3625 cm^{-1}, while the waters of crystallisation give rise to bands at 3371 {ν(OH)} and 1624 cm^{-1} {δ(H-O-H)}.

3.2.3 Reactions to form the Binuclear Cation $[(\eta^6\text{-}C_{16}H_{16})RuCl_3Ru(\eta^6\text{-}C_{16}H_{16})]^+$.

(i) The reaction of $[Ru(\eta^6\text{-}C_{16}H_{16})Cl_2]_2$ (1) with $NH_4[PF_6]$ in methanol.

When $[Ru(\eta^6\text{-}C_{16}H_{16})Cl_2]_2$ (1) is stirred with $NH_4[PF_6]$ in methanol at ambient temperature for 24h a fine brown precipitate is obtained. This precipitate analysed closely for $[Ru_2(\eta^6\text{-}C_{16}H_{16})_2Cl_3][PF_6]$ (43). In the infrared spectrum a broad ν(Ru-Cl) band is observed at 275 cm^{-1}, which is inconsistent with the spectrum of the starting material (1), which exhibits two bands in this region at 295 and 254 cm^{-1}. This observation is very similar to that made for $[Ru_2(\eta^6\text{-}C_6H_6)_2Cl_3][PF_6]$, which exhibits two closely spaced

bands at 264 and 276 cm^{-1}, and was prepared by an analogous method[99]. In the FAB mass spectrum the highest mass peak is observed at 870 mass units, which corresponds to $\{[Ru_2(\eta^6\text{-}C_{16}H_{16})_2Cl_3][PF_6]\}^+$. The peak at 725 mass units is due to the cation $[Ru_2(\eta^6\text{-}C_{16}H_{16})_2Cl_3]^+$, while other fragmentation peaks are listed below:

m/e	Fragment
690	$[Ru_2(\eta^6\text{-}C_{16}H_{16})_2Cl_2]^+$
345	$[Ru(\eta^6\text{-}C_{16}H_{16})Cl]^+$
310	$[Ru(\eta^6\text{-}C_{16}H_{16})]^+$

The ^1H n.m.r. spectrum, recorded in CD_3NO_2 exhibits the usual pattern of cyclophane resonances (Table 3.4). A number of attempts were made to grow crystals employing a variety of solvent systems and temperatures, but none were successful.

(ii) $[Ru_2(\eta^6\text{-}C_{16}H_{16})_2Cl_3][BPh_4]$ (44).

The compound (44) was prepared and characterised similarly to (43). The details are given in the experimental section. All attempts to grow crystals were unsuccessful.

(iii) The reaction of $[Ru(\eta^6\text{-}C_{16}H_{16})Cl_2(py)]$ (20) and $[Ru(\eta^6\text{-}C_{16}H_{16})Cl(py)_2][PF_6]$ (25) with $H[BF_4]$ in methanol.

The high yield synthesis of $[M_2(\eta^6\text{-arene})_2X_3][BF_4]$ from $[M(\eta^6\text{-arene})X_2(py)]$, $[M(\eta^6\text{-arene})X(py)_2][PF_6]$ and $H[BF_4]$ in methanol has been demonstrated[63,100] for a number of systems: a) M=Ru,Os, arene=C_6H_6, X=Cl; b) M=Ru, arene=C_6H_6, X=Br; and c) M=Ru, arene=1,3,5-$C_6H_3Me_3$, X=Cl,Br,I. A mechanism has been proposed[63,100] for this reaction whereby the pyridyl ligands are first labilised by protonation and exchanged for solvent molecules, leading to $[M(\eta^6\text{-arene})X_2(MeOH)]$ and $[M(\eta^6\text{-arene})X(MeOH)_2]^+$ in solution, which then couple to form the stable triple-bridged cations.

When a suspension of (20) and (25) was treated with $H[BF_4]$ in methanol a red/brown solid was obtained after *ca.* 1.5 h. This solid analysed closely for $[Ru_2(\eta^6\text{-}C_{16}H_{16})_2Cl_3][BF_4]$ (45). In the infrared spectrum a band was observed at 1050 cm^{-1} confirming the presence of the $[BF_4]^-$ anion. Two strong, closely spaced, ν(Ru-Cl) bands were observed at 262 and 275 cm^{-1}, which is very similar to the bands at 264 and

276 cm^{-1} observed for $[Ru_2(\eta^6\text{-}C_6H_6)_2Cl_3][PF_6]$[99]. The ^1H n.m.r. spectrum of (45), recorded in CD_3NO_2, was identical to that recorded for (43) (Table 3.4). $^{13}C\text{-}\{^1H\}$ n.m.r. data are presented in the experimental section.

(iv) The reaction of $[Ru_2(\eta^6\text{-}C_{16}H_{16})_2(OMe)_3][PF_6]$ (38) with *conc.* HCl in methanol.

When a solution of $[Ru_2(\eta^6\text{-}C_{16}H_{16})_2(OMe)_3][PF_6]$ (38) in methanol was treated with an excess of *conc.* HCl in methanol, a pale brown precipitate formed immediately. This solid was isolated by filtration and identified as $[Ru_2(\eta^6\text{-}C_{16}H_{16})_2Cl_3][PF_6]$ (43) by its infrared spectrum, which contained no ν(C-O) band in the region of 1050 cm^{-1}, but did exhibit a broad band at *ca.* 275 cm^{-1}, which is readily assigned to ν(Ru-Cl). A band at 844 cm^{-1} confirmed the presence of the $[PF_6]^-$ anion. It should be noted that $[Ru_2(\eta^6\text{-}C_6H_6)_2(OMe)_3][BPh_4]$ is reported[103] to react with anhydrous HCl to give a mixture of $[Ru(\eta^6\text{-}C_6H_6)Cl_2]_2$ and $[Ru_2(\eta^6\text{-}C_6H_6)_2Cl_3][BPh_4]$. There is no evidence for the formation of $[Ru(\eta^6\text{-}C_{16}H_{16})Cl_2]_2$ (1) in this case.

(v) The reaction of $[Ru(\eta^6\text{-}C_{16}H_{16})Cl_2]_2$ (1) with CsCl and *conc.* HCl in ethanol.

The reaction of $[Ru(\eta^6\text{-}C_6H_6)Cl_2]_2$ with an excess of CsCl and *conc.* HCl in ethanol over a period of five days is reported[98,99] to produce the anionic ruthenium salt $Cs[Ru(\eta^6\text{-}C_6H_6)Cl_3]$. An exactly analogous reaction was performed using the compound (1), but only the starting material was recovered. The compound $Cs[Ru(\eta^6\text{-}C_6H_6)Cl_3]$ has been shown[99] to lose one of the chloride ligands very readily in reactions with ligands L=H_2O, py, PR_3, Me_2SO, etc. Reported attempts to prepare the analogous anionic compounds $Cs[Ru(\eta^6\text{-}C_6H_6)X_3]$ (X^-=Br^-,I^-) also resulted in the recovery of the starting materials $[Ru(\eta^6\text{-}C_{16}H_{16})X_2]_2$. It is possible that for (1) and the compounds $[Ru(\eta^6\text{-}C_{16}H_{16})X_2]_2$ a similar reaction occurs as for $[Ru(\eta^6\text{-}C_6H_6)Cl_2]_2$, but that the products are unstable with respect to loss of a halide ion, and therefore re-dimerise.

3.2.4 The Reaction of $[Ru_2(\eta^6\text{-}C_{16}H_{16})_2Cl_3][PF_6]$ (43) with Pyridine in Methanol: The Crystal Structure of *trans*-$[Ru(py)_4Cl_2]$ (46).

When the compound $[Ru_2(\eta^6\text{-}C_{16}H_{16})_2Cl_3][PF_6]$ (43) was treated with an excess of pyridine in methanol over an extended period of time (*ca.* 12h) red crystals were obtained. These crystals were identified as the well known[98,99,124] compound *trans*-$[Ru(py)_4Cl_2]$ (46). A thorough search of the literature and crystallographic data bases indicates that, remarkably, the crystal structure has not thus far been reported. Since the crystals obtained directly from the reaction solution were of good quality we have undertaken this structure determination.

The structures of a number of *trans*-dichloride metal tetrakis(pyridine) complexes have been reported. These fall into two main categories, those of metals in the +2 oxidation state, and those of metals in the +3 oxidation state. Of those in the latter

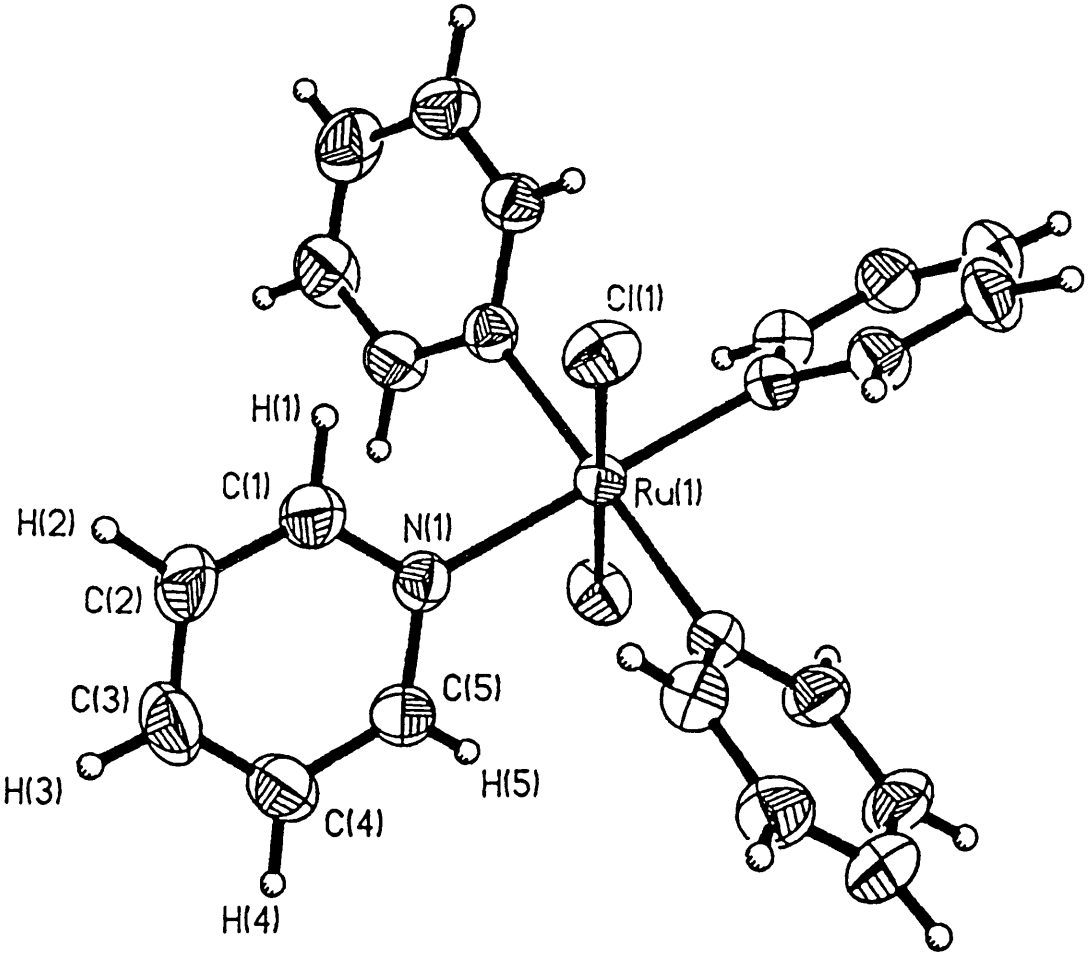

Fig. 3.5 A thermal ellipsoid plot of *trans*-$[Ru(py)_4Cl_2]$ (46) at the 50% confidence level. Ru-Cl=2.406(1) Å, Ru-N=2.073(3) Å, N-Ru-Cl=89.6(1)°.

category, the *trans*-$[M(py)_4Cl_2]^+$ (M=Ru[125],Rh[126,127]) cations, have been used in the isolation of the hydrogendinitrate anion. This anion had been the subject of controversy regarding the way in which it is hydrogen bonded. The cation has therefore often not been the main focus of attention when these structures were reported. Nevertheless the relevant structural parameters are available. The structures of two compounds of Group 13 elements have also been reported, namely *trans*-$[M(py)_4Cl_2][MCl_4]$ (M=Al[128],Ga[129]). The most comprehensive study in this field, by Long and Clarke[130], reports the structures of the three isomorphous anhydrous compounds *trans*-$[M(py)_4Cl_2]$ (M=Fe,Co,Ni), and the hydrated compound *trans*-$[Fe(py)_4Cl_2].H_2O$. In each of these four compounds the metal is in the +2 oxidation state.

The crystals of *trans*-$[Fe(py)_4Cl_2].H_2O$ were grown by the slow evaporation of a reaction solution open to the air[130]. The anhydrous analogue was obtained only under a moisture free atmosphere[130]. In contrast, the anhydrous compound *trans*-$[Ru(py)_4Cl_2]$ (46) was obtained simply by evaporation of the methanolic reaction solution in air. The crystals of compounds of the first transition series, namely *trans*-$[M(py)_4Cl_2]$ (M=Fe,Co,Ni) and *trans*-$[Fe(py)_4Cl_2].H_2O$, are reported[130] to lose pyridine from their surfaces, and were mounted in capillaries containing the mother liquor during their structure determinations. No such surface degradation has been observed for the crystals of compound (46), nor did the crystal degrade in the X-ray beam during the diffraction experiment.

A thermal ellipsoid plot of (46) and some important structural parameters are presented in Fig. 3.5, and a crystal packing diagram, viewed along the a-axis is presented in Fig. 3.6. Details of the structure determination and refinement are given in Section 3.3.4, while the crystal data, fractional coordinates, bond lengths, and bond angles are presented in Tables 3.10-3.13

The asymmetric unit comprises one quarter of the formula unit and the structure is isomorphous with the compounds *trans*-$[M(py)_4Cl_2]$ (M=Fe,Co,Ni)[130]. Table 3.1 gives crystal data for these four isomorphous compounds. The most striking feature is the decrease in unit cell dimensions, and hence unit cell volume, on going across the first transition series, and on moving from the first to the second row in Group 8. The explanation for this trend is a significant decrease in the M-N distance on going from Fe to Ni and from Fe to Ru, and a rather smaller decrease in the M-Cl distance on going from Fe to Ru. These bond length differences will be discussed in more detail later.

Fig. 3.6 is a packing plot of (46), viewed along the a-axis, and shows that the molecules are well separated from each other. Long and Clarke give a detailed description[130] of the packing in the unit cell and, since there is essentially no difference between the structures they report and that of (46), it shall not be repeated here. It is worth

TABLE 3.1 Crystal Data for *trans*-[M(py)$_4$Cl$_2$] Compounds.

	Fe(py)$_4$Cl$_2$[a]	Co(py)$_4$Cl$_2$[a]	Ni(py)$_4$Cl$_2$[a,b]	Ru(py)$_4$Cl$_2$[c]
Molecular weight	443.16	446.24	446.02	**488.38**
Space group	$I4_1/acd$	$I4_1/acd$	$I4_1/acd$	**$I4_1/acd$**
a, Å	15.945(2)	15.966(2)	15.920(3)	**15.664(2)**
c, Å	17.287(6)	17.153(6)	17.046(12)	**16.970(2)**
V, Å^3	4395(3)	4373(3)	4320(5)	**4164(1)**
d_{calc}	1.34	1.36	1.37	**1.56**
μ, cm^{-1}	9.6	10.7	11.6	**9.7**
Refined parameters	63	63	63	**83[d]**
Reflections observed	533	686	848	**757**
R	4.77	4.83	4.98	**4.53**
R'	6.52	6.68	7.48	**3.20**

a. Ref. 130

b. Crystal used corresponded to $Ni_{0.97}Fe_{0.3}(py)_4Cl_2$ with 0.42 wt % Fe.

c. This work.

d. Hydrogen atoms were refined.

noting however that the Cl-Ru-Cl vector is not parallel with the tetragonal axis and as a result there is no crystallographically imposed restriction on the N-Ru-Cl angle, which is 89.6°.

Table 3.2 gives M-N and M-Cl distances for a range of *trans*-[M(py)$_4$Cl$_2$] compounds. Among the anhydrous iron, cobalt and nickel compounds the difference in M-Cl bond distances is no greater than *ca.* 3 e.s.d.s. This observation is attributed[130] to the predominantly σ-bonded character of the M-Cl interactions and constant number of electrons in the e_g orbitals of the metal ions. By comparison, the M-N distances vary significantly. The nitrogen atoms participate in partial π-bonding to the metal ions, and therefore as the number of electrons in the metal t_{2g} bonding orbitals increases from 4 to 6 from Fe to Ni, the M-N bondlength is successively shortened[130]. Long and Clarke[130] note that this is part of a systematic shortening in M-N bond lengths observed across the first

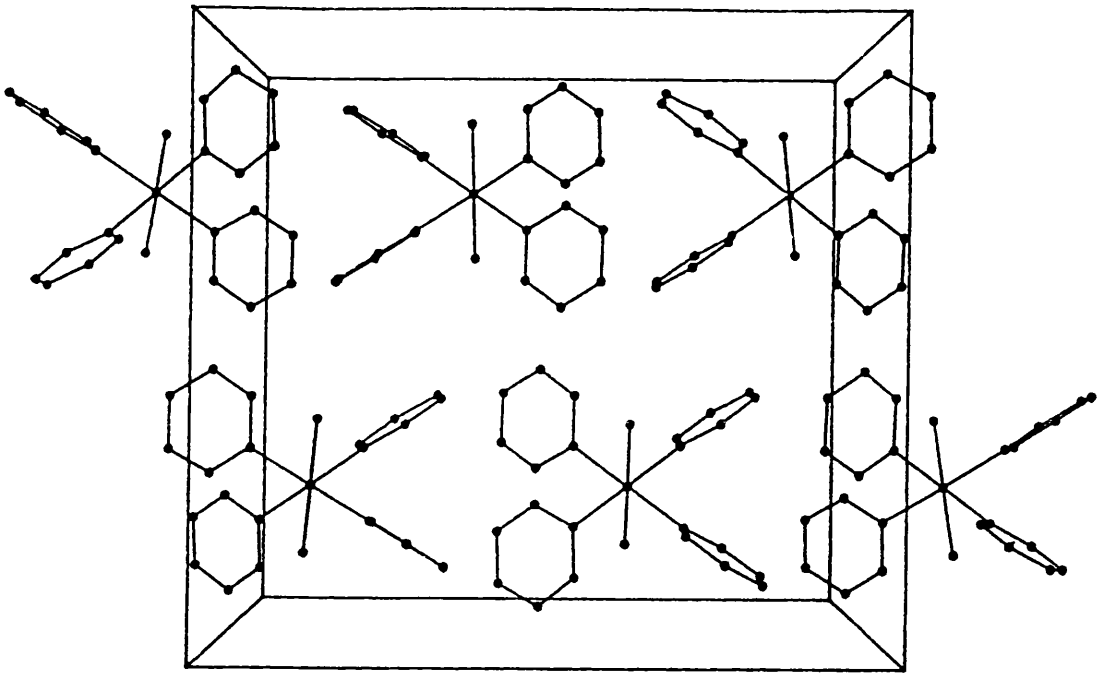

Fig. 3.6 A packing plot of *trans*-$[Ru(py)_4Cl_2]$ (46) viewed along the a-axis.

transition series from Mn to Zn and suggest that this is due to three main factors:

(i) Increasing effective nuclear charge.

(ii) Decreasing ionic radius.

(iii) Increasing number of t_{2g} π-bonding electrons.

For (46) the M-Cl distance is significantly shorter than those found in the compounds of iron, cobalt and nickel. The dominant factor here would appear to be the increase in effective nuclear charge. The Ru-N distance, 2.073(3) Å, is *ca.* 0.16 Å shorter than that in the anhydrous Fe compound and *ca.* 0.06 Å shorter than that in the nickel compound. These are large, and clearly very real differences, and result from greater M-L bond strength due to greater orbital overlap on going from the first to the second row of the transition series, since the number of t_{2g} electrons in Ru^{2+} is equal to that in Fe^{2+} and two less than that in Ni^{2+}!

The Ru(III) and Rh(III) compounds have significantly shorter M-Cl distances, which reflects the combination of both greater effective nuclear charge and smaller ionic radius of the metal ions. The M-N distances of the Ru(III) and Rh(III) compounds do not

TABLE 3.2 M-Cl and M-N Distances in *trans*-$M(py)_4Cl_2$ Compounds.

Compound.	M-Cl (Å)	M-N (Å)
$Fe(py)_4Cl_2.H_2O$[a,130]	2.429(2)	2.247(4)
$Fe(py)_4Cl_2$[a,130]	2.430(3)	2.229(6)
$Co(py)_4Cl_2$[a,130]	2.444(2)	2.183(4)
$Ni(py)_4Cl_2$[a,c,130]	2.437(2)	2.133(4)
$Ru(py)_4Cl_2$ (46)[a,d]	**2.406(1)**	**2.073(3)**
$[Ru(py)_4Cl_2][H(NO_3)_2]$[a,125]	2.326(4)	2.090(12)
$[Rh(py)_4Cl_2][H(NO_3)_2]$[b,126]	2.331(1)	2.060(2)
$[Rh(py)_4Cl_2][H(NO_3)_2]$[a,127]	2.34(1)	2.09(2)
$[Al(py)_4Cl_2][AlCl_4]$[a,128]	2.279(3)	2.070(4)
$[Ga(py)_4Cl_2][GaCl_4]$[a,129]	2.313(5)	2.108(12)

a. X-ray study.

b. Neutron study.

c. Crystal used corresponded to $Ni_{0.97}Fe_{0.3}(py)_4Cl_2$ with 0.42 wt % Fe.

d. This work.

e. Averaged value.

show a marked shortening compared with that in (46).

Long and Clarke suggest[130] that if the M-N distance becomes too short, unfavourable pyridine-pyridine interactions at H1 and C5 would result. Indeed, the compound *trans*-$[Zn(py)_4Cl_2]$ is not known. On the basis of the trend in M-N distances across the first transition period, this compound is predicted to have a Zn-N distance of *ca.* 1.99 Å. A tetrahedral complex, $[Zn(py)_2Cl_2]$, is known, and exhibits a Zn-N distance of 2.049(6) Å. The distance of 2.073 Å in (46) is therefore long enough for these unfavourable interactions to be small, and not cause a change in geometry.

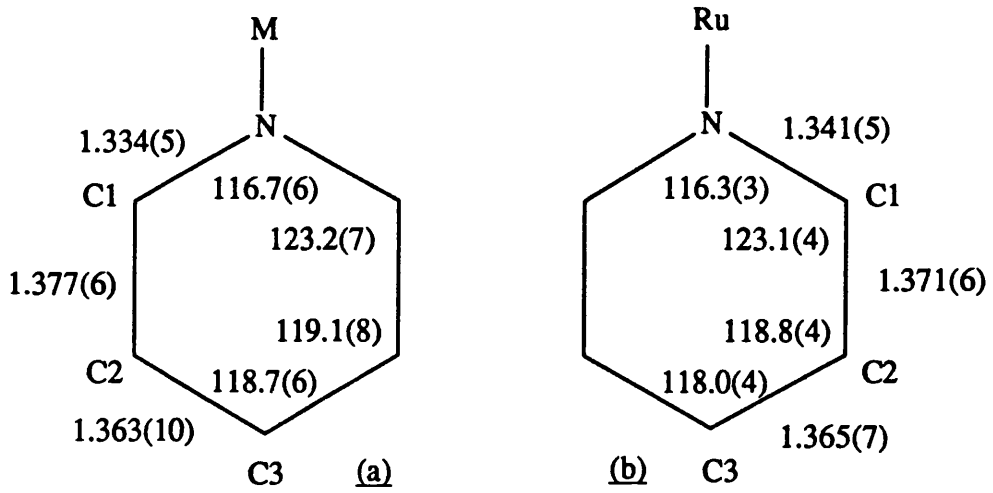

Fig. 3.7 The averaged bond lengths (Å) and angles (°) in the pyridine ligands of a) *trans*-$[M(py)_4Cl_2]$ (M=Fe,Co,Ni) and *trans*-$[Fe(py)_4Cl_2].H_2O$[130], and b) *trans*-$[Ru(py)_4Cl_2]$ (46).

Long and Clarke[130] structurally investigated seven independent pyridine ligands under very similar conditions and presented an averaged value for each of the bond lengths and angles. This data is shown in Fig. 3.7 alongside the relevant values found in the structure of (46). There is agreement between the two sets of data to within two e.s.d.s for each parameter.

3.3 EXPERIMENTAL.

3.3.1 Instrumentation and Physical Measurements.

As described in Section 2.3.1.

3.3.2 Materials.

The compound $[Ru(\eta^6\text{-}C_{16}H_{16})Cl_2]_2$ (1) was prepared as described in Section 2.3.3. Materials were otherwise obtained and used as described in Section 2.3.2.

3.3.3 Synthesis.

The synthesis of $[Ru_2(\eta^6\text{-}C_{16}H_{16})_2(OCH_3)_3][BPh_4]$ (37).

$[Ru(\eta^6\text{-}C_{16}H_{16})Cl_2]_2$ (0.08 g; 0.11 mmol) was added to a freshly prepared and filtered solution of sodium methoxide in methanol {sodium (0.20 g) dissolved in methanol (10 cm^3)}. The mixture was stirred at 315 K for 2.5 h., during which time the solution turned first yellow, then orange. The solution was allowed to cool to room temperature and was then filtered. To the clear orange filtrate a solution of $Na[BPh_4]$ in methanol was added. An orange microcrystalline solid formed immediately. The solid was filtered off and washed with methanol (5 cm^3), diethyl ether (5 cm^3), and air dried. Yield: 0.06 g; 0.05 mmol; 55%. Satisfactory microanalytical data were not obtained.

Infrared spectrum: ν(O-C): 1046 (s); δ(Ru-O-C): 1153 (m); ν(Ru-O): 515 (w); $[BPh_4]^-$: 708 (s), 722 (s), 734 (s) cm^{-1}.

The synthesis of $[Ru_2(\eta^6\text{-}C_{16}H_{16})_2(OCH_3)_3][PF_6]$ (38).

Using the method described for compound (37) an orange solution was obtained by reaction of $[Ru(\eta^6\text{-}C_{16}H_{16})Cl_2]_2$ (0.14 g; 0.18 mmol) with sodium methoxide. To this, a solution of $K[PF_6]$ in methanol was added, which caused an orange, microcrystalline solid to form. The solution was cooled to *ca.* 258 K for 30 min., during which time more of the product precipitated. The solid was filtered off and washed with methanol (5 cm^3), diethyl ether (15 cm^3), and air dried. The reaction solution was kept at *ca.* 258 K for a further 3

days, which gave a second crop of the product. This was isolated as before. Combined yield: 0.11 g; 0.14 mmol; 37%.

Infrared spectrum: ν(O-C): 1046 (m, br); δ(Ru-O-C): 1153 (m); ν(Ru-O): 514 (s); $[PF_6]^-$: 842 (s, br), cm^{-1}.

The synthesis of $[Ru_2(\eta^6\text{-}C_{16}H_{16})_2(OCH_2CH_3)_3][PF_6]$ (39).

$[Ru(\eta^6\text{-}C_{16}H_{16})Cl_2]_2$ (0.09 g; 0.10 mmol) was added to a freshly prepared and filtered solution of sodium ethoxide in ethanol {sodium (0.20 g) dissolved in ethanol (15 cm^3)}. The solution was stirred and heated to ca. 315 K for 20 min. An orange solution formed, which was filtered and allowed to cool to room temperature. A filtered solution of $K[PF_6]$ in ethanol (3 cm^3) was added, and the solution cooled to *ca.* 258 K overnight. The orange, microcrystalline product which formed was filtered off, washed with ethanol (5 cm^3), diethyl ether (5 cm^3), then air dried. The filtrate was reduced to half volume and kept at *ca.* 258 K for a further 24 h. A second smaller crop of product was isolated. Combined yield: 0.04 g; 0.04 mmol; 38%.

Infrared spectrum: ν(O-C): 1052 (m); δ(Ru-O-C): 1155 (m); ν(Ru-O): 509 (m); $[PF_6]^-$: 842 (s, br) cm^{-1}.

The synthesis of $[Ru_2(\eta^6\text{-}C_{16}H_{16})_2(OCH_2CH_3)_3][BPh_4]$ (41).

Using a method similar to that given for (39) an orange solution was obtained. To this solution a filtered solution of $Na[BPh_4]$ in ethanol was added which caused the immediate precipitation of the orange product. The product was filtered off, washed with ethanol (5 cm^3), diethyl ether (5 cm^3), then air dried. Yield: 0.08 g; 0.07 mmol; 64% {based on $[Ru(\eta^6\text{-}C_{16}H_{16})Cl_2]_2$ (0.09 g; 0.12 mmol)}.

Infrared spectrum: ν(O-C): 1050 (m); δ(Ru-O-C): 1153 (m); ν(Ru-O): 515 (m); $[BPh_4]^-$: 710 (s), 722 (s), 735 (s) cm^{-1}.

The synthesis of $[Ru_2(\eta^6\text{-}C_{16}H_{16})_2(OH)_3][PF_6].2H_2O$ (42).

Complex (38) (0.10 g; 0.12 mmol) was treated with water (15 cm^3) under reflux conditions for *ca.* 2 h. A small quantity of a brown solid was removed by filtration leaving

a clear orange solution. A little orange precipitate was obtained from this solution on cooling in an ice bath. More precipitate was obtained on addition of a filtered solution of $K[PF_6]$ in water. The precipitate was filtered off, washed with water (2 cm^3), ethanol (0.5 cm^3), and diethyl ether (5 cm^3), and then dried *in vacuo*. Yield 0.05g; 0.06 mmol; 46%.

Infrared spectrum: [OH]: ν(OH) 3625 (w, sharp); [H_2O]: ν(OH) 3371 (w, v br), δ(H-O-H) 1624 (w); ν(Ru-O): 507 (m); $[PF_6]^-$: 842 (s, br).

The synthesis of $[Ru_2(\eta^6\text{-}C_{16}H_{16})_2Cl_3][PF_6]$ (43).

Ammonium hexafluorophosphate (0.03 g; 0.20 mmol) was added to a suspension of $[Ru(\eta^6\text{-}C_{16}H_{16})Cl_2]_2$ (0.06 g; 0.09 mmol) in methanol (10 cm^3). The suspension was stirred at room temperature for 24 h. The product, a very fine brown precipitate, was filtered off, washed with methanol (5 cm^3), diethyl ether (5 cm^3), and then air dried. The product was purified by removing free [2_2]paracyclophane by sublimation under reduced pressure at *ca.* 373 K for 4 h. Yield after purification: 0.05 g; 0.06 mmol; 74%.

Infrared spectrum: ν(Ru-Cl): 275 (s, br); $[PF_6]^-$: 844 (s, br) cm^{-1}.

Mass spectrum:

m/e	Fragment
870	$[Ru_2(\eta^6\text{-}C_{16}H_{16})_2Cl_3][PF_6]^+$
725	$[Ru_2(\eta^6\text{-}C_{16}H_{16})_2Cl_3]^+$
690	$[Ru_2(\eta^6\text{-}C_{16}H_{16})_2Cl_2]^+$
345	$[Ru(\eta^6\text{-}C_{16}H_{16})Cl]^+$
310	$[Ru(\eta^6\text{-}C_{16}H_{16})]^+$

The synthesis of $[Ru_2(\eta^6\text{-}C_{16}H_{16})_2Cl_3][BPh_4]$ (44).

Tetraphenylboron sodium (0.05 g; 0.16 mmol) was added to a suspension of $[Ru(\eta^6\text{-}C_{16}H_{16})Cl_2]_2$ (0.09 g; 0.11 mmol) in methanol (10 cm^3). The suspension was stirred at room temperature for 5 h. A fine brown precipitate was filtered off, washed with methanol (5 cm^3), diethyl ether (5 cm^3), then air dried. The product was purified by removing some free [2_2]paracyclophane by sublimation under reduced pressure at *ca.* 373 K for 3 h. Yield after purification: 0.09 g; 0.09 mmol; 77%.

Infrared spectrum: ν(Ru-Cl): 267 (m, br); $[BPh_4]^-$: 704 (s), 721 (s), 734 (s) cm^{-1}.

The synthesis of $[Ru_2(\eta^6\text{-}C_{16}H_{16})_2Cl_3][BF_4]$ (45).

To a suspension of $[Ru(\eta^6\text{-}C_{16}H_{16})Cl_2(NC_5H_5)]$ (20) (0.026 g; 0.05 mmol) and $[Ru(\eta^6\text{-}C_{16}H_{16})Cl(NC_5H_5)_2][PF_6]$ (25) (0.035 g; 0.05 mmol) in methanol (5 cm^3), $H[BF_4]$ (40% approx., 0.05 cm^3) was added, and the solution was stirred for 90 min. A red/brown precipitate formed which was filtered off and washed with methanol (2 cm^3), diethyl ether (5 cm^3), then air dried. Yield: 0.04 g; 0.05 mmol; 88%.

Infrared spectrum: ν(Ru-Cl): 262 (s), 275 (s); $[BF_4]^-$: 1050 (s, br) cm^{-1}.

^{13}C n.m.r. Data: Solvent: CD_3NO_2. Operating frequency: 100 MHz.

	δ, ppm.
Metallated $C_2\underline{C}_4H_4$	74.3
Non-metallated $C_2\underline{C}_4H_4$	134.9
Metallated $\underline{C}_2C_4H_4$	115.7
Non-metallated $\underline{C}_2C_4H_4$	141.0
$-\underline{C}H_2\underline{C}H_2-$	32.3, 34.1

The synthesis of *trans*-$[Ru(NC_5H_5)Cl_2]$ (46).

Compound (43) (*ca.* 0.01 g; 0.01 mmol) was suspended in methanol (3 cm^3), and treated with an excess of pyridine (0.5 cm^3, 6.5 mmol) overnight at ambient temperature. Red crystals formed which were identified as (46).

3.3.4 Details of the Crystal Structure Determinations.

See Section 2.3.5 for the general experimental procedure employed in the crystal structure determinations.

(i) Details of the crystal structure determination of $[Ru_2(\eta^6\text{-}C_{16}H_{16})_2(OCH_2CH_3)_3][PF_6]$ (39).

The orange crystals used for this experiment were grown directly from the reaction solution. From the systematically absent data the space group was either C2/c or Cc. The refinement of the structure proceeded most smoothly in C2/c.

The positions of the two ruthenium ions were derived by direct methods. Iterative application of least-squares refinement and difference-Fourier synthesis led to the development of the entire structure. The C37-C38 bond length initially refined to an unreasonably short value, 1.30 Å. This bond length was set to 1.52 Å (a value comparable to the that of similar bonds in the structure), and was allowed to shift by a maximum of 0.01 Å per cycle for four least-squares cycles and then by a maximum of 0.005 Å for a further four cycles, after which convergence was achieved at a more reasonable value of 1.47 Å.

The asymmetric unit contains one cation and two half-anions. One half-anion has its phosphorus atom positioned on an inversion centre, while the other has its phosphorus atom and two fluorine atoms contained in a mirror plane. The two half-anions show no appreciable disorder. Although several of the hydrogen atoms were apparent in the final difference-Fourier map they were not included in the refinement. The final difference-Fourier had a highest peak of 1.15 $eÅ^{-3}$, which was in a possible alternative position for C37. All attempts at refining the structure employing a disordered model for C37 resulted in a poorer overall result and were not adopted. The remaining peaks in the difference-Fourier map were below 1 $eÅ^{-3}$. The crystallographic data, fractional coordinates, bond lengths, and bond angles are presented in Tables 3.6-3.9.

(ii) Details of the structure determination of *trans*-$[Ru(NC_5H_5)_4Cl_2]$ (46).

A red crystal was grown directly from the reaction solution. From the systematically absent data the space group was uniquely defined as $I4_1/acd$. The full data set was collected as if the crystal was orthorhombic rather than tetragonal.

The positions of all of the non-hydrogen atoms were found by direct methods. The

asymmetric unit contains one quarter of the ruthenium ion, half of a chloride ion, and one complete pyridine ligand. Iterative application of least-squares refinement and difference-Fourier synthesis led to the development of the entire structure, including the hydrogen atoms. All of the non-hydrogen atoms were refined anisotropically, while the hydrogen atoms were refined isotropically. The crystallographic data, fractional coordinates, bond lengths, and bond angles are presented in Tables 3.10-3.13.

TABLE 3.3 Microanalytical Data for the Compounds $[Ru_2(\eta^6\text{-}C_{16}H_{16})_2Y_3][X]$ (Y=OH,OMe,OEt,Cl).

Compound.		Microanalytical data.					
		%C		%H		%Cl	
		found	calc.	found	calc.	found	calc.
$[Ru_2(\eta^6\text{-}C_{16}H_{16})_2(OMe)_3][PF_6]$	(38)	49.1	51.5	4.8	4.9		
$[Ru_2(\eta^6\text{-}C_{16}H_{16})_2(OEt)_3][PF_6]$	(39)	48.2	52.7	5.2	5.1		
$[Ru_2(\eta^6\text{-}C_{16}H_{16})_2(OEt)_3][BPh_4]$	(41)	68.5	69.4	6.2	6.3		
$[Ru_2(\eta^6\text{-}C_{16}H_{16})_2(OH)_3][PF]_6.2H_2O$	(42)	45.2	45.4	4.6	4.9		
$[Ru_2(\eta^6\text{-}C_{16}H_{16})_2(Cl)_3][PF_6]$	(43)	44.3	44.2	3.8	3.7	13.3	12.2
$[Ru_2(\eta^6\text{-}C_{16}H_{16})_2(Cl)_3][BPh_4]$	(44)	63.8	64.4	5.0	5.0		
$[Ru_2(\eta^6\text{-}C_{16}H_{16})_2(Cl)_3][BF_4]$	(45)	45.2	47.3	3.8	4.0		

TABLE 3.4 ^{1}H n.m.r. Data for the Compounds $[Ru_2(\eta^6\text{-}C_{16}H_{16})_2Y_3][X]$ (Y=OH,OMe,OEt,Cl) at 298 K.

Compound.		Solvent.	^{1}H n.m.r. data. δ, ppm.			
			Cyclophane resonances.			Other resonances.
			non-coord. C_6H_4	coord. C_6H_4	$-CH_2CH_2-$ (AA'XX')	
$[Ru_2(\eta^6\text{-}C_{16}H_{16})_2(OMe)_3][BPh_4]$	(37)	CD_2Cl_2[a]	6.57 (s)	4.44 (s)	2.58, 3.04	4.07 (s): OCH_3 [c].
$[Ru_2(\eta^6\text{-}C_{16}H_{16})_2(OMe)_3][PF_6]$	(38)	CD_3NO_2[a]	6.67 (s)	4.67 (s)	2.70, 3.08	4.12 (s): OCH_3.
$[Ru_2(\eta^6\text{-}C_{16}H_{16})_2(OEt)_3][PF_6]$	(39)	$(CD_3)_2CO$[b]	6.91 (s)	5.28 (s)	2.98, 3.25	0.80 (t)[d]: CH_3CH_2O
						4.11 (q)[d]: CH_3CH_2O.
$[Ru_2(\eta^6\text{-}C_{16}H_{16})_2(OEt)_3][BPh_4]$	(41)	CD_2Cl_2[b]	6.57 (s)	4.41 (s)	2.57, 3.05	1.18 (t)[d]: CH_3CH_2O
						4.14 (q)[d]: CH_3CH_2O[c].
$[Ru_2(\eta^6\text{-}C_{16}H_{16})_2(OH)_3][PF_6].2H_2O$	(42)	CD_3NO_2[a]	6.65 (s)	4.63 (s)	2.62, 3.05	
$[Ru_2(\eta^6\text{-}C_{16}H_{16})_2Cl_3][PF_6]$	(43)	CD_3NO_2[a]	6.81 (s)	5.09 (s)	2.74, 3.19	
$[Ru_2(\eta^6\text{-}C_{16}H_{16})_2Cl_3][BF_4]$	(45)	CD_3NO_2[a]				
$[Ru_2(\eta^6\text{-}C_{16}H_{16})_2Cl_3][BPh_4]$[e]	(44)	CD_2Cl_2[b]	6.63 (s)	4.74 (s)	2.62, 3.13	[c].

a) Operating frequency: 400 MHz.

b) Operating frequency: 200 MHz.

c) $[BPh_4]^-$ resonances observed at *ca.* δ 6.92 (t), 7.08 (t) and 7.38 ppm.

d) $^3J_{H\text{-}H}$ = 6.8 Hz.

TABLE 3.6 **Crystallographic Data for $[Ru_2(\eta^6\text{-}C_{16}H_{16})_2(OCH_2CH_3)_3][PF_6]$ (39).**

Formula	$Ru_2O_3C_{38}H_{47}P_1F_6$
fw, g	934.9
Space group	C2/c
a, Å	18.170(3)
b, Å	21.560(3)
c, Å	19.696(2)
α, deg	90.0
β, deg	105.54(1)
γ, deg	90.0
V, Å^3	7432(2)
Z	8
F(000)	3648
d_{calc}, g/cm^3	1.61
Crystal size, mm	0.52 x 0.25 x 0.06
Scan technique	ω-2Θ
μ(Mo-K_α), cm^{-1}	8.70
Orientation reflections, no.; range (2Θ)	35; ($6° \leq 2\Theta \leq 28°$)
Temperature, °C	20
Total No. of reflections measured	10370
No. of unique data	6582
Total with $I \geq 1.5\sigma(I)$	5054
No. of parameters	454
R[a]	0.0641
R'[b]	0.0693
Weighting scheme	$w = 1.000/(\sigma^2F + 0.000596F^2)$
Largest shift/esd, final cycle	0.036
Largest peak, e/Å^3	1.15

a) $R = \Sigma[|F_o|-|F_c|]/\Sigma|F_o|$

b) $R' = \Sigma[(|F_o|-|F_c|).w^{\frac{1}{2}}]/\Sigma[|F_o|.w^{\frac{1}{2}}]$

TABLE 3.7 **Atomic Coordinates (x10^4) and Equivalent Isotropic Displacement Parameters for $[Ru_2(\eta^6\text{-}C_{16}H_{16})_2(OCH_2CH_3)_3][PF_6]$ (39).**

Atom	x		y		z		U(eq)[a]	
Ru1	2010	(1)	948	(1)	1594	(1)	34	(1)
Ru2	1261	(1)	1999	(1)	650	(1)	30	(1)
O1	2067	(3)	1902	(2)	1620	(3)	38	(2)
O2	2012	(3)	1285	(2)	605	(3)	38	(2)
O3	918	(3)	1259	(3)	1147	(3)	45	(2)
C1	2363	(5)	666	(4)	2746	(4)	37	(3)
C2	2999	(5)	783	(4)	2465	(5)	49	(3)
C3	3082	(7)	438	(5)	1882	(6)	64	(4)
C4	2537	(8)	-19	(5)	1578	(5)	67	(5)
C5	1846	(7)	-34	(4)	1762	(5)	67	(4)
C6	1748	(5)	313	(4)	2350	(4)	44	(3)
C7	3138	(5)	-217	(4)	3622	(5)	52	(3)
C8	3825	(6)	-194	(5)	3440	(6)	73	(5)
C9	3894	(9)	-545	(7)	2851	(8)	96	(7)
C10	3284	(11)	-906	(6)	2459	(7)	96	(7)
C11	2654	(8)	-1016	(4)	2748	(6)	75	(5)
C12	2607	(6)	-669	(4)	3338	(5)	56	(4)
C13	2428	(7)	838	(5)	3504	(5)	64	(4)
C14	2929	(7)	331	(5)	4022	(5)	62	(4)
C15	2772	(12)	-539	(6)	1170	(6)	127	(8)
C16	3202	(12)	-1064	(6)	1692	(7)	133	(9)
C17	452	(5)	2811	(4)	602	(4)	44	(3)
C18	1203	(5)	2999	(4)	645	(5)	43	(3)
C19	1563	(5)	2816	(4)	116	(4)	39	(3)
C20	1162	(5)	2438	(4)	-453	(4)	41	(3)
C21	494	(5)	2132	(4)	-402	(4)	42	(3)
C22	128	(5)	2329	(4)	130	(4)	40	(3)
C23	-248	(5)	3754	(4)	-231	(5)	53	(4)
C24	424	(6)	4035	(4)	-295	(5)	57	(4)
C25	779	(6)	3843	(5)	-811	(5)	62	(4)
C26	466	(5)	3374	(5)	-1277	(5)	53	(3)

C27	-278	(6)	3185	(5)	-1309	(5)	55	(4)
C28	-628	(5)	3371	(4)	-787	(5)	53	(3)
C29	-39	(6)	3184	(4)	970	(5)	57	(4)
C30	-439	(6)	3737	(5)	457	(5)	60	(4)
C31	1400	(6)	2426	(5)	-1128	(5)	56	(4)
C32	957	(6)	2977	(5)	-1620	(5)	63	(4)
C33	2149	(7)	2261	(4)	2249	(5)	67	(4)
C34	1437	(9)	2243	(6)	2504	(6)	92	(6)
C35	1967	(6)	906	(4)	5	(5)	51	(3)
C36	1256	(7)	495	(5)	-210	(5)	66	(4)
C37	200	(8)	924	(7)	967	(9)	125	(8)
C38	-294	(12)	1143	(11)	1400	(11)	164	(12)
P1	0		999	(2)	7500		66	(2)
F1	0		1685	(6)	7500		275	(14)
F2	0		300	(7)	7500		219	(13)
F3	806	(5)	991	(5)	8020	(6)	159	(5)
F4	347	(8)	971	(9)	6900	(7)	236	(11)
P2	2500		2500		5000		80	(2)
F7	2665	(6)	1786	(5)	4984	(6)	155	(6)
F8	2105	(8)	2414	(7)	5595	(7)	198	(8)
F9	3264	(6)	2556	(7)	5547	(7)	212	(8)

a) Equivalent isotropic U defined as $\frac{1}{3}$ of the trace of the orthoganalised U_{ij} tensor.

TABLE 3.8 **Selected Bond Lengths (Å) for $[Ru_2(\eta^6\text{-}C_{16}H_{16})_2(OCH_2CH_3)_3][PF_6]$ (39)**

Ru1-Ru2	3.015	(1)	Ru1-O1	2.058	(5)
Ru1-O2	2.081	(5)	Ru1-O3	2.055	(5)
Ru1-C1	2.269	(7)	Ru1-C2	2.155	(9)
Ru1-C3	2.175	(10)	Ru1-C4	2.298	(9)
Ru1-C5	2.177	(9)	Ru1-C6	2.167	(8)
Ru2-O1	2.084	(5)	Ru2-O2	2.076	(5)
Ru2-O3	2.054	(5)	Ru2-C17	2.271	(9)
Ru2-C18	2.159	(8)	Ru2-C19	2.196	(7)
Ru2-C20	2.332	(8)	Ru2-C21	2.183	(8)
Ru2-C22	2.159	(8)	O1-C33	1.436	(10)
O2-C35	1.420	(9)	O3-C37	1.450	(16)
C1-C2	1.430	(12)	C1-C6	1.403	(11)
C1-C13	1.513	(12)	C2-C3	1.410	(14)
C3-C4	1.412	(16)	C4-C5	1.397	(16)
C4-C15	1.507	(14)	C5-C6	1.430	(14)
C7-C8	1.388	(14)	C7-C12	1.381	(13)
C7-C14	1.525	(14)	C8-C9	1.418	(19)
C9-C10	1.406	(20)	C10-C11	1.429	(20)
C10-C16	1.515	(18)	C11-C12	1.403	(14)
C13-C14	1.603	(13)	C15-C16	1.587	(16)
C17-C18	1.405	(12)	C17-C22	1.413	(12)
C17-C29	1.522	(12)	C18-C19	1.426	(12)
C19-C20	1.419	(12)	C20-C21	1.409	(12)
C20-C31	1.505	(12)	C21-C22	1.447	(12)
C23-C24	1.399	(14)	C23-C28	1.397	(14)
C23-C30	1.521	(13)	C24-C25	1.405	(15)
C25-C26	1.381	(14)	C26-C27	1.397	(13)
C26-C32	1.520	(14)	C27-C28	1.404	(14)
C29-C30	1.588	(13)	C31-C32	1.606	(13)
C33-C34	1.508	(18)	C35-C36	1.517	(14)
C37-C38	1.472	(5)			

TABLE 3.9 **Selected Bond Angles (°) for $[Ru_2(\eta^6\text{-}C_{16}H_{16})_2(OCH_2CH_3)_3][PF_6]$ (39)**

O1-Ru1-Ru2	43.6	(1)	O2-Ru1-Ru2	43.5	(1)
O2-Ru1-O1	70.3	(2)	O3-Ru1-Ru2	42.8	(1)
O3-Ru1-O1	73.8	(2)	O3-Ru1-O2	74.3	(2)
C1-Ru1-Ru2	141.1	(2)	C1-Ru1-O1	104.1	(2)
C1-Ru1-O2	163.6	(3)	C1-Ru1-O3	119.8	(3)
C2-Ru1-Ru2	139.3	(2)	C2-Ru1-O1	96.9	(3)
C2-Ru1-O2	126.4	(3)	C2-Ru1-O3	153.9	(3)
C2-Ru1-C1	37.6	(3)	C3-Ru1-Ru2	140.0	(3)
C3-Ru1-O1	117.6	(4)	C3-Ru1-O2	101.2	(3)
C3-Ru1-O3	166.0	(4)	C3-Ru1-C1	67.1	(3)
C3-Ru1-C2	38.0	(4)	C4-Ru1-Ru2	142.6	(2)
C4-Ru1-O1	152.7	(4)	C4-Ru1-O2	101.4	(3)
C4-Ru1-O3	130.3	(4)	C4-Ru1-C1	76.3	(3)
C4-Ru1-C2	66.4	(4)	C4-Ru1-C3	36.7	(4)
C5-Ru1-Ru2	140.1	(3)	C5-Ru1-O1	167.5	(4)
C5-Ru1-O2	121.1	(3)	C5-Ru1-O3	103.1	(4)
C5-Ru1-C1	66.5	(3)	C5-Ru1-C2	80.6	(4)
C5-Ru1-C3	67.5	(4)	C5-Ru1-C4	36.2	(4)
C6-Ru1-Ru2	138.8	(2)	C6-Ru1-O1	129.3	(3)
C6-Ru1-O2	156.9	(3)	C6-Ru1-O3	97.8	(3)
C6-Ru1-C1	36.8	(3)	C6-Ru1-C2	68.8	(3)
C6-Ru1-C3	81.2	(3)	C6-Ru1-C4	66.7	(4)
C6-Ru1-C5	38.4	(4)	O1-Ru2-Ru1	43.0	(1)
O2-Ru2-Ru1	43.6	(1)	O2-Ru2-O1	69.8	(2)
O3-Ru2-Ru1	42.8	(2)	O3-Ru2-O1	73.3	(2)
O3-Ru2-O2	74.4	(2)	C17-Ru2-Ru1	141.8	(2)
C17-Ru2-O1	113.8	(3)	C17-Ru2-O2	174.7	(2)
C17-Ru2-O3	110.1	(3)	C18-Ru2-Ru1	140.0	(2)
C18-Ru2-O1	97.2	(3)	C18-Ru2-O2	140.5	(3)
C18-Ru2-O3	139.2	(3)	C18-Ru2-C17	36.9	(3)
C19-Ru2-Ru1	140.2	(2)	C19-Ru2-O1	108.4	(3)
C19-Ru2-O2	108.8	(3)	C19-Ru2-O3	176.7	(3)
C19-Ru2-C17	66.6	(3)	C19-Ru2-C18	38.2	(3)
C20-Ru2-Ru1	142.1	(2)	C20-Ru2-O1	139.0	(3)

C20-Ru2-O2	98.5	(2)	C20-Ru2-O3	143.3	(3)
C20-Ru2-C17	76.2	(3)	C20-Ru2-C18	66.4	(3)
C20-Ru2-C19	36.4	(3)	C21-Ru2-Ru1	138.7	(2)
C21-Ru2-O1	175.1	(3)	C21-Ru2-O2	108.4	(3)
C21-Ru2-O3	110.9	(3)	C21-Ru2-C17	67.6	(3)
C21-Ru2-C18	81.2	(3)	C21-Ru2-C19	67.5	(3)
C21-Ru2-C20	36.2	(3)	C22-Ru2-Ru1	139.1	(2)
C22-Ru2-O1	144.6	(3)	C22-Ru2-O2	141.1	(3)
C22-Ru2-O3	96.3	(3)	C22-Ru2-C17	37.1	(3)
C22-Ru2-C18	68.3	(3)	C22-Ru2-C19	80.6	(3)
C22-Ru2-C20	66.4	(3)	C22-Ru2-C21	38.9	(3)
Ru2-O1-Ru1	93.4	(2)	C33-O1-Ru1	123.6	(5)
C33-O1-Ru2	128.5	(6)	Ru2-O2-Ru1	93.0	(2)
C35-O2-Ru1	124.4	(5)	C35-O2-Ru2	124.8	(5)
Ru2-O3-Ru1	94.4	(2)	C37-O3-Ru1	130.2	(6)
C37-O3-Ru2	129.6	(7)	C2-C1-Ru1	66.9	(4)
C6-C1-Ru1	67.7	(4)	C6-C1-C2	119.1	(8)
C13-C1-Ru1	147.9	(6)	C13-C1-C2	118.8	(8)
C13-C1-C6	121.4	(8)	C1-C2-Ru1	75.5	(5)
C3-C2-Ru1	71.8	(6)	C3-C2-C1	119.7	(9)
C2-C3-Ru1	70.2	(5)	C4-C3-Ru1	76.4	(6)
C4-C3-C2	119.8	(10)	C3-C4-Ru1	66.9	(5)
C5-C4-Ru1	67.2	(5)	C5-C4-C3	118.9	(9)
C15-C4-Ru1	149.4	(7)	C15-C4-C3	118.6	(13)
C15-C4-C5	121.6	(13)	C4-C5-Ru1	76.6	(6)
C6-C5-Ru1	70.4	(5)	C6-C5-C4	120.8	(10)
C1-C6-Ru1	75.6	(5)	C5-C6-Ru1	71.2	(5)
C5-C6-C1	118.9	(9)	C12-C7-C8	120.0	(11)
C14-C7-C8	118.1	(10)	C14-C7-C12	120.9	(9)
C9-C8-C7	118.3	(13)	C10-C9-C8	121.1	(13)
C11-C10-C9	118.1	(12)	C16-C10-C9	121.7	(17)
C16-C10-C11	119.0	(17)	C12-C11-C10	118.3	(12)
C11-C12-C7	121.4	(10)	C14-C13-C1	110.0	(8)
C13-C14-C7	112.2	(7)	C16-C15-C4	110.2	(9)
C15-C16-C10	112.7	(9)	C18-C17-Ru2	67.2	(5)
C22-C17-Ru2	67.1	(5)	C22-C17-C18	118.7	(8)

C29-C17-Ru2	147.4	(6)	C29-C17-C18	120.2	(8)
C29-C17-C22	120.5	(8)	C17-C18-Ru2	75.9	(5)
C19-C18-Ru2	72.3	(5)	C19-C18-C17	120.2	(8)
C18-C19-Ru2	69.5	(4)	C20-C19-Ru2	77.1	(5)
C20-C19-C18	119.9	(7)	C19-C20-Ru2	66.6	(4)
C21-C20-Ru2	66.2	(4)	C21-C20-C19	118.8	(7)
C31-C20-Ru2	148.0	(6)	C31-C20-C19	120.0	(8)
C31-C20-C21	120.8	(8)	C20-C21-Ru2	77.7	(5)
C22-C21-Ru2	69.6	(4)	C22-C21-C20	119.1	(7)
C17-C22-Ru2	75.8	(5)	C21-C22-Ru2	71.4	(5)
C21-C22-C17	120.1	(8)	C28-C23-C24	116.5	(9)
C30-C23-C24	120.7	(9)	C30-C23-C28	121.2	(9)
C25-C24-C23	121.2	(9)	C26-C25-C24	120.6	(10)
C27-C26-C25	117.7	(10)	C32-C26-C25	121.4	(9)
C32-C26-C27	119.4	(10)	C28-C27-C26	120.4	(9)
C27-C28-C23	121.1	(9)	C30-C29-C17	109.5	(7)
C29-C30-C23	113.6	(7)	C32-C31-C20	107.7	(8)
C31-C32-C26	114.1	(7)	C34-C33-O1	111.9	(9)
C36-C35-O2	114.5	(8)	C38-C37-O3	110.3	(15)

TABLE 3.10 Crystallographic Data for *trans*-[$Ru(NC_5H_5)_4Cl_2$] (46).

Formula	$Ru_1C_{20}H_{20}N_4Cl_2$
fw, g	488.4
Space group	$I4_1/acd$
a, Å	15.664(2)
b, Å	15.664(2)
c, Å	16.970(2)
α, deg	90.0
β, deg	90.0
γ, deg	90.0
V, Å^3	4164(1)
Z	8
F(000)	1968
d_{calc}, g/cm^3	1.56
Crystal size, mm	0.40 x 0.16 x 0.13
Scan technique	ω-2Θ
μ(Mo-K_α), cm^{-1}	9.66
Orientation reflections, no.; range (2Θ)	25; ($12° \leq 2\Theta \leq 31°$)
Temperature, °C	20
Total No. of reflections measured	4139
No. of unique data	933
Total with $I \geq 1.5\sigma(I)$	757
No. of parameters	83
R[a]	0.0453
R'[b]	0.0320
Weighting scheme	$w = 1.000/(\sigma^2F + 0.000029F^2)$
Largest shift/esd, final cycle	0.002
Largest peak, e/Å^3	0.45

a) $R = \Sigma[|F_o|-|F_c|] / \Sigma|F_o|$

b) $R' = \Sigma[(|F_o|-|F_c|) . w^{\frac{1}{2}}] / \Sigma [|F_o| . w^{\frac{1}{2}}]$

TABLE 3.11 **Atomic Coordinates (x10^4) and Equivalent Isotropic Displacement Parameters for *trans*-[$Ru(NC_5H_5)_4Cl_2$] (46).**

Atom	x		y		z		U(eq)[a]	
Ru1	0		2500		1250		29	(1)
Cl1	1086	(2)	1414	(2)	1250		45	(1)
N1	668	(2)	3155	(2)	386	(2)	34	(1)
C1	1042	(3)	2752	(3)	-221	(3)	43	(1)
C2	1487	(3)	3173	(3)	-798	(3)	55	(2)
C3	1566	(4)	4040	(4)	-771	(3)	59	(2)
C4	1188	(3)	4466	(3)	-154	(3)	50	(2)
C5	749	(3)	4016	(3)	402	(3)	40	(1)
H1	993	(27)	2135	(27)	-236	(23)	51	(12)
H2	1744	(28)	2849	(27)	-1226	(25)	60	(13)
H3	1803	(33)	4315	(33)	-1138	(30)	79	(15)
H4	1220	(29)	5080	(31)	-132	(28)	73	(16)
H5	492	(24)	4278	(25)	767	(22)	37	(12)

a) Equivalent isotropic U defined as $\frac{1}{3}$ of the trace of the orthoganalised U_{ij} tensor.

TABLE 3.12 **Selected Bond Lengths (Å) for *trans*-[$Ru(NC_5H_5)_4Cl_2$] (46).**

Ru1-Cl1	2.406	(1)	Ru1-N1	2.073	(3)
N1-C1	1.341	(5)	N1-C5	1.355	(5)
C1-C2	1.371	(6)	C1-H1	0.97	(4)
C2-C3	1.365	(7)	C2-H2	0.97	(4)
C3-C4	1.375	(7)	C3-H3	0.84	(5)
C4-C5	1.365	(6)	C4-H4	0.96	(5)
C5-H5	0.85	(4)			

TABLE 3.13 **Selected Bond Angles (°) for *trans*-[$Ru(NC_5H_5)_4Cl_2$] (46).**

N1-Ru1-Cl1	89.6	(1)	C1-N1-Ru1	122.1	(3)
C5-N1-Ru1	121.7	(3)	C5-N1-C1	116.3	(3)
C2-C1-N1	123.0	(4)	H1-C1-N1	117	(2)
H1-C1-C2	120	(2)	C3-C2-C1	120.0	(5)
H2-C2-C1	120	(3)	H2-C2-C3	120	(3)
C4-C3-C2	118.0	(4)	H3-C3-C2	122	(4)
H3-C3-C4	120	(4)	C5-C4-C3	119.6	(4)
H4-C4-C3	120	(3)	H4-C4-C5	121	(3)
C4-C5-N1	123.2	(4)	H5-C5-N1	117	(3)
H5-C5-C4	120	(3)			

CHAPTER 4.

FURTHER REACTIONS AND PROPERTIES OF THE COMPOUNDS $[M(\eta^6\text{-ARENE})(\eta^6\text{-}[2_2]\text{PARACYCLOPHANE})][X]_2$ (M=Ru,Os).

4.1 INTRODUCTION.

During studies on a wide range of ruthenium-cyclophane compounds Boekelheide *et al* prepared a number of mononuclear compounds of the type $[Ru(\eta^6\text{-arene})(\eta^6\text{-}[2_2]\text{paracyclophane})][BF_4]_2$. The syntheses and characterisation by elemental analysis and ^1H n.m.r. spectroscopy were reported, together with a few reactions of the corresponding reduced species, $[Ru(0)(\eta^6\text{-arene})(\eta^6\text{-}[2_2]\text{paracyclophane})]$, with protons. Boekelheide *et al* had not structurally characterised any of the Ru(II)-$[2_2]$paracyclophane complexes, nor were any ^{13}C n.m.r. data published. New data in both of these areas have now been obtained and are presented in this chapter. The mononuclear compounds studied here are precursors to the chain compounds, which are the subject of Chapter 5. Therefore it was important to characterise these complexes fully, so that comparisons might be made with the chain compounds, where both faces of the cyclophane are coordinated to metal ions. The reactions of some of the ruthenium(II) compounds with nucleophiles have also been briefly investigated. Several osmium analogues of the previously reported[73,75] ruthenium compounds have been prepared and characterised.

4.2 RESULTS AND DISCUSSION.

4.2.1 The Synthesis and Characterisation of New Osmium(II)-$[2_2]$Paracyclophane Compounds.

(i) $[Os(\eta^6\text{-}C_6H_6)(\eta^6\text{-}C_{16}H_{16})][BF_4]_2$ (17).

The compound $[Os(\eta^6\text{-}C_6H_6)(\eta^6\text{-}C_{16}H_{16})][BF_4]_2$ (17) (Fig. 4.1) was prepared by a procedure strictly analogous to that reported for the ruthenium derivative (11)[73]. The ^1H n.m.r. spectrum (Table 4.2), recorded in CD_3NO_2, exhibits a singlet resonance due to the benzene protons at δ 6.91 (6H), singlets at 6.54 and 7.11 ppm (each 4H) due to the protons of the coordinated and non-coordinated aromatic rings of the paracyclophane ligand, and two six-line multiplets of an AA'XX' coupling pattern at δ 3.21 and 3.51 ppm (each 4H). Integration of the spectrum supports the proposed stoichiometry. When the ^1H n.m.r. spectrum of this osmium compound is compared with that of its ruthenium analogue (11) (Table 4.2), recorded in the same solvent, the most noteworthy feature is the shifting of the signals due to the various aromatic protons to higher frequency. The resonances due to the

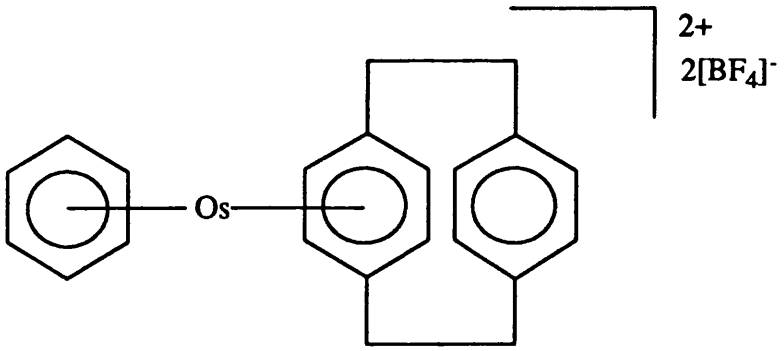

Fig. 4.1 $[Os(\eta^6\text{-}C_6H_6)(\eta^6\text{-}C_{16}H_{16})][BF_4]_2$ (17).

protons of the coordinated benzene and paracyclophane rings are shifted by *ca.* 0.25 ppm as might be expected on the basis of a comparison of the ^1H n.m.r. spectra of the compounds $[M(\eta^6\text{-}C_6H_6)Cl_2]_2$ (Table 2.1). However, the protons of the non-coordinated paracyclophane deck are also shifted significantly, by 0.07 ppm, emphasising the considerable electronic interaction between the two aromatic paracyclophane decks.

When the $^{13}C\text{-}\{^1H\}$ n.m.r. spectra (Table 4.3) of the two compounds are compared, the resonances due to the carbon atoms of the bridging functions and those due to the non-coordinated cyclophane ring are essentially unchanged for the two metals. However, the resonances due to the non-bridgehead carbon atoms of the coordinated cyclophane ring and that due to the carbon atoms of the benzene ring exhibit shifts of *ca.* 7 ppm to lower frequency in the osmium compound. The resonance of the bridgehead carbon atoms of the coordinated cyclophane ring only shift by *ca.* 2 ppm. This smaller shift for the coordinated bridgehead carbon atoms has two possible origins. Firstly, a lesser capacity for orbital rehybridisation, and secondly, a slightly weaker interaction with the metal due to the greater Os-C distance.

Single crystals of (17) were obtained by slow evaporation of a dilute solution of the complex in acetonitrile, and the structure confirmed by X-ray diffraction. The molecular structure of the cation is presented in Fig. 4.2 with some important structural data. The crystallographic data, fractional coordinates, bond lengths, and bond angles are presented in Tables 4.5-4.8, while details of the structure determination and refinement are presented in Section 4.3.4.

The asymmetric unit contains one quarter of the cation, which sits on a site with mm symmetry, and half of a $[BF_4]^-$ anion. Each component of the structure is subject to disorder. The cation is disordered in two respects. The cyclophane ligand is disordered over two positions related by a 90° rotation, with the two sites having equal occupancy.

Lengths, Å.	
Os-C1	2.22(2)
Os-C2	2.19(2)
Os-C3	2.20(2)
Os-C4	2.37(2)
Os-Ar(C_6H_6)	1.73
Os-Ar($C_{16}H_{16}$)	1.70
Inter-ring sep.	2.99
Angles, °.	
Torsion 0.0, required by crystal symmetry	

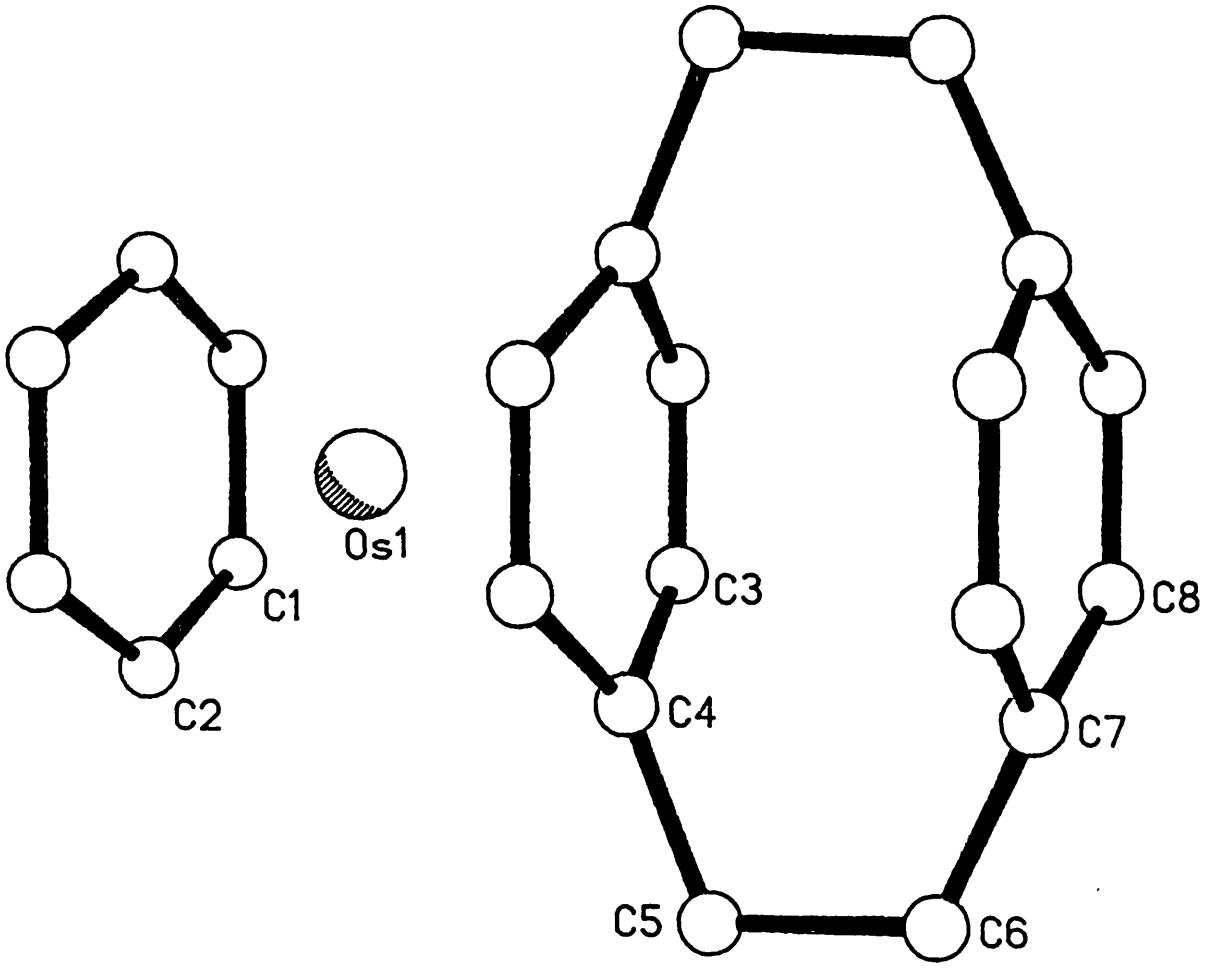

Fig. 4.2 The structure of $[Os(\eta^6\text{-}C_6H_6)(\eta^6\text{-}C_{16}H_{16})]^{2+}$ (17) in the solid state with some important structural parameters (averaged values).

Efficient crystal packing is achieved by having the cyclophane oriented alternately throughout the lattice. The benzene ring is similarly disordered, though in this case one site is occupied 75% of the time, the other 25% of the time. The $[BF_4]^-$ anion is highly disordered.

The osmium(II) ion is sandwiched between the benzene ring and one ring of the paracyclophane ligand, in a similar fashion to that reported for structures of bis(η^6-arene)ruthenium(II) compounds[66,131]. For reported (η^6-arene)osmium(II) structures typical Os-C distances[65,73,104,131-134] lie in the range 2.15-2.25 Å, while the corresponding metal to ring centroid distances average 1.68 Å. The corresponding values for the new structure are given in the caption to Fig. 4.2, and are generally in agreement with previous data. The clear exception is the Os to cyclophane bridgehead carbon distance Os1-C4, 2.37(2) Å, which is significantly longer than the other Os-C bond lengths. This feature was noted for the paracyclophane structures already discussed in previous chapters. The distance between the aromatic decks of the cyclophane is 2.99 Å, which represents the same 0.10 Å shortening when compared with the free ligand[7] as was observed for the ruthenium(II)-paracyclophane structures already described. Crystal symmetry accounts for the apparently 0° torsion angle in the interdeck connectivity, C4-C5-C6-C7. This angle typically has a value of *ca.* 3-11° (see previously described structures and ref. 24). Early crystal structure determinations of the cyclophane ligand also gave a torsion angle of 0°, but a subsequent careful redetermination[7] identified a dynamic disorder that occurs by a twist of the aromatic rings and results in a torsion angle of *ca.* 3°. A similar disorder is undoubtedly present in this metal complex, but due to the presence of the heavy metal atom it was not possible to refine an acceptable model.

(ii) $[Os(\eta^6\text{-}C_{16}H_{16})_2][BF_4]_2$ (47).

The compound $[Os(\eta^6\text{-}C_{16}H_{16})_2][BF_4]_2$ (47) (Fig. 4.3) was prepared by a procedure strictly analogous to that reported[66,75] for $[Ru(\eta^6\text{-}C_{16}H_{16})_2][BF_4]_2$ (13). The details of the syntheses and characterisation are presented in the experimental section. ^1H and $^{13}C\text{-}\{^1H\}$ n.m.r. data for the two compounds are presented in Tables 4.2 and 4.3.

The ^1H n.m.r. spectra exhibit the usual pattern of resonances observed for the η^6-coordinated [2_2]paracyclophane ligand. Comparing the ^1H n.m.r. spectra of (13) and (47), the same chemical shift differences are observed as found for the compounds (11) and (17) i.e. shifts to higher frequency for the osmium compound, (47), of *ca.* 0.3 ppm for the protons of the coordinated deck, and *ca.* 0.1 ppm for those of the non-coordinated

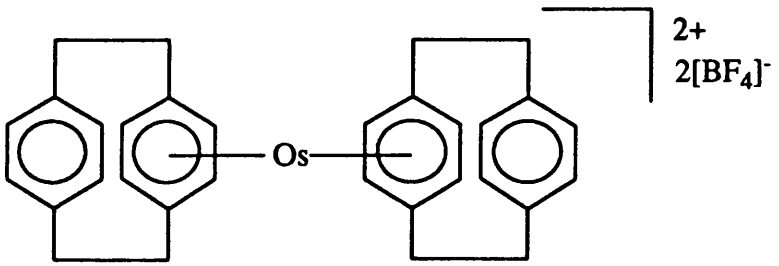

Fig. 4.3 $[Os(\eta^6\text{-}C_{16}H_{16})_2][BF_4]_2$ (47).

deck. When comparing the $^{13}C\text{-}\{^1H\}$ n.m.r. spectra, only the chemical shifts of the non-bridgehead carbon atoms differ significantly. That for the osmium compound, δ 79.6 ppm, being 7 ppm to lower frequency than that observed for (13). This is in contrast to compounds (11) and (17) where, in addition, a 2 ppm chemical shift difference was observed for the bridgehead carbon atoms.

Attempts were made to grow crystals of (13) and (47) from a variety of solvent systems, including by the slow evaporation of nitromethane, acetonitrile, and acetone solutions, and by vapour diffusion of diethyl ether into these solutions. Unfortunately, whenever X-ray quality crystals were obtained they were identified as the cyclophane ligand by measurement of the unit cell parameters. Thus one can conclude that (13) and (47) decompose over a period of a few days in these solvents.

4.2.2 The Crystal Structures of $[Ru(\eta^6\text{-arene})(\eta^6\text{-}C_{16}H_{16})][X]_2$ Compounds.

(i) The Crystal structure of $[Ru(\eta^6\text{-}C_6H_6)(\eta^6\text{-}C_{16}H_{16})][BF_4]_2$ (11).

Single crystals of $[Ru(\eta^6\text{-}C_6H_6)(\eta^6\text{-}C_{16}H_{16})][BF_4]_2$ (11) were obtained from a solution of the compound in nitromethane. The unit cell parameters were determined as described in Section 2.3.5. The parameters are a 7.739(4), b 18.603(10), c 14.880(8) Å, $\alpha=\beta=\gamma$ 90.0°, V 2142(2) $Å^3$. These are identical, within experimental error, to those determined for the osmium analogue, (17), and the two compounds are therefore isomorphous.

(ii) The Crystal Structures of $[Ru(\eta^6\text{-}p\text{-cymene})(\eta^6\text{-}C_{16}H_{16})][BF_4]_2$ (48) and $[Ru((\eta^6\text{-}p\text{-cymene})(\eta^6\text{-}C_{16}H_{16})][BPh_4]_2.\frac{1}{2}Me_2CO$ (49).

The compound $[Ru(\eta^6\text{-p-cymene})(\eta^6\text{-}C_{16}H_{16})][BF_4]_2$ (48) was prepared as described previously[73]. Single crystals were obtained by slow evaporation of a nitromethane solution of the compound, and the structure determined by X-ray crystallography. The structure is not reported in full as the data set was of rather poor quality. This was due to broad peak profiles giving centring difficulties and hence a less accurately determined unit cell than is usually desirable. Nevertheless, the structure determination was considered worthwhile due to the total absence of any (η^6-arene)ruthenium(II)-[2_2]paracyclophane structures in the chemical literature at the time. Although the final residuals were high (R=0.12), and a few peaks between 1 and 2 $eÅ^{-3}$ remained in the final electron density map, the refinement of the structure proceeded smoothly, and gave a result with no grave anomalies in terms of bond lengths or angles. The structure of the cation is presented in Fig. 4.4 with some important structural parameters.

Due to the difficulties encountered with the structure of (48) an alternative anion was sought to the often crystallographically troublesome $[BF_4]^-$. Since (48) was water soluble it was dissolved in this solvent and treated with an excess of $Na[BPh_4]$ resulting in the immediate precipitation of the yellow compound $[Ru((\eta^6\text{-p-cymene})(\eta^6\text{-}C_{16}H_{16})][BPh_4]_2$ (49) which was characterised by elemental analysis (Table 4.1) and by ^1H n.m.r. spectroscopy (Table 4.4).

Single crystals were obtained by the slow evaporation of an acetone solution of the complex, and the structure was determined by X-ray diffraction. The result represents a large improvement over that obtained for (48). Details of the structure determination and refinement are presented in Section 4.3.4, while Tables 4.9-4.12 contain the crystallographic data, fractional coordinates, bond lengths, and bond angles respectively. The molecular structure of the cation is presented in Fig. 4.5 with some important structural parameters.

The ruthenium ion is sandwiched between one aromatic deck of the cyclophane ligand and the *p*-cymene ring, in a similar fashion to (17), (48), and reported bis(η^6-arene)ruthenium(II) structures[66,131]. The Ru-C distances to the cyclophane ligand fall into two groups. The Ru to bridgehead carbon distances, 2.341(9) and 2.360(11) Å, being significantly longer than the Ru to non-bridgehead carbon distances, 2.183-2.212(10) Å. There is little variation within the groups and, as suggested previously, this is due to the uniform geometry of the ligand in the *trans* coordination site. The

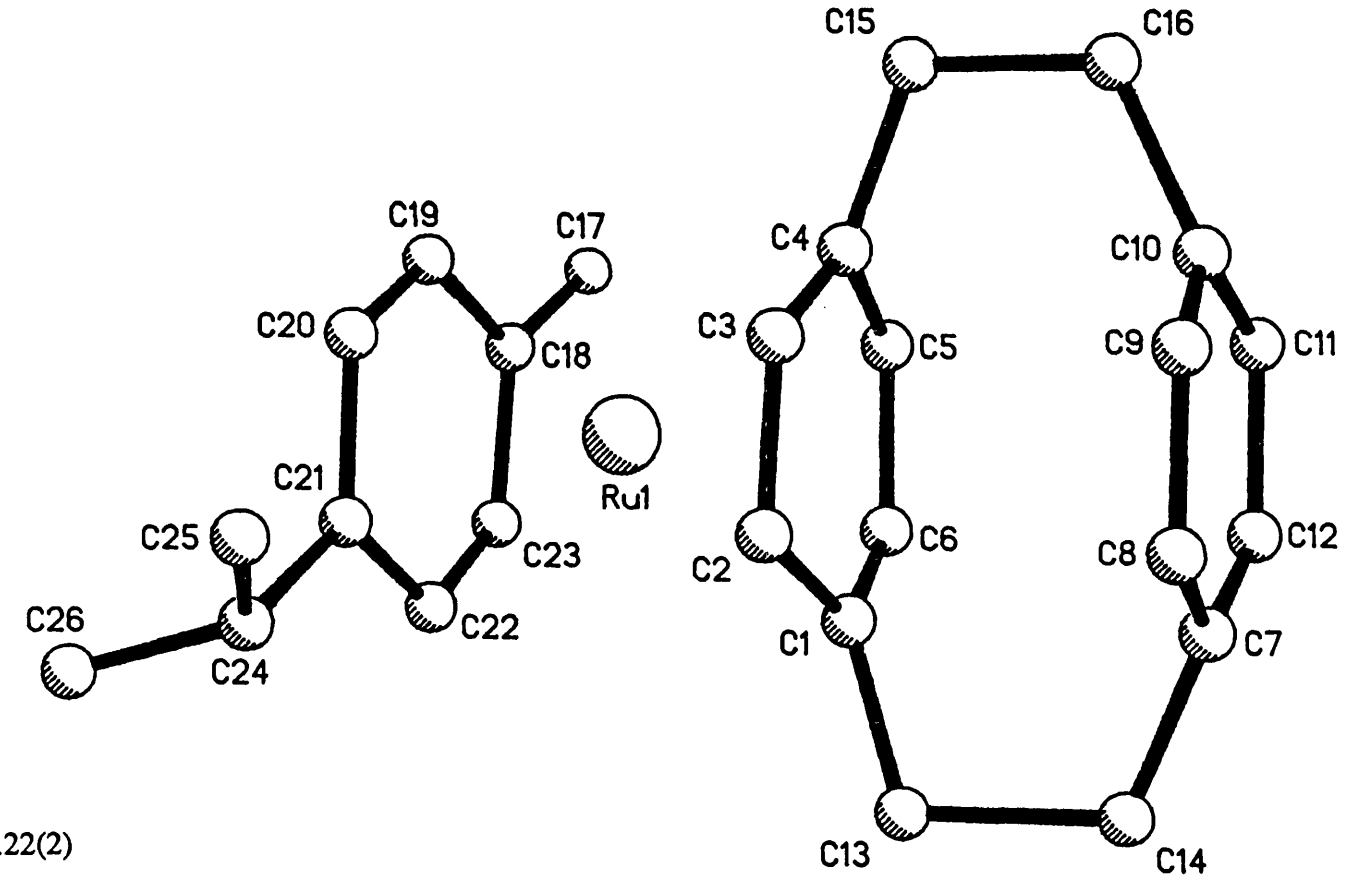

Lengths, Å.	
Ru-Ar(*p*-cymene)	1.72
Ru-Ar($C_{16}H_{16}$)	1.75
Ru-C(*p*-cymene)	*av.* 2.22(2)
Ru-C1,4	*av.* 2.35(2)
Ru-C2,3,5,6	*av.* 2.23(2)

Fig. 4.4 The molecular structure of the cation of [Ru(η^6-*p*-cymene)(η^6-$C_{16}H_{16}$)][BF_4]$_2$ (48), with some important structural parameters

absolute values of the Ru-C distances are in good agreement with similar values reported elsewhere in this thesis. The Ru-C distances to the *p*-cymene ligand lie in the range 2.185-2.262(11) Å, which is in accord with similar distances reported[95,101,109,113,115] for many (η^6-*p*-cymene)ruthenium(II) compounds (2.14-2.21 Å). The Ru-C21 distance is marginally longer than the others, though in the reported structures there is no evidence for the Ru to isopropyl-substituted carbon atom distance being any different from the other Ru-C bond lengths.

The cyclophane inter-ring separation of of 2.99 Å is similar to corresponding distances reported elsewhere in this thesis, while the Ru-Ar distances, Ru-(η^6-*p*-cymene)=1.701 Å, and Ru-(η^6-$C_{16}H_{16}$)=1.705 Å, are slightly longer. The small torsion angles of the cyclophane bridges, 4.1 and 0.8°, are similar to the values observed in other structures where the coordination sites *trans* to the cyclophane are uniformly occupied, e.g. (37), (39) and (17). In common with many other structures[65,90,95,101,109,113-115] containing the *p*-cymene ligand, the *p*-cymene ligand here has one methyl group of the isopropyl substituent oriented towards the metal ion and one pointing away from it. Unusually however, the methyl and isopropyl groups are distorted out of the ring plane away from the metal, by 1.6 and 4.3° respectively. These groups are more generally distorted towards the metal atom[65,90,95].

The most noteworthy difference between the structures of (48) and (49) is illustrated in Fig. 4.6. This figure gives views perpendicular to the ring planes for the two cations. In the structure of the $[BF_4]^-$ salt, (48), the two coordinated aromatic rings are exactly eclipsed, whereas in that of the $[BPh_4]^-$ salt, (49) they are staggered by *ca.* 15°. Therefore one might conclude that there is no overwhelming driving force governing the mutual orientation of the two arenes to be either staggered or eclipsed, but that efficiency in crystal packing determines this geometry.

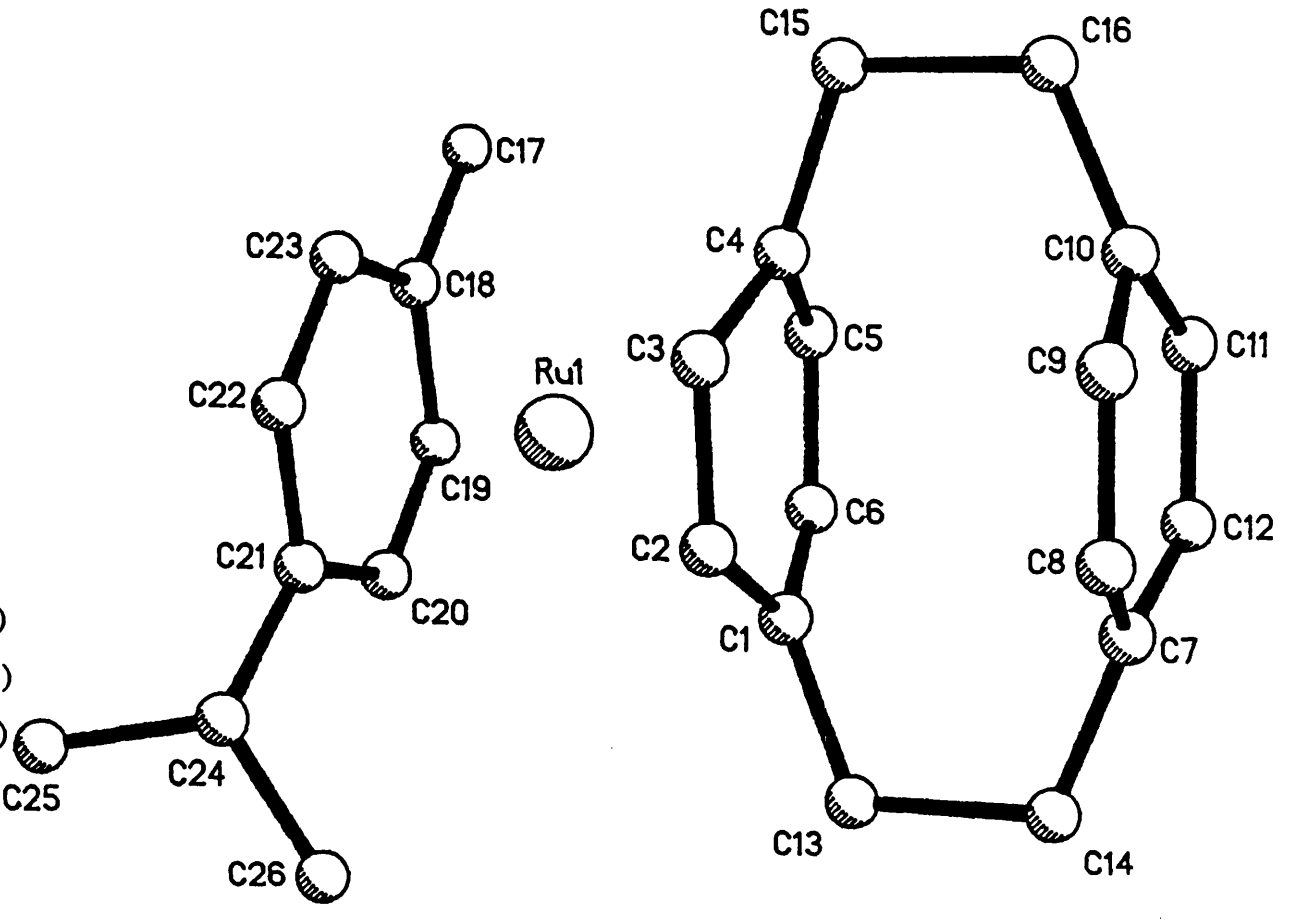

Lengths, Å.	
Ru-Ar(*p*-cymene)	1.70
Ru-Ar($C_{16}H_{16}$)	1.71
Ru-C(*p*-cymene)	21.9-2.26(1)
Ru-C1,4	2.34, 2.36(1)
Ru-C2,3,5,6	2.18-2.21(1)
Inter-ring sep.	2.99
Angles, °.	
Torsion	0.8, 4.1

Fig. 4.6 The molecular structure of the cation of [Ru(η^6-*p*-cymene)(η^6-$C_{16}H_{16}$)][BPh_4]$_2$.½Me_2CO (49) with some important structural parameters.

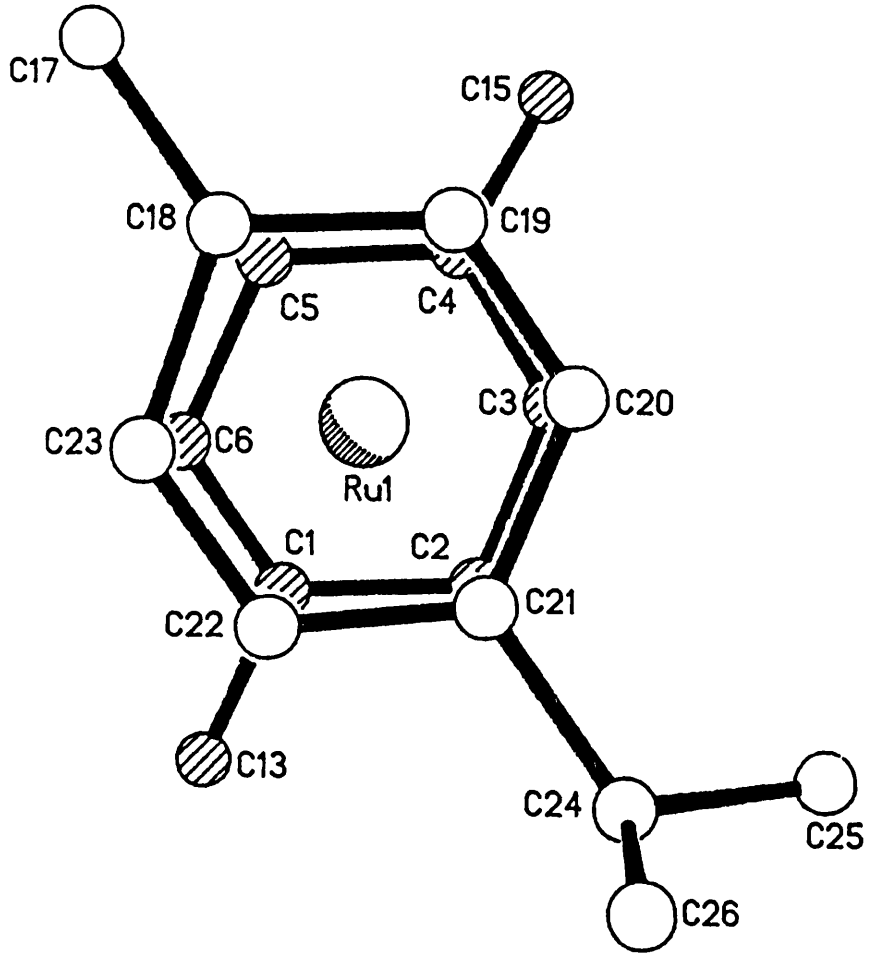

[Ru(η⁶-*p*-cymene)(η⁶-$C_{16}H_{16}$)][BF_4]$_2$ (48).

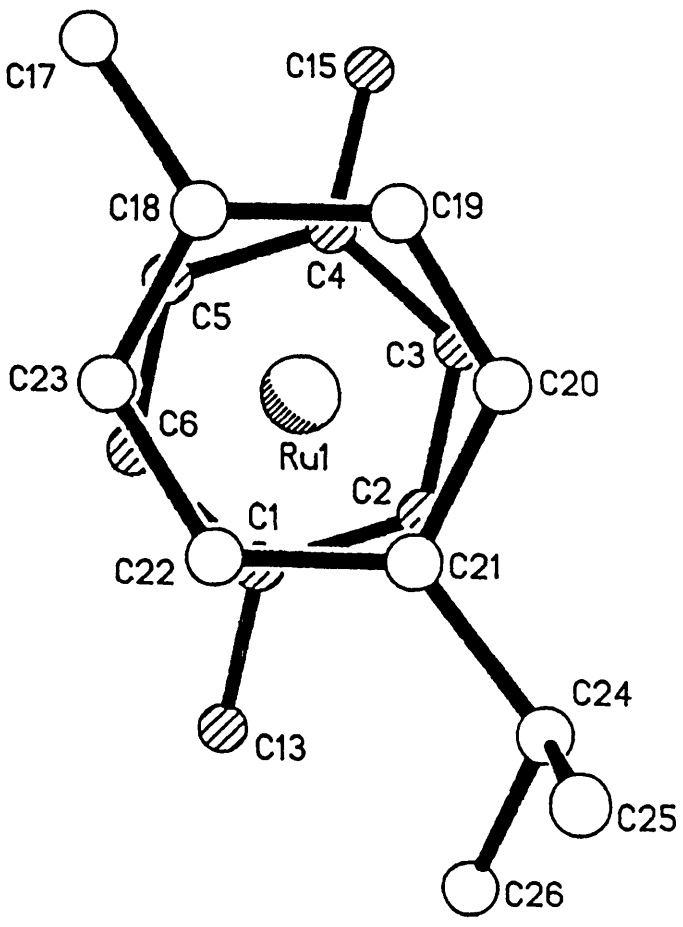

[Ru(η⁶-*p*-cymene)(η⁶-$C_{16}H_{16}$)][BPh_4].½Me_2CO (49).

Fig. 4.6 Plots of (48) and (49) viewed perpendicualar to the ring planes.

4.2.3 Further Studies on $[M(\eta^6\text{-arene})(\eta^6\text{-}C_{16}H_{16})][X]_2$ Compounds.

(i) $^{13}C\text{-}\{^1H\}$ n.m.r. Studies on $[M(\eta^6\text{-arene})(\eta^6\text{-}C_{16}H_{16})][X]_2$ Compounds.

The measurement of the $^{13}C\text{-}\{^1H\}$ n.m.r. spectra of all the $[M(\eta^6\text{-arene})(\eta^6\text{-}C_{16}H_{16})][X]_2$ compounds, to be used in the synthesis of chain compounds, was considered an essential precursor to the unambiguous characterisation of those compounds. Boekelheide *et al* had not published $^{13}C\text{-}\{^1H\}$ n.m.r. spectral data for the compounds he reported. The compounds studied are $[Ru(\eta^6\text{-}C_6H_6)(\eta^6\text{-}C_{16}H_{16})][BF_4]_2$ (11), $[Ru(\eta^6\text{-}C_{16}H_{16})_2][BF_4]_2$ (13), $[Ru(\eta^6\text{-}p\text{-cymene})(\eta^6\text{-}C_{16}H_{16})][BF_4]_2$ (48), and $[Ru(\eta^6\text{-}C_6Me_6)(\eta^6\text{-}C_{16}H_{16})][BF_4]_2$ (50). The spectra of the new osmium compounds (17) and (47) have also been recorded. The data are presented in Table 4.3. The ^{13}C n.m.r. spectrum of (11), recorded in d_6-DMSO, has been reported by Mori *et al*[81] but as this strongly coordinating solvent tends to displace the coordinated arenes over a period of hours the data have now been recorded in CD_3NO_2.

(ii) The Reaction of $[Ru(\eta^6\text{-}C_{16}H_{16})_2][BF_4]_2$ (13) with $[Os(\eta^6\text{-}C_6H_6)(acetone)_3][BF_4]_2$ under Reflux Conditions.

As described in Chapter 1, Boekelheide *et al* prepared triple-layered complexes of the type $[(\eta^6\text{-arene})Ru(\eta^6,\eta^6\text{-}C_{16}H_{16})Ru(\eta^6\text{-arene})][BF_4]_4$[66,73]. It was our intention to prepare a mixed-metal analogue of this type of compound, namely $[(\eta^6\text{-}C_6H_6)Os(\eta^6,\eta^6\text{-}C_{16}H_{16})Ru(\eta^6\text{-}C_6H_6)][BF_4]_4$. To this end $[Ru(\eta^6\text{-}C_6H_6)(\eta^6\text{-}C_{16}H_{16})][BF_4]_2$ (11) was treated with $[Os(\eta^6\text{-}C_6H_6)(acetone)_3][BF_4]_2$ (1:1 mol ratio) in a refluxing mixture of acetone/CF_3CO_2H for 30 minutes. Cooling, followed by precipitation with diethyl ether, gave a pale yellow powder. The ^1H n.m.r. spectrum, recorded in d_6-DMSO, showed two sets of resonances, which were attributed to the cations $[Ru(\eta^6\text{-}C_6H_6)(\eta^6\text{-}C_{16}H_{16})]^{2+}$ (11) and $[Os(\eta^6\text{-}C_6H_6)(\eta^6\text{-}C_{16}H_{16})]^{2+}$ (17). These compounds were present in solution in an approximate ratio of 1:3, and thus we conclude that under these experimental conditions the paracyclophane ligand has been substantially transferred to the osmium ion. It had previously been reported[85] that when the iron(II) complex $[Fe(\eta^6\text{-octamethylparacyclophane})_2]^{2+}$ is treated with $[Ru(\eta^6\text{-}p\text{-cymene})(acetone)_3]^{2+}$ in CF_3CO_2H, the arene-iron bonds are disrupted and only $[Ru(\eta^6\text{-}p\text{-cymene})(\eta^6\text{-octamethylparacyclophane})]^{2+}$ is isolated. Thus under the appropriate conditions iron will be displaced by ruthenium, and ruthenium by osmium.

(iii) The Synthesis of $[Ru(\eta^6\text{-}p\text{-cymene})(\eta^6\text{-}C_{16}H_{16})][(CF_3CO_2)_2H]_2$ (51)

Due to the problems of disorder often encountered with the $[BF_4]^-$ anion in crystal structures, and the more general lack of success in crystallising the (η^6-arene)ruthenium(II)-[2$_2$]paracyclophane compounds, alternative counter-ions were sought. One of the counter-ions considered was trifluoroacetate $[CF_3CO_2]^-$. With this as the aim, $[Ru(\eta^6\text{-}p\text{-cymene})Cl_2]_2$ was treated with $Ag[CF_3CO_2]$ in acetone to remove the chloride ions. After removal of the AgCl by filtration, the red solution was refluxed with [2$_2$]paracyclophane and trifluoroacetic acid in the usual way. Infrared and microanalytical data confirmed the presence of the dimeric anion $[(CF_3CO_2)_2H]^-$ in the product (51). Attempts at growing crystals of this compound were unsuccessful.

4.2.4 Reactions of $[M(\eta^6\text{-arene})(\eta^6\text{-}C_{16}H_{16})][X]_2$ Compounds with Nucleophiles.

(i) The Reactions of $[Ru(\eta^6\text{-}C_6H_6)(\eta^6\text{-}C_{16}H_{16})][BF_4]_2$ (11) with $Na[BH_4]$ and K[CN].

When $[Ru(\eta^6\text{-}C_6H_6)(\eta^6\text{-}C_{16}H_{16})][BF_4]_2$ (11) was treated with sodium borohydride in methanol a yellow/green solution was formed from which a pale yellow solid was isolated. This solid analysed closely for $[Ru(\eta^5\text{-}C_6H_7)(\eta^6\text{-}C_{16}H_{16})][BF_4]$ (52) (Table 4.1). The ^{1}H n.m.r. spectrum was recorded in CD_3NO_2 and is presented in Fig. 4.7. An analysis of the spectrum reveals that the cyclophane ligand has been untouched by the H^- nucleophile, since all the usual cyclophane resonances are observed (Table 4.4). The singlet resonance in the spectrum of (11) due to the protons of the benzene ring is no longer apparent, but five new resonances are observed. These resonances are assigned to the protons of the η^5-coordinated cyclohexadienyl ligand. A series of decoupling experiments has verified the assignment of the chemical shifts as follows: δ 6.23 (t, 1H) H_5, 4.85 (t, 2H) $H_{4,6}$, 3.35 (t, 2H) $H_{3,7}$, 2.37 ppm (dt, 1H) H_2(*endo*), 2.08 (d, 1H) H_1(*exo*), (Fig. 4.8 gives the hydrogen atom numbering scheme). The resonance for H_1 is partially masked by the peak due to the water in the CD_3NO_2 solvent, but was clearly observed when the spectrum was recorded in CD_2Cl_2. Thus it is clear that the benzene ring has been attacked by the hydride ion. Stephenson *et al* have reported[91] that the reaction of H^- with $[Ru(\eta^6\text{-}C_6H_6)(PMe_2Ph)phen][PF_6]_2$ also yields a product containing a cyclohexadienyl ligand, namely $[Ru(\eta^5\text{-}C_6H_7)(PMe_2Ph)(phen)][PF_6]$. This compound exhibited resonances at δ 5.79, 4.78, 2.80 and 2.38 ppm which were similarly assigned.

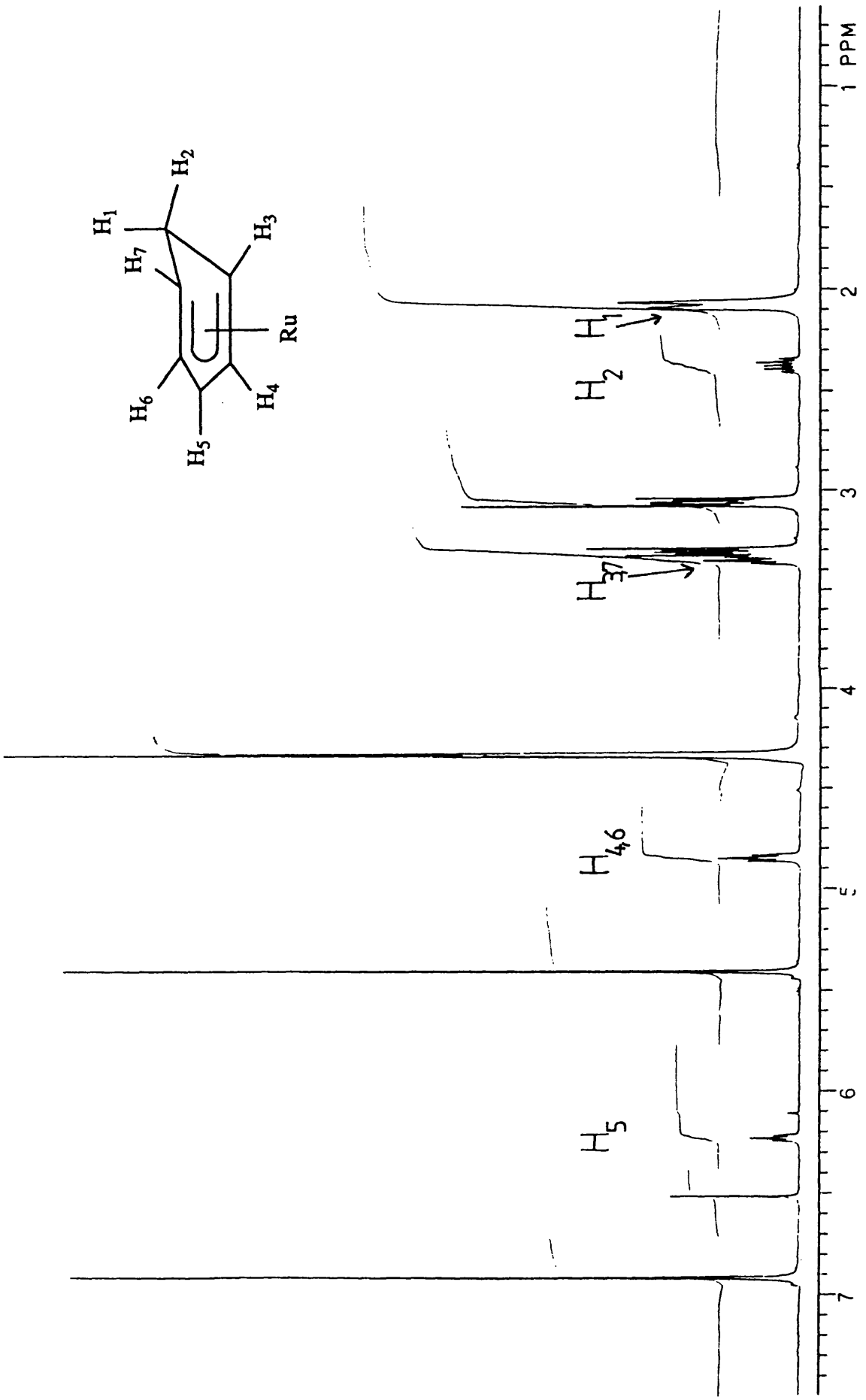

Fig. 4.7 The ^1H n.m.r. spectrum of $[Ru(\eta^5\text{-}C_6H_7)(\eta^6\text{-}C_{16}H_{16})][BF_4]$ (52), recorded in CD_3NO_2 at 298 K.

When compound (11) was treated with $[CN]^-$ in a similar fashion to that described above in various stoichiometric ratios (1:1, 1:1.5, 1:excess), the solutions rapidly turned yellow. However, the isolated solids were shown by ^1H n.m.r. spectroscopy to be a mixture of products. The cleanest spectra were obtained for solids isolated from reactions in which a low stoichiometric ratio of (11):$[CN]^-$ was employed. These spectra showed that in the major product the benzene ring had been attacked by the nucleophile, leaving the cyclophane ligand intact.

(ii) **The Reaction of $[Ru(\eta^6\text{-}p\text{-cymene})(\eta^6\text{-}C_{16}H_{16})][BF_4]_2$ (48) with $Na[BH_4]$**

When compound (48) was treated with an excess of $Na[BH_4]$, as described above, a pale yellow solid was obtained. An analysis of the ^1H n.m.r. spectrum of this solid, recorded in $CDCl_3$, indicates that two products are formed, in which the *p*-cymene ligand has been attacked by the hydride in both cases. A detailed series of ^1H n.m.r. decoupling experiments has confirmed that the two compounds formed are (53) and (54) (Fig. 4.8), which are present in a 3:1 ratio. The full assignment of the n.m.r. spectrum is presented in

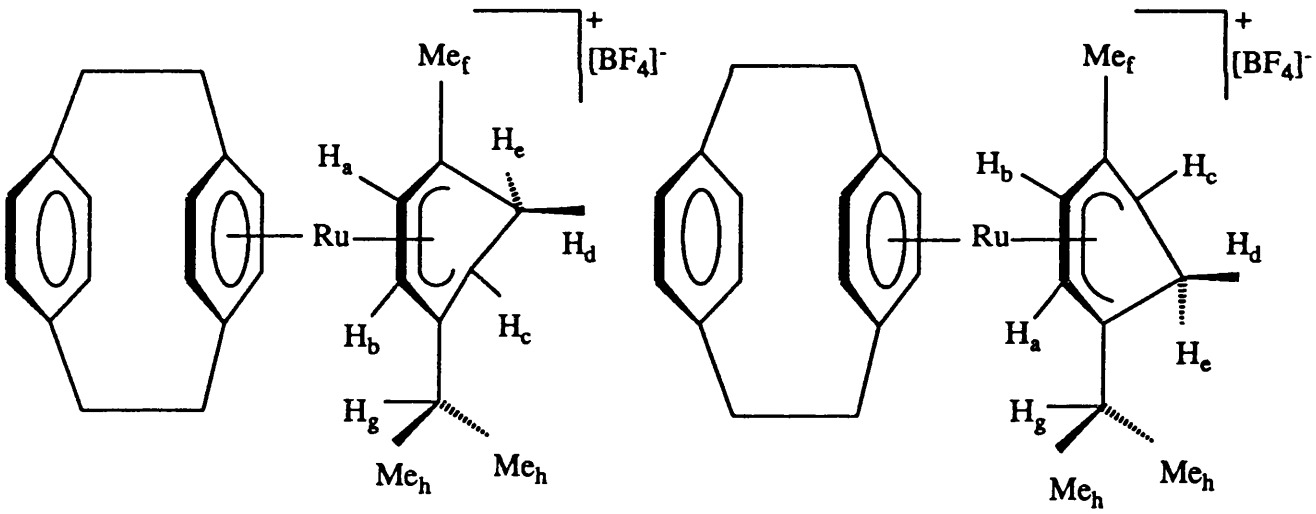

(53) (54)

Fig. 4.8 The two products formed in the reaction of (48) and $Na[BH_4]$.

the experimental section. The *exo*-protons H_d give rise to doublet resonances with $^2J_{Hd\text{-}He}$ *ca.* 14 Hz, while the *endo*-protons H_e give rise to doublets of doublets with $^2J_{Hd\text{-}He}$ *ca.* 14 Hz and $^3J_{Hc\text{-}He}$ *ca.* 6 Hz. A Newman projection showing the orientation of the C-H bonds to H_c and H_d shows that they are almost perpendicular, and hence give rise to very small

couplings (< 1Hz), while that of the C-H bonds to H_e and H_c shows that they are twisted by only a few degrees, and therefore exhibit larger coupling constants. Since the *p*-cymene ligand is substituted by three different groups, the cation is chiral. This results in the cyclophane resonances exhibiting a characteristic pattern, previously described in Chapter 2 for the compounds $[Ru(\eta^6\text{-}C_{16}H_{16})Cl(NC_5H_5)(PR_3)][X]$.

Attack by the hydride ion has occurred at the two unsubstituted sites on the *p*-cymene ring, but in unequal proportions. There are two reasons for this. The first is steric, the smaller methyl group allowing easier approach to the ring position *ortho* to it. The second reason is electronic. Green *et al* have shown that hydride attack is favoured at sites *meta* to electron releasing groups[135]. The isopropyl group, being more alkylated than the methyl, is the better electron donor, again promoting attack at the ring position *ortho* to the methyl group.

The FAB mass spectrum exhibits a peak at 445 mass units which corresponds to $RuC_{26}H_{31}$, and supports the proposed addition of one H^- ion to the cation. Although mass spectra have been found to be accurate to within one mass unit, in this instance this data could not be used in isolation to verify the identity of the compound, and cannot distinguish between the two isomers. The simulated isotopic pattern matched that observed experimentally.

4.2.5 The Reaction of $[Ru(\eta^6\text{-}C_{16}H_{16})Cl_2]_2$ (1) with TlCp: An Alternative Synthesis of $[Ru(\eta^5\text{-}C_5H_5)(\eta^6\text{-}C_{16}H_{16})][PF_6]$ (10).

When $[Ru(\eta^6\text{-}C_{16}H_{16})Cl_2]_2$ (1) was treated with cyclopentadienylthallium in acetonitrile, a brown solution and a precipitate of TlCl was obtained. The solution was filtered, concentrated, and diethyl ether added causing a brown solid to form. This solid was shown to contain the cation $[Ru(\eta^5\text{-}C_5H_5)(\eta^6\text{-}C_{16}H_{16})]^+$ by its ^1H n.m.r. spectrum. The chloride counter-ion was exchanged for $[PF_6]^-$ by dissolving the compound in water and treating with $NH_4[PF_6]$. The tan solid, $[Ru(\eta^5\text{-}C_5H_5)(\eta^6\text{-}C_{16}H_{16})][PF_6]$ (10), was identified by ^1H and $^{13}C\text{-}\{^1H\}$ n.m.r. spectroscopy (Tables 4.4 and 4.3). In the ^1H n.m.r. spectrum the protons of the $[C_5H_5]^-$ ring give rise to a singlet resonance at δ 5.07 ppm, those of the coordinated and non-coordinated cyclophane rings exhibit singlet resonances at δ 5.43 and 6.89 ppm respectively, and the usual multiplet resonances are observed at δ 2.98 and 3.28 ppm. The chemical shift observed for the cyclopentadiene protons is similar to that reported[48] for $[Ru(\eta^5\text{-}C_5H_5)(\eta^6\text{-arene})][X]$ compounds (4.9-5.4 ppm). It is noteworthy that in the $^{13}C\text{-}\{^1H\}$ n.m.r. spectrum of (10) the resonances due to the cyclophane ligand are closely similar to those observed for (1) (Table 2.2), but different to

those observed for the [Ru(η^6-arene)(η^6-$C_{16}H_{16}$)][BF_4]$_2$ compounds. The resonances due to C_1 (Table 4.3) occur *ca.* 12 ppm to lower frequency of those observed in the spectra of the η^6-arene compounds, while the resonance due to C_3 is observed *ca.* 6 ppm to lower frequency. The carbon atoms of the cyclopentadiene ring resonate at δ 79.0 ppm, which is similar to that reported[48] in various [Ru(η^5-C_5H_5)(η^6-arene)][X] compounds (79-82 ppm). Compound (10) was previously prepared by Mann *et al*[46] by reaction of [2_2]paracyclophane with [CpRu(MeCN)$_3$][PF_6] (9) under reflux conditions. The ^{1}H n.m.r. spectroscopic data reported[46] are in agreement with those presented here, although a different solvent was employed in their measurements (d_6-acetone), and the resonance due to the -CH_2CH_2- protons was described simply as a single multiplet.

4.3 EXPERIMENTAL.

4.3.1 Instrumentation and Physical Measurements.

As described in Section 2.3.1.

4.3.2 Materials.

The compounds $[M(\eta^6\text{-}C_{16}H_{16})Cl_2]_2$ {M=Ru (1), M=Os (16)} were prepared as described in Section 2.3.3. The complexes $[Ru(\eta^6\text{-arene})Cl_2]_2$ (arene=C_6H_6, 1,4-$MeC_6H_4CHMe_2$) were prepared by literature methods[21,31]. The complex $[Ru(\eta^6\text{-}C_6Me_6)Cl_2]_2$ was prepared by heating $[Ru(\eta^6\text{-}1,4\text{-}MeC_6H_4CHMe_2)Cl_2]_2$ with a large excess of molten hexamethylbenzene at ca. 460 K for 4-5 h in the absence of a solvent[51]. The excess ligand was removed by washing with ether and the pure product was obtained by recrystallisation from $CHCl_3$. The complex $[Os(\eta^6\text{-}C_6H_6)Cl_2]_2$ was obtained by the published method[63].

To prepare the complexes $[Ru(\eta^6\text{-arene})(\eta^6\text{-}C_{16}H_{16})][BF_4]_2$, {arene=$C_6H_6$ (11), C_6Me_6 (51), 1,4-$MeC_6H_4CHMe_2$ (49), $C_{16}H_{16}$ (48)}, the appropriate $[Ru(\eta^6\text{-arene})Cl_2]_2$ complex was first treated with a slight excess of $Ag[BF_4]$ in acetone to give the compounds $[Ru(\eta^6\text{-arene})(acetone)_3][BF_4]_2$. The solvates were then refluxed for 30 min. with an equimolar quantity of $[2_2]$paracyclophane in a 1:1 mixture of acetone and trifluoroacetic acid to give the essentially pure products in high yield[66,73]. Cyclopentadienylthallium (TlCp) was prepared by the published method[50]. Other materials were obtained and used as described in Section 2.3.2.

4.3.3 Synthesis.

The synthesis of $[Os(\eta^6\text{-}C_6H_6)(\eta^6\text{-}C_{16}H_{16})][BF_4]_2$ (17).

Silver tetrafluoroborate (0.55 g; 2.83 mmol) was added to a suspension of $[Os(\eta^6\text{-}C_6H_6)Cl_2]_2$ (0.42 mg; 0.62 mmol) in acetone (10 cm^3). The solution was stirred at room temperature for 30 min. and the silver chloride precipitate removed by filtration through celite. The silver chloride was washed with acetone (20 cm^3) until no longer yellow in colour. The clear orange solution of $[Os(\eta^6\text{-}C_6H_6)(acetone)_3][BF_4]_2$ was concentrated to 10 cm^3. Trifluoroacetic acid (5 cm^3) and $[2_2]$paracyclophane (0.25 g; 1.20

mmol) were added and the mixture refluxed for 30 min. The solution was cooled in an ice-bath and diluted with diethyl ether (50 cm^3). A pale yellow product precipitated. The solid was filtered off, washed with acetone (5 cm^3), then diethyl ether (15 cm^3), and dried *in vacuo*. Yield, based on $[Os(\eta^6\text{-}C_6H_6)Cl_2]_2$: 0.44 g; 0.68 mmol; 55%.

Infrared spectrum: $[BF_4]^-$: 1062 (s, br); δ(CCC): 661 (m) cm^{-1}.

The synthesis of $[Os(\eta^6\text{-}C_{16}H_{16})_2][BF_4]_2$ (47).

This complex was prepared similarly to (17). $[Os(\eta^6\text{-}C_{16}H_{16})Cl_2]_2$ (16) (0.16 g; 0.17 mmol), $Ag[BF_4]$ (0.16 g; 0.82 mmol), acetone (10 cm^3), [2$_2$]paracyclophane (0.05 g; 0.26 mmol). Yield, based on $[Os(\eta^6\text{-}C_{16}H_{16})Cl_2]_2$: 0.08 g; 0.11 mmol; 40%.

Infrared spectrum: $[BF_4]^-$ 1053 (s, br); δ(CCC) 661 (w); $\nu(CH)_{ar}$ 3061 cm^{-1}.

Mass spectrum:

m/e	Fragment.
695	$[Os(\eta^6\text{-}C_{16}H_{16})_2][BF_4]^+$
608	$[Os(\eta^6\text{-}C_{16}H_{16})_2]^+$
400	$[Os(\eta^6\text{-}C_{16}H_{16})]^+$
487	$[(\eta^6\text{-}C_{16}H_{16})][BF_4]^+$

The synthesis of $[Ru(\eta^6\text{-}p\text{-cymene})(\eta^6\text{-}C_{16}H_{16})][BPh_4]_2$ (49).

Tetraphenylboron sodium (0.04 g; 0.10 mmol) was added to a filtered solution of $[Ru(\eta^6\text{-}p\text{-cymene})(\eta^6\text{-}C_{16}H_{16})][BF_4]_2$ (0.03 g; 0.05 mmol) in water (5 cm^3) at ambient temperature which caused the bright yellow product to precipitate from solution immediately. The yellow solid was filtered off and washed with water (2 cm^3), methanol (2 cm^3), and diethyl ether (10 cm^3). Yield after air drying: 0.04 g; 0.04 mmol; 70%.

Infrared spectrum: $[BPh_4]^-$: 706 (s), 736 (s), 751 (s); δ(CCC): 658 (m); $\nu(CH)_{ar}$: 3039 (m).

The synthesis of $[Ru(\eta^6\text{-}p\text{-cymene})(\eta^6\text{-}C_{16}H_{16})][(CF_3CO_2)_2H]_2$ (51).

Silver trifluoroacetate (0.40 g; 1.79 mmol) was added to a suspension of $[Ru(\eta^6\text{-}p\text{-cymene})Cl_2]_2$ (0.24 g; 0.40 mmol) in acetone (10 cm^3). The mixture was stirred at room temperature for 1 h., then filtered through celite to remove the precipitated silver chloride. Trifluoroacetic acid (5 cm^3) and $[2_2]$paracyclophane (0.16 g; 0.77 mmol) were added to the deep red solution. The solution was refluxed for 40 min., allowed to cool to room temperature, and then diluted with diethyl ether (60 cm^3). The pale, silvery yellow, microcrystalline product which precipitated, was isolated by filtration, washed with diethyl ether (10 cm^3), and dried *in vacuo*. Yield, based on $[Ru(\eta^6\text{-}p\text{-}cymene)Cl_2]_2$: 0.57 g; 0.64 mmol; 80%.

Infrared spectrum: ν(CF): 1135 (s, br), 1199 (s, br); ν(CO): 1751 (vs, br), 1781 (vs, br); ν(OH): 2721 (m); δ(CCC): 670 (w), $\nu(CH)_{ar}$: 3071 cm^{-1}.

The syntheses of $[Ru(\eta^5\text{-}C_5H_5)(\eta^6\text{-}C_{16}H_{16})][X]$ {X=Cl^-, $[PF_6]^-$ (10)}.

Cyclopentadienylthallium (0.08 g; 0.30 mmol) was added to a suspension of $[Ru(\eta^6\text{-}C_{16}H_{16})Cl_2]_2$ (1) (0.21 g; 0.28 mmol) in acetonitrile (40 cm^3). A brown solution formed while stirring for 80 min. Thallium chloride precipitated from the solution and was removed by filtration through celite. The volume of the solution was reduced to *ca.* 10 cm^3, and then diethyl ether (40 cm^3) was added to precipitate a brown solid. The solid was isolated by filtration and washed with diethyl ether (10 cm^3), then air dried. The brown solid was identified by ^1H n.m.r. spectroscopy as $[Ru(\eta^5\text{-}C_5H_5)(\eta^6\text{-}C_{16}H_{16})]Cl$. Yield: 0.09 g; 0.22 mmol, 38%.

Purification of $[Ru(\eta^5\text{-}C_5H_5)(\eta^6\text{-}C_{16}H_{16})]^+$ was attempted on a small scale. $[Ru(\eta^5\text{-}C_5H_5)(\eta^6\text{-}C_{16}H_{16})]Cl$ was dissolved in water, filtered to remove any undissolved material, and treated with an excess of $NH_4[PF_6]$. The product, $[Ru(\eta^5\text{-}C_5H_5)(\eta^6\text{-}C_{16}H_{16})][PF_6]$ (10), formed as a tan precipitate, which was isolated by filtration and washed with water (2 cm^3), ethanol (2cm^3), and diethyl ether (10 cm^3), then air dried.

The synthesis of $[Ru(\eta^5\text{-}C_6H_7)(\eta^6\text{-}C_{16}H_{16})][BF_4]$ (52).

Sodium borohydride (0.01 g; 0.26 mmol) was added a little at a time to a suspension of $[Ru(\eta^6\text{-}C_6H_6)(\eta^6\text{-}C_{16}H_{16})][BF_4]_2$ (11) (0.05 g; 0.09 mmol) in methanol (5

cm^3). The solution effervesced and then cleared after *ca.* 2 min. Water (1.0 cm^3) was added dropwise to the yellow/green solution to destroy any unreacted hydride. Dichloromethane (25 cm^3) was added, and the organic layer was then separated from the aqueous layer. The organic layer was reduced in volume to *ca.* 2 cm^3 and stored at *ca.* 255 K overnight. A pale yellow precipitate formed which was isolated by filtration, washed with diethyl ether (10 cm^3), and air dried. Yield: 0.01 g; 0.02 mmol; 22%.

Infrared spectrum: $[BF_4]^-$: 1049 (s, br); δ(CCC): 678 (m); $\nu(CH)_{ar}$: 3041 (m); $\nu(CH_{exo})$: 2813 (m) cm^{-1}.

The synthesis of $[Ru(\eta^5\text{-}1\text{-}Me,2\text{-}H_2,4\text{-}CHMe_2\text{-}C_6H_3)(\eta^6\text{-}C_{16}H_{16})][BF_4]$ (53) and $[Ru(\eta^5\text{-}1\text{-}Me,3\text{-}H_2,4\text{-}CHMe_2\text{-}C_6H_3)(\eta^6\text{-}C_{16}H_{16})][BF_4]$ (54).

Sodium borohydride (0.01 g; 0.26 mmol) was added to a suspension of $[Ru(\eta^6\text{-}p\text{-cymene})(\eta^6\text{-}C_{16}H_{16})][BF_4]_2$ (48) (0.09 g, 0.14 mmol) in methanol (5 cm^3). The solution cleared and became olive green after *ca.* 5 min., and was stirred for a total of 20 min. Water (2 cm^3) was added to destroy any remaining hydride, and the solution was pumped to dryness. Nitromethane (20 cm^3) was added to extract the product. The resulting solution was filtered to remove a dark residue, leaving a clear yellow filtrate. This was reduced in volume to *ca.* 5 cm^3 and cooled to 255 K, which caused the pale yellow product to precipitate. The solid was isolated by filtration, washed with diethyl ether (10 cm^3) and dried *in vacuo*. Yield: 0.04 g; 0.08 mmol; 55%.

Infrared spectrum: $[BF_4]^-$: 1055 (s, br); δ(CCC): 665 (w), 679 (s); $\nu(CH)_{ar}$: 3026 (s); $\nu(CH_{exo})$: 2804 cm^{-1}.

Mass spectrum:

m/e	Fragment
445	$[Ru(\eta^5\text{-}1\text{-}Me,2\text{-}H_2,4\text{-}CHMe_2\text{-}C_6H_3)(\eta^6\text{-}C_{16}H_{16})]^+$ and $[Ru(\eta^5\text{-}1\text{-}Me,3\text{-}H_2,4\text{-}CHMe_2\text{-}C_6H_3)(\eta^6\text{-}C_{16}H_{16})]^+$
310	$[Ru(\eta^6\text{-}C_{16}H_{16})]^+$

^{1}H n.m.r. data: Solvent: $CDCl_3$. Operating frequency: 400 MHz.

H_a	4.72 (d,1H)	H_b	5.95 (d,1H)

(53)

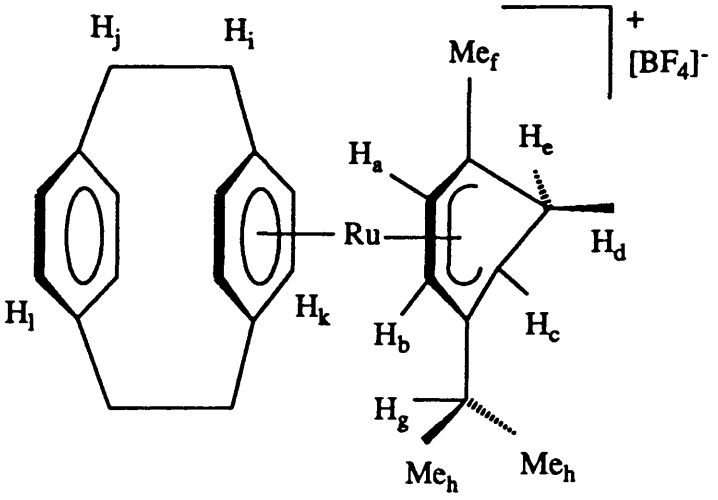

H_c	3.44 (d,1H)	H_f	1.36 (s,3H)
H_d(*exo*)	2.24 (d,1H)	H_g	1.88 (sept,1H)
H_e(*endo*)	2.34 (dd,1H)	H_h	0.97 (dd,6H)
Cyclophane resonances:			
H_i	2.82, 2.95 (each m,2H)	H_k	5.02, 5.61 (each d,2H)
H_j	3.24 (m,4H)	H_l	6.84 (s)

(54)

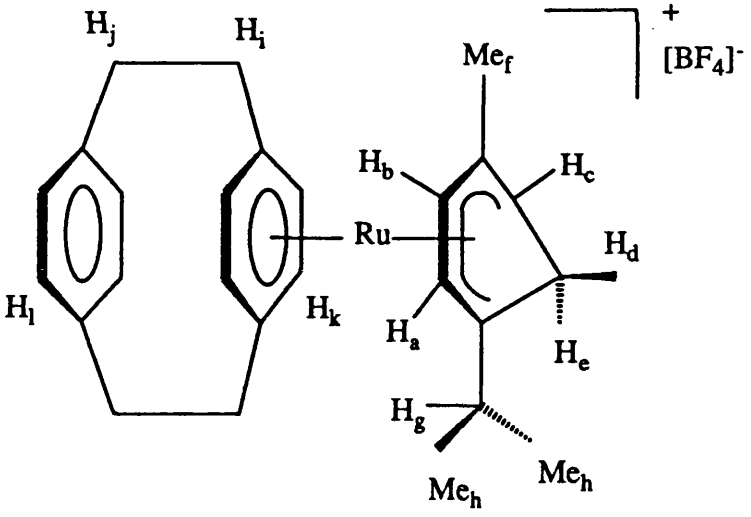

H_a	4.70 (d,1H)	H_e(*endo*)	2.30 (dd,1H)
H_b	6.05 (d,1H)	H_f	1.71 (s,3H)
H_c	3.43 (d,1H)	H_g	1.65 (sept,1H)
H_d(*exo*)	2.09 (d,1H)	H_h	0.78, 0.90 (each d,3H)
Cyclophane resonances:			
H_i	2.82, 2.95 (each m,2H)	H_k	5.04, 5.54 (each d,2H)
H_j	3.24 (m,4H)	H_l	6.83 (s,4H)

4.3.4 Details of the Crystal Structure Determinations.

The general experimental method for the crystal structure determinations is given in Section 2.3.5.

(i) Details of the crystal structure determination of $[Os(\eta^6\text{-}C_6H_6)(\eta^6\text{-}C_{16}H_{16})][BF_4]_2$ (17).

The pale yellow crystals were grown by the slow evaporation of an acetonitrile solution of the compound. The data collection was routine. From the systematic absences the space group was either Cmcm or $Cmc2_1$. Refinement proceeded most smoothly in Cmcm.

The asymmetric unit contains one quarter of the cation and one half of a $[BF_4]^-$ anion. The position of the osmium atom was derived from a three dimensional Patterson function. Least-squares refinement followed by difference-Fourier synthesis were used to locate the remaining non-hydrogen atoms.

Each component of the structure is subject to disorder. The cation is disordered in two respects. Firstly, the cyclophane ligand is disordered over two positions related by a 90° rotation with the two sites having equal occupancy. The benzene ring is similarly disordered, though in this case the refinement resulted in one site being occupied 75% of the time, the alternative site 25% of the time. The $[BF_4]^-$ anion is located on the mirror plane at (0,y,z). The boron atom and two fluorines lie in that plane. The anion is highly disordered. Attempts to refine chemically reasonable models based on interpenetrating rigid tetrahedra were largely unsuccessful. When the atoms of the anion were allowed to refine freely a chemically unsatisfactory solution was obtained. This solution did however result in the best overall refinement, and more importantly, led to the greatest precision for the parameters describing the chemically more interesting cation. As there are no short contacts between cation and anions this imperfect result was accepted. The osmium, boron and fluorine atoms were refined anisotropically. The hydrogen atoms were included in fixed positions with a common isotropic temperature factor ($U=0.08$ Å^2). In the final electron density map the largest peak was 1.1 eÅ^{-3}, which was close to the metal atom.

The crystallographic data are presented in Table 4.4, and the fractional coordinates, bond lengths, and bond angles are presented in Tables 4.5-4.7 respectively.

(ii) Details of the crystal structure determination of $[Ru(\eta^6\text{-}p\text{-cymene})(\eta^6\text{-}C_{16}H_{16})][BPh_4]_2.\frac{1}{2}(CH_3)_2CO$ (49).

The yellow crystals were grown by the slow evaporation of an acetone solution of the compound. The crystal structure determination was undertaken in an attempt to achieve a more acceptable result than had been obtained for the tetrafluoroborate salt of this compound (48). The data collection was routine. The space group was $P\bar{1}$.

The position of the ruthenium ion was found using a three-dimensional Patterson function. Iterative application of least-squares refinement and difference-Fourier synthesis led to the development of the entire structure. The asymmetric unit comprises one cation, two $[BPh_4]^-$ anions, and half an acetone of crystallisation. All non-hydrogen atoms, other than those in the acetone molecule, have been refined anisotropically. Hydrogen atoms were included in a riding model for the cation and anions, and were given a common, fixed, isotropic temperature factor (U=0.08 $Å^2$).

For the atoms of the acetone molecule a common site occupancy factor was allowed to refine freely in the early cycles, and was then fixed at the refined value of 50%. It was not possible to distinguish the oxygen atom from the two methyl carbon atoms, so the molecule was refined with all atoms as carbon atoms. The geometry was fixed such that the molecule was planar with the C-C bond lengths allowed to refine by up to 0.001 Å per cycle. This bond distance converged to a value of 1.25 (4) Å.

The highest peak in the final electron density map was 0.94 $eÅ^{-3}$, and was associated with the acetone molecule. The crystallographic data are presented in Table 4.8, and the fractional coordinates, bond lengths, and bond angles are presented in Tables 4.9-4.11 respectively.

TABLE 4.1 Microanalytical Data.

Compound.		Microanalytical data.			
		%C		%H	
		found.	calc.	found.	calc.
$[Os(\eta^6\text{-}C_6H_6)(\eta^6\text{-}C_{16}H_{16})][BF_4]_2$	(17)	40.6	40.7	3.4	3.4
$[Os(\eta^6\text{-}C_{16}H_{16})_2][BF_4]_2$.[a]	(47)	48.3	49.3	4.1	4.1
$[Ru(\eta^6\text{-}p\text{-cymene})(\eta^6\text{-}C_{16}H_{16})][BPh_4]_2.\frac{1}{2}Me_2CO$	(49)	81.3	79.7	6.7	6.4
$[Ru(\eta^6\text{-}p\text{-cymene})(\eta^6\text{-}C_{16}H_{16})][(CF_3CO_2)_2H]_2$	(51)	45.5	45.5	3.6	3.6
$[Ru(\eta^5\text{-}C_6H_7)(\eta^6\text{-}C_{16}H_{16})][BF_4]$	(52)	55.6	55.1	4.9	4.4
$[Ru(\eta^5\text{-}1\text{-Me},2\text{-}H_2,4\text{-}CHMe_2\text{-}C_6H_3)(\eta^6\text{-}C_{16}H_{16})][BF_4]$	(53)	57.9	58.7	5.6	5.9
$[Ru(\eta^5\text{-}1\text{-Me},3\text{-}H_2,4\text{-}CHMe_2\text{-}C_6H_3)(\eta^6\text{-}C_{16}H_{16})][BF_4]$	(54)				

a) Found values recalculated to allow for 2 moles of CF_3CO_2H.

TABLE 4.2 ^{1}H n.m.r. Data for the Compounds $[M(\eta^6\text{-arene})(\eta^6\text{-}C_{16}H_{16})][BF_4]_2$ at 298 K.

Compound.		Solvent.	^{1}H n.m.r. data. δ, ppm.			
			Cyclophane resonances.			Other resonances.
			non-coord. C_6H_4	coord. C_6H_4	$-CH_2CH_2-$ (AA'XX')	
$[Ru(\eta^6\text{-}C_6H_6)(\eta^6\text{-}C_{16}H_{16})][BF_4]_2$	(11)	CD_3NO_2[a]	7.04 (s)	6.25 (s)	3.22, 3.46	6.71 (s): C_6H_6
$[Os(\eta^6\text{-}C_6H_6)(\eta^6\text{-}C_{16}H_{16})][BF_4]_2$	(17)	CD_3NO_2[a]	7.11 (s)	6.54 (s)	3.21, 3.51	6.91 (s): C_6H_6
$[Ru(\eta^6\text{-}p\text{-cymene})(\eta^6\text{-}C_{16}H_{16})][BF_4]_2$	(48)	CD_3NO_2[a]	7.02 (s)	6.22 (s)	3.20, 3.46	1.24 (d)[b], 2.37 (s)[c], 2.81 (sept)[d], 6.64 (br. s)[e]: *p*-cymene.
$[Ru(\eta^6\text{-}C_6Me_6)(\eta^6\text{-}C_{16}H_{16})][BF_4]_2$	(50)	CD_3NO_2[a]	6.95 (s)	5.91 (s)	3.12, 3.41	2.46 (s): $C_6(CH_3)_6$
$[Ru(\eta^6\text{-}C_{16}H_{16})_2][BF_4]_2$	(13)	CD_3NO_2[a]	6.94 (s)	5.90 (s)	3.04, 3.35	
$[Os(\eta^6\text{-}C_{16}H_{16})_2][BF_4]_2$	(47)	CD_3NO_2[a]	7.01 (s)	6.22 (s)	3.02, 3.40	

a) Operating frequency: 400 MHz. b) $ArCH(CH_3)_2$, 6H, $^3J_{H\text{-}H}$=6.9 Hz. c) CH_3Ar, 3H.

d) $ArCHMe_2$, 1H, $^3J_{H\text{-}H}$=6.9 Hz. e) $MeC_6H_4CHMe_2$, 4H.

TABLE 4.3 ^{13}C-{^1H} n.m.r. Data at 298 K.

Compound.		Solvent.	^{13}C-{^1H} n.m.r. data. δ, ppm.						
			Cyclophane resonances[a].						Other resonances.
			C_1	C_2	C_3	C_4	C_5	C_6	
$[Ru(\eta^6\text{-}C_6H_6)(\eta^6\text{-}C_{16}H_{16})][BF_4]_2$	(11)	CD_3NO_2	134.9	141.1	90.0	135.8	33.5	35.2	94.0: $\underline{C}_6H_6$
$[Os(\eta^6\text{-}C_6H_6)(\eta^6\text{-}C_{16}H_{16})][BF_4]_2$	(17)	CD_3NO_2	133.0	141.2	83.4	135.8	33.8	34.9	87.2: $\underline{C}_6H_6$
$[Ru(\eta^6\text{-}p\text{-cymene})(\eta^6\text{-}C_{16}H_{16})][BF_4]_2$	(48)	CD_3NO_2	135.5	141.1	90.3	135.7	33.3	35.1	[b].
$[Ru(\eta^6\text{-}C_6Me_6)(\eta^6\text{-}C_{16}H_{16})][BF_4]_2$	(50)	CD_3NO_2	131.2	141.2	91.2	135.6	32.3	34.9	109.2: $\underline{C}_6Me_6$, 18.0: $C_6(\underline{C}H_3)_6$
$[Ru(\eta^6\text{-}C_{16}H_{16})_2][BF_4]_2$	(13)	CD_3NO_2	133.7	140.9	87.2	135.5	33.2	35.1	
$[Os(\eta^6\text{-}C_{16}H_{16})_2][BF_4]_2$	(47)	CD_3NO_2	133.6	140.9	79.6	135.5	33.4	34.9	
$[Ru(\eta^5\text{-}C_5H_5)(\eta^6\text{-}C_{16}H_{16})][PF_6]$	(10)	CD_3NO_2	120.9	141.4	84.0	135.1	33.5	35.2	79.0: $\underline{C}_5H_5$

a)

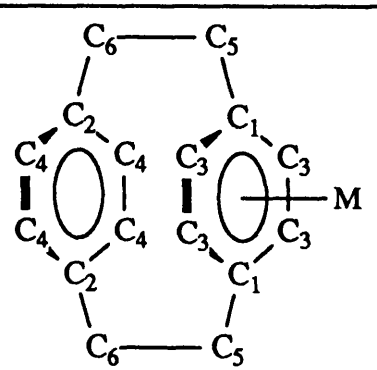

b)

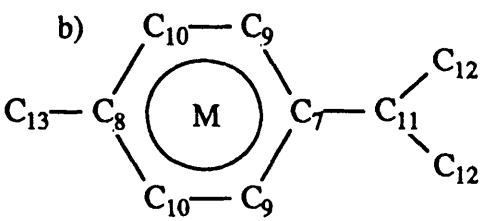

p-cymene resonances: 121.8 (C_7), 111.3 (C_8), 93.7 (C_9), 91.7 (C_{10}), 33.1 (C_{11}), 22.8 (C_{12}), 19.9 (C_{13}).

TABLE 4.4 ^{1}H n.m.r. Data for the Compounds (10), (49), (51) and (52) at 298 K.

Compound.		Solvent.	^{1}H n.m.r. data. δ, ppm.			
			Cyclophane resonances.			Other resonances.
			non-coord. C_6H_4	coord. C_6H_4	-CH_2CH_2- (AA'XX')	
$[Ru(\eta^6\text{-}p\text{-cymene})(\eta^6\text{-}C_{16}H_{16})][BPh_4]_2$	(49)	CD_3CN[a]	6.91 (s)	5.94 (s)	3.02, 3.34	1.13 (d)[b], 2.18 (s)[c], 2.64 (sept)[d], 6.33 (s)[e]: *p*-cymene, [f].
$[Ru(\eta^6\text{-}p\text{-cymene})(\eta^6\text{-}C_{16}H_{16})]$-$[(CF_3CO_2)_2H]_2$	(51)	CD_3NO_2[a]	7.02 (s)	6.24 (s)	3.20, 3.45	1.24 (d)[b], 2.37 (s)[c], 2.81 (sept)[d], 6.65 (A_2B_2)[e]: *p*-cymene.
$[Ru(\eta^5\text{-}C_5H_5)(\eta^6\text{-}C_{16}H_{16})][PF_6]$	(10)	CD_3NO_2[a]	6.89 (s)	5.43 (s)	2.98, 3.28	5.07 (s): C_5H_5
$[Ru(\eta^5\text{-}C_6H_7)(\eta^6\text{-}C_{16}H_{16})][BF_4]$	(52)	CD_3NO_2[a]	6.92 (s)	5.40 (s)	3.05, 3.31	2.08 (d,1H), 2.37 (dt,1H), 3.35 (t,2H), 4.85 (t,2H) 6.23 (t,1H): η^5-C_6H_7[g].

a) Operating frequency: 400 MHz. b) $ArCH(CH_3)_2$, 6H, $^3J_{H\text{-}H}$=6.9 Hz. c) CH_3Ar, 3H.

d) $ArCHMe_2$, 1H, $^3J_{H\text{-}H}$=6.9 Hz. e) $MeC_6H_4CHMe_2$, 4H. f) $[BPh_4]^-$: 6.83 (t,8H), 6.99 (t,16H), 7.26 (m,16H).

g) See Fig. 4.7 for full assignment of resonances.

TABLE 4.5 **Crystallographic data for $[Os(\eta^6\text{-}C_6H_6)(\eta^6\text{-}C_{16}H_{16})][BF_4]_2$ (17).**

Formula	$Os_1C_{22}H_{22}B_2F_8$
fw, g	650.3
Space group	Cmcm
a, Å	7.728(2)
b, Å	18.642(5)
c, Å	14.852(4)
α, deg	90.0
β, deg	90.0
γ, deg	90.0
V, Å^3	2140(1)
Z	4
F(000)	1248
d_{calc}, g/cm^3	2.02
Crystal size, mm	0.80 x 0.12 x 0.02
Scan technique	ω-2Θ
μ(Mo-K_α), cm^{-1}	60.39
Orientation reflections, no.; range (2Θ)	28; ($10^o \leq 2\Theta \leq 23^o$)
Temperature, °C	20
Total No. of reflections measured	1085
No. of unique data	1050
Total with $I \geq 1.5\sigma(I)$	928
No. of parameters	101
R[a]	0.0380
R'[b]	0.0402
Weighting scheme	$w = 1.000/(\sigma^2F + 0.001122F^2)$
Largest shift/esd, final cycle	0.021
Largest peak, e/Å^3	1.10

a) $R = \Sigma[|F_o|-|F_c|]/\Sigma|F_o|$

b) $R' = \Sigma[(|F_o|-|F_c|) . w^{\frac{1}{2}}]/\Sigma[|F_o|.w^{\frac{1}{2}}]$

TABLE 4.6 **Atomic Coordinates (x10^4) and Equivalent Isotropic Displacement Parametars (Å^{2}x10^3) for [Os(η^6-C_6H_6)(η^6-$C_{16}H_{16}$)[BF_4]$_2$ (17).**

Atom	x		y		z		U(eq)[a]	
Os1	0		1282	(1)	2500		33	(1)
C1	956	(16)	2203	(6)	3336	(9)	49	(3)
C2	1811	(29)	2180	(10)	2500		52	(5)
C3	883	(20)	326	(7)	3296	(10)	28	(3)
C4	1870	(31)	234	(12)	2500		36	(5)
C5	3639	(31)	-78	(12)	2500		51	(6)
C6	3502	(36)	-887	(14)	2500		67	(7)
C7	1794	(32)	-1215	(12)	2500		40	(5)
C8	871	(24)	-1275	(7)	3302	(11)	37	(3)
C1A	1480	(54)	2231	(20)	2921	(29)	51	(8)
C2A	0		2224	(17)	3397	(23)	19	(7)
C3A	1552	(19)	399	(7)	2967	(10)	31	(3)
C4A	0		314	(10)	3475	(15)	33	(4)
C5A	0		33	(15)	4384	(21)	66	(7)
C6A	0		-787	(11)	4388	(16)	45	(5)
C7A	0		-1133	(12)	3451	(15)	38	(5)
C8A	1519	(21)	-1202	(8)	2980	(11)	36	(3)
B1	0		3605	(14)	5391	(14)	83	(8)
F1	0		3603	(13)	6284	(14)	211	(12)
F2	0		3496	(32)	4570	(29)	249	(33)
F3	1541	(31)	3447	(23)	5139	(18)	208	(19)
F2A	0		2817	(16)	5459	(28)	173	(19)
F3A	1128	(41)	4134	(16)	5307	(26)	224	(19)

a) Equivalent isotropic U defined as $\frac{1}{3}$ of the trace of the orthoganalised U_{ij} tensor.

TABLE 4.7 **Selected Averaged Bond Lengths (Å) for $[Os(\eta^6\text{-}C_6H_6)(\eta^6\text{-}C_{16}H_{16})[BF_4]_2$ (17).**

Os1-C1	2.22	(2)	Os1-C2	2.19	(2)
Os1-C3	2.20	(2)	Os1-C4	2.37	(2)
C1-C2	1.38	(3)	C3-C4	1.42	(2)
C4-C5	1.47	(3)	C5-C6	1.52	(3)
C6-C7	1.49	(3)	C7-C8	1.38	(2)
C1-C1*	1.36	(5)	C3-C3*	1.37	(3)
C8-C8*	1.39	(3)			

* Starred atoms generated by crystal symmetry.

TABLE 4.8 **Selected Averaged Bond Angles (°) for $[Os(\eta^6\text{-}C_6H_6)(\eta^6\text{-}C_{16}H_{16})[BF_4]_2$ (17).**

C1*-C1-C2	120	(2)	C1-C2-C1*	120	(3)
C3*-C3-C4	122	(1)	C3-C4-C3*	114	(2)
C3-C4-C5	123	(1)	C3*-C4-C5	113	(2)
C4-C5-C6	110	(2)	C5-C6-C7	117	(2)
C6-C7-C8	120	(1)	C6-C7-C8*	120	(1)
C8-C7-C8*	118	(2)	C8*-C8-C7	121	(1)

* Starred atoms generated by crystal symmetry.

TABLE 4.9 **Crystallographic Data for $[Ru(\eta^6\text{-}p\text{-cymene})(\eta^6\text{-}C_{16}H_{16})][BPh_4]_2.\frac{1}{2}(CH_3)_2CO$ (49).**

Formula	$Ru_1C_{76}H_{73}B_2$
fw, g	1109.1
Space group	$P\bar{1}$
a, Å	13.546(5)
b, Å	13.726(4)
c, Å	17.917(6)
α, deg	106.47(2)
β, deg	106.80(3)
γ, deg	95.45(3)
V, Å^3	3001(2)
Z	2
F(000)	1166
d_{calc}, g/cm^3	1.23
Crystal size, mm	0.76 x 0.35 x 0.04
Scan techniqe	ω-2Θ
μ(Mo-K_α), cm^{-1}	2.96
Orientation reflections, no.; range (2Θ)	27; ($8° \leq 2\Theta \leq 22°$)
Temperature, °C	20
Total No. of reflections measured	10705
No. of unique data	10242
Total with $I \geq 2.5\sigma(I)$	5284
No. of parameters	711
R[a]	0.0705
R'[b]	0.0757
Weighting scheme	$w = 1.000/(\sigma^2F + 0.004373F^2)$
Largest shift/esd, final cycle	0.008
Largest peak, e/Å^3	0.94

a) $R = \Sigma[|F_o|-|F_c|]/\Sigma|F_o|$

b) $R' = \Sigma[(|F_o|-|F_c|) . w^{\frac{1}{2}}]/\Sigma[|F_o|.w^{\frac{1}{2}}]$

TABLE 4.10 **Atomic Coordinates ($x10^4$) and Equivalent Isotropic Displacement Parameters ($Å^2x10^3$) for $[Ru(\eta^6\text{-}p\text{-cymene})(\eta^6\text{-}C_{16}H_{16})][BPh_4]_2.\frac{1}{2}Me_2CO$ (49).**

Atom	x		y		z		U(eq)[a]	
Ru1	2403	(1)	2152	(1)	2931	(1)	44	(1)
C1	1876	(7)	353	(7)	2514	(5)	51	(4)
C2	2728	(8)	757	(7)	3254	(6)	58	(4)
C3	3666	(7)	1319	(7)	3284	(6)	53	(4)
C4	3764	(7)	1427	(6)	2544	(6)	53	(4)
C5	2855	(7)	1257	(7)	1886	(5)	51	(4)
C6	1915	(7)	720	(6)	1884	(5)	51	(4)
C7	2516	(8)	-1417	(7)	2014	(6)	60	(4)
C8	3433	(8)	-1204	(7)	2692	(6)	61	(4)
C9	4349	(8)	-676	(8)	2698	(6)	60	(4)
C10	4404	(7)	-346	(7)	2038	(6)	54	(4)
C11	3552	(8)	-777	(7)	1319	(6)	60	(4)
C12	2628	(8)	-1299	(7)	1304	(5)	60	(4)
C13	1043	(8)	-529	(7)	2388	(7)	67	(5)
C14	1446	(8)	-1572	(8)	2098	(7)	76	(5)
C15	4849	(8)	1639	(8)	2494	(7)	69	(5)
C16	6190	(7)	582	(8)	2160	(6)	66	(5)
C17	2808	(12)	4039	(9)	2129	(7)	99	(7)
C18	2403	(9)	3661	(7)	2710	(6)	64	(5)
C19	1373	(10)	3151	(8)	2496	(7)	75	(5)
C20	1031	(8)	2784	(8)	3056	(7)	66	(5)
C21	1664	(8)	2963	(7)	3857	(6)	63	(5)
C22	2694	(9)	3449	(8)	4071	(6)	66	(5)
C23	3083	(8)	3806	(7)	3523	(6)	63	(4)
C24	1322	(11)	2679	(10)	4507	(9)	101	(7)
C25	908	(15)	3554	(12)	4950	(11)	174	(14)
C26	553	(15)	1747	(13)	4203	(11)	154	(13)
B1	2787	(8)	7099	(8)	4600	(6)	49	(4)
C27	1881	(7)	6285	(7)	3780	(6)	61	(4)
C28	1039	(8)	5656	(8)	3827	(7)	76	(5)

C29	187	(10)	5086	(9)	3148	(11)	102 (7)
C30	119	(13)	5111	(13)	2372	(11)	120 (8)
C31	892	(15)	5676	(12)	2286	(8)	117 (8)
C32	1776	(10)	6262	(8)	2964	(6)	85 (5)
C33	3053	(7)	6563	(6)	5308	(5)	50 (4)
C34	2477	(8)	6603	(8)	5850	(6)	67 (5)
C35	2688	(9)	6111	(9)	6450	(7)	81 (6)
C36	3456	(9)	5531	(8)	6515	(7)	72 (5)
C37	4035	(7)	5463	(7)	5990	(6)	61 (4)
C38	3856	(7)	5978	(6)	5423	(5)	49 (4)
C39	2321	(7)	8141	(7)	4892	(5)	52 (4)
C40	1483	(7)	8420	(8)	4384	(6)	60 (4)
C41	1146	(8)	9331	(8)	4654	(7)	68 (5)
C42	1598	(9)	10009	(7)	5431	(8)	72 (5)
C43	2422	(8)	9779	(7)	5957	(7)	67 (5)
C44	2765	(8)	8852	(7)	5691	(6)	61 (4)
C45	3869	(7)	7424	(7)	4416	(5)	54 (4)
C46	4480	(7)	8404	(8)	4751	(5)	56 (4)
C47	5434	(8)	8645	(8)	4622	(6)	62 (5)
C48	5760	(9)	7914	(10)	4128	(7)	76 (6)
C49	5220	(10)	6941	(10)	3772	(8)	87 (7)
C50	4279	(9)	6709	(7)	3906	(6)	66 (5)
B2	7691	(8)	8481	(8)	838	(6)	50 (4)
C51	8577	(7)	8046	(8)	435	(5)	54 (4)
C52	9172	(7)	8625	(8)	133	(5)	56 (4)
C53	9896	(7)	8240	(9)	-238	(6)	63 (5)
C54	10053	(8)	7260	(9)	-310	(6)	64 (5)
C55	9479	(8)	6641	(8)	-49	(6)	71 (5)
C56	8746	(7)	7031	(8)	310	(6)	63 (4)
C57	6525	(7)	8082	(7)	98	(5)	52 (4)
C58	5743	(7)	8654	(9)	64	(6)	65 (5)
C59	4729	(8)	8277	(11)	-492	(8)	82 (6)
C60	4466	(8)	7309	(10)	-1059	(7)	74 (5)
C61	5230	(8)	6715	(9)	-1044	(6)	75 (5)
C62	6228	(7)	7088	(8)	-483	(6)	64 (5)
C63	7913	(6)	9737	(7)	1230	(5)	53 (4)

C64	7846	(7)	10362	(8)	731	(6)	60 (4)
C65	7990	(7)	11443	(9)	1055	(7)	70 (5)
C66	8166	(8)	11913	(9)	1855	(8)	76 (5)
C67	8231	(9)	11332	(10)	2369	(6)	80 (5)
C68	8112	(7)	10258	(8)	2061	(6)	60 (4)
C69	7632	(7)	7966	(7)	1553	(6)	58 (4)
C70	8496	(8)	7787	(8)	2081	(6)	71 (5)
C71	8455	(9)	7384	(9)	2705	(7)	81 (6)
C72	7497	(11)	7146	(10)	2806	(7)	94 (7)
C73	6637	(10)	7354	(11)	2301	(8)	102 (7)
C74	6701	(8)	7750	(9)	1704	(6)	75 (5)
C75	7139	(16)	4264	(17)	151	(12)	115 (9)
C76	6767	(25)	4052	(26)	-611	(17)	153 (13)
C77	6781	(23)	4885	(24)	610	(17)	137 (11)
C78	7903	(23)	3897	(24)	454	(17)	137 (11)

a) Equivalent isotropic U defined as $\frac{1}{3}$ of the trace of the orthoganalised U_{ij} tensor.

TABLE 4.11 **Selected Bond Lengths (Å) for $[Ru(\eta^6\text{-}p\text{-cymene})(\eta^6\text{-}C_{16}H_{16})[BPh_4]_2.\frac{1}{2}Me_2CO$ (49).**

Ru1-C1	2.341	(9)	Ru1-C2	2.199	(10)
Ru1-C3	2.189	(10)	Ru1-C4	2.360	(11)
Ru1-C5	2.212	(10)	Ru1-C6	2.183	(7)
Ru1-C18	2.216	(11)	Ru1-C19	2.185	(13)
Ru1-C20	2.167	(11)	Ru1-C21	2.262	(12)
Ru1-C22	2.199	(9)	Ru1-C23	2.191	(8)
C1-C2	1.405	(11)	C1-C6	1.373	(15)
C1-C13	1.492	(13)	C2-C3	1.401	(14)
C3-C4	1.417	(15)	C4-C5	1.382	(12)
C4-C15	1.504	(16)	C5-C6	1.408	(14)
C7-C8	1.401	(13)	C7-C12	1.377	(16)
C7-C14	1.500	(17)	C8-C9	1.372	(16)
C9-C10	1.399	(16)	C10-C11	1.386	(11)
C10-C16	1.501	(14)	C11-C12	1.371	(15)
C13-C14	1.585	(15)	C15-C16	1.571	(15)
C17-C18	1.496	(20)	C18-C19	1.391	(17)
C18-C23	1.427	(13)	C19-C20	1.409	(19)
C20-C21	1.379	(14)	C21-C22	1.380	(15)
C21-C24	1.503	(22)	C22-C23	1.417	(17)
C24-C25	1.495	(24)	C24-C26	1.429	(24)

The $[BPh_4]^-$ ions have B-C distances in the range 1.613-1.663 (15) Å, and C-C distances in the range 1.32-1.42 (2) Å.

TABLE 4.12 **Selected Bond Angles (°) for [Ru(η^6-*p*-cymene)(η^6-$C_{16}H_{16}$)][BPh_4]$_2$.½Me_2CO (49).**

C1-Ru1-C2	35.9	(3)	C1-Ru1-C18	152.5	(3)
C18-Ru1-C19	36.8	(4)	Ru1-C1-C2	66.6	(5)
C2-C1-C6	116.8	(9)	C2-C1-C13	121.1	(9)
C6-C1-C13	121.7	(9)	Ru1-C1-C13	146.5	(7)
C1-C2-C3	120.9	(10)	C2-C3-C4	118.8	(7)
Ru1-C4-C15	146.1	(6)	C3-C4-C5	118.0	(9)
C3-C4-C15	118.4	(8)	C5-C4-C15	123.4	(10)
C4-C5-C6	119.2	(9)	C1-C6-C5	121.9	(8)
C8-C7-C12	117.1	(10)	C8-C7-C14	121.6	(10)
C12-C7-C14	120.4	(9)	C7-C8-C9	119.8	(10)
C8-C9-C10	122.0	(8)	C9-C10-C11	115.1	(9)
C9-C10-C16	121.7	(7)	C11-C10C16	121.7	(10)
C10-C11-C12	122.2	(10)	C7-C12-C11	120.6	(8)
C1-C13-C14	108.2	(9)	C7-C14-C13	113.9	(8)
C4-C15-C16	109.2	(8)	C10-C16-C15	113.4	(9)
Ru1-C18-C17	129.5	(8)	Ru1-C18-C19	70.4	(7)
C17-C18-C19	123.0	(10)	C17-C18-C23	120.2	(10)
C19-C18-C23	116.9	(11)	C18-C19-C20	121.1	(9)
C19-C20-C21	122.6	(10)	C20-C21-C22	116.6	(11)
Ru1-C21-C24	133.7	(8)	C20-C21-C24	125.4	(10)
C22-C21-C24	117.9	(9)	C21-C22-C23	122.7	(9)
C18-C23-C22	119.9	(10)	C21-C24-C25	109.1	(13)
C21-C24-C26	114.6	(12)	C25-C24-C26	109.4	(15)

CHAPTER 5.

EXTENDED TRANSITION METAL-CYCLOPHANE COMPLEXES: BINUCLEAR AND TRINUCLEAR COMPOUNDS.

5.1 INTRODUCTION.

In Chapter 1 (Section 1.3.6) we discussed the reasons for choosing ruthenium as a suitable metal for extended transition metal cyclophane compounds. The work presented in Chapters 2 and 4 demonstrates that the chemistry is readily extended to osmium. Boekelheide *et al* have prepared a number of symmetrical bis-ruthenium compounds of the type $[(\eta^6\text{-arene})Ru(\eta^6,\eta^6\text{-}C_{16}H_{16})Ru(\eta^6\text{-arene})][BF_4]_4$ (Scheme 1.10). In these compounds the cyclophane is capped at both external faces by treating the ligand with a large molar excess of $[Ru(\eta^6\text{-arene})(acetone)_3][BF_4]_2$. It was our intention to develop a synthetic method for the preparation of mixed-metal (Ru/Os) analogues of these compounds. We also proposed to prepare mixed-metal analogues of the triruthenium compound $[(\eta^6\text{-}C_6Me_6)Ru(\eta^6,\eta^6\text{-}C_{16}H_{16})Ru(\eta^6,\eta^6\text{-}C_{16}H_{16})Ru(\eta^6\text{-}C_6Me_6)][BF_4]_6$ (14) (Fig. 1.16).

5.2 RESULTS AND DISCUSSION.

5.2.1 Development of the Synthetic Strategy.

(i) Reactions under Reflux Conditions.

The first synthetic strategy investigated is illustrated in Scheme 5.1. When $[Ru(\eta^6\text{-}C_6H_6)(\eta^6\text{-}C_{16}H_{16})][BF_4]_2$ was treated with a one molar equivalent of $[Os(\eta^6\text{-}C_6H_6)(acetone)_3][BF_4]_2$ the cyclophane was substantially transferred to the osmium ion and a 3:1 mixture of $[Os(\eta^6\text{-}C_6H_6)(\eta^6\text{-}C_{16}H_{16})][BF_4]_2$ (17) and $[Ru(\eta^6\text{-}C_6H_6)(\eta^6\text{-}C_{16}H_{16})][BF_4]_2$ (11) was isolated (see Section 4.2.3). None of the desired binuclear complex was obtained.

The reaction was also attempted with the cyclophane coordinated to the osmium ion in the starting material. In this instance (17) was treated with a one molar equivalent of $[Ru(\eta^6\text{-}p\text{-cymene})(acetone)_3][BF_4]_2$. The ^1H n.m.r. spectrum of the solid isolated, indicated that (17) was recovered as the major component of a mixture, but that a small amount of the desired binuclear compound $[(\eta^6\text{-}p\text{-cymene})Ru(\eta^6,\eta^6\text{-}C_{16}H_{16})Os(\eta^6\text{-}C_6H_6)][BF_4]_4$ (55) was also formed. Treatment of $[Ru(\eta^6\text{-}p\text{-cymene})(\eta^6\text{-}C_{16}H_{16})][BF_4]_2$ (48) with two equivalents of $[Os(\eta^6\text{-}C_6H_6)(acetone)_3][BF_4]_2$ under similar conditions led to the isolation of an approximately 1:1 mixture of (48) and (55). Thus the strategy outlined in Scheme 5.1 did not facilitate the formation of pure mixed-metal compounds.

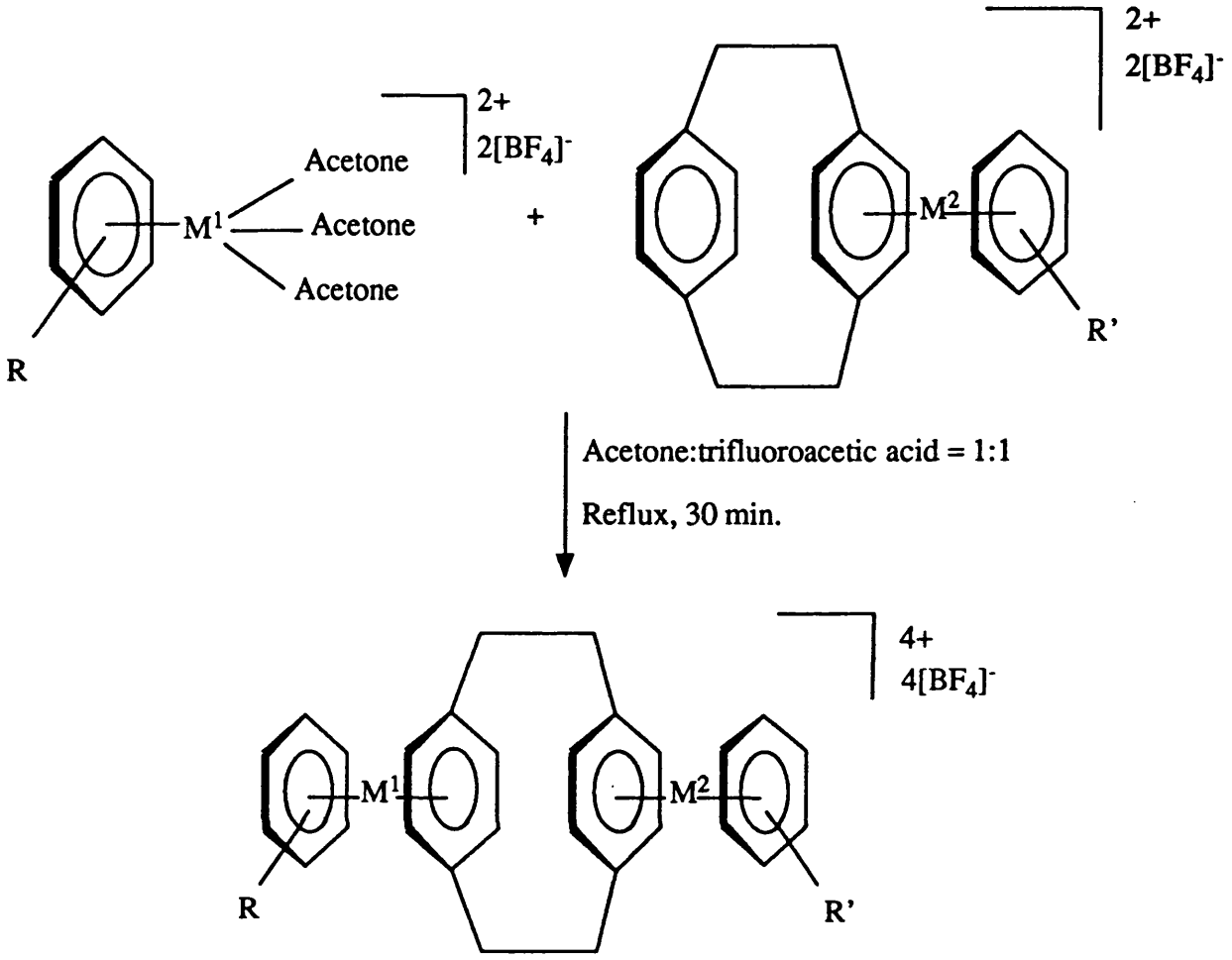

Scheme 5.1 A proposed synthetic stragegy designed to lead to mixed-metal compounds.

Boekelheide *et al*[66] used neat trifluoroacetic acid as the solvent in the synthesis of (14). This approach was adopted as a modification to Scheme 5.1. The solutions of the solvate complexes $[M^1(\eta^6\text{-arene})(acetone)_3][BF_4]_2$ were therefore pumped to dryness before the addition of CF_3CO_2H and $[M^2(\eta^6\text{-arene})(\eta^6\text{-}C_{16}H_{16})][BF_4]_2$. The modified strategy proved successful in the preparation of a pure sample of (55), by reaction of (17) with $[Ru(\eta^6\text{-}p\text{-cymene})(acetone)_3][BF_4]_2$. However, this procedure was less successful for other metal-ligand combinations, mixtures being frequently obtained. The products isolated vary according to the relative solubilities of the reagent $[M(\eta^6\text{-arene})(\eta^6\text{-}C_{16}H_{16})][BF_4]_2$ and the binuclear product in the trifluoroacetic acid solvent. Thus the concentrations used were critical. The reaction time was also an important variable, as too long a reaction time resulted in a scrambling of the arene

ligands, while too short a reaction time resulted in the recovery of a substantial amount of unreacted starting materials. As a result of this unpredictability a new strategy was developed, and is described below.

(ii) Reactions at Ambient Temperature.

Due to the hit and miss nature of strategies involving refluxing solvents, reactions were attempted at ambient temperature. The reaction was first attempted on a trial scale in an n.m.r. tube with the aim being to prepare a new unsymmetrical hetero(η^6-arene)bisruthenium compound, namely $[(\eta^6\text{-}C_6H_6)Ru(\eta^6,\eta^6\text{-}C_{16}H_{16})Ru(\eta^6\text{-}p\text{-cymene})][BF_4]_4$ (56).

The reaction of $[Ru(\eta^6\text{-}C_6H_6)(\eta^6\text{-}C_{16}H_{16})][BF_4]_2$ (11) with $[Ru(\eta^6\text{-}p\text{-cymene})(acetone)_3][BF_4]_2$ in trifluoroacetic acid at 293 K.

Compound (11) was dissolved in trifluoroacetic acid and a little deuterated acetone. The ^1H n.m.r. spectrum was recorded. A sample of $[Ru(\eta^6\text{-}p\text{-cymene})(acetone)_3][BF_4]_2$ (57) was prepared and pumped to dryness. The solvate complex (57) was mixed with the contents of the n.m.r. tube. The ^1H n.m.r. spectrum was recorded immediately and exhibited two sets of resonances due to (11) and (57). After 30 minutes at 293 K the spectrum was re-recorded. This spectrum exhibited a third, minor set of resonances, attributable to the binuclear compound $[(\eta^6\text{-}C_6H_6)Ru(\eta^6,\eta^6\text{-}C_{16}H_{16})Ru(\eta^6\text{-}p\text{-cymene})][BF_4]_4$ (56). A small amount of solid material was also observed in the n.m.r. tube at this stage. The n.m.r. tube was allowed to stand at room temperature for 24 hours. The ^1H n.m.r. spectrum was then re-recorded. This spectrum exhibited no resonances due to (11), a minor set of resonances due to (56), and a major set of resonances due unreacted (57), which was in excess. A significant amount of precipitate was now present in the n.m.r. tube. The precipitate was isolated by filtration. The ^1H n.m.r. spectrum of the disolved precipitate was recorded in CD_3NO_2 and only exhibited resonances attributable to (56).

The new strategy (Scheme 5.2) of employing an excess of the solvate complex, trifluoroacetic acid as the solvent, and reaction over a prolonged time period at room temperature, proved successful. The reaction was scaled up and has allowed the preparation of a range of new hetero(η^6-arene)bisruthenium-[2_2]paracyclophane compounds, and binuclear and trinuclear heterometallic-[2_2]paracyclophane compounds.

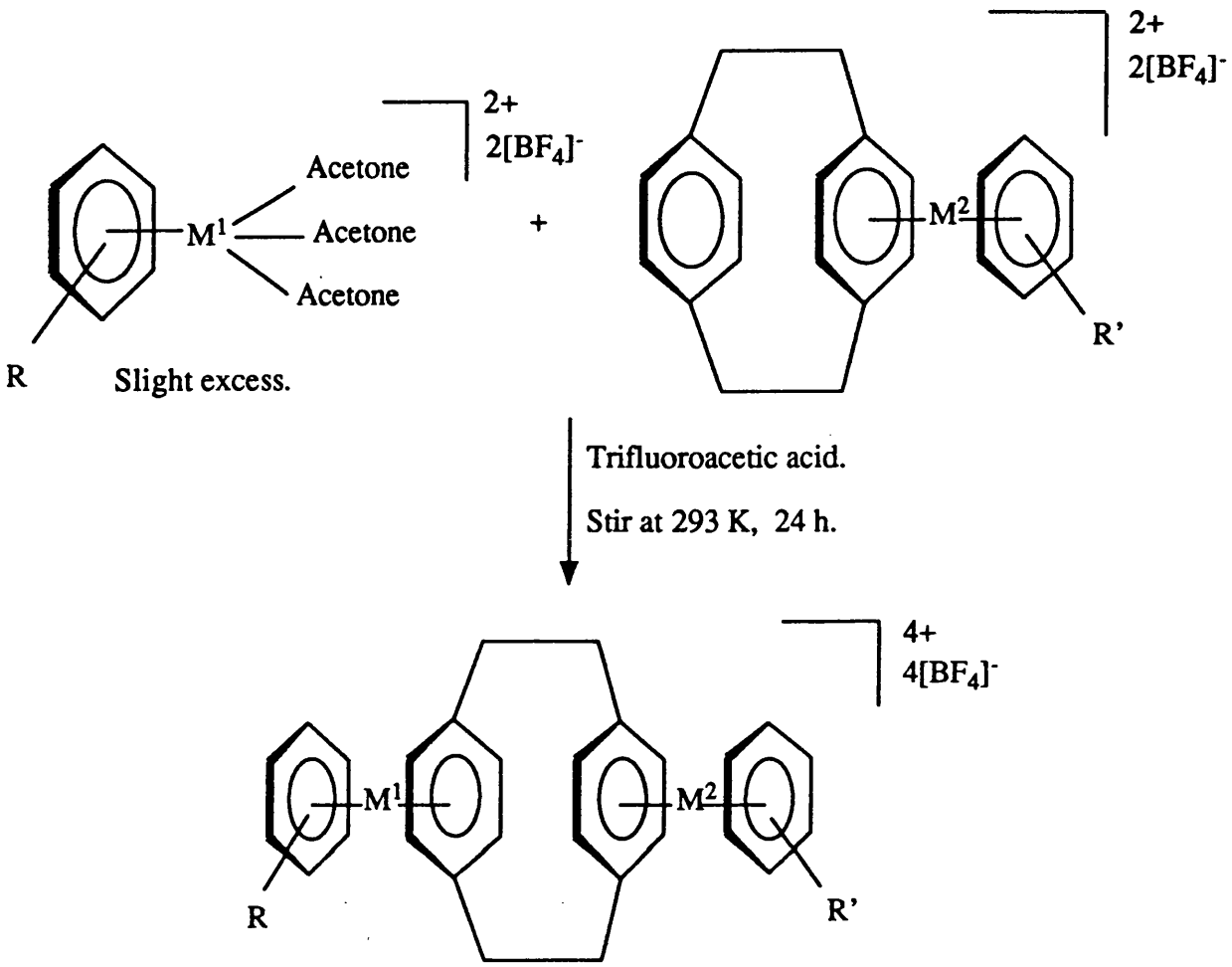

Scheme 5.2 The successful synthetic method developed for the preparation of extended transition metal-cyclophane compounds.

High yields are obtained, typically 60-90%. In some cases the reaction may still be incomplete after 24 h. and some of the mononuclear compound $[M^1(\eta^6\text{-arene})(\eta^6\text{-}C_{16}H_{16})][BF_4]_2$ is isolated along with the desired product. In these instances purification is reliably achieved by further treatment of the impure mixture with a fresh solution of $[M^2(\eta^6\text{-arene})(\text{acetone})_3][BF_4]_2$.

5.2.2 The Preparation and Characterisation of Hetero(η^6-arene)bisruthenium-[2_2]paracyclophane Compounds: [(η^6-arene^1)Ru(η^6,η^6-$C_{16}H_{16}$)Ru(η^6-arene^2)][BF_4]$_4$.

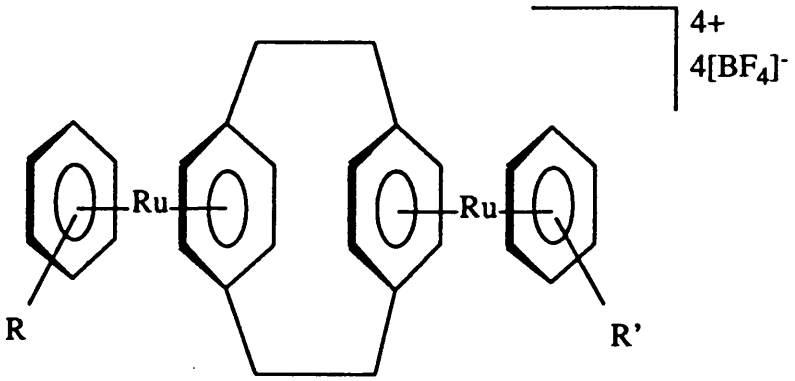

(i) [(η^6-C_6H_6)Ru(η^6,η^6-$C_{16}H_{16}$)Ru(η^6-*p*-cymene)][BF_4]$_4$ (56).

Compound (56) was prepared by the method outlined in Scheme 5.2. The ^{1}H n.m.r. spectrum, recorded in CD_3NO_2, exhibits the usual resonances due to the benzene and *p*-cymene ligands (Section 5.3.3). The pattern of resonances due to the protons of the η^6,η^6-coordinated cyclophane ligand is markedly different from that for η^6-coordinated ligands. The resonances due to the protons of the aromatic rings appear as two closely spaced singlets at δ 6.71 and 6.72 ppm (Fig. 5.1). The small chemical shift difference results from the inequivalent capping ligands, benzene and *p*-cymene. In contrast, when only one face of the cyclophane is coordinated the resonances of the protons of the coordinated and non-coordinated decks appear at least 0.6 ppm apart. In the symmetrical compounds of the type [(η^6-arene)Ru(η^6,η^6-$C_{16}H_{16}$)Ru(η^6-arene)][BF_4]$_4$, prepared by Boekelheide *et al*[73], where the two terminal arenes are identical, the eight aromatic cyclophane protons exhibit one singlet resonance at *ca.* δ 6.5 ppm.

The -CH_2CH_2- protons of (56) give rise to a broad singlet resonance at δ 3.64 ppm (Fig. 5.1), which is significantly to higher frequency of similar resonances observed for η^6-coordinated cyclophane ligands, and totally different in appearance. In compounds where only one face of the cyclophane is metal coordinated, these protons give rise to an AA'XX' pattern of resonances comprising two multiplets at least 0.25 ppm apart at a maximum mean chemical shift of *ca.* δ 3.35 ppm (Fig. 5.1). The previously reported[73] symmetrical compounds exhibit sharp singlet resonances at *ca.* δ 3.5 ppm. Integration of the spectrum supports the proposed 1:1:1 ratio of C_6H_6:$C_{16}H_{16}$:*p*-cymene.

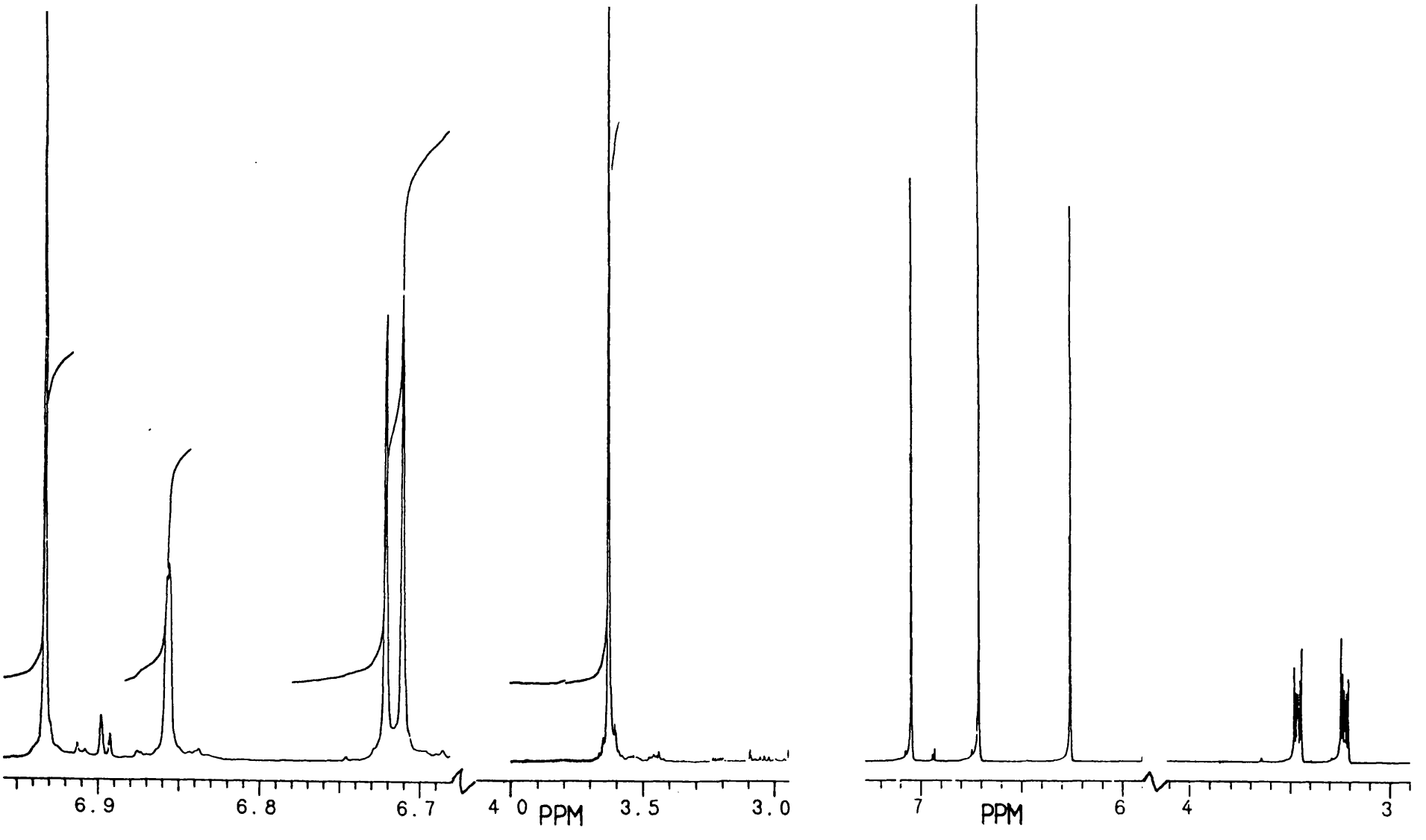

a) [(η^6-C_6H_6)Ru(η^6,η^6-$C_{16}H_{16}$)Ru(η^6-*p*-cymene)][BF_4]$_4$ (56).

b) [Ru(η^6-C_6H_6)(η^6-$C_{16}H_{16}$)][BF_4]$_2$ (11).

Fig. 5.1 The ^{1}H n.m.r. resonances of the aromatic and -CH_2CH_2- protons of (56) and (11) (δ, ppm).

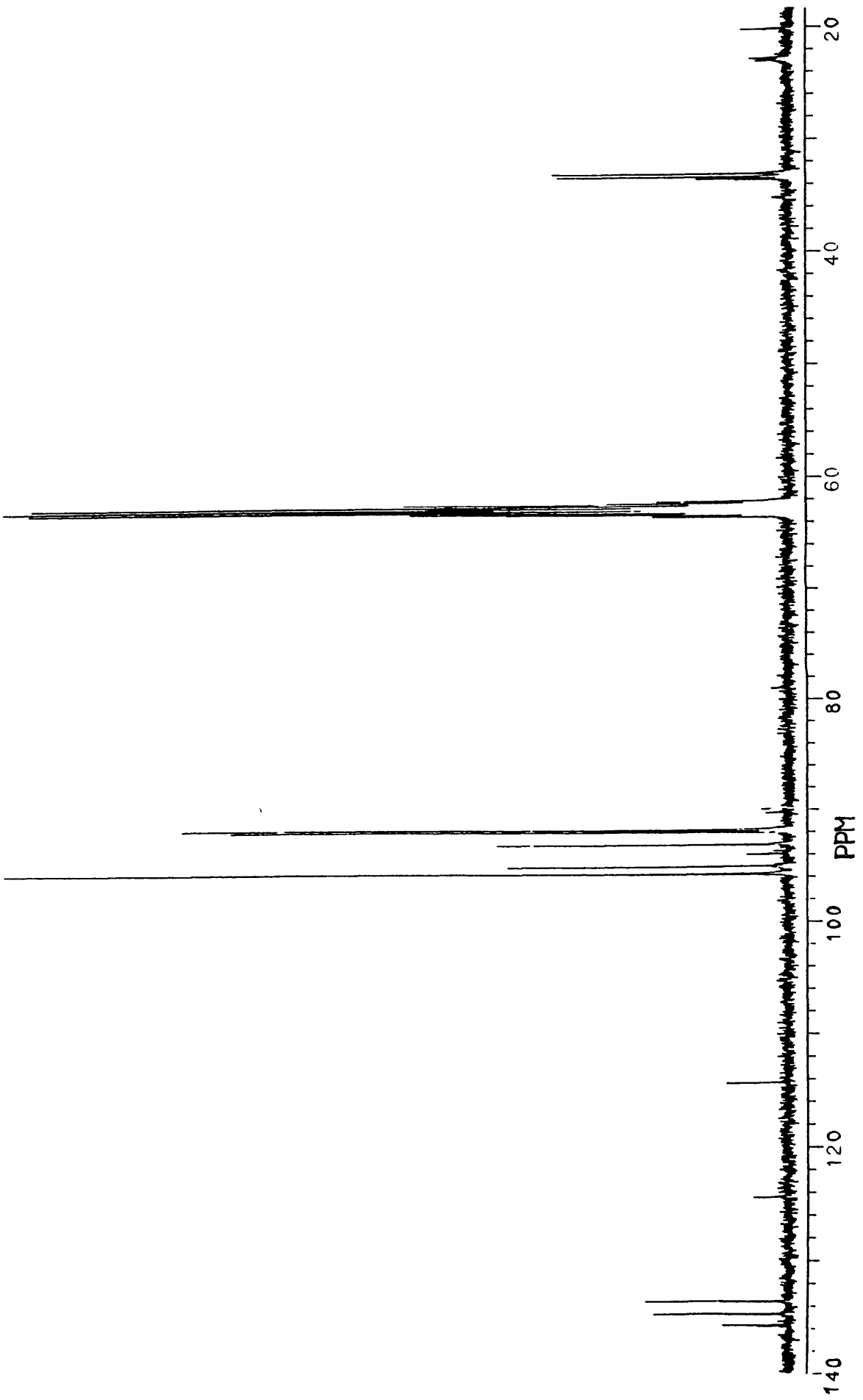

Fig. 5.2 The ^{13}C-{^{1}H} n.m.r. spectrum of $[(\eta^6\text{-}C_6H_6)Ru(\eta^6,\eta^6\text{-}C_{16}H_{16})Ru(\eta^6\text{-}p\text{-cymene})][BF_4]_4$ (56).

The ^{13}C-{^{1}H} n.m.r. spectrum of (56) (Fig. 5.2, Section 5.3.3), recorded in CD_3NO_2, also reflects the similar chemical and magnetic environments of the two cyclophane decks. The resonances of the non-bridgehead carbon atoms in the cyclophane rings appear as two closely spaced singlets at δ 91.8 and 92.0 ppm {c.f. δ 90.0 and 135.8 ppm for those of the carbon atoms in the coordinated and non-coordinated rings respectively in the spectrum of (11) (Table 2.2)}. The resonances due to the carbon atoms of the ethylenic bridging functions appear only 0.3 ppm apart {c.f. a separation of *ca.* 2 ppm for (11)}.

Christiani *et al*[26] have assigned the band at 621 cm^{-1} in the infrared spectrum of the pure [2$_2$]paracyclophane ligand either to the δ(CCC) mode or to the particular geometry of the cyclophane molecule. This band splits and one band then moves to higher wavenumbers when one face of the cyclophane is coordinated to a metal atom or ion. Bands at 650, 680, and 675 cm^{-1} are reported[26] for the compounds [M(η^6-$C_{16}H_{16}$)$(CO)_3$] (M=Cr,Mo,W) respectively, while bands are observed in the range 655-665 cm^{-1} for most of the "Ru(η^6-$C_{16}H_{16}$)" compounds reported in this study. The infrared spectrum of (56) exhibits a band at 681 cm^{-1}, but no band in the region 655-665 cm^{-1}. Indeed, all of the compounds reported in this chapter exhibit a band in the narrow range 677-681 cm^{-1}. Thus it appears that this band has moved a further 20 cm^{-1} on coordination of a second metal atom, suggesting an additional subtle change in geometry of the cyclophane ligand. The spectrum also exhibits ν(CO) (1634-1670 cm^{-1}) and ν(OH) (3645, 3545 cm^{-1}) bands. These are due to some residual CF_3CO_2H, which is stubbornly retained despite thorough drying of the sample. This problem was encountered with most of the chain compounds described in this chapter, and resulted in problems in calculating accurate microanalytical figures (Table 5.1).

The FAB mass spectrum has been recorded. The parent peak is observed at 885 mass units which corresponds to [(η^6-C_6H_6)Ru(η^6,η^6-$C_{16}H_{16}$)Ru(η^6-p-cymene)][BF_4]$_3^+$. Peaks are also observed for fragments containing the metal complex and two, one and no [BF_4]$^-$ anions. Other peaks in the spectrum correspond to [(η^6-arene)Ru(η^6-$C_{16}H_{16}$)][BF_4]$_x^+$ {arene=C_6H_6, *p*-cymene; X=0,1,2 (not all combinations)}, which indicates that the metal complex is most readily cleaved at the metal-arene bonds.

(ii) $[(\eta^6\text{-}C_6H_6)Ru(\eta^6,\eta^6\text{-}C_{16}H_{16})Ru(C_6Me_6)][BF_4]_4$ (58).

Compound (58) was prepared by the method shown in Scheme 5.2. The full details of the synthesis and characterisation are presented in the experimental section. There is a substantial difference in the magnetic influence of the benzene and hexamethylbenzene ligands in this compound compared with the terminal arene ligands in (56). The cyclophane resonances in the ^1H and $^{13}C\text{-}\{^1H\}$ n.m.r. spectra reflect this fact (Section 5.3.3, Tables 5.2 and 5.3). In particular, the $-CH_2CH_2-$ protons give rise to a multiplet resonance with an AA'BB' coupling pattern rather than a singlet as observed for (56).

(iii) $[(\eta^6\text{-}p\text{-cymene})Ru(\eta^6,\eta^6\text{-}C_{16}H_{16})Ru(C_6Me_6)][BF_4]_4$ (59).

Compound (59) was prepared by the method outlined in Scheme 5.2. Full details of the synthesis and characterisation are presented in the experimental section (5.3.3).

5.2.3 The Preparation and Characterisation of Binuclear Mixed-Metal Compounds: $[(\eta^6\text{-}C_6H_6)Os(\eta^6,\eta^6\text{-}C_{16}H_{16})Ru(\eta^6\text{-arene})][BF_4]_4$.

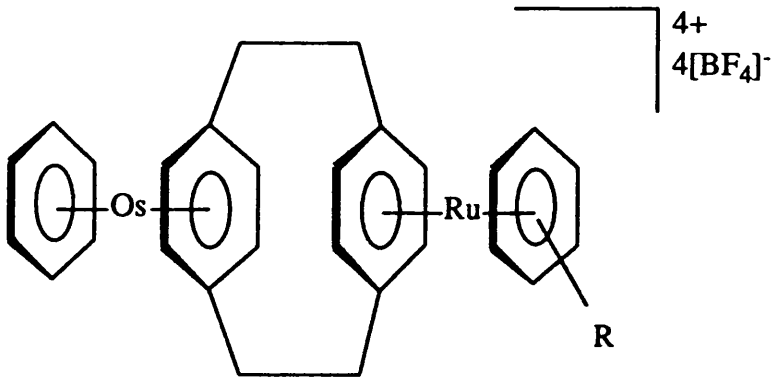

(i) $[(\eta^6\text{-}C_6H_6)Os(\eta^6,\eta^6\text{-}C_{16}H_{16})Ru(\eta^6\text{-}p\text{-cymene})][BF_4]_4$ (55).

Compound (55) can be prepared in refluxing trifluoroacetic acid (see experimental section), but the method outlined in Scheme 5.2 should be employed if the success of the synthesis is to be guaranteed. The ^1H and $^{13}C\text{-}\{^1H\}$ n.m.r. spectra are presented in Figs. 5.3 and 5.4 respectively.

There are two noteworthy features in the ^1H n.m.r. spectrum. Firstly, the resonances of the aromatic ring protons of the cyclophane appear *ca.* 0.2 ppm apart, with the protons of the ring coordinated to the osmium ion resonating at higher frequency. This assignment is made on the basis of observations made for pairs of mononuclear compounds (i.e. (11) and (17), and (13) and (47) Table 4.3). The separation is much greater than that observed in the spectrum of the analogous bisruthenium compound (56) (0.01 ppm). Secondly, two multiplet resonances with an AA'BB' coupling pattern are observed for the $-CH_2CH_2-$ protons of the cyclophane. The two multiplets appear much closer together than in the spectra of compounds where only one cyclophane deck is metal coordinated, and as a result exhibit much greater second order character. In the spectrum of compound (56) this resonance appears as a slightly broadened singlet, so the substantial splitting of the degeneracy observed for (55) is due to the difference in the magnetic anisotropy of the two metal ions. The assignment of resonances observed in the $^{13}C\text{-}\{^1H\}$ n.m.r. spectrum was made with reference to the spectra reported in Chapter 4. Thus the resonances at δ 84.2 and 92.0 ppm are assigned to the non-bridgehead carbon atoms of the cyclophane rings coordinated to the osmium and ruthenium ions respectively.

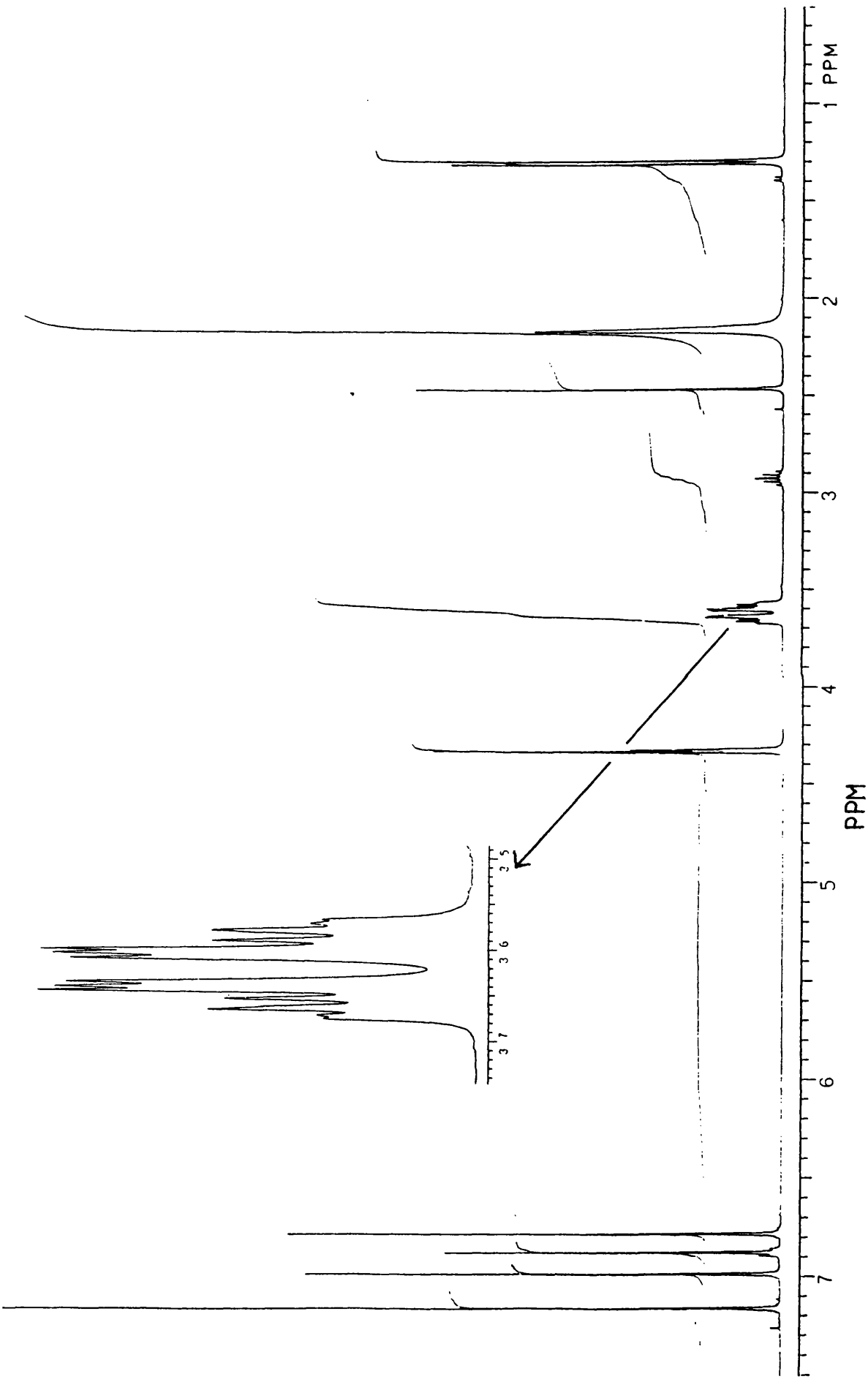

Fig. 5.3 The ^{1}H n.m.r. spectrum of $[(\eta^6\text{-}C_6H_6)Os(\eta^6,\eta^6\text{-}C_{16}H_{16})Ru(\eta^6\text{-}p\text{-cymene})][BF_4]_4$ (55).

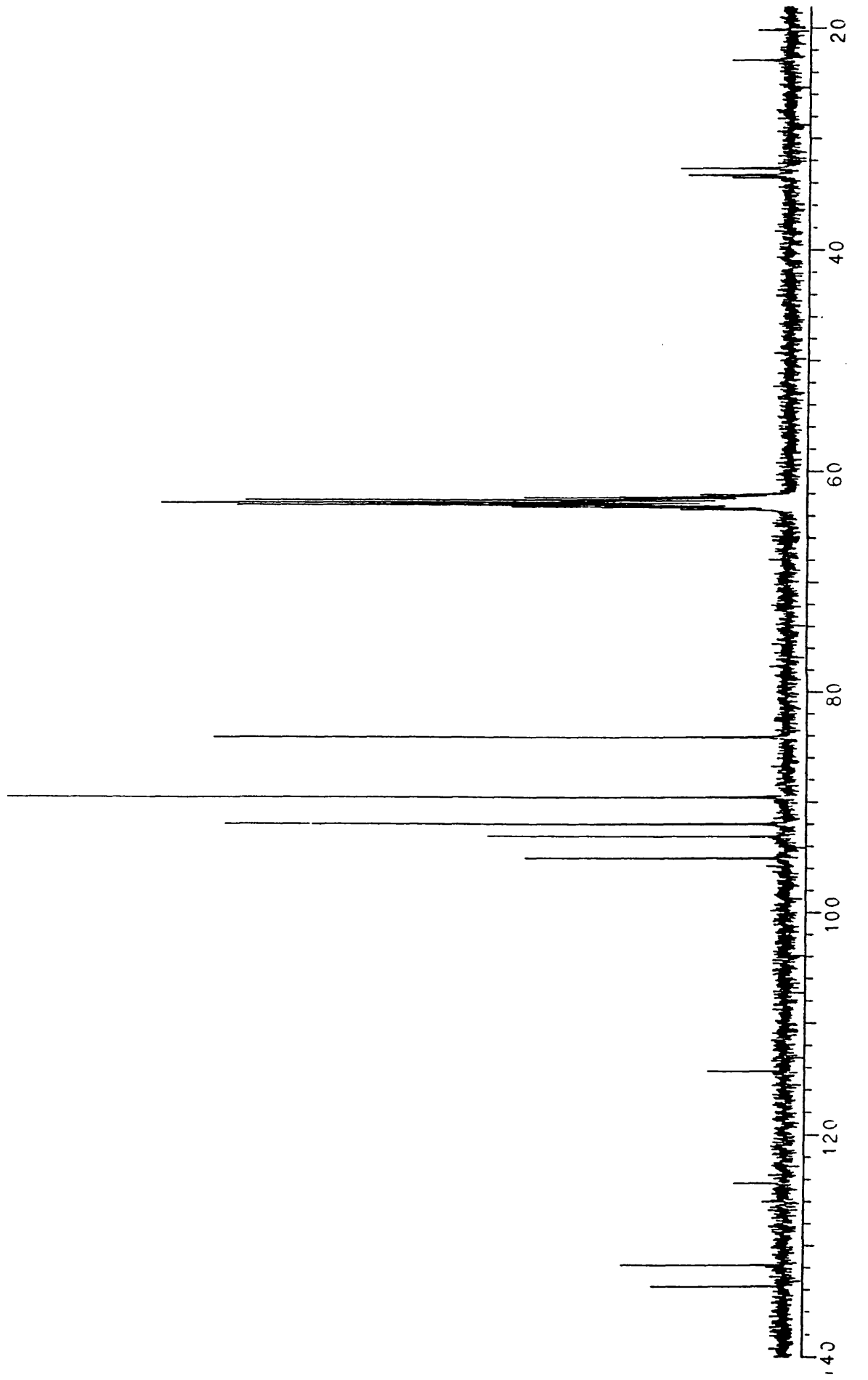

Fig. 5.4 The $^{13}C-\{^{1}H\}$ n.m.r. spectrum of $[(\eta^6\text{-}C_6H_6)Os(\eta^6,\eta^6\text{-}C_{16}H_{16})Ru(\eta^6\text{-}p\text{-cymene})][BF_4]_4$ (55).

The similar compounds $[(\eta^6\text{-}C_6H_6)Os(\eta^6,\eta^6\text{-}C_{16}H_{16})Ru(\eta^6\text{-}C_6H_6)][BF_4]_4$ (60) and $[(\eta^6\text{-}C_6H_6)Os(\eta^6,\eta^6\text{-}C_{16}H_{16})Ru(\eta^6\text{-}C_6Me_6)][BF_4]_4$ (61) were prepared by the method outlined in Scheme 5.2 and were characterised similarly to (55). The full details are given in the experimental section.

(ii) $[(\eta^6\text{-}C_6H_6)Os(\eta^6,\eta^6\text{-}C_{16}H_{16})Ru(\eta^6\text{-}C_{16}H_{16})][BF_4]_4$ (62).

Compound (62) was obtained as a minor product in the room temperature synthesis of (63) (see below). (62) could readily be converted to (63) by further treatment with $[Os(\eta^6\text{-}C_6H_6)(acetone)_3][BF_4]_2$, but is of interest in its own right since it contains one cyclophane ligand coordinated at one external face and another coordinated at both. The infrared spectrum of (62) exhibits δ(CCC) bands at both 660 and 680 cm^{-1}, the former arising from the η^6-coordinated cyclophane, and the latter from the η^6,η^6-coordinated ligand.

The ^1H n.m.r. spectrum exhibits two sets of resonances, one set typical of the ligand coordinated at one aromatic deck, the other set typical of the ligand with both faces metal coordinated. The two sets of resonances have integrals of equal intensity, supporting the proposed 1:1 ratio of the two types of cyclophane present in the molecule. The $^{13}C\text{-}\{^1H\}$ n.m.r. spectrum provides additional evidence supporting the proposed structure. Four resonances are observed in the δ 80-90 ppm region, and are assigned to the carbon atoms of the four coordinated aromatic rings. A fifth resonance is observed at δ 135.7 ppm, which is typical of the non-bridgehead carbon atoms of a non-coordinated cyclophane deck.

5.2.4 The Preparation and Characterisation of Trinuclear Mixed-Metal Compounds: $[(\eta^6\text{-arene})M^1(\eta^6,\eta^6\text{-}C_{16}H_{16})M^2(\eta^6,\eta^6\text{-}C_{16}H_{16})M^1(\eta^6\text{-arene})][BF_4]_6$.

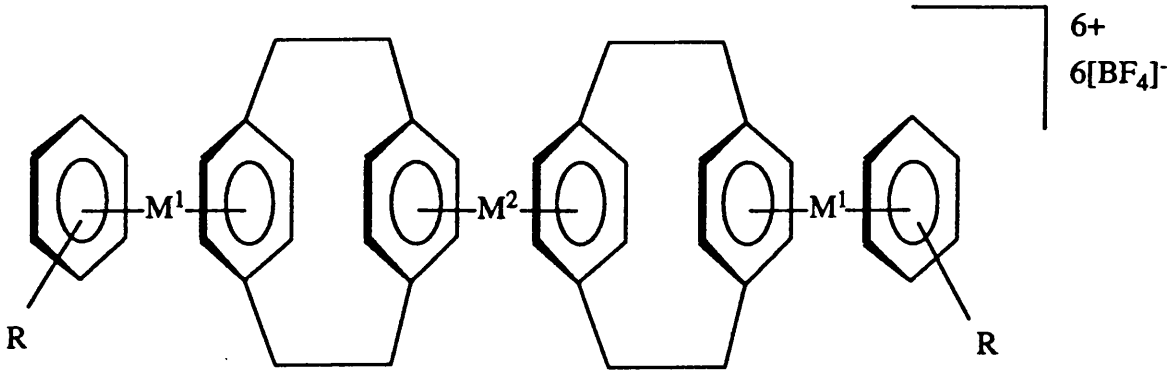

(i) $[(\eta^6\text{-}C_6H_6)Os(\eta^6,\eta^6\text{-}C_{16}H_{16})Ru(\eta^6,\eta^6\text{-}C_{16}H_{16})Os(\eta^6\text{-}C_6H_6)][BF_4]_6$ (63).

Compound (63) has been prepared under reflux conditions and at room temperature. The synthetic strategy shown in Scheme 5.2 was readily extended to the preparation of trinuclear species, i.e. the bis-cyclophane compounds $[M^1(\eta^6\text{-}C_{16}H_{16})_2][BF_4]_2$ were capped at both external cyclophane faces by treatment with an excess of the solvate complexes $[M^2(\eta^6\text{-arene})(acetone)_3][BF_4]_2$. For (63) M^1=Ru, M^2=Os and arene=C_6H_6. The full details of the syntheses and of the characterisation are given in the experimental section. Integration of the ^1H n.m.r. spectrum supports the proposed 1:1 ratio of benzene:η^6,η^6-coordinated [2$_2$]paracyclophane. The ^1H and $^{13}C\text{-}\{^1H\}$ n.m.r. spectra are similar in general appearance to those observed for the binuclear heterometallic compounds described above. In the ^1H n.m.r. spectrum, recorded in CD_3NO_2, the aromatic protons of the cyclophane ligands resonate at δ 6.68 and 6.95 ppm, while those of the C_6H_6 ligands reonate at δ 7.14 ppm. The cyclophane protons proximate to the osmium ions resonate at the higher frequency. In the spectrum[66] of the closely related tri-ruthenium analogue (14), recorded in the same solvent, these protons resonate at δ 6.36 and 6.47 ppm. The infrared spectrum exhibits a δ(CCC) band at 678 cm^{-1}, which is typical for the doubly metallated cyclophane.

Using similar procedures the compounds $[(\eta^6\text{-}C_6H_6)Ru(\eta^6,\eta^6\text{-}C_{16}H_{16})Os(\eta^6,\eta^6\text{-}C_{16}H_{16})Ru(\eta^6\text{-}C_6H_6)][BF_4]_6$ (64), $[(\eta^6\text{-p-cymene})Ru(\eta^6,\eta^6\text{-}C_{16}H_{16})Os(\eta^6,\eta^6\text{-}C_{16}H_{16})Ru(\eta^6\text{-p-cymene})][BF_4]_6$ (65), and

$[(\eta^6\text{-}C_6Me_6)Ru(\eta^6,\eta^6\text{-}C_{16}H_{16})Os(\eta^6,\eta^6\text{-}C_{16}H_{16})Ru(\eta^6\text{-}C_6Me_6)][BF_4]_6$ (66) were prepared and characterised. The full details are given in the experimental section.

5.2.5 Some Comments on Attempts to Crystallise the Chain Compounds.

Even though spectroscopic data provide clear evidence as to the identity of the chain compounds described in this chapter, an X-ray crystallographic characterisation was considered highly desirable. At the time of writing there is no published structural data for an η^6,η^6-coordinated [2$_2$]paracyclophane ligand. One important question that would be answered by such a study would be to what extent does the geometry of the cyclophane change when a second metal coordinates. It has already been noted that a shift in the i.r. band at *ca.* 660 cm^{-1} for an η^6-coordinated ligand to *ca.* 680 cm^{-1} when a second metal coordinates, indicates that some further structural change may have occured. Crystallographic study could elucidate the nature of this change.

Attempts have been made under various conditions to crystallise each of the eleven compounds reported in this chapter. Some crystals have been obtained. Compounds (55) and (56) crystallised as thin plates, while (59) crystallised as needles. In these cases crystals were either twinned or diffracted too weakly for the crystallographic experiment to be undertaken. Crystals obtained from solutions of (55) and (56) were shown to be compounds (17) and (11) respectively, indicating that the chain compounds break down in solution over a few days. A solution of (60) deposited two sets of crystals, one type identified as the cyclophane ligand, the other as (11) or (17). Thus all efforts were in vain.

There are two factors which may have inhibited the formation of good quality crystals. Firstly, the $[BF_4]^-$ anion is often crystallographically problematic in terms of disorder and, being basically spherical in shape, might pack poorly with the linear cations. A change to a more linear counterion, e.g. $[SCN]^-$, might be more compatible with the chain compounds. Secondly, the metal-[2$_2$]paracyclophane bonds break in coordinating solvents before the compound has chance to crystallise. A switch to the octamethyparacyclophane ligand should result in more stable products due to the expected greater metal-ligand bond strength.

5.3 EXPERIMENTAL.

5.3.1 Instrumentation and Physical Measurements.

As described in Section 2.3.1.

5.3.2 Materials.

The compounds $[M(\eta^6\text{-}C_{16}H_{16})Cl_2]_2$ {M=Ru (1), M=Os (16)} were prepared as described in Section 2.3.3. The compounds $[M(\eta^6\text{-arene})Cl_2]_2$ (M=Ru,Os η^6-arene=C_6H_6; M=Ru η^6-arene=C_6Me_6, 1,4-$MeC_6H_4CHMe_2$) were prepared as described in Section 4.3.2. The compounds $[M(\eta^6\text{-}C_{16}H_{16})_2][BF_4]_2$ were prepared as described in Sections 4.3.2 (M=Ru) and 4.3.3 (M=Os). Other materials were obtained and used as described in section 2.3.2.

5.3.3 Synthesis and Characterisation.

$[(\eta^6\text{-}C_6H_6)Ru(\eta^6,\eta^6\text{-}C_{16}H_{16})Ru(\eta^6\text{-}p\text{-cymene})][BF_4]_4$ (56).

Silver tetrafluoroborate (0.08 g; 0.42 mmol) was added to a suspension of $[Ru(\eta^6\text{-}p\text{-cymene})Cl_2]_2$ (0.06 g; 0.09 mmol). The mixture was stirred at room temperature for 1 h., and filtered through celite to remove the precipitated silver chloride. The red filtrate was pumped to dryness. Trifluoracetic acid (5 cm^3) and $[Ru(\eta^6\text{-}C_6H_6)(\eta^6\text{-}C_{16}H_{16})][BF_4]_2$ (0.10 g; 0.18 mmol) were added, and the solution was stirred overnight at ambient temperature. The volume of the deep orange solution was reduced to *ca.* 2-3 cm^3, and diethyl ether (20 cm^3) was added to precipitate the pale yellow product. The solid was filtered off, washed with diethyl ether (15 cm^3), then dried *in vacuo*. Yield: 0.17 g; 0.18 mmol; 93% (based on $[Ru(\eta^6\text{-}C_6H_6)(\eta^6\text{-}C_{16}H_{16})][BF_4]_2$).

Infrared spectrum: $[BF_4]^-$: 1059 (s, br); δ(CCC): 681 (m); $\nu(CH)_{ar}$: 3072 (s).

^1H n.m.r. Data: Solvent: CD_3NO_2. Operating frequency: 400 MHz.

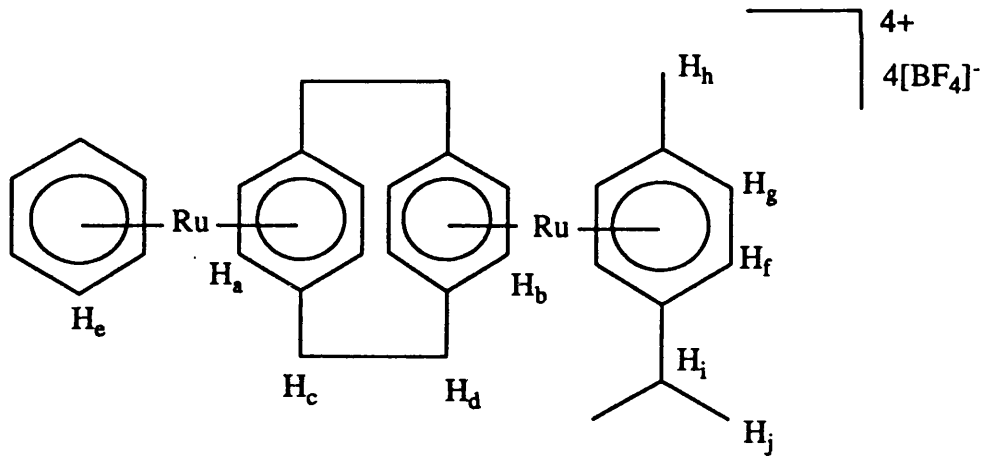

Cyclophane resonances δ, ppm:

H_a, H_b	6.71 (s,4H), 6.72 (s,4H)
H_c, H_d	3.64 (s,8H)

Other resonances δ, ppm:

H_e	6.93 (s,6H)
H_f, H_g	6.85 (br s,4H)
H_h	2.45 (s,3H)
H_i	2.91 (sept,1H,$^3J_{H\text{-}H}$=7Hz)
H_j	1.28 (d,6H,$^3J_{H\text{-}H}$=7Hz)

$^{13}C-\{^{1}H\}$ n.m.r. Data: Solvent: CD_3NO_2. Operating frequency: 100 MHz.

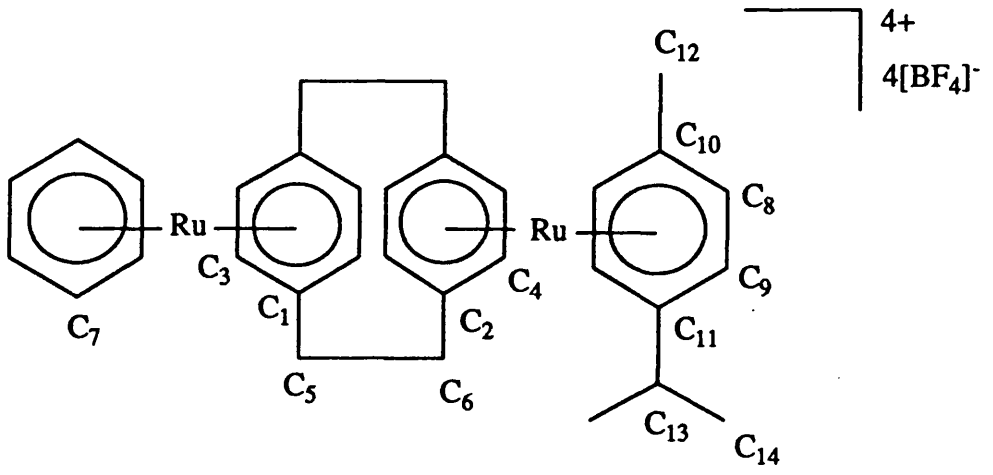

Cyclophane resonances:

C_1, C_2	133.6, 134.7
C_3, C_4	91.8, 92.0
C_5, C_6	33.0, 33.3

Other resonances:

C_7	95.7	C_{11}	124.4
C_8	93.1	C_{12}	20.1
C_9	95.1	C_{13}	33.5
C_{10}	114.3	C_{14}	23.0

Mass spectrum: m/e range: 400-1000 mass units.

m/e	Fragment
885	$[(\eta^6\text{-}C_6H_6)Ru(\eta^6,\eta^6\text{-}C_{16}H_{16})Ru(\eta^6\text{-}p\text{-cymene})][BF_4]_3^+$
798	$[(\eta^6\text{-}C_6H_6)Ru(\eta^6,\eta^6\text{-}C_{16}H_{16})Ru(\eta^6\text{-}p\text{-cymene})][BF_4]_2^+$
711	$[(\eta^6\text{-}C_6H_6)Ru(\eta^6,\eta^6\text{-}C_{16}H_{16})Ru(\eta^6\text{-}p\text{-cymene})][BF_4]^+$
624	$[(\eta^6\text{-}C_6H_6)Ru(\eta^6,\eta^6\text{-}C_{16}H_{16})Ru(\eta^6\text{-}p\text{-cymene})]^+$
562	$[(\eta^6\text{-}C_6H_6)Ru(\eta^6\text{-}C_{16}H_{16})][BF_4]_2^+$
531	$[(\eta^6\text{-}C_{16}H_{16})Ru(\eta^6\text{-}p\text{-cymene})][BF_4]^+$
475	$[(\eta^6\text{-}C_6H_6)Ru(\eta^6\text{-}C_{16}H_{16})][BF_4]^+$
444	$[(\eta^6\text{-}C_{16}H_{16})Ru(\eta^6\text{-}p\text{-cymene})]^+$

[(η^6-C_6H_6)Ru(η^6,η^6-$C_{16}H_{16}$)Ru(η^6-C_6Me_6)][BF_4]$_4$ (58).

A crude sample of (58) was obtained by the method described for the preparation of (56). [Ru(η^6-C_6Me_6)Cl_2]$_2$ (0.05 g; 0.08 mmol), Ag[BF_4] (0.07 g; 0.35 mmol), [Ru(η^6-C_6H_6)(η^6-$C_{16}H_{16}$)][BF_4]$_2$ (0.07 g; 0.13 mmol). Mass of solid isolated : 0.09 g. The ^{1}H n.m.r. spectrum recorded for this solid indicated the presence of 15-20% of the mononuclear starting material, [Ru(η^6-C_6H_6)(η^6-$C_{16}H_{16}$)][BF_4]$_2$, in addition to the desired product. Purification was achieved as follows: [Ru(η^6-C_6Me_6)Cl_2]$_2$ (0.02 g; 0.04 mmol) was treated with Ag[BF_4] (0.04 g; 0.21 mmol) as previously. The impure solid (0.09 g) and CF_3CO_2H (5 cm^3) were then added to the dried solvate complex and the solution stirred at room temperature overnight. The pale yellow product was isolated as before. Yield after purification: 0.10 g; 0.10 mmol; 77% (based on [Ru(η^6-C_6H_6)(η^6-$C_{16}H_{16}$)][BF_4]$_2$).

Infrared spectrum: [BF_4]$^-$: 1057 (s, br); δ(CCC): 680 (m); ν(CH)$_{ar}$: 3063 (s).

^{1}H n.m.r. Data: Solvent: CD_3NO_2. Operating frequency: 400 MHz.

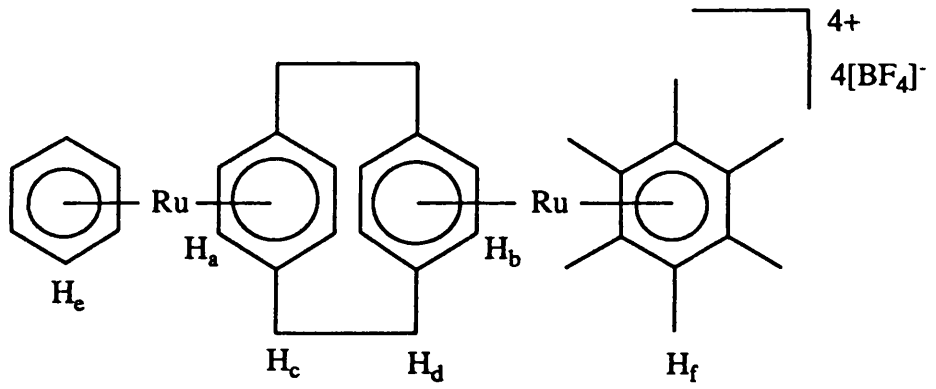

Cyclophane resonances δ, ppm:

H_a	6.62 (s,4H).
H_b	6.42 (s,4H).
H_c, H_d	3.52-3.61 (m,8H,AA'BB').

Other resonances δ, ppm:

H_e	6.92 (s,6H).
H_f	2.53 (s,18H).

^{13}C-{^{1}H} n.m.r. Data: Solvent: CD_3NO_2. Operating frequency: 100 MHz.

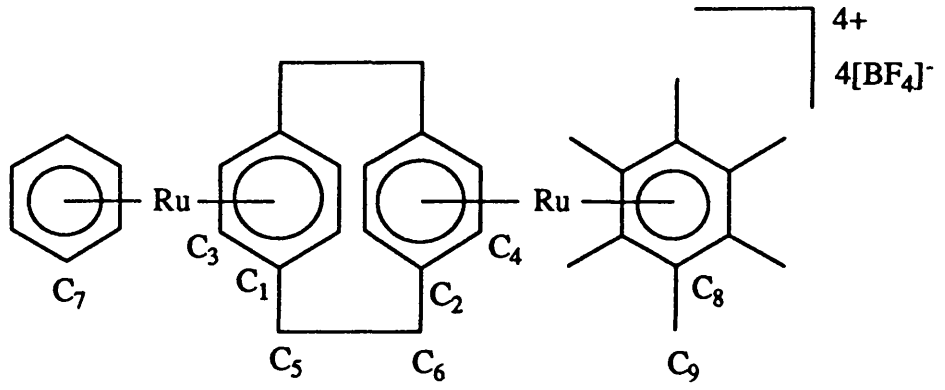

Cyclophane resonances δ, ppm:

C_1	134.6	C_4	92.6
C_2	131.0	C_5, C_6	33.0, 31.7
C_3	91.8		

Other resonances δ, ppm:

C_7	95.6
C_8	111.2
C_9	18.1

Mass spectrum: m/e range: 400-1000 mass units.

m/e	Fragment
913	$[(\eta^6\text{-}C_6H_6)Ru(\eta^6,\eta^6\text{-}C_{16}H_{16})Ru(\eta^6\text{-}C_6Me_6)][BF_4]_3^+$
826	$[(\eta^6\text{-}C_6H_6)Ru(\eta^6,\eta^6\text{-}C_{16}H_{16})Ru(\eta^6\text{-}C_6Me_6)][BF_4]_2^+$
739	$[(\eta^6\text{-}C_6H_6)Ru(\eta^6,\eta^6\text{-}C_{16}H_{16})Ru(\eta^6\text{-}C_6Me_6)][BF_4]^+$
652	$[(\eta^6\text{-}C_6H_6)Ru(\eta^6,\eta^6\text{-}C_{16}H_{16})Ru(\eta^6\text{-}C_6Me_6)]^+$
559	$[(\eta^6\text{-}C_{16}H_{16})Ru(\eta^6\text{-}C_6Me_6)][BF_4]^+$
472	$[(\eta^6\text{-}C_{16}H_{16})Ru(\eta^6\text{-}C_6Me_6)]^+$

[(η^6-C_6Me_6)Ru(η^6,η^6-$C_{16}H_{16}$)Ru(η^6-*p*-cymene)][BF_4]$_4$ (59).

A crude sample of (59) was obtained by the method used to prepare (56). [Ru(η^6-C_6Me_6)Cl_2]$_2$ (0.05 g; 0.08 mmol), Ag[BF_4] (0.07 g; 0.37 mmol), [Ru(η^6-*p*-cymene)(η^6-$C_{16}H_{16}$)][BF_4]$_2$ (0.08 g; 0.12 mmol). Mass of solid isolated: 0.12 g. The ^{1}H n.m.r. spectrum recorded for this solid indicated the presence of ca. 20% of the starting material, [Ru(η^6-*p*-cymene)(η^6-$C_{16}H_{16}$)][BF_4]$_2$, in addition to the desired product. The crude product was purified by further overnight treatment with a fresh solution of the solvate complex {[Ru(η^6-C_6Me_6)Cl_2]$_2$ (0.03 g; 0.04 mmol), Ag[BF_4] (0.04 g; 0.18 mmol)}. The pale yellow purified product was isolated as before. Yield: 0.12 g; 0.12 mmol; 93% (based on [Ru(η^6-*p*-cymene)(η^6-$C_{16}H_{16}$)][BF_4]$_2$).

Infrared spectrum: [BF_4]$^-$: 1057 (s, br); δ(CCC): 680 (m); ν(CH)$_{ar}$: 3063 (s).

^{1}H n.m.r. Data: Solvent: CD_3NO_2. Operating frequency: 400 MHz.

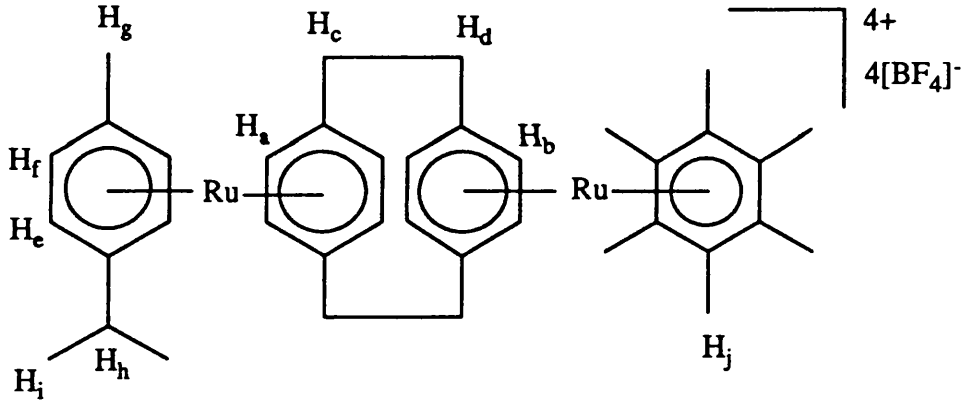

Cyclophane resonances δ, ppm:

H_a	6.41 (s,4H)
H_b	6.60 (s,4H)
H_c, H_d	3.55 (s,8H)

Other resonances δ, ppm:

H_e, H_f	6.84 (s,4H)
H_g	2.45 (s,3H)
H_h	2.91 (sept,1H,$^3J_{H\text{-}H}$=7Hz)
H_i	1.28 (d,6H,$^3J_{H\text{-}H}$=7Hz)
H_j	2.53 (s,18H)

^{13}C-{^{1}H} n.m.r. Data: Solvent: CD_3NO_2. Operating frequency: 100 MHz.

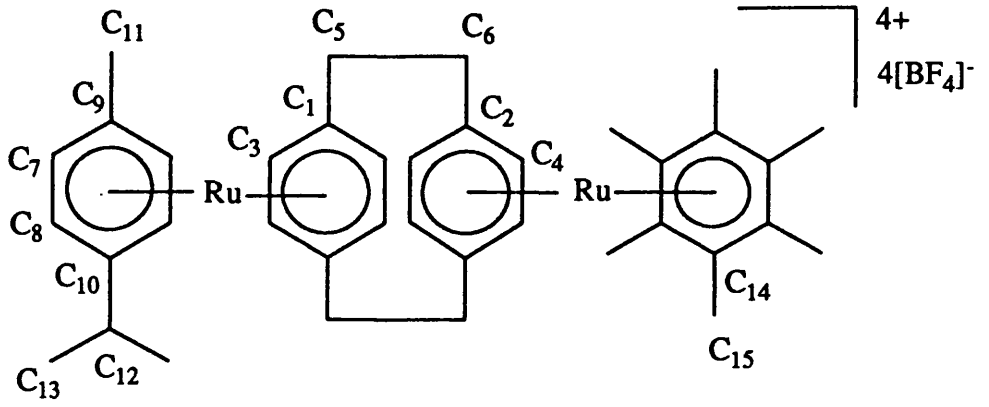

Cyclophane resonances δ, ppm:

C_1	133.4	C_4	91.9
C_2	130.9	C_5, C_6	31.7, 32.7
C_3	92.6		

Other resonances δ, ppm:

C_7	93.3	C_{12}	33.5
C_8	95.3	C_{13}	22.6
C_9	113.7	C_{14}	111.3
C_{10}	124.0	C_{15}	18.1
C_{11}	20.2		

Mass spectrum: m/e range: 400-1100 mass units.

m/e	Fragment
1056	$[(\eta^6\text{-}C_6Me_6)Ru(\eta^6,\eta^6\text{-}C_{16}H_{16})Ru(\eta^6\text{-}p\text{-cymene})][BF_4]_4^+$
969	$[(\eta^6\text{-}C_6Me_6)Ru(\eta^6,\eta^6\text{-}C_{16}H_{16})Ru(\eta^6\text{-}p\text{-cymene})][BF_4]_3^+$
882	$[(\eta^6\text{-}C_6Me_6)Ru(\eta^6,\eta^6\text{-}C_{16}H_{16})Ru(\eta^6\text{-}p\text{-cymene})][BF_4]_2^+$
795	$[(\eta^6\text{-}C_6Me_6)Ru(\eta^6,\eta^6\text{-}C_{16}H_{16})Ru(\eta^6\text{-}p\text{-cymene})][BF_4]^+$
708	$[(\eta^6\text{-}C_6Me_6)Ru(\eta^6,\eta^6\text{-}C_{16}H_{16})Ru(\eta^6\text{-}p\text{-cymene})]^+$
559	$[(\eta^6\text{-}C_6Me_6)Ru(\eta^6\text{-}C_{16}H_{16})][BF_4]^+$
472	$[(\eta^6\text{-}C_6Me_6)Ru(\eta^6\text{-}C_{16}H_{16})]^+$
444	$[(\eta^6\text{-}C_{16}H_{16})Ru(\eta^6\text{-}p\text{-cymene})]^+$

[(η^6-C_6H_6)Os(η^6,η^6-$C_{16}H_{16}$)Ru(η^6-C_6H_6)][BF_4]$_4$ (60).

A crude sample of (60) was obtained by the method employed for (56). [Ru(η^6-C_6H_6)Cl_2]$_2$ (0.05 g; 0.11 mmol) Ag[BF_4] (0.01 g; 0.050 mmol), [Os(η^6-C_6H_6)(η^6-$C_{16}H_{16}$)][BF_4]$_2$ (0.09 g; 0.14 mmol). The solid was filtered off, washed with diethyl ether (10 cm^3), and dried *in vacuo* for 2 h. Mass of solid isolated: 0.16 g. The ^{1}H n.m.r. spectrum of this solid indicated the presence of some unreacted [Os(η^6-C_6H_6)(η^6-$C_{16}H_{16}$)][BF_4]$_2$ and [Ru(η^6-C_6H_6)(acetone)$_3$][BF_4]$_2$. The sample was purified by addition of trifluoroacetic acid (5 cm^3) and stirring overnight. The solid was filtered off, mass isolated: 0.11 g. The ^{1}H n.m.r. spectrum of this solid indicated a greater proportion of the desired dimetallic product, but also the presence of a little unreacted [Os(η^6-C_6H_6)(η^6-$C_{16}H_{16}$)][BF_4]$_2$. Further overnight treatment with a fresh solution of [Ru(η^6-C_6H_6)(acetone)$_3$][BF_4]$_2$ {[Ru(η^6-C_6H_6)Cl_2]$_2$ (0.03 g; 0.06 mmol), Ag[BF_4] (0.05 g; 0.27 mmol)}, and filtration of the solid without the addition of diethyl ether afforded the pure, off-white product which was washed with diethyl ether and dried *in vacuo* for 1 h. Yield: 0.08 g; 0.08 mmol; 58% (based on [Os(η^6-C_6H_6)(η^6-$C_{16}H_{16}$)][BF_4]$_2$).

Infrared spectrum: [BF_4]$^-$: 1034 (s, br); δ(CCC): 678 (m); ν(CH)$_{ar}$: 3069 (s), 3094 (s).

^{1}H n.m.r. Data: Solvent: CD_3NO_2. Operating frequency: 400 MHz.

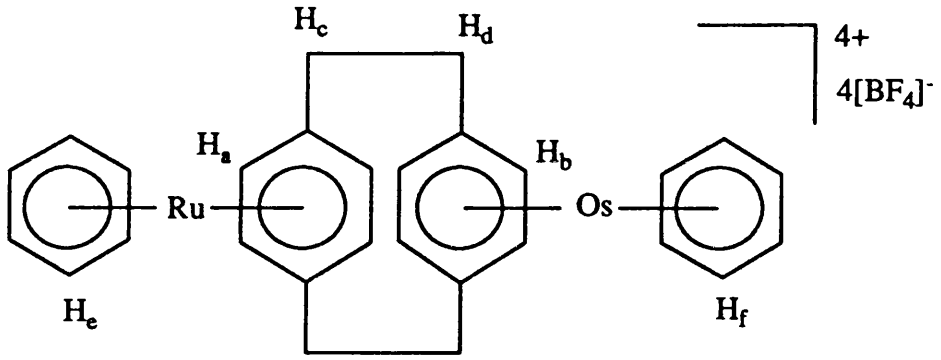

Cyclophane resonances δ, ppm:

H_a	6.82 (s,4H)
H_b	7.02 (s,4H)
H_c, H_d	3.57-3.67 (m,8H,AA'BB')

Other resonances δ, ppm:

H_e	6.96 (s,6H)
H_f	7.17 (s,6H)

^{13}C-{^{1}H} n.m.r. Data: Solvent: CD_3NO_2. Operating frequency: 100 MHz.

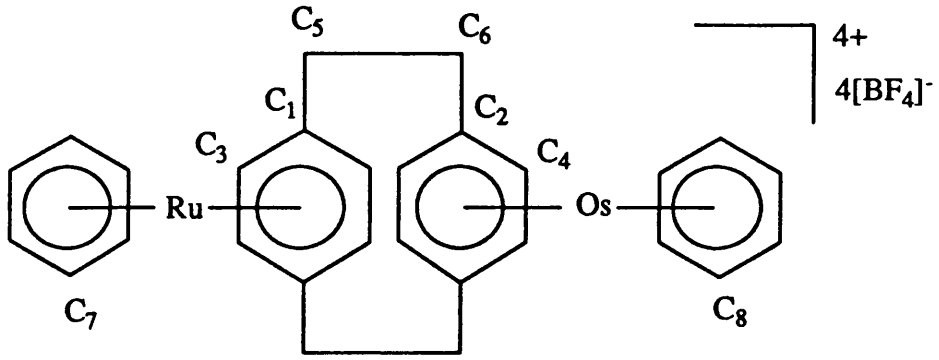

Cyclophane resonances δ, ppm:

C_1	135.0	C_4	84.1
C_2	132.0	C_5, C_6	33.1, 33.4
C_3	91.7		

Other resonances δ, ppm:

C_7	95.8	C_8	89.6

[(η^6-C_6H_6)Os(η^6,η^6-$C_{16}H_{16}$)Ru(η^6-*p*-cymene)][BF_4]$_4$ (55).

Silver tetrafluoroborate (0.30 g; 1.54 mmol) was added to a suspension of [Ru(η^6-*p*-cymene)Cl_2]$_2$ (0.20 g; 0.33 mmol) in acetone (10 cm^3), and the mixture stirred for 30 min. at room temperature. The precipitated silver chloride was removed by filtration through celite, giving a clear, red solution which was pumped to dryness. Trifluoroacetic acid (7 cm^3) and [Os(η^6-C_6H_6)(η^6-$C_{16}H_{16}$)][BF_4]$_2$ (0.08 g; 0.13 mmol) were added, and the mixture was refluxed for 30 min. The solution was cooled in an ice-bath and diluted with diethyl ether (20 cm^3) to precipitate the pale yellow product. The product was filtered off, washed with diethyl ether (25 cm^3) and air dried. Yield: 0.13 g; 0.12 mmol; 95% (based on [Os(η^6-C_6H_6)(η^6-$C_{16}H_{16}$)][BF_4]$_2$).

Infrared spectrum: $[BF_4]^-$: 1048 (s, br); δ(CCC): 679 (s); $\nu(CH)_{ar}$: 3073 (s).

^{1}H n.m.r. Data: Solvent: CD_3NO_2. Operating frequency: 400 MHz.

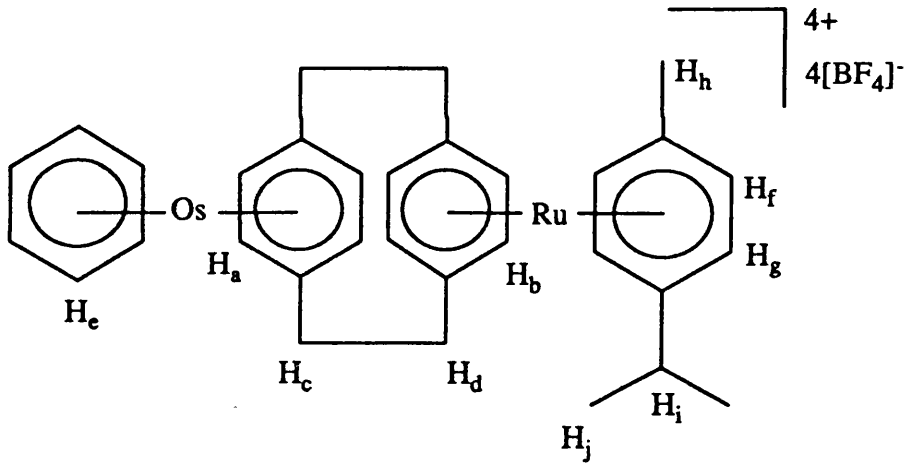

Cyclophane resonances δ, ppm:

H_a	6.99 (s,4H)
H_b	6.78 (s,4H)
H_c, H_d	3.58-3.65 (m,8H,AA'BB')

Other resonances δ, ppm:

H_e	7.16 (s,6H)
H_f, H_g	6.88 (br s,4H)
H_h	2.47 (s,3H)
H_i	2.93 (sept,1H,$^3J_{H\text{-}H}$=7Hz)
H_j	1.29 (d,6H,$^3J_{H\text{-}H}$=7Hz)

$^{13}C-\{^{1}H\}$ n.m.r. Data: Solvent: CD_3NO_2. Operating frequency: 100 MHz.

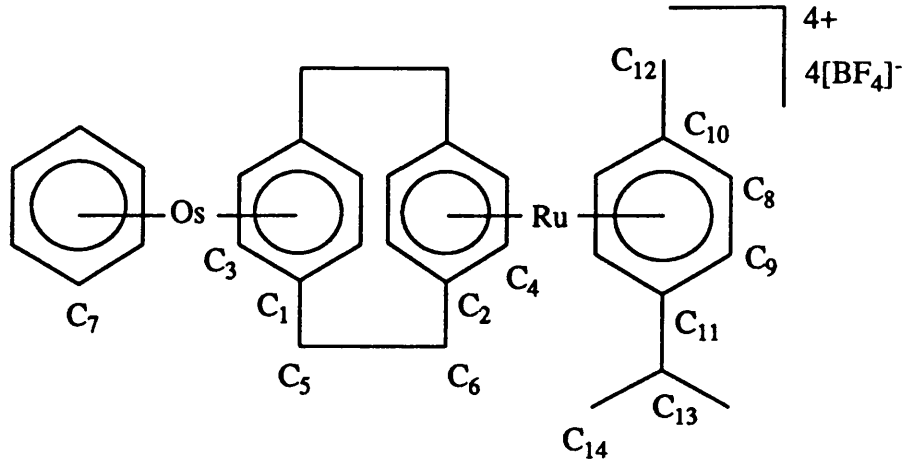

Cyclophane resonances δ, ppm:

C_1	131.2	C_4	92.0
C_2	133.7	C_5, C_6	33.3, 32.7
C_3	84.2		

Other resonances δ, ppm:

C_7	89.6	C_{11}	124.4
C_8	93.1	C_{12}	20.2
C_9	95.1	C_{13}	33.5
C_{10}	114.4	C_{14}	22.9

[(η^6-C_6H_6)Os(η^6,η^6-$C_{16}H_{16}$)Ru(η^6-C_6Me_6)][BF_4]$_4$ (61).

Compound (61) was prepared similarly to (56). [Ru(η^6-C_6Me_6)Cl_2]$_2$ (0.05 g; 0.07 mmol), Ag[BF_4] (0.07 g; 0.33 mmol), [Os(η^6-C_6H_6)(η^6-$C_{16}H_{16}$)][BF_4]$_2$ (0.06 g 0.10 mmol). The pale yellow solid was filtered off, washed with diethyl ether (10 cm^3) and dried *in vacuo* for 2 h. Yield: 0.08 g; 0.07 mmol; 73% (based on [Os(η^6-C_6H_6)(η^6-$C_{16}H_{16}$)][BF_4]$_2$).

Infrared spectrum: $[BF_4]^-$: 1055 (s, br); δ(CCC): 677 (m); $\nu(CH)_{ar}$: 3062 (s).

^{1}H n.m.r. Data: Solvent: CD_3NO_2. Operating frequency: 400 MHz.

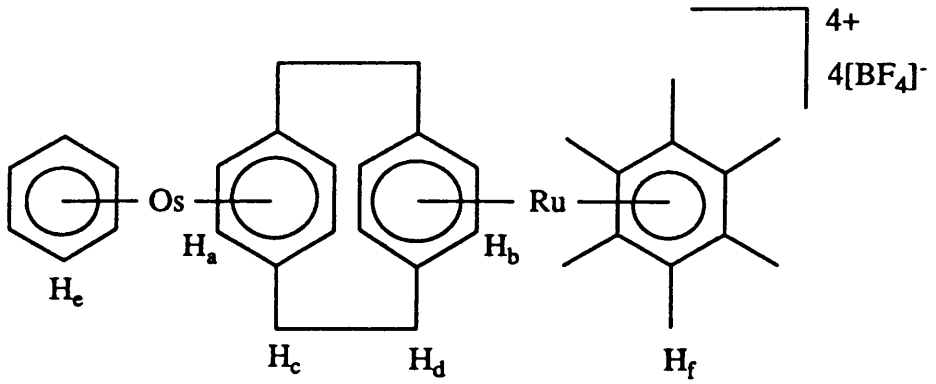

Cyclophane resonances δ, ppm:

H_a	6.90 (s,4H)
H_b	6.50 (s,4H)
H_c, H_d	3.51-3.61 (m,8H,AA'BB')

Other resonances δ, ppm:

H_e	7.15 (s,6H)
H_f	2.54 (s,18H)

^{13}C-{^{1}H} n.m.r. Data: Solvent: CD_3NO_2. Operating frequency: 100 MHz.

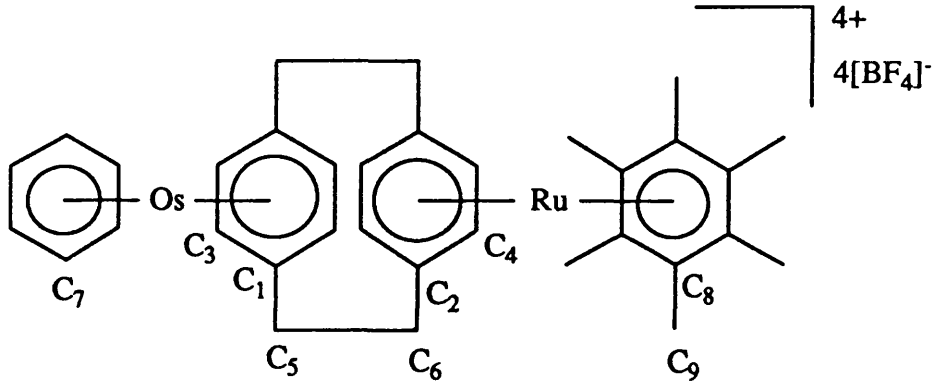

Cyclophane resonances δ, ppm:

C_1, C_2	131.1, 131.7
C_3	84.2
C_4	92.6
C_5, C_6	31.4, 33.0

Other resonances δ, ppm:

C_7	89.5
C_8	111.3
C_9	18.2

Mass spectrum: m/e range: 450-1200 mass units.

m/e	Fagment
1003	$[(\eta^6\text{-}C_6H_6)Os(\eta^6,\eta^6\text{-}C_{16}H_{16})Ru(\eta^6\text{-}C_6Me_6)][BF_4]_3^+$
916	$[(\eta^6\text{-}C_6H_6)Os(\eta^6,\eta^6\text{-}C_{16}H_{16})Ru(\eta^6\text{-}C_6Me_6)][BF_4]_2^+$
829	$[(\eta^6\text{-}C_6H_6)Os(\eta^6,\eta^6\text{-}C_{16}H_{16})Ru(\eta^6\text{-}C_6Me_6)][BF_4]^+$
742	$[(\eta^6\text{-}C_6H_6)Os(\eta^6,\eta^6\text{-}C_{16}H_{16})Ru(\eta^6\text{-}C_6Me_6)]^+$
559	$[(\eta^6\text{-}C_{16}H_{16})Ru(\eta^6\text{-}C_6Me_6)][BF_4]^+$
478	$[(\eta^6\text{-}C_6H_6)Os(\eta^6\text{-}C_{16}H_{16})]^+$
472	$[(\eta^6\text{-}C_{16}H_{16})Ru(\eta^6\text{-}C_6Me_6)]^+$

$[(\eta^6\text{-}C_6H_6)Os(\eta^6,\eta^6\text{-}C_{16}H_{16})Ru(\eta^6\text{-}C_{16}H_{16})][BF_4]_4$ (62).

Silver tetrafluroborate (0.06 g; 0.31 mmol) was added to a suspension of $[Os(\eta^6\text{-}C_6H_6)Cl_2]_2$ (0.05 g; 0.08 mmol) in acetone (5 cm^3) and the mixture stirred for 1 h. The precipitated silver chloride was removed by filtration, giving a clear yellow solution which was pumped to dryness. Trifluoroacetic acid (5 cm^3) and $[Ru(\eta^6\text{-}C_{16}H_{16})_2][BF_4]_2$ (0.03 g; 0.05 mmol) were added. The mixture was stirred for 48 h. at room temperature. The solid deposited after this time was isolated by filtration, washed with trifluoroacetic acid (2 cm^3) and diethyl ether, and dried *in vacuo*. The ^1H n.m.r. spectrum of this product identified it as $[(\eta^6\text{-}C_6H_6)Os(\eta^6,\eta^6\text{-}C_{16}H_{16})Ru(\eta^6,\eta^6\text{-}C_{16}H_{16})Os(\eta^6\text{-}C_6H_6)][BF_4]_6$ (63) (see below). Yield 0.01 g, 0.006 mmol, 14% (based on $[Ru(\eta^6\text{-}C_{16}H_{16})_2][BF_4]_2$). Diethyl ether (10 cm^3) was added to the deep yellow filtrate, which caused a second precipitate to form. This was isolated as before. This second solid was shown by its ^1H and $^{13}C\text{-}\{^1H\}$ n.m.r. spectra to contain predominantly $[(\eta^6\text{-}C_6H_6)Os(\eta^6,\eta^6\text{-}C_{16}H_{16})Ru(\eta^6\text{-}C_{16}H_{16})]\text{-}[BF_4]_4$ (62). Approximate yield: 0.04 g, 0.04 mmol, 78% (based on $[Ru(\eta^6\text{-}C_{16}H_{16})_2][BF_4]_2$).

Infrared spectrum: $[BF_4]^-$: 1059 (s, br); δ(CCC): 660 (w), 678 (m); $\nu(CH)_{ar}$: 3070 (s).

^1H n.m.r. Data: Solvent: CD_3NO_2. Operating frequency: 400 MHz.

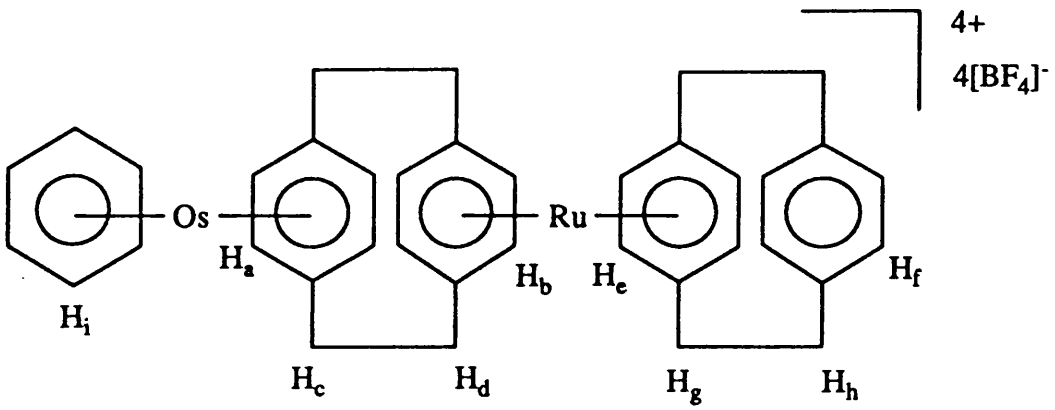

Cyclophane resonances δ, ppm:

$(\eta^6,\eta^6\text{-}C_{16}H_{16})$:

H_a	6.99 (s,4H)
H_b	6.46 (s,4H)
H_c, H_d	3.50 (s,8H)

(η^6-$C_{16}H_{16}$):

H_e	6.13 (s,4H)
H_f	6.91 (s,4H)
H_g, H_h	3.12, 3.41 (m, each 4H, AA'XX')

Other resonances δ, ppm:

H_i	7.12 (s,6H)

^{13}C-{^1H} n.m.r. Data: Solvent: CD_3NO_2. Operating frequency: 100 MHz.

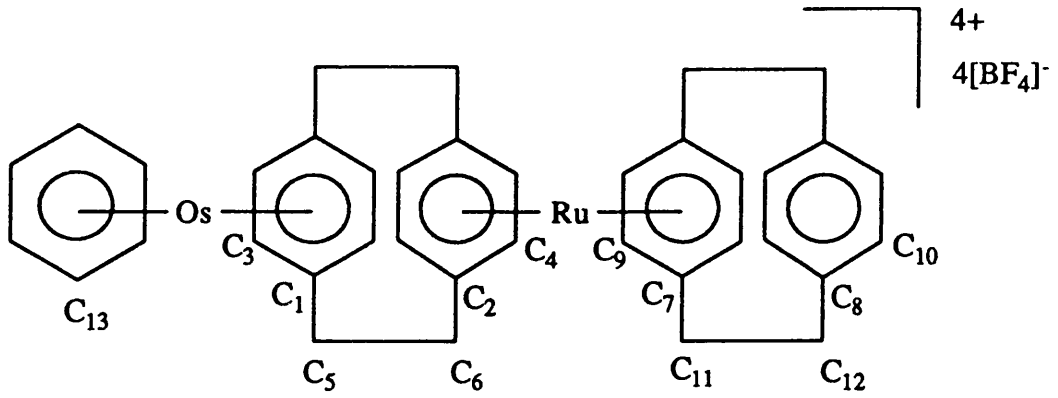

Cyclophane resonances δ, ppm:

C_1	131.7	C_7	133.7
C_2	136.5	C_8	140.9
C_3	84.0	C_{10}	135.7
C_4, C_9	89.0, 88.3		
C_5, C_6, C_{11}, C_{12}	33.3, 35.2, 33.2, 33.3		

Other resonances δ, ppm:

C_{13}	89.4

$[(\eta^6\text{-}C_6H_6)Os(\eta^6,\eta^6\text{-}C_{16}H_{16})Ru(\eta^6,\eta^6\text{-}C_{16}H_{16})Os(\eta^6\text{-}C_6H_6)][BF_4]_6$ (63).

Silver tetrafluoroborate (0.15 g; 0.77 mmol) was added to a suspension of $[Os(\eta^6\text{-}C_6H_6)Cl_2]_2$ (0.12 g; 0.17 mmol) in acetone. The mixture was stirred for 1 h. at room temperature, and then filtered through celite to remove the precipitated silver chloride. The solvent was removed *in vacuo*. To the yellow/orange residue trifluoroacetic acid (5 cm^3) and $[Ru(\eta^6\text{-}C_{16}H_{16})_2][BF_4]_2$ (0.06 g; 0.09 mmol) were added, and the mixture was refluxed for 10 min. The solution was cooled in an ice-bath and a pale yellow precipitate formed. The solid was filtered off and washed with diethyl ether (10 cm^3). Addition of diethyl ether to the filtrate caused a second crop of the product to be precipitated. Combined yield after drying *in vacuo*: 0.11 g; 0.07 mmol; 74% (based on $[Ru(\eta^6\text{-}C_{16}H_{16})_2][BF_4]_2$). (63) may also be prepared by an analogous reaction at room temperature {see above, (62)}.

Infrared spectrum: $[BF_4]^-$: 1059 (s, br); δ(CCC): 660 (m); $\nu(CH)_{ar}$: 3069 (s).

^1H n.m.r. Data: Solvent: CD_3NO_2. Operating frequency: 400 MHz.

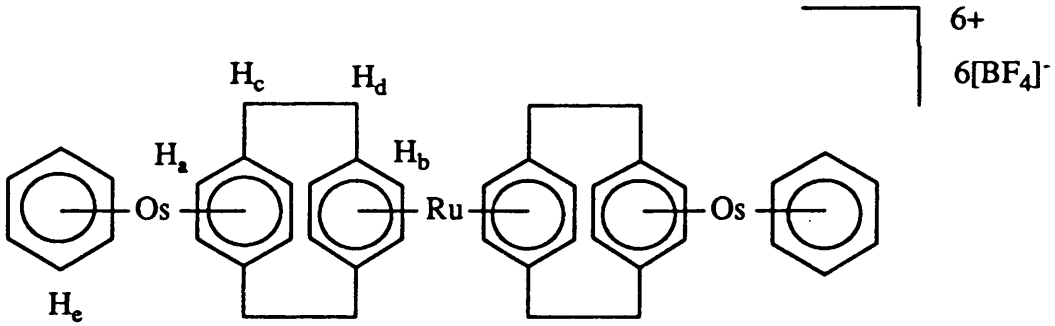

Cyclophane resonances δ, ppm:

H_a	6.95 (s,8H)
H_b	6.68 (s,8H)
H_c, H_d	3.51-3.61 (m,16H,AA'BB')

Other resonances δ, ppm:

H_e	7.14 (s,12H)

$^{13}C-\{^{1}H\}$ n.m.r. Data: Solvent: CD_3NO_2. Operating frequency: 100 MHz.

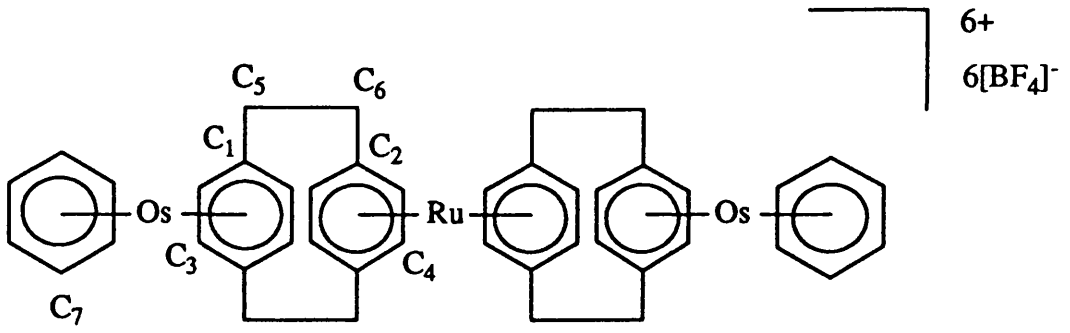

Cyclophane resonances δ, ppm:

C_1	131.5	C_4	90.2
C_2	136.6	C_5, C_6	33.3, 32.9
C_3	84.0		

Other resonances δ, ppm:

C_7	89.6

[(η^6-C_6H_6)Ru(η^6,η^6-$C_{16}H_{16}$)Os(η^6,η^6-$C_{16}H_{16}$)Ru(η^6-C_6H_6)][BF_4]$_6$ (64).

Silver tetrafluoroborate (0.09 g mg; 0.46 mmol) was added to a suspension of [Ru(η^6-C_6H_6)Cl_2]$_2$ (0.05 g; 0.10 mmol) in acetone (5 cm^3). The mixture was stirred for 1 h. and filtered through celite to remove the precipitated silver chloride. The solution was pumped to dryness and trifluoroacetic acid (5 cm^3) and [Os(η^6-$C_{16}H_{16}$)$_2$][BF_4]$_2$ (51.9 mg; 0.067 mmol) were added. The solution was stirred for 60 h. at room temperature. The product formed as a pale yellow precipitate which was filtered off and washed with diethyl ether (10 cm^3), then air dried. Yield: 0.09 g; 0.06 mmol; 95% (based on [Os(η^6-$C_{16}H_{16}$)$_2$][BF_4]$_2$).

Infrared spectrum: $[BF_4]^-$: 1061 (s, br); δ(CCC): 678 (s); $\nu(CH)_{ar}$: 3073 (s).

^{1}H n.m.r. Data: Solvent: CD_3NO_2. Operating frequency: 400 MHz.

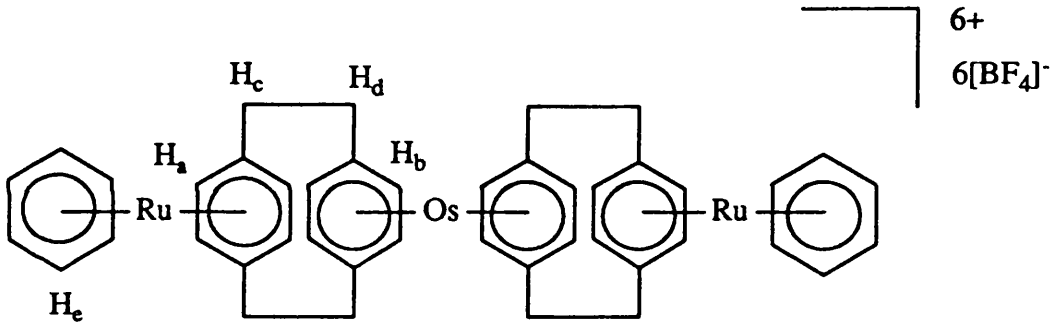

Cyclophane resonances δ, ppm:

H_a	6.75 (s,8H)
H_b	6.93 (s,8H)
H_c, H_d	3.49-3.62 (m,16H,AA'BB')

Other resonances δ, ppm:

H_e	6.93 (s,12H)

$^{13}C-\{^{1}H\}$ n.m.r. Data: Solvent: CD_3NO_2. Operating frequency: 100 MHz.

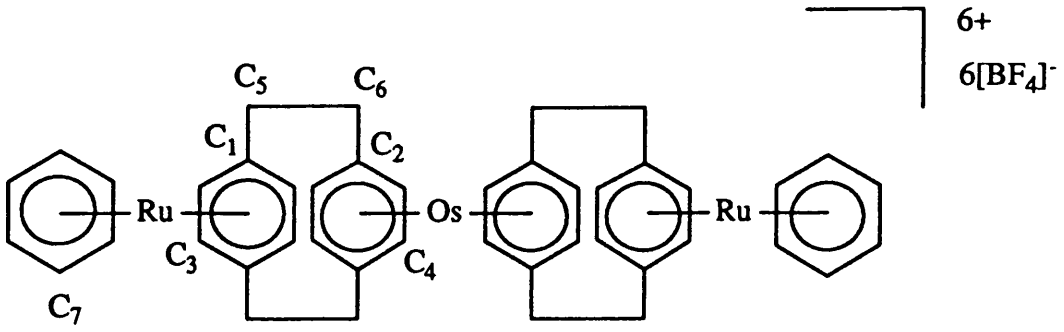

Cyclophane resonances δ, ppm:

C_1	135.8	C_4	82.4
C_2	134.4	C_5, C_6	33.1, 33.2
C_3	91.7		

Other resonances δ, ppm:

C_7	95.8

[(η^6-*p*-cymene)Ru(η^6,η^6-$C_{16}H_{16}$)Os(η^6,η^6-$C_{16}H_{16}$)Ru(η^6-*p*-cymene)][BF_4]$_6$ (65).

Silver tetrafluoroborate (0.11 g; 1.81 mmol) was added to a suspension of [Ru(η^6-*p*-cymene)Cl_2]$_2$ (0.08 g; 0.12 mmol) in acetone (5 cm^3). The mixture was stirred for 1 h., and filtered through celite to remove the precipitated silver chloride. The resulting clear orange solution was pumped to dryness. Trifluoroacetic acid (5 cm^3) and [Os(η^6-$C_{16}H_{16}$)$_2$][BF_4]$_2$ (0.06 g; 0.08 mmol) were then added, and the solution stirred for 60 h. at room temperature. After this time a tan coloured oil had formed, which was smeared around the bottom of the flask, in addition to a little yellow solid which was suspended in the solution. The solid and the solution were decanted from the oil. Diethyl ether (20 cm^3) was added to the solution, which precipitated a further crop of pale yellow solid. This solid was filtered off, washed with diethyl ether (10 cm^3), then air dried. The ^{1}H n.m.r. spectrum of this solid indicated that (65) was the major product, but that there were impurities present. The tan coloured oil was stirred with a fresh aliquot of trifluoroacetic acid (5 cm^3), in which it fully dissolved after 48 h. The addition of diethyl ether (30 cm^3) precipitated a second crop of the pale yellow solid, which was collected as before. This second solid was identified by its ^{1}H n.m.r. spectrum as a pure sample of (65). Yield of second crop of product: 0.09 g; 0.06 mmol; 72% (based on [Os(η^6-$C_{16}H_{16}$)$_2$][BF_4]$_2$).

Infrared spectrum: $[BF_4]^-$: 1054 (s, br); δ(CCC): 677 (m); ν$(CH)_{ar}$: 3066 (m) cm^{-1}.

^{1}H n.m.r. Data: Solvent: CD_3NO_2. Operating frequency: 400 MHz.

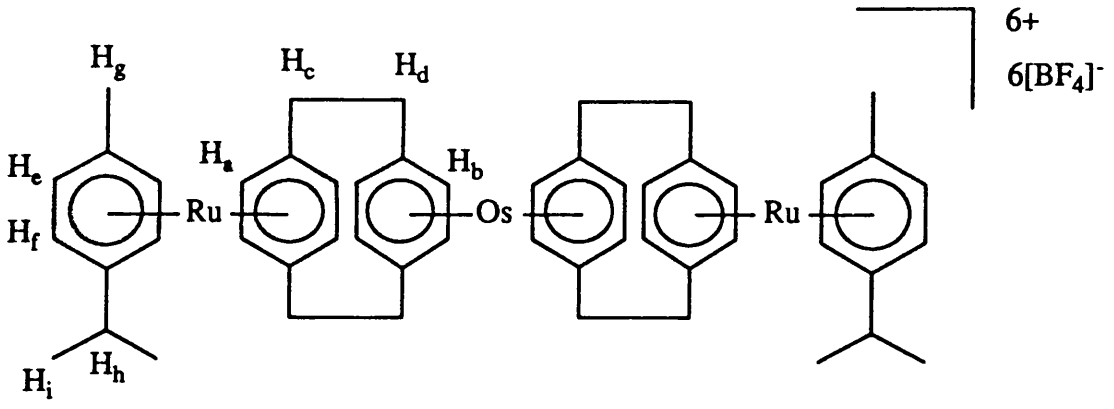

Cyclophane resonances δ, ppm:

H_a	6.73 (s,8H)	H_c, H_d	3.49-3.59 (m,16H,AA'BB')
H_b	6.91 (s,8H)		

Other resonances δ, ppm:

H_e, H_f	6.85 (m,8H,A_2B_2)
H_g	2.44 (s,6H)
H_h	2.90 (sept,2H,$^3J_{H-H}$=7Hz)
H_i	1.27 (d,12H,$^3J_{H-H}$=7Hz)

$^{13}C-\{^1H\}$ n.m.r. Data: Solvent: CD_3NO_2. Operating frequency: 100 MHz.

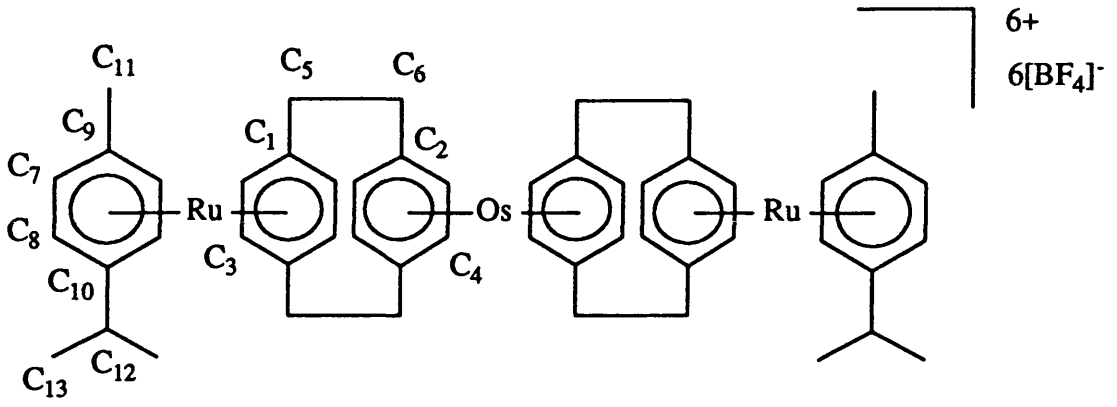

Cyclophane resonances δ, ppm:

C_1	135.5	C_4	82.4
C_2	133.0	C_5, C_6	32.7, 33.2
C_3	91.9		

Other resonances δ, ppm:

C_7	93.1	C_{11}	20.1
C_8	95.1	C_{12}	33.5
C_9	114.3	C_{13}	22.8
C_{10}	124.4		

Mass spectrum: m/e range: 400-1620 mass units.

m/e	Fragment
1515	$[(\eta^6\text{-}p\text{-cymene})Ru(\eta^6,\eta^6\text{-}C_{16}H_{16})Os(\eta^6,\eta^6\text{-}C_{16}H_{16})Ru(\eta^6\text{-}p\text{-cymene})][BF_4]_5^+$
1428	$[(\eta^6\text{-}p\text{-cymene})Ru(\eta^6,\eta^6\text{-}C_{16}H_{16})Os(\eta^6,\eta^6\text{-}C_{16}H_{16})Ru(\eta^6\text{-}p\text{-cymene})][BF_4]_4^+$
1341	$[(\eta^6\text{-}p\text{-cymene})Ru(\eta^6,\eta^6\text{-}C_{16}H_{16})Os(\eta^6,\eta^6\text{-}C_{16}H_{16})Ru(\eta^6\text{-}p\text{-cymene})][BF_4]_3^+$
1254	$[(\eta^6\text{-}p\text{-cymene})Ru(\eta^6,\eta^6\text{-}C_{16}H_{16})Os(\eta^6,\eta^6\text{-}C_{16}H_{16})Ru(\eta^6\text{-}p\text{-cymene})][BF_4]_2^+$
1167	$[(\eta^6\text{-}p\text{-cymene})Ru(\eta^6,\eta^6\text{-}C_{16}H_{16})Os(\eta^6,\eta^6\text{-}C_{16}H_{16})Ru(\eta^6\text{-}p\text{-cymene})][BF_4]^+$

1366 $[(\eta^6\text{-}p\text{-cymene})Ru(\eta^6,\eta^6\text{-}C_{16}H_{16})Os(\eta^6\text{-}C_{16}H_{16})][BF_4]_6^+$

1192 $[(\eta^6\text{-}p\text{-cymene})Ru(\eta^6,\eta^6\text{-}C_{16}H_{16})Os(\eta^6\text{-}C_{16}H_{16})][BF_4]_4^+$

1105 $[(\eta^6\text{-}p\text{-cymene})Ru(\eta^6,\eta^6\text{-}C_{16}H_{16})Os(\eta^6\text{-}C_{16}H_{16})][BF_4]_3^+$

1018 $[(\eta^6\text{-}p\text{-cymene})Ru(\eta^6,\eta^6\text{-}C_{16}H_{16})Os(\eta^6\text{-}C_{16}H_{16})][BF_4]_2^+$

931 $[(\eta^6\text{-}p\text{-cymene})Ru(\eta^6,\eta^6\text{-}C_{16}H_{16})Os(\eta^6\text{-}C_{16}H_{16})][BF_4]^+$

844 $[(\eta^6\text{-}p\text{-cymene})Ru(\eta^6,\eta^6\text{-}C_{16}H_{16})Os(\eta^6\text{-}C_{16}H_{16})]^+$

531 $[(\eta^6\text{-}p\text{-cymene})Ru(\eta^6\text{-}C_{16}H_{16})][BF_4]^+$

443 $[(\eta^6\text{-}p\text{-cymene})Ru(\eta^6\text{-}C_{16}H_{16})]^+$

[(η^6-C_6Me_6)Ru(η^6,η^6-$C_{16}H_{16}$)Os(η^6,η^6-$C_{16}H_{16}$)Ru(η^6-C_6Me_6)][BF_4]$_6$ (66).

Silver tetrafluoroborate (0.10 g; 0.49 mmol) was added to a suspension of [Ru(η^6-C_6Me_6)Cl_2]$_2$ (0.07 g; 0.11 mmol) in acetone (5 cm^3). The mixture was stirred at room temperature for 1 h., and filtered through celite to remove the precipitated silver chloride. The resultant clear orange solution was pumped to dryness, and trifluoroacetic acid (5 cm^3) and [Os(η^6-$C_{16}H_{16}$)$_2$][BF_4]$_2$ (0.06 g; 0.07 mmol) were added. The solution was stirred for 60 h. During this time the product had precipitated from solution as a pale yellow powder, which was filtered off, washed with diethyl ether (10 cm^3) and dried *in vacuo*. Yield: 0.07 g; 0.04 mmol; 57% (based on [Os(η^6-$C_{16}H_{16}$)$_2$][BF_4]$_2$).

Infrared spectrum: $[BF_4]^-$: 1057 (s, br); δ(CCC): 677 (m); ν$(CH)_{ar}$: 3063 (s).

^{1}H n.m.r. Data: Solvent: CD_3NO_2. Operating frequency: 400 MHz.

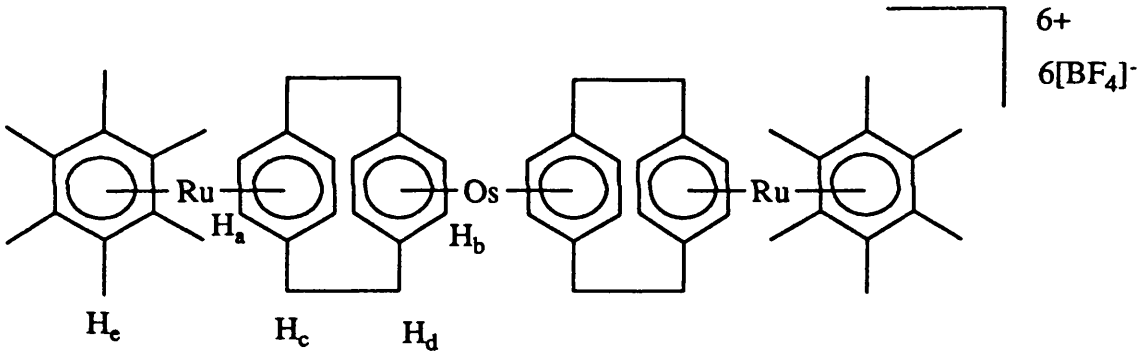

Cyclophane resonances δ, ppm:

H_a	6.43 (s,8H)
H_b	6.80 (s,8H)
H_c, H_d	3.44-3.51 (m,16H,AA'BB')

Other resonances δ, ppm:

H_e	2.51 (s,32H)

^{13}C-{^{1}H} n.m.r. Data: Solvent: CD_3NO_2. Operating frequency: 100 MHz.

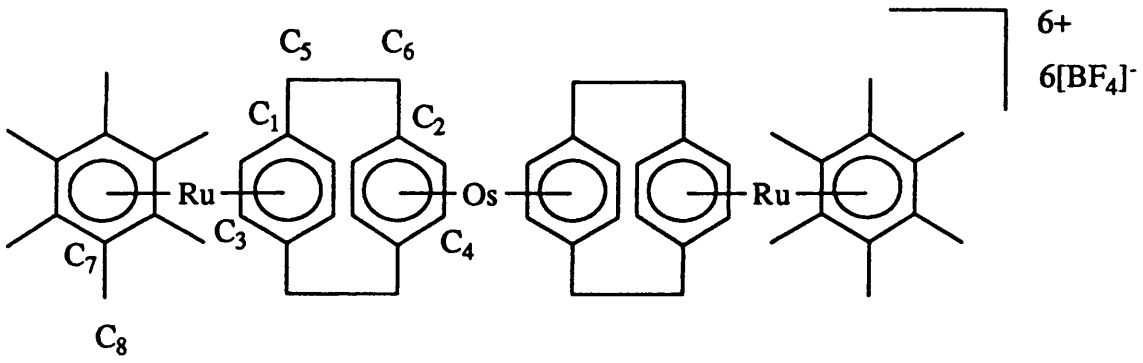

Cyclophane resonances δ, ppm:

C_1	135.4	C_4	82.4
C_2	130.5	C_5, C_6	31.4, 32.9
C_3	92.5		

Other resonances δ, ppm:

C_7	111.3
C_8	18.0

Mass spectrum: m/e range: 450-1700 mass units.

m/e	Fragment
1571	$[(\eta^6\text{-}C_6Me_6)Ru(\eta^6,\eta^6\text{-}C_{16}H_{16})Os(\eta^6,\eta^6\text{-}C_{16}H_{16})Ru(\eta^6\text{-}C_6Me_6)][BF_4]_5^+$
1484	$[(\eta^6\text{-}C_6Me_6)Ru(\eta^6,\eta^6\text{-}C_{16}H_{16})Os(\eta^6,\eta^6\text{-}C_{16}H_{16})Ru(\eta^6\text{-}C_6Me_6)][BF_4]_4^+$
1397	$[(\eta^6\text{-}C_6Me_6)Ru(\eta^6,\eta^6\text{-}C_{16}H_{16})Os(\eta^6,\eta^6\text{-}C_{16}H_{16})Ru(\eta^6\text{-}C_6Me_6)][BF_4]_3^+$
1310	$[(\eta^6\text{-}C_6Me_6)Ru(\eta^6,\eta^6\text{-}C_{16}H_{16})Os(\eta^6,\eta^6\text{-}C_{16}H_{16})Ru(\eta^6\text{-}C_6Me_6)][BF_4]_2^+$
1223	$[(\eta^6\text{-}C_6Me_6)Ru(\eta^6,\eta^6\text{-}C_{16}H_{16})Os(\eta^6,\eta^6\text{-}C_{16}H_{16})Ru(\eta^6\text{-}C_6Me_6)][BF_4]^+$
1046	$[(\eta^6\text{-}C_6Me_6)Ru(\eta^6,\eta^6\text{-}C_{16}H_{16})Os(\eta^6\text{-}C_{16}H_{16})][BF_4]_2^+$
959	$[(\eta^6\text{-}C_6Me_6)Ru(\eta^6,\eta^6\text{-}C_{16}H_{16})Os(\eta^6\text{-}C_{16}H_{16})][BF_4]^+$
782	$[(\eta^6\text{-}C_{16}H_{16})Os(\eta^6\text{-}C_{16}H_{16})][BF_4]_2^+$
559	$[(\eta^6\text{-}C_6Me_6)Ru(\eta^6,\eta^6\text{-}C_{16}H_{16})][BF_4]^+$
472	$[(\eta^6\text{-}C_6Me_6)Ru(\eta^6\text{-}C_{16}H_{16})]^+$

TABLE 5.1 Microanalytical Data for Extented Transition Metal-Cyclophane Compounds.

Compound.	%C		%H	
	calc.	found[a]	calc.	found[a]
(56)	39.6	37.8	3.7	3.5
(58)	40.9	36.3	4.0	3.8
(59)	43.3	43.2	4.6	4.6
(60)	33.5	31.8	2.8	2.7
(55)	36.3	38.7	3.4	3.7
(61)	37.6	36.8	3.7	3.8
(63)	33.6	34.6	2.8	2.8
(64)	35.6	32.1	3.0	2.8
(65)	39.6	34.7	3.8	3.6
(66)	40.7	34.5	4.1	4.0

a) Some samples stubbornly retain varying amounts of the trifluoroacetic acid solvent, resulting in the observed discrepancies. See text in Section 5.2.2.

CHAPTER 6

SOME STRUCTURAL AND SPECTROSCOPIC FEATURES OF THE METAL-COORDINATED [2.2]PARACYCLOPHANE LIGAND.

6.1 INTRODUCTION.

Chapter 1 reviewed the important properties of [2_2]paracyclophane and described several of its known transition metal compounds. Chapters 2-5 have described the preparation of many new compounds. These include the first Os(II)-[2_2]paracyclophane compounds. A wealth of new structural data has been obtained for the η^6-coordinated [2_2]paracyclophane ligand, together with spectroscopic data for the ligand coordinated to the metal ions Ru(II) and Os(II) via one or both external faces. Crystal structures of η^6-coordinated ligand on these metal ions are reported for the first time, while the understanding of the sometimes complex n.m.r. spectroscopic characteristics has been enhanced by some detailed experiments.

This chapter aims to draw together some of the important new structural and spectroscopic data. It discusses the factors which affect the observed geometry of the ligand in the solid state, and govern the extremely variable appearance of the ^1H and ^{13}C resonances in the solution n.m.r. spectra.

6.2 RESULTS AND DISCUSSION.

6.2.1 Factors Affecting the Structural Geometry of [2_2]Paracyclophane when Coordinated to Ru(II) or Os(II).

The reported[24] crystal structure of [Cr(η^6-$C_{16}H_{16}$)$(CO)_3$] (4) indicated that a number of geometrical changes result when a transition metal atom coordinates to one external face of the [2_2]paracyclophane ligand. The most noteworthy features when compared with the structure[7] of the ligand itself are:

(i) a significant decrease in the interdeck separation,

(ii) a flattening of the aromatic rings, the coordinated ring more so than the non-coordinated one,

(iii) a relaxation of the distortion from ideal geometries for the sp^2 and sp^3 hybridised carbon atoms of the ligand skeleton.

The current study has determined the structure of the η^6-coordinated ligand in a variety of chemical environments. Structures have been determined with complexes having a range of charges per metal ion: 0, ½+, 1+ and 2+. In some molecules the cyclophane ligand lies *trans* to an unsymmetrical coordination environment, e.g. two chloride ions and a Lewis base, while in others the environment is more

symmetrical, e.g. three alkoxide ions or an η^6-coordinated arene. This section aims to discuss how these factors influence the geometry of the [2_2]paracyclophane ligand. Tables 6.1, 6.2, and 6.3 present the important structural parameters.

The data presented in Tables 6.1, 6.2, and 6.3 provides no evidence that the net charge on the metal centre has any significant effect on the cyclophane geometry. The nature and spatial arrangement of the ligands *trans* to the cyclophane has important implications however.

When the *trans* coordination sites are occupied by either two chloride ions and a Lewis base, or one chloride ion and two Lewis bases, two geometrical changes result. Firstly, the M-C bonds *trans* to the M-N or M-P bonds are lengthened. This feature is observed for compounds (18), (20), and (25) and is also reported for [Ru(η^6-C_6H_6)Cl_2($PMePh_2$)] and [Ru(η^6-*p*-cymene)Cl_2($PMePh_2$)][86]. The second change is in the torsion angles of the ethylenic bridging functions. The largest angles are observed for those compounds with an unsymmetrical arrangement of *trans* ligands in which there is a large variation in M-C distances. In these compounds the coordinated aromatic deck is not only distorted into a boat shape by the intrinsic strain of the cyclophane geometry, but additionally distorted by the influence of the Lewis base in the *trans* coordination site. This unsymmetrical puckering of the coordinated ring causes an additional twist of one cyclophane deck with respect to the other.

Compounds (37), (39), (17), (48), and the previously reported[24] Chromium(0) compound (4) all have symmetrically occupied *trans* coordination sites. These compounds exhibit little variation in M-C bond lengths, other than that due to the natural boat shape of the cyclophane, and small ethylenic bridge torsion angles.

The inter-ring separations of the Ru(II) and Os(II) compounds show little variation. The distance, *ca.* 2.99 Å, is consistently 0.10 Å shorter than that observed for the uncoordinated cyclophane[7], 3.09 Å. The value of 3.02 Å, observed for (4) is greater than any that have been determined in the current study. This is due to Cr(0) having poorer electron withdrawing properties compared with Ru(II) or Os(II). This difference also accounts for the rather longer M-C bonds in (4) when compared with the Group VIII compounds.

The M-Ar distance, i.e. the distance from the metal to the centroid of the non-bridgehead carbon atoms of the coordinated cyclophane deck, is *ca.* 1.66 Å for each of the compounds other than (17) and (48). In that pair of compounds the two aromatic ligands sandwich the metal ion. In these compounds the M-Ar distance is rather longer at 1.71 Å. This may be caused by electronic repulsions between the two coordinated aromatic rings.

We have already mentioned that coordination of a transition metal ion to the cyclophane ligand results in a withdrawal of electron density from the cyclophane π-electron system, and hence decreases the electronic repulsion between the two rings. Table 6.2 presents angular data which show how the strain is accommodated in different parts of the cyclophane skeleton. Angles α and γ provide a measure of the distortion of the coordinated and non-coordinated rings respectively, into a boat conformation, while β and δ give the distortion from planarity of the ring-bridge linkages to the coordinated and non-coordinated rings respectively.

The way in which the decrease in inter-deck separation is manifested in terms of angular changes is rather surprising. The general trend in these changes is consistent for all of the compounds studied, including that reported[24] for (4), although the magnitude of the effect varies somewhat. When compared with the angle in the uncoordinated ligand, β decreases markedly from 11° to *ca.* 5-9° in all complexes. The angle φ relaxes completely to its ideal value of *ca.* 109.5°. The remaining angle associated with the coordinated deck, α, shows no significant change. Thus the angles associated with the linkages to the coordinated cyclophane deck relax towards to their ideal values, while the coordinated benzene ring is just as boat shaped when metal-coordinated as in the free state. Of the angles associated with the non-coordinated deck only γ shows any real variation, a small decrease, indicating that the non-coordinated deck adopts a slightly shallower boat conformation.

The data presented in Table 6.3 shows that the bond lengths of the interdeck connectivity remain almost identical for all of the compounds studied. The CH_2-CH_2 bond (C, Table 6.3) lengthens slightly, but the lengths from the rings to the bridges (A and B) are essentially the same as in the free ligand. Thus the decrease in the inter-ring separation when the ligand coordinates, is brought about almost exclusively by changes in the angles β and φ.

6.2.2 Factors Affecting the ^1H and ^{13}C-{^1H} n.m.r. Spectra of Ru(II)- and Os(II)-[2_2]paracyclophane Compounds

The general features of the ^1H and ^{13}C-{^1H} n.m.r. spectra of [2_2]paracyclophane and some of its transition metal compounds have been documented previously and were discussed in the introductory chapter {Section 1.3.2 for [M(η^6-$C_{16}H_{16}$)$(CO)_3$] (M=Cr,Mo,W) and Section 1.3.7 for [2_2]paracyclophane-ruthenium compounds}. In the present study [2_2]paracyclophane is found in a far wider range of chemical environments

than was previously the case. This allows an investigation into more of the factors which influence the appearance of these spectra. It is the aim of this section to identify and comment upon these factors.

(i) ^{1}H n.m.r. Spectra.

Let us first recall the simplicity of the spectrum of the free cyclophane ligand. It comprises two singlet resonances, one at δ 3.05 due to the aliphatic protons, the other at 6.47 ppm due to the aromatic protons[66]. The effect of coordinating a transition metal to one face, or both faces of the cyclophane shall be dealt with in turn.

In the simplest cases, when a transition metal coordinates to one face of the [2$_2$]paracyclophane ligand in an η^6-fashion, the degeneracy of the resonances observed for the pure ligand is split. Two resonances are observed in the aromatic region, one for the protons of each ring, while two six-line multiplet resonances forming an AA'XX' coupling pattern are observed for the -CH_2CH_2- protons of the bridging functions. A number of factors influence the chemical shifts of these resonances and are discussed below:

The first section quantifies the influence of the metal ion. Subsequent sections deal with only ruthenium compounds. Comparisons are made between spectra recorded in the same solvent whenever possible. Table 6.4 presents the important data.

1. The influence of the metal ion.

When the spectra of analogous pairs of Ru and Os compounds are compared, (19) and (21), or (20) and (22) for example, the chemical shifts for the Os compounds appear to higher frequency by *ca.* 0.4 and *ca.* 0.06 ppm for the aromatic protons of the coordinated and non-coordinated rings respectively. The chemical shifts of the multiplets arising from the aliphatic protons are essentially unchanged. This latter observation is probably due to the fact that the methylenic protons are too distant from the metal to be influenced directly by its magnetic anisotropy.

2. The influence of the counter-ion.

When the spectra of $[PF_6]^-$ and $[BPh_4]^-$ salts of a given cation are compared, (25) and (26), or (28) and (29), for example, the resonances of the coordinated and non-coordinated ring protons of the $[BPh_4]^-$ salts appear *ca.* 0.3 and *ca.* 0.1 ppm respectively, to lower frequency. The multiplet resonance due to the methylenic protons

closer to the metal ion appears *ca.* 0.1 ppm to lower frequency in the $[BPh_4]^-$ salts. The counter-ion has a dramatic influence on the appearance of the aromatic resonances in the chiral compounds (34) and (35). In the $[PF_6]^-$ salt, both resonances appear with an A_2B_2 coupling pattern, whereas for the $[BPh_4]^-$ salt, the resonance due to the protons of the non-coordinated ring appears as a singlet, while that of the coordinated ring appears with an A_2B_2 coupling pattern.

3. The influence of *trans* ligands.

By far the largest influence on the chemical shifts is the type of *trans* ligand. The two aromatic resonances may appear at high frequencies, *ca.* δ 7.05 and 6.25 ppm, with a separation of 0.75 ppm, or at much lower frequencies, *ca.* δ 6.55 and 4.45 ppm, with separations as large as 2.10 ppm. The two chemical shifts of the aliphatic signals show an equally large variation. This ranges from δ 3.20 and 3.45 ppm, with a separation of 0.25 ppm, to δ 2.85 and 1.60 ppm, with a separation of 1.25 ppm. The compounds spilt into three groups, arene-cyclophane compounds, triply-bridged dinuclear compounds, and compounds containing Lewis bases, which can be discussed separately.

The arene-cyclophane compounds exhibit aromatic resonances at *ca.* δ 6.9-7.0 and 5.9-6.3 ppm, while the aliphatic protons resonate at chemical shifts in the range δ 3.05-3.45 ppm with small separations of *ca.* 0.3 ppm. The *trans* arene ligands cause these resonances to appear to lower frequency in the order benzene (11), *p*-cymene (48), hexamethylbenzene (50), [2$_2$]paracyclophane (13). The aromatic resonances of the arene-cyclophane compounds generally appear to higher frequency than those observed for the other classes of compounds.

For compounds containing Lewis bases, the chemical shift of the non-coordinated ring protons was generally invariant at *ca.* δ 6.75 ppm. That for the coordinated ring protons appearing to lower frequency for the compounds containing tertiary phosphines {(18), (19), (27), (28), (29)} than those containing heterocyclic nitrogen donor ligands {(20), (25), (26), (32)}. The phosphine ligands also cause the largest chemical shift differences for the aliphatic resonances, with the splitting being significantly greater when two tertiary phosphine ligands are coordinated rather than one. Compound (27) exhibited the largest such chemical shift difference.

The triply akloxide- (37) or chloro-bridged (44) compounds exhibit aromatic resonances at rather lower frequencies than the other types of compounds mentioned above (*ca.* δ 6.6 and 4.4-4.7 ppm), while the separation between the aliphatic resonances is *ca.* 0.5 ppm.

4. The influence of the nett charge on the molecule.

The effect of the nett charge on the molecule is difficult to determine directly from the compounds in this study but is probably fairly small in comparison with other influences, i.e. counter-ion or type of *trans* ligand. Previous studies[87,89,108,136] on the compounds $[M(\eta^6\text{-}C_6H_6)Cl_2(S)]$ and $[M(\eta^6\text{-}C_6H_6)Cl(S)_2]^+$ (M=Ru,Os; S=dimethyl sulphoxide, water) have shown that the charge difference causes a change of *ca.* 0.1 ppm in the chemical shift of the benzene protons, with the resonance in the spectrum of the cation appearing at the lower frequency.

When the $[2_2]$paracyclophane ligand is metal-coordinated at both external faces the two decks are in much more similar chemical environments than in the compounds where only one face is coordinated. The relevant data are presented in Table 6.5.

The spectra of the doubly metallated cyclophane compounds are different from those of the singly metallated ones in a number of respects. The cyclophane aromatic resonances appear with smaller chemical shift separations, or as singlets if the cyclophane is symmetrically coordinated. The resonances due to the aliphatic protons appear at a higher frequency than any observed for the η^6-coordinated compounds, and exhibit singlet resonances when symmetrically coordinated, or complex multiplet resonances with a second order AA'BB' coupling pattern when the cyclophane is unsymmetrically coordinated.

Two factors cause a variation in the chemical shifts of the aromatic resonances, firstly the identity of the coordinated metal ion, and secondly the *trans* arene ligand. Osmium(II) causes the chemical shifts for coordinated arene protons to appear to high frequency of those observed for ruthenium(II). The difference is *ca.* 0.2 ppm. As mentioned above, the *trans* arene causes the chemical shifts of the coordinated cyclophane ring to appear to lower frequency in the order: benzene, *p*-cymene, C_6Me_6, $[2_2]$paracyclophane (e.g. the trend in the chemical shift of H_a in compounds (60), (55), (61) and (62), Table 6.5).

(ii) $^{13}C\text{-}\{^1H\}$ n.m.r. Spectra.

The $^{13}C\text{-}\{^1H\}$ n.m.r. data are presented in Tables 2.2, 2.5, 6.6, and 6.7. Figure 6.1 gives the carbon atom numbering scheme adopted.

A comparison of the spectra of analogous pairs of ruthenium and osmium compounds, e.g. (1) and (16), or (11) and (17), indicates that only the chemical shifts of the carbon atoms directly coordinated to the metal ions show any significant variation

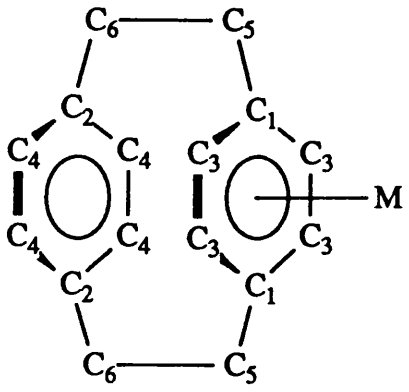

Fig. 6.1 The cyclophane carbon atom numbering scheme for ^{13}C-{^1H} n.m.r. resonances.

when the metal ion is changed. For the osmium compounds the chemical shift of C_1 appears *ca.* 2.0 ppm to lower frequency of that observed when the metal is ruthenium, while for C_3 the chemical shift difference is *ca.* 7 ppm.

The chemical shift range for C_1 among all of the compounds studied is *ca.* 115 to 135 ppm. For the compounds with coordinated Lewis bases, (19), (20), and (31), or chloride bridges, (1), (16), and (45), the value lies at the lower end of this range, 115-122 ppm, while the arene-M-cyclophane compounds have values in the range 130-135 ppm. The chemical shifts for C_3 lie in the range 72-91 ppm, and exhibit a similar pattern.

As was observed in the ^1H n.m.r. spectra, *trans* arene ligands cause a systematic variation in the chemical shifts of the metal-coordinated cyclophane carbon atoms. For the η^6-coordinated cyclophane ligands in compounds (11), (48), and (50) the trend is for the chemical shift of C_3 to appear to higher frequency in the order: benzene, *p*-cymene, C_6Me_6. However, the signal from C_1 appears at a significantly lower frequency for (50) than in (11) or (48). For the doubly metallated cyclophane ligands the same trend is observed in compounds (56), (58), and (59), in (60), (55) and (61), and in (64), (65), and (66) (Table 6.7). i.e. for the non-bridgehead carbon atoms there is a systematic shift to higher frequency, while for the bridgehead carbon atoms there is a larger shift to lower frequency.

For the singly metallated cyclophane ligands the resonances of the carbon atoms of the non-coordinated ring (C_2 and C_4) exhibit little variation in chemical shift. Chemical shifts for C_2 lie in the range 138-141 ppm, while those for C_4 lie in the range 132-136 ppm. These are very similar values to those observed for the free cyclophane, C_2: 139.1 ppm, C_4: 132.8 ppm. This reinforces the conclusion drawn from the structural data discussed above, that the geometry of the non-coordinated deck is little influenced by a

metal coordinated to the opposite face.

The carbon atoms of the bridging functions give rise to two resonances in the range 31-35 ppm. In general terms the chemical shift difference reflects the degree of asymmetry in the chemical environments of the two faces of the cyclophane ligand. The chemical shift separation is typically *ca.* 2 ppm for the singly metallated cyclophane ligands. However, for the doubly metallated cyclophane compounds, there are two important factors. The first is the identity of the metal ions. Compound (60) is symmetrical in all respects other than the metal ions. In this compound the signals due to the carbon atom bridging functions appear with a separation of 0.3 ppm. The bis-ruthenium(II) compounds (56), (58), and (59), allow the effect of different *trans* arene ligands to be determined. This influence is rather greater since when the two arene ligands are very different, e.g. C_6H_6 and C_6Me_6, a chemical shift separation of 1.3 ppm is observed.

From the discussion above, the following factors are seen to be dominant for the ^1H n.m.r. spectra. Fundamental differences occur depending on whether the cyclophane is singly or doubly metallated. For the singly metallated compounds, the chief influence on the chemical shifts is the type of *trans* ligand, with the metal ion and counter ion type having a rather smaller effect. For the doubly metallated cyclophane compounds the spectra reflect the greater symmetry of the chemical environments of the cyclophane ligands. The cyclophane chemical shifts show less variation than in the singly metallated examples, with the type of metal ion having a fairly small effect, and that of the type of *trans* arene ligand a rather larger one. The appearance of the $-CH_2CH_2-$ resonances varies substantially however, from a singlet in the symmetrically coordinated compounds, to complex and highly variable multiplet patterns with substantial second order character when the cyclophane is unsymmetrically coordinated.

In the ^{13}C n.m.r. spectra, only the resonances of the metallated carbon atoms show any substantial variation in chemical shift. The *trans* ligands again have a greater influence on the chemical shifts than the type of metal ion. This is true for both singly and doubly metallated compounds.

TABLE 6.1 Structural Data for [2$_2$]Paracyclophane Compounds.

Compound.		M-C (bridgehead) (Å) {*trans* ligand}	M-C (non-bridgehead) (Å) {*trans* ligand}	Inter-ring separation (Å)	M-Ar (Å)	Torsion (°) -CH_2CH_2-
[Ru(η^6-$C_{16}H_{16}$)Cl_2(PPh_3)]	(18)	2.38(1) {P}	2.28(1) {P}	2.99	1.69	10.5
		2.30(1) {Cl}	2.16(1) {Cl}			
[Ru(η^6-$C_{16}H_{16}$)Cl_2(py)]	(20)	2.35(2) {N}	2.21(2) {N}	2.99	1.66	12.2
		2.29(2) {Cl}	2.15(2) {Cl}			
[Ru(η^6-$C_{16}H_{16}$)Cl(py)$_2$][PF_6]	(25)	2.36(2) {N}	2.20(2) {N}	3.01	1.67	7.5
		2.30(2) {Cl}	2.17(2) {Cl}			
[Ru(η^6-$C_{16}H_{16}$)Cl(phen)][PF_6]	(31)	2.33(1)[a] {N,Cl}	2.18(1)[a] {N,Cl}	2.97	1.68	4.5
[Ru$_2$(η^6-$C_{16}H_{16}$)$_2$($OMe)_3$][BPh_4]	(37)	2.29(1) {O}	2.16(1) {O}	3.00	1.64	2.1
[Ru$_2$(η^6-$C_{16}H_{16}$)$_2$($OEt)_3$][PF_6]	(39)	2.30(1) {O}	2.19(1) {O}	2.99	1.65	2.9
[Os(η^6-C_6H_6)(η^6-$C_{16}H_{16}$)][BF_4]$_2$	(17)	2.37(2) {C}	2.20(2) {C}	2.99	1.71	0.0[b]
[Ru(η^6-*p*-cymene)(η^6-$C_{16}H_{16}$)][BPh_4]$_2$	(48)	2.35(1) {C}	2.19(1) {C}	2.99	1.71	2.5
[Cr(η^6-$C_{16}H_{16}$)$(CO)_3$]	(4)	2.34(1) {CO}	2.21(1) {CO}	3.02	-	3.8
[2$_2$](1,4)$C_{16}H_{16}$	(3)	-	-	3.09	-	3.2[c]

a) No significant variation between Ru-C bond lengths *trans* to N or Cl.

b) 0.0° torsion angle imposed by crystal symmetry.

c) This angle was determined by an analysis of anisotropic thermal parameters[7].

TABLE 6.2 Structural Data for [2$_2$]Paracyclophane Compounds.

Compound.		Cyclophane angular deformations (°). α	β	γ	δ	φ	ψ
[Ru(η^6-$C_{16}H_{16}$)Cl_2(PPh_3)]	(18)		7.0		10.6	109.2(5)	112.6(5)
[Ru(η^6-$C_{16}H_{16}$)Cl_2(py)]	(20)	13.6	8.0	10.7	13.9	109(2)	114(2)
[Ru(η^6-$C_{16}H_{16}$)Cl(py)$_2$][PF_6]	(25)	13.9	5.1	12.7	11.6	107(2)	115(2)
[Ru(η^6-$C_{16}H_{16}$)Cl(phen)][PF_6]	(31)	13.1	7.1	11.2	12.2	108.5(8)	114.5(8)
[Ru_2(η^6-$C_{16}H_{16}$)$_2$(OMe)$_3$][BPh_4]	(37)	14.0	6.4	11.4	11.6	109.7(10)	113.3(9)
[Ru_2(η^6-$C_{16}H_{16}$)$_2$(OEt)$_3$][PF_6]	(39)	12.1	8.0	11.2	11.4	109.4(8)	113.2(8)
[Os(η^6-C_6H_6)(η^6-$C_{16}H_{16}$)][BF_4]$_2$	(17)	12.3	9.8	9.6	15.2	110(2)	117(2)
[Ru(η^6-*p*-cymene)(η^6-$C_{16}H_{16}$)][BPh_4]$_2$	(48)					108.7(8)	113.7(8)
[Cr(η^6-$C_{16}H_{16}$)(CO)$_3$]	(4)	12.2	8.9	11.4	11.2	110.9(1)	112.8(3)
[2$_2$](1,4)$C_{16}H_{16}$	(3)	12.6	11.2	12.6	11.2	113.7	113.7

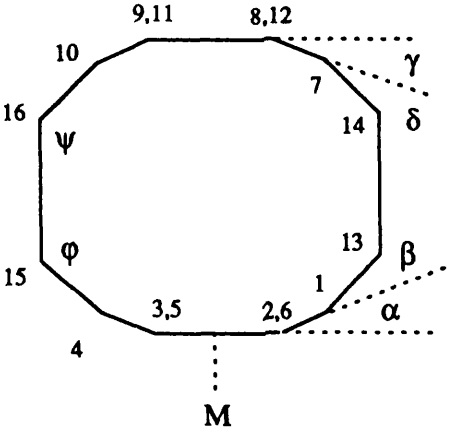

TABLE 6.3 Cyclophane Bridge Bondlengths, (Å).

Compound.	A	B	C
(3)[7]	1.51	1.51	1.57
(4)[24]	1.51(1)	1.52(1)	1.60(4)
(18)	1.51(1)	1.51(1)	1.59(1)
(20)	1.51(3)	1.51(3)	1.58(3)
(25)	1.55(3)	1.52(3)	1.60(3)
(31)	1.49(1)	1.50(2)	1.57(1)
(37)	1.49(2)	1.52(2)	1.58(2)
(39)	1.51(1)	1.52(2)	1.60(1)
(48)	1.49(3)	1.54(3)	1.58(4)
(49)	1.50(1)	1.50(2)	1.59(2)
(17)	1.47(3)	1.49(3)	1.52(3)

Values are averaged over all similar bond lengths in each structure, and generally do not vary by more than +/- 0.03 Å from the quoted figure.

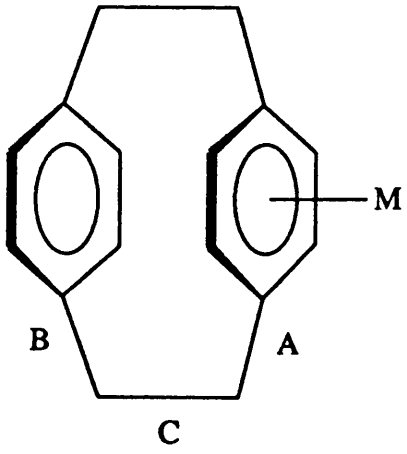

TABLE 6.4 ^{1}H n.m.r. Data for Ru(II) and Os(II)-η^6-[2$_2$]Paracyclophane Compounds

Compound	Solvent	Non-coord. C_6H_4 [a]	Coord. C_6H_4 [a]	$-CH_2CH_2-$ [b] δ, ppm.
(18)	$CDCl_3$	6.69	4.70	3.01, 2.31
(19)	$CDCl_3$	6.68	4.52	3.03, 2.38
(20)	$CDCl_3$	6.77	4.90	3.18, 2.76
(21)	$CDCl_3$	6.75	4.88	3.05, 2.36
(22)	$CDCl_3$	6.81	5.43	3.18, 2.70
(25)	CD_2Cl_2	6.88	5.15	3.26, 2.79
(26)	CD_2Cl_2	6.80	4.81	3.22, 2.67
(27)	$CDCl_3$	6.82	5.18	2.86, 1.60
(28)	$CDCl_3$	6.78	4.95	2.98, 2.00
(29)	CD_2Cl_2	6.71	4.67	3.01, 2.06
(32)	CD_2Cl_2	6.82	4.92	3.26, 2.86
(34)	$CDCl_3$	6.81 (A_2B_2)	5.03 (A_2B_2)	3.09, 2.38
(35)	$CDCl_3$	6.65	4.56 (A_2B_2)	3.00 (4H), 2.28/2.12 (2H+2H)
(37)	CD_2Cl_2	6.57	4.44	3.04, 2.58
(44)	CD_2Cl_2	6.63	4.74	3.12, 2.61
(11)	CD_3NO_2	7.04	6.25	3.46, 3.22
(48)	CD_3NO_2	7.02	6.22	3.46, 3.20
(50)	CD_3NO_2	6.95	5.91	3.41, 3.12
(13)	CD_3NO_2	6.94	5.90	3.35, 3.04

a) Singlet 4H, unless otherwise stated.

b) Six-line multiplet resonances with AA'XX' coupling pattern, unless otherwise stated.

TABLE 6.5 ^{1}H n.m.r. Data for Compounds Containing η^6,η^6- Coordinated [2$_2$]Paracyclophane Ligands.

Compound.	^{1}H n.m.r. Data. δ, ppm. CD_3NO_2, 298 K, 400 MHz.		
	H_a	H_b	H_c,H_d
(56) Ru,Ru	6.71 / 6.72[a,b,e]		3.64 (s)
(58) Ru,Ru	6.62[a,e]	6.42[c,e]	3.52-3.61 (m, AA'BB')
(59) Ru,Ru	6.60[b,e]	6.41[c,e]	3.55 (s)
(60) Ru,Os	6.82[a,e]	7.02[a,f]	3.57-3.67 (m, AA'BB')
(55) Ru,Os	6.78[b,e]	6.99[a,f]	3.58-3.65 (m, AA'BB')
(61) Ru,Os	6.50[c,e]	6.90[a,f]	3.51-3.61 (m, AA'BB')
(62) Ru,Os	6.46[d,e]	6.99[a,f]	3.50 (s)
(63) Os,Ru,Os	6.68[e]	6.95[f]	3.51-3.61 (m, AA'BB')
(64) Ru,Os,Ru	6.75[e]	6.93[f]	3.49-3.62 (m, AA'BB')
(65) Ru,Os,Ru	6.73[e]	6.91[f]	3.49-3.59 (m, AA'BB')
(66) Ru,Os,Ru	6.43[e]	6.80[f]	3.44-3.51 (m, AA'BB')

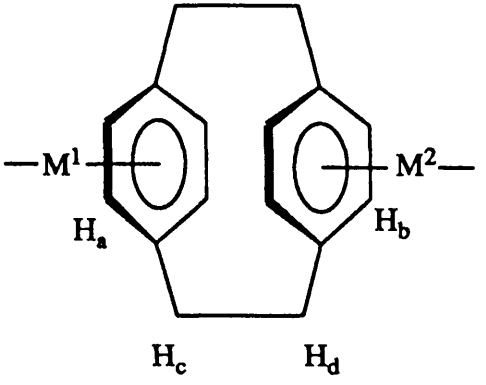

trans to: a) η^6-C_6H_6

b) η^6-*p*-cymene

c) η^6-C_6Me_6

d) η^6-$C_{16}H_{16}$

e) Ru

f) Os

TABLE 6.6 ^{13}C-{^{1}H} n.m.r. Data for η^6-Coordinated Cyclophane Compounds.

Compound.	Solvent.	C1	C2	C3	C4	C5	C6
(19)	$CDCl_3$	121.0	139.3	84.6	132.9	31.8	33.6
(20)	CD_2Cl_2	115.5	139.9	79.6	133.6	31.9	33.7
(26)	CD_2Cl_2	a	139.5	81.9	133.8	32.0	33.7
(30)	CD_2Cl_2	a	139.7	73.1	133.7	32.1	33.8
(31)	CD_3NO_2	120.7	141.4	84.0	135.0	32.8	34.5
(37)	CD_2Cl_2	a	138.9	72.8	132.9	31.7	33.4
(45)	CD_3NO_2	115.7	141.0	74.3	134.9	32.3	34.1

a) Not observed, or unambiguous assignment not possible.

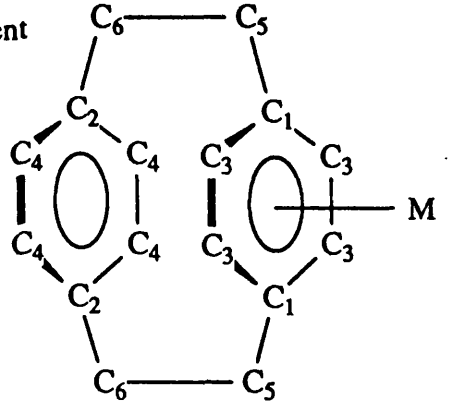

TABLE 6.7 ^{13}C-{^{1}H} n.m.r. Data for Compounds Containing η^6,η^6- Coordinated [2_2]Paracyclophane Ligands.

Compound.	^{13}C-{^{1}H} n.m.r. Data. δ, ppm. CD_3NO_2, 298 K, 100 MHz.				
	C_1	C_2	C_3	C_4	C_5,C_6
(56) Ru,Ru	133.6[b,e]	134.7[a,e]	91.8[b,e]	92.0[a,e]	33.3, 33.0
(58) Ru,Ru	131.0[c,e]	134.6[a,e]	91.8[c,e]	92.6[a,e]	33.0, 31.7
(59) Ru,Ru	130.9[c,e]	133.4[b,e]	91.9[c,e]	92.6[b,e]	32.7, 31.7
(60) Ru,Os	135.0[a,]	132.0[a,f]	91.7[a,e]	84.1[a,f]	33.4, 33.1
(55) Ru,Os	133.7[b,e]	131.2[a,f]	92.0[b,e]	84.2[a,f]	33.3, 32.7
(61) Ru,Os	131.7[c,e]	131.1[a,f]	92.6[c,e]	84.2[a,f]	33.0, 31.4
(62) Ru,Os	136.5[d,e]	131.7[a,f]	89.0/88.3[d,e]	84.0[a,f]	33.3, 33.2
(63) Os,Ru,Os	136.6[e]	131.5[a,f]	90.2[e]	84.0[a,f]	33.3, 32.9
(64) Ru,Os,Ru	134.4[a,e]	135.8[f]	91.7[a,e]	82.4[f]	33.2, 33.1
(65) Ru,Os,Ru	133.0[b,e]	135.5[f]	91.9[b,e]	82.4[f]	33.2, 32.7
(66) Ru,Os,Ru	130.5[c,e]	135.4[f]	92.5[c,e]	82.4[f]	32.9, 31.4

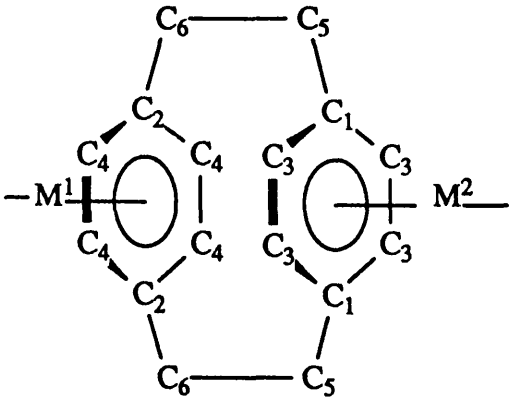

trans to: a) η^6-C_6H_6

b) η^6-*p*-cymene

c) η^6-C_6Me_6

d) η^6-$C_{16}H_{16}$

e) Ru

f) Os

APPENDIX I.

List of Compound Numbers.

1. $[Ru(\eta^6\text{-}C_{16}H_{16})Cl_2]_2$
2. $[Ru(\eta^6\text{-}C_{16}H_{16})(acetone)_3][BF_4]_2$
3. $[2_2](1,4)C_{16}H_{16}$
4. $[Cr(\eta^6\text{-}C_{16}H_{16})(CO)_3]$
5. $[Cr(C_6H_6)(CO)_3]$
6. $[Fe(\eta^5\text{-}C_5H_5)(\eta^6\text{-}C_{16}H_{16})][PF_6]$
7. $[(\eta^5\text{-}C_5H_5)Fe(\eta^6,\eta^6\text{-}C_{16}H_{16})Fe(\eta^6\text{-}C_5H_5)][PF_6]_2$
8. $[Fe(\eta^5\text{-}C_5H_5)(\eta^6\text{-}p\text{-xylene})]^+$
9. $[Ru(\eta^5\text{-}C_5H_5)(CH_3CN)_3][PF_6]$
10. $[Ru(\eta^5\text{-}C_5H_5)(\eta^6\text{-}C_{16}H_{16})][PF_6]$
11. $[Ru(\eta^6\text{-}C_6H_6)(\eta^6\text{-}C_{16}H_{16})][BF_4]_2$
12. $[Ru(\eta^4\text{-}C_6H_8)(\eta^6\text{-}C_{16}H_{16})]$
13. $[Ru(\eta^6\text{-}C_{16}H_{16})_2][BF_4]_2$
14. $[(\eta^6\text{-}C_6Me_6)Ru(\eta^6,\eta^6\text{-}C_{16}H_{16})Ru(\eta^6,\eta^6\text{-}C_{16}H_{16})Ru(\eta^6\text{-}C_6Me_6)][BF_4]_6$
15. $[(\eta^6\text{-}C_{16}H_{16})Ru(\eta^6,\eta^6\text{-}C_{16}H_{16})Ru(\eta^6\text{-}C_{16}H_{16})][BF_4]_4$
16. $[Os(\eta^6\text{-}C_{16}H_{16})Cl_2]_2$
17. $[Os(\eta^6\text{-}C_6H_6)(\eta^6\text{-}C_{16}H_{16})][BF_4]_2$
18. $[Ru(\eta^6\text{-}C_{16}H_{16})Cl_2(PPh_3)]$
19. $[Ru(\eta^6\text{-}C_{16}H_{16})Cl_2(PMe_2Ph)]$
20. $[Ru(\eta^6\text{-}C_{16}H_{16})Cl_2(NC_5H_5)]$
21. $[Os(\eta^6\text{-}C_{16}H_{16})Cl_2(PMe_2Ph)]$
22. $[Os(\eta^6\text{-}C_{16}H_{16})Cl_2(NC_5H_5)]$
23. $[Ru(\eta^6\text{-}C_{16}H_{16})Cl_2(1,4\text{-}N_2C_4H_4)]$
24. $[\{Ru(\eta^6\text{-}C_{16}H_{16})Cl_2\}(1,4\text{-}N_2C_4H_4)]$
25. $[Ru(\eta^6\text{-}C_{16}H_{16})Cl(NC_5H_5)_2][PF_6]$
26. $[Ru(\eta^6\text{-}C_{16}H_{16})Cl(NC_5H_5)_2][BPh_4]$
27. $[Ru(\eta^6\text{-}C_{16}H_{16})Cl(PPh_3)_2][PF_6]$
28. $[Ru(\eta^6\text{-}C_{16}H_{16})Cl(PMe_2Ph)_2][PF_6]$
29. $[Ru(\eta^6\text{-}C_{16}H_{16})Cl(PMe_2Ph)_2][BPh_4]$
30. $[Os(\eta^6\text{-}C_{16}H_{16})Cl(NC_5H_5)_2][BPh_4]$
31. $[Ru(\eta^6\text{-}C_{16}H_{16})Cl(1,10\text{-phen})][PF_6]$
32. $[Ru(\eta^6\text{-}C_{16}H_{16})Cl(2,2'\text{-bipy})][BPh_4]$

33. $[Ru(\eta^6\text{-}C_{16}H_{16})Cl(2,2'\text{-bipy})][PF_6]$
34. $[Ru(\eta^6\text{-}C_{16}H_{16})Cl(PPh_3)(NC_5H_5)][PF_6]$
35. $[Ru(\eta^6\text{-}C_{16}H_{16})Cl(PPh_3)(NC_5H_5)][BPh_4]$
36. $[Ru(\eta^6\text{-}C_{16}H_{16})Cl(PMe_2Ph)(NC_5H_5)][BPh_4]$
37. $[Ru_2(\eta^6\text{-}C_{16}H_{16})_2(OMe)_3][BPh_4]$
38. $[Ru_2(\eta^6\text{-}C_{16}H_{16})_2(OMe)_3][PF_6]$
39. $[Ru_2(\eta^6\text{-}C_{16}H_{16})_2(OEt)_3][PF_6]$
40. $[Ru_2(\eta^6\text{-}C_6H_6)_2(OMe)_3]^+$
41. $[Ru_2(\eta^6\text{-}C_{16}H_{16})_2(OEt)_3][BPh_4]$
42. $[Ru_2(\eta^6\text{-}C_{16}H_{16})_2(OH)_3][PF_6]$
43. $[Ru_2(\eta^6\text{-}C_{16}H_{16})_2Cl_3][PF_6]$
44. $[Ru_2(\eta^6\text{-}C_{16}H_{16})_2Cl_3][BPh_4]$
45. $[Ru_2(\eta^6\text{-}C_{16}H_{16})_2Cl_3][BF_4]$
46. *trans*-$[Ru(NC_5H_5)_4Cl_2]$
47. $[Os(\eta^6\text{-}C_{16}H_{16})_2[BF_4]_2$
48. $[Ru(\eta^6\text{-}p\text{-cymene})(\eta^6\text{-}C_{16}H_{16})][BF_4]_2$
49. $[Ru(\eta^6\text{-}p\text{-cymene})(\eta^6\text{-}C_{16}H_{16})][BPh_4]_2.\frac{1}{2}Me_2CO$
50. $[Ru(\eta^6\text{-}C_6Me_6)(\eta^6\text{-}C_{16}H_{16})][BF_4]_2$
51. $[Ru(\eta^6\text{-}p\text{-cymene})(\eta^6\text{-}C_{16}H_{16})][(CF_3CO_2)_2H]_2$
52. $[Ru(\eta^5\text{-}C_6H_7)(\eta^6\text{-}C_{16}H_{16})][BF_4]$
53. $[Ru(\eta^5\text{-1-Me,2-}H_2\text{,4-}CHMe_2\text{-}C_6H_3)(\eta^6\text{-}C_{16}H_{16})][BF_4]$
54. $[Ru(\eta^5\text{-1-Me,3-}H_2\text{,4-}CHMe_2\text{-}C_6H_3)(\eta^6\text{-}C_{16}H_{16})][BF_4]$
55. $[(\eta^6\text{-}p\text{-cymene})Ru(\eta^6,\eta^6\text{-}C_{16}H_{16})Os(\eta^6\text{-}C_6H_6)][BF_4]_4$
56. $[(\eta^6\text{-}C_6H_6)Ru(\eta^6,\eta^6\text{-}C_{16}H_{16})Ru(\eta^6\text{-}p\text{-cymene})][BF_4]_4$
57. $[Ru(\eta^6\text{-}p\text{-cymene})(acetone)_3][BF_4]_2$
58. $[(\eta^6\text{-}C_6H_6)Ru(\eta^6,\eta^6\text{-}C_{16}H_{16})Ru(\eta^6\text{-}C_6Me_6)][BF_4]_4$
59. $[(\eta^6\text{-}p\text{-cymene})Ru(\eta^6,\eta^6\text{-}C_{16}H_{16})Ru(\eta^6\text{-}C_6Me_6)][BF_4]_4$
60. $[(\eta^6\text{-}C_6H_6)Os(\eta^6,\eta^6\text{-}C_{16}H_{16})Ru(\eta^6\text{-}C_6H_6)][BF_4]_4$
61. $[(\eta^6\text{-}C_6H_6)Os(\eta^6,\eta^6\text{-}C_{16}H_{16})Ru(\eta^6\text{-}C_6Me_6)][BF_4]_4$
62. $[(\eta^6\text{-}C_6H_6)Os(\eta^6,\eta^6\text{-}C_{16}H_{16})Ru(\eta^6\text{-}C_{16}H_{16})][BF_4]_4$
63. $[(\eta^6\text{-}C_6H_6)Os(\eta^6,\eta^6\text{-}C_{16}H_{16})Ru(\eta^6,\eta^6\text{-}C_{16}H_{16})Os(\eta^6\text{-}C_6H_6)][BF_4]_6$
64. $[(\eta^6\text{-}C_6H_6)Ru(\eta^6,\eta^6\text{-}C_{16}H_{16})Os(\eta^6,\eta^6\text{-}C_{16}H_{16})Ru(\eta^6\text{-}C_6H_6)][BF_4]_6$
65. $[(\eta^6\text{-}p\text{-cymene})Ru(\eta^6,\eta^6\text{-}C_{16}H_{16})Os(\eta^6,\eta^6\text{-}C_{16}H_{16})Ru(\eta^6\text{-}p\text{-cymene})][BF_4]_6$
66. $[(\eta^6\text{-}C_6Me_6)Ru(\eta^6,\eta^6\text{-}C_{16}H_{16})Os(\eta^6,\eta^6\text{-}C_{16}H_{16})Ru(\eta^6\text{-}C_6Me_6)][BF_4]_6$

REFERENCES

1. C.J. Brown. and A.C. Farthing, *Nature (London), 164, (1949), 915.*

2. V. Boekelheide, *Top. Curr. Chem., 113, (1983), 87.*

3. D.J. Cram and H. Steinberg, *J. Am. Chem. Soc., 73, (1951), 5691.*

4. T. Reichstein and R. Oppenaur, *Helv. Chim. Acta, 16, (1933), 1373.*

5. C.J. Brown, *J. Chem. Soc., (1953), 3265.*

6. K. Lonsdale, J.J. Milledge, and K.V.K. Rao, *Proc. Roy. Soc. A225, (1960), 82.*

7. H. Hope, J. Bernstein, and K.N. Trueblood, *Acta Cryst., B28, (1972), 1733.*

8. J.T.S. Andrews and E.F. Westrum, Jr., *J. Phys. Chem., 74, (1970), 2170.*

9. D.J. Cram and J.M. Cram, *Acc. Chem. Res., 4, (1971), 204.*

10. V. Boekelheide, *Acc. Chem. Res., 13, (1980), 65.*

11. F. Gerson, *Top. Curr. Chem., 115, (1984), 57.*

12. F. Gerson and W.B. Martin, Jr., *J. Am. Chem. Soc., 91, (1969), 1883.*

13. E. Heilbronner and Z-z. Yang, *Top. Curr. Chem., 115, (1984), 1.*

14. B. Kovač, M. Mohraz, E. Heilbronner, V. Boekelheide, and H. Hopf, *J. Am. Chem. Soc., 102, (1980), 4314.*

15. R. Hoffmann, *Acc. Chem. Res., 4, (1971), 1.*

16. D.J. Cram, N.L. Allinger, and H. Steinberg, *J. Am. Chem. Soc., 76, (1954), 5691.*

17. D.J. Cram and R.H. Bauer, *J. Am. Chem. Soc., 81, (1959), 5971.*

18. S. Canuto and C. Zerner, *J. Am. Chem. Soc., 112, (1990), 2114.*

19. P.M. Keehn and S.M. Rosenfeld (ed), *Cyclophanes, Academic Press, (1983), and references therein.*

20. M.G. Newton, T.J. Walter, and N.L. Allinger, *J. Am. Chem. Soc., 95, (1973), 5652.*

21. S. Misumi and T. Otsubo, *Acc. Chem. Res., 11, (1978), 251.*

22. D.J. Cram and D.I. Wilkinson, *J. Am. Chem. Soc., 82,* (1960), *5721.*

23. H. Ohno, H. Horita, T. Otsubo, Y. Sakata, and S. Misumi, *Tett. Lett., 3, (1977), 265.*

24. Y. Kai, N. Yasuoka, and N. Kasai, *Acta Cryst., B34, (1978), 2840.*

25. B. Rees and P. Coppens, *Acta Cryst., B29, (1973), 2516.*

26. F. Christiani, D. De Filippo, P. Deplano, F. Devillanova, A. Diaz, F. Trogu, and G. Verani, *Inorg. Chim. Acta, 12, (1975), 119.*

27. W. McFarlane and S.O. Grim, *J. Organomet. Chem., 5, (1966), 147.*

28. E. Langer and H. Lehner, *J. Organomet. Chem., 173, (1973), 47.*

29. M. Takamori and N. Mori, *J. Organomet. Chem., 301, (1986), 321.*

30. C. Elschenbroich, R. Möckel, and U. Zenneck, *Angew. Chem. Int. Ed. Engl., 17, (1978), 7.*

31. R. Benn, N.E. Blank, M.W. Haenel, J. Klein, A.R. Koray, K. Weidenhammer, and M.L. Ziegler, *Angew. Chem. Int. Ed. Engl., 19, (1980), 44.*

32. A.R. Koray, M.L. Ziegler, N.E. Blank, and W. Haenel, *Tett. Lett., 26, (1979), 2465.*

33. N.E. Blank, M.W. Haenel, A.R. Koray, K. Weidenhammer, and M.L. Ziegler, *Acta Cryst., B36, (1980), 2054.*

34. E. Keulen and F. Jellinek, *J. Organomet. Chem., 5, (1966), 490.*

35. T.H. Coffield, V. Sandel, and R.D. Closson, *J. Am. Chem. Soc., 79, (1957), 5826.*

36. A.N. Nesmeyanov, N.A. Vol'Kenau, and I.N. Bolesova, *Tett. Lett., 25, (1963), 1725.*

37. A.R. Koray, *J. Organomet. Chem., 212, (1981), 233.*

38. T.P. Gill and K.R. Mann, *J. Organomet. Chem., 216, (1981), 65.*

39. P.L. Timms, *J. Chem. Soc. Chem. Commun., (1969), 1033.*

40. J. Elzinger and M. Rosenblum, *Tett. Lett., 23, (1982), 1535.*

41. D.J. Cram, R.C. Helgeson, D. Lock, and L.A. Singer, *J. Am. Chem. Soc., 88, (1966), 1324.*

42. P. Pertici and G. Vitulli, *Inorg. Synth., 22, (1983), 180.*

43. A.N. Nesmeyanov, N.A. Vol'Kenau, I.N. Bolesova, and L.S. Shul'Pina, *J. Organomet. Chem.,* 182, (1979), C36.

44. E. Roman and D. Astruc, *Inorg. Chim. Acta, 37, (1979), L465.*

45. N.A. Vol'Kenau, I.N. Bolesova, L.S. Shul'Pina, A.N. Kitaigorodskii, and D.N. Kravtsov, *J. Organomet. Chem., 288, (1985), 341.*

46. T.P. Gill and K.R. Mann, *Organometallics, 1, (1982), 485.*

47. R.A. Zelonka and M.C. Baird, *J. Organomet. Chem. 44, (1972), 383.*

48. I.W. Robertson, T.A. Stephenson, and D.A. Tocher, *J. Organomet. Chem.*, 228, *(1982), 171.*

49. E.O. Fischer, *Angew. Chem. 69, (1957), 207.*

50. A.J. Nelson, C.E.F. Rickard, and J.M. Smith, *Inorg. Synth., 24, (1986), 97.*

51. A.M. McNair, D.C. Boyd, and K.R. Mann, *Organometallics, 5, (1986), 303.*

52. I.U. Khand, P.L. Pauson, and W.E. Watts, *J. Chem. Soc. (C), (1968), 2257.*

53. I.U. Khand, P.L. Pauson, and W.E. Watts, *J. Chem. Soc. (C), (1968), 2261.*

54. P.M. Maitlis, *Chem. Soc. Revs., 10, (1981), 1, and references therein.*

55. W.E. Silverthorn, *Adv. Organomet. Chem., 13, (1975), 47, and references therein.*

56. E.O. Fischer and R. Böttcher, *Z. Anorg. Allg. Chem., 291, (1957), 305.*

57. E.O. Fischer and C. Elschenbroich, *Chem. Ber., 103, (1970), 162.*

58. G. Huttner and S. Lange, *Acta Cryst., B28, (1972), 2049.*

59. M.Y. Darensberg and E.I. Muetterties, *J. Am. Chem. Soc., 100, (1978), 7425.*

60. M.A. Bennett and T.W. Matheson, *J. Organomet. Chem., 175, (1979), 87.*

61. M.A. Bennett, T.N. Huang, T.W. Matheson, and A.K. Smith, *Inorg. Synth., 21, 74.*

62. F.B. McCormick and W.B. Gleason, *Acta Cryst., C44, (1987), 603.*

63. T. Arthur and T.A. Stephenson, *J. Organomet. Chem., 208, (1981), 369.*

64. J.A. Cabeza and P.M. Maitlis, *J. Chem. Soc. Dalton Trans., (1985), 573.*

65. S.W. Watkins and F.R. Fronczek, *Acta Cryst., B38, (1982), 270.*

66. R.T. Swan, A.W. Hanson, and V. Boekelheide, *J. Am. Chem. Soc., 108, (1986), 3324.*

67. C. LeVanda, K. Bechgaard, D.O. Cowan, U.T. Müller-Westerhoff, P. Eilbracht, G.A. Candela, and R.L. Collins, *J. Am. Chem. Soc., 98, (1976), 3181.*

68. M-H. Desbois, J. Guillin, J-P. Mariot, F. Varret, and D. Astruc, *J. Chem. Soc. Chem. Commun., (1985), 447.*

69. M-H. Desbois, D. Astruc, J. Guillin, J-P. Mariot, and F. Varret, *J. Am. Chem. Soc., 107, (1985), 5280.*

70. T-Y. Dang, M.J. Cohn, D.N. Hendrickson, and C.G. Pierpont, *J. Am. Chem. Soc., 107, (1985), 4777.*

71. M.J. Cohn, T-Y. Dang, D.N. Hendrickson, S.J. Geib, and A.L. Rheingold, *J. Chem. Soc. Chem. Commun., (1985), 1095.*

72. C. Elschenbroich and J. Heck, *J. Am. Chem. Soc., 101, (1979), 6773.*

73. E.D. Laganis, R.H Voegeli, R.T. Swann, R.G. Finke, H. Hopf, and V. Boekelheide, *Organometallics, 1, (1982), 1415.*

74. E.D. Laganis, R.G. Finke, and V. Boekelheide, *Tett. Lett., 21, (1980), 4405.*

75. R.T. Swann and V. Boekelheide, *Tett. Lett., 25, (1984), 899.*

76. H.C. Kang, K-D. Plitzko, V. Boekelheide, H. Higuchi, and S. Misumi, *J. Organomet. Chem., 321, (1987), 79.*

77. R.T. Swann, A.W. Hanson, and V. Boekelheide, *J. Am. Chem. Soc., 106, (1984), 818.*

78. A.W. Hanson, *Cryst. Struc. Commun., 11, (1982), 1019.*

79. R.H. Voegeli, H.C. Kang, R.G. Finke, and V. Boekelheide, *J. Am. Chem. Soc., 108, (1986), 7010.*

80. R.G. Finke, R.H. Voegeli, E.D. Laganis, and V. Boekelheide, *Organometallics, 2, (1983), 347.*

81. T. Miura, T. Horishita, and N. Mori, *J. Organomet. Chem., 333, (1987), 387.*

82. E.L. Muetterties, J.R. Bleeke, E.J. Wuchter, and T.A. Albright, *Chem. Rev., 82, (1982), 499.*

83. M.A. Bennett, *Comp. Organomet. Chem., Vol. 4, (1982), Ch. 32, Pergamon Press.*

84. G. Consiglio and F. Morandini, *Chem. Rev., 87, (1987), 761.*

85. H. Le Bozec, D. Touchard, and P.H. Dixneuf, *Adv. Organomet. Chem., 29, (1989), 163, and references therein.*

86. M.A. Bennett, G.B. Robertson, and A.K. Smith, *J. Organomet. Chem. 43, (1972), C41.*

87. R.A. Zelonka and M.C. Baird, *J. Organomet. Chem., 35, (1972), C43.*

88. H. Werner, and R. Werner, *Chem. Ber., 115, (1982), 3766.*

89. R.A. Zelonka and M.C. Baird, *Can. J. Chem., 50, (1972), 3063.*

90. J.A. Cabeza, H. Adams, and A.J. Smith, *Inorg. Chim. Acta, 114, (1986), L17.*

91. D.R. Robertson, I.W. Robertson, and T.A. Stephenson, *J. Organomet. Chem., 202, (1980), 309.*

92. F. Faraone, G.A. Loprete, and G. Tresoldi, *Inorg. Chim. Acta, 34, (1979), L251.*

93. R. Werner and H. Werner, *J. Organomet. Chem., 210, (1981), C11.*

94. Y. Hung, W-J. Kung, and H. Taube, *Inorg. Chem., 20, (1981), 457.*

95. D.A. Tocher, R.O. Gould, T.A. Stephenson, M.A. Bennett, J.P. Ennett, T.W. Matheson, L. Sawyer, and V.K. Shah, *J. Chem. Soc. Dalton Trans., (1983), 1571.*

96. E.C. Morrison, C.A. Palmer, and D.A. Tocher, *J. Organomet. Chem. 349, (1988), 405.*

97. P.A. Downton, B. Mailvaganam, C.S. Frampton, B.G. Sayer, and M.J. McGlinchey, *J. Am. Chem. Soc., 112, (1990), 27.*

98. D.R. Robertson and T.A. Stephenson, *J. Organomet. Chem., 116, (1976), C29.*

99. D.R. Robertson, T.A. Stephenson, and (in part) T. Arthur, *J. Organomet. Chem., 162, (1978), 121.*

100. T. Arthur and T.A. Stephenson, *J. Organomet. Chem., 168, (1979), C39.*

101. D.A. Tocher and M.D. Walkinshaw, *Acta Cryst. B38, (1982), 3083.*

102. T. Arthur, D.R. Robertson, D.A. Tocher, and T.A. Stephenson, *J. Organomet. Chem., 208, (1981), 389.*

103. R.O. Gould, T.A. Stephenson, and D.A. Tocher, *J. Organomet. Chem., 263, (1984), 375.*

104. R.O. Gould, C.L. Jones, T.A. Stephenson, and D.A. Tocher, *J. Organomet. Chem., 264, (1984), 365.*

105. R.O. Gould, C.L. Jones, D.R. Robertson, and T.A. Stephenson, *J. Chem. Soc. Chem. Commun., (1977), 222.*

106. R.O. Gould, C.L. Jones, D.R. Robertson, D.A. Tocher, and T.A. Stephenson, *J. Organomet. Chem., 226, (1982), 199.*

107. D.R. Robertson and T.A. Stephenson, *J. Organomet. Chem., 142, (1977), C31.*

108. M.A. Bennett and A.K. Smith, *J. Chem. Soc. Dalton Trans., (1974), 233.*

109. P. Lahuerta, J. Latorre, M. Sanaù, F.A. Cotton, and W. Schwotzer, *Polyhedron, 7, (1988), 1311.*

110. P. Barabotti, P. Diversi, G. Ingrosso, A. Lucherini, F. Marchetti, L. Sagramora, V. Adovasio, and M. Nardelli, *J. Chem. Soc. Chem. Commun., (1990), 179.*

111. T. Wilczewski and Z. Dauter, *J. Organomet. Chem., 312, (1986), 349.*

112. I.S. Thorburn, S.J. Rettig, and B.R. James, *J. Organomet. Chem., 296, (1985), 103.*

113. M.P. Garcia, A. Portilla, L.A. Oro, C. Foces-Foces, and F.H. Cano, *J. Organomet. Chem., 322, (1987), 111.*

114. R.D. Brost, G.C. Bruce, and S.R. Stobart, *J. Chem. Soc., Chem. Commun., (1986), 1580.*

115. R.S. Bates, M.J. Begley, and A.H. Wright, *Polyhedron, 9, (1990), 1113.*

116. F.M. Conroy-Lewis and S.J. Simpson, *J. Organomet. Chem., 396, (1990), 83.*

117. M.O. Albers, D.C. Liles, D.J. Robinson, and E. Singleton, *Organometallics, 6, (1987), 2179.*

118. R.J. Restivo, G. Ferguson, D.J. O'Sullivan, and F.J. Lalor, *Inorg. Chem., 14, (1975), 3046.*

119. D.P. Rillema, D.S. Jones, and H.A. Levy, *J. Chem. Soc. Chem. Commun., (1979), 849.*

120. B.E. Buchanan, J.G. Vos, M. Kaneko, W.J.M. van der Putten, J.M. Kelly, R. Hage, R.A.G. de Graaff, R. Prins, J.G. Haasnoot, and J. Reedijk, *J. Chem. Soc. Dalton Trans., (1990), 2425.*

121. L.A. Oro, D. Carmona, M.A. Esteruelas, C. Foces-Foces, and F.H. Cano, *J. Organomet. Chem., 307, (1986), 83.*

122. M.T. Youinou and R. Ziessel, *J. Organomet. Chem., 363, (1989), 197.*

123. M. Calligaris, L. Campana, G. Mestroni, M. Tornatore, and E. Alessio, *Inorg. Chim. Acta, 127, (1987), 103.*

124. E.W. Abel, M.A. Bennett, and G. Wilkinson, *J. Chem. Soc., (1959), 3178.*

125. N.S. Al-Zamil, E.H.M. Evans, R.D. Gillard, D.W. James, T.E. Jenkins, R.J. Lancashire, and P.A. Williams, *Polyhedron, 1, (1982), 525.*

126. J. Rozière, M.S. Lehmann, and J. Potier, *Acta Cryst., B35, (1979), 1099.*

127. G.C. Dobinson, R. Mason, and D.R. Russell, *J. Chem. Soc. Chem. Commun., (1967), 62.*

128. P. Pullmann, K. Hensen, and J.W. Bats, *Z. Naturforsch., 37b, (1982), 1312.*

129. I. Sinclair, R.W.H. Small, and I.J. Worrall, *Acta Cryst., B37, 1290.*

130. G.J. Long and P.J. Clarke, *Inorg. Chem., 17, (1978), 1394.*

131. H. Werner, H. Kletzin, and Ch. Burschka, *J. Organomet. Chem. 276, (1984), 231.*

132. J.A. Cabeza, A.J. Smith, H. Adams, and P. Maitlis, *J. Chem. Soc. Dalton Trans., (1986), 1155.*

133. M.A. Bennett, I.J. McMahon, S. Pelling, G.B. Robertson, and W.A. Wickramasinghe, *Organometallics, 4, (1985), 754.*

134. H. Werner, W. Knaup, and M. Dziallas, *Angew. Chem. Int. Ed. Engl., 26, (1987), 248.*

135. S.G. Davies, M.L.H. Green, and D.P. Mingos, *Tetrahedron, 34, (1978), 3047.*

136. G. Winkhaus, H. Singer, and M. Kricke, *Z. Naturforsch., 21b, (1966), 1109.*

Journal of Organometallic Chemistry, 356 (1988) C29–C31
Elsevier Sequoia S.A., Lausanne – Printed in The Netherlands

Preliminary communication

The synthesis of new paracyclophane complexes of ruthenium(II): Crystal structure of $[Ru(\eta^6\text{-}C_{16}H_{16})Cl(C_5H_5N)_2][PF_6]$

Mark R.J. Elsegood and Derek A. Tocher *

Department of Chemistry, University College London, 20 Gordon Street, London WC1H 0AJ (Great Britain)

(Received August 15th, 1988)

Abstract

The dimer $[Ru(\eta^6\text{-}C_{16}H_{16})Cl_2]_2$ reacts with ligands L ($L = PMe_2Ph$, PPh_3, C_5H_5N) to give both neutral monomeric $[Ru(\eta^6\text{-}C_{16}H_{16})Cl_2L]$ and cationic monomeric $[Ru(\eta^6\text{-}C_{16}H_{16})ClL_2]^+$ products. One example, $[Ru(\eta^6\text{-}C_{16}H_{16})Cl(C_5H_5N)_2][PF_6]$, has been characterised by X-ray crystallography. Reaction with the bidentate ligand 2,2′-bipyridyl gives the mononuclear cation $[Ru(\eta^6\text{-}C_{16}H_{16})Cl(bipy)]^+$, isolated as its $[BPh_4]^-$ salt, whereas reaction with OMe^- or OEt^- gives dinuclear products $[Ru_2(\eta^6\text{-}C_{16}H_{16})_2(OR)_3]^+$.

During synthetic studies on a number of bis(η^6-[2*n*]cyclophane)ruthenium(II) and related oligomeric compounds, Boekelheide et al. made the dinuclear molecules $[Ru(\eta^6\text{-}C_{16}H_{16})Cl_2]_2$ [1,2]. These species were of interest to us as they are clearly closely related to the $[Ru(\eta^6\text{-arene})Cl_2]_2$ compounds whose chemistry we have extensively studied [3–10]. We now report the results of our preliminary investigations into the reactions of the paracyclophane complex, bis(η^6-[2_2](1,4)cyclophane)-dichlorobis(η-chloro)diruthenium(II), with a range of ligands.

We have prepared a range of orange red adducts $[Ru(\eta^6\text{-}C_{16}H_{16})Cl_2L]$ ($L = PMe_2Ph$, PPh_3, C_5H_5N) * by reaction of an excess of the appropriate ligand with a toluene suspension of the metal complex. All the complexes are monomeric in chloroform and are non-electrolytes in acetonitrile and nitromethane. The ^1H NMR spectrum of each complex typically shows three sets of resonances for the cyclophane ligand. The coordinated ring gives rise to a singlet ($L = C_5H_5N$) or doublet ($L = PPh_3$, PMe_2Ph; ^3J(P–H) ca. 1.5 Hz) resonance in the range δ 4.7–4.9 ppm, the uncoordinated ring appears as a singlet at ca. δ 6.7 ppm, and the methylene protons appear as an AA′BB′ pattern at ca. δ 2.8 ppm. Integration of the complete ^1H NMR spectra confirms that the products are 1/1 adducts.

* Satisfactory elemental analyses have been obtained.

0022-328X/88/$03.50

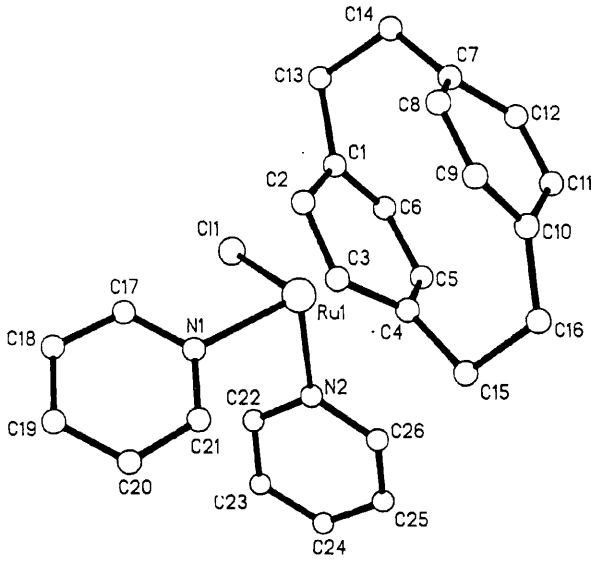

Fig. 1. View of the structure of one of the $[Ru(\eta^6\text{-}C_{16}H_{16})Cl(C_5H_5N)_2]^+$ cations showing the atom labelling scheme. Important parameters: Ru(1)–Cl(1) 2.404(6), Ru(1)–N(1) 2.166(16), Ru(1)–N(2) 2.133(20), Ru(1)–C(1) 2.365(21), Ru(1)–C(2) 2.248(22), Ru(1)–C(3) 2.161(21), Ru(1)–C(4) 2.312(20), Ru(1)–C(5) 2.164(17), Ru(1)–C(6) 2.175(17) Å, Cl(1)–Ru(1)–N(1) 90.1(5), Cl(1)–Ru(1)–N92) 86.4(6), N(1)–Ru(1)–N(2) 84.8(6)°.

In contrast, if the reactions are carried out in methanolic solution and $[NH_4]PF_6$ is added to the reaction mixture then the compounds $[Ru(\eta^6\text{-}C_{16}H_{16})ClL_2][PF_6]$ * can be obtained. Integration of the ^1H NMR spectra was consistent with formation of the cationic 2/1 adducts. The monomeric nature of the products has been confirmed by X-ray structural analysis of a representative compound, $[Ru(\eta^6\text{-}C_{16}H_{16})Cl(C_5H_5N)_2][PF_6]$ (see Fig. 1) *.

The geometry about the ruthenium ion is that of a distorted tetrahedron, with the paracyclophane and the other ligands adopting a "piano stool" configuration. The complex has a similar arrangement of ligands to that in several $[Ru(\eta^6\text{-arene})Cl_2L]$ and $[Ru(\eta\text{-arene})ClL_2]^+$ molecules [7,13]. The coordination of the chloride and heterocyclic nitrogen donor ligands closely resembles that observed in the cation $[Ru(\eta\text{-}p\text{-cymene})Cl(C_4H_4N_2)_2]^+$ [7]. The most marked contrast between the structures of (η^6-arene)ruthenium(II) compounds and the paracyclophane compound discussed here is the significant variation in the metal–carbon distances observed in the latter. In the case of (η^6-arene)ruthenium(II) compounds the metal–carbon distances typically fall in a narrow range about 2.14–2.21 Å [4,6–10,13], while the compound reported here has close distances in the range 2.16–2.36 Å. However this large variation in metal carbon distances has been observed previously [1,14], and is

* *Crystal data for* $C_{26}H_{26}ClF_6N_2PRu$: $M = 647.99$, a 7.814(1), b 20.251(3), c 32.785(5) Å, V 5186(1) Å^3, $Z = 8$, d_{calc} 1.66 g/cm^3, $F(000)$ 2608, μ(Mo-K_α) 7.74 cm^{-1}, orthorhombic space group $P2_12_12_1$ (the asymmetric unit contains two cations and two $[PF_6]^-$ anions).
Structure determination: A crystal of dimensions 0.15×0.10×0.40 mm was used to collect 6648 unique data up to θ 25° on a Nicolet R3m/V diffractometer. The positions of the ruthenium atoms were derived by direct methods and the remaining non-hydrogen atoms found by iterative application of least-squares refinement and difference-fourier synthesis [11]. The $[PF_6]^-$ anions are extensively disordered and this led to less than ideal refinement [12*]. The current R value is 0.075 from the 3399 reflections with $I > 2.5\sigma(I)$. The weighting scheme was $w = 1.0/(\sigma^2(F) + 0.000024\ F^2)$. The structure of one of the cations (the other is essentially identical) is presented in Fig. 1.

attributed to the presence of the two ethylenic bridges between the aromatic rings. Indeed it is a feature of the free ligand, as well as of its metal complexes, that the aromatic rings are non-planar [15].

When a solution of $[Ru(\eta^6\text{-}C_{16}H_{16})Cl_2]_2$ in methanol is stirred with an excess of 2,2′-bipyridyl for less than ca. 1 h a red solution is formed, and a brown solid separates on addition of $Na[BPh_4]$. Analytical and spectroscopic data are consistent with the formulation of this solid as $[Ru(\eta^6\text{-}C_{16}H_{16})Cl(bipy)][BPh_4]$. Prolonged interaction between the dimer and 2,2′-bipyridyl results in the formation of the well-known cation $[Ru(bipy)_3]^{2+}$.

Finally reaction of $[Ru(\eta^6\text{-}C_{16}H_{16})Cl_2]_2$ with solutions of Na[OR] in ROH (R = Me, Et) gives yellow solutions from which solids can be precipitated by addition of $K[PF_6]$ or $Na[BPh_4]$. These solids have been identified as the dinuclear species $[(\eta^6\text{-}C_{16}H_{16})Ru(OR)_3Ru(\eta^6\text{-}C_{16}H_{16})]X$, ($X = PF_6^-$ or BPh_4^-) in which the cation has confacial bioctahedral geometry [16*].

Acknowledgements. We thank Johnson–Matthey plc for generous loans of ruthenium trichloride and the SERC for financial support (M.R.J.E.) and for provision of the X-ray equipment.

References

1 R.T. Swann, A.W. Hanson and V. Boekelheide, J. Am. Chem. Soc., 108 (1986) 3324.
2 R.H. Voegeli, H.C. Kang, R.G. Finke and V. Boekelheide, J. Am. Chem. Soc., 108 (1986) 7010.
3 T. Arthur, D.R. Robertson, D.A. Tocher and T.A. Stephenson, J. Organomet. Chem., 208 (1981) 389.
4 R.O. Gould, C.L. Jones, D.R. Robertson, D.A. Tocher and T.A. Stephenson, J. Organomet. Chem., 226 (1982) 199.
5 I.W. Robertson, T.A. Stephenson and D.A. Tocher, J. Organomet. Chem., 228 (1982) 177.
6 D.A. Tocher and M.D. Walkinshaw, Acta Cryst. B, 38 (1982) 3083.
7 D.A. Tocher, R.O. Gould, T.A. Stephenson, M.A. Bennett, J.P. Ennett, T.W. Matheson, L. Sawyer and V.K. Shah, J. Chem. Soc. Dalton Trans., (1983) 1571.
8 R.O. Gould, C.L. Jones, T.A. Stephenson and D.A. Tocher, J. Organomet. Chem., 264 (1984) 365.
9 R.O. Gould, T.A. Stephenson and D.A. Tocher, J. Organomet. Chem., 263 (1984) 375.
10 E.C. Morrison, C.A. Palmer and D.A. Tocher, J. Organomet. Chem., 349 (1988) 405.
11 G.M. Sheldrick, SHELXTL PLUS, An integrated system for refining and displaying crystal structures from diffraction data. University of Gottingen, Federal Republic of Germany, 1986.
12 The problems encountered during refinement of the X-ray data set will be discussed in detail in the full paper.
13 M.A. Bennett, G.B. Robertson and A.K. Smith, J. Organomet. Chem., 43 (1972) C41.
14 Y. Kai, N. Yasuoka and N. Kasai, Acta Cryst. B, 34 (1978) 2840.
15 H. Hope, J. Bernstein and K.N. Trueblood, Acta Cryst. B, 28 (1972) 1733.
16 Preliminary X-ray examination has confirmed this geometry for the compound $[Ru_2(\eta^6\text{-}C_{16}H_{16})_2(OEt)_3]PF_6$.

* Reference numbers with asterisks indicate notes in the list of references.

Journal of Organometallic Chemistry, 391 (1990) 239–245
Elsevier Sequoia S.A., Lausanne
JOM 20851

Studies on transition metal paracyclophane compounds. Synthesis and crystal structure of $[Os(\eta^6\text{-}C_6H_6)(\eta^6\text{-}[2_2](1,4)\text{-}C_{16}H_{16})][BF_4]_2$: synthesis and NMR characterisation of the trinuclear heterometallic complex $[(\eta^6\text{-}C_6H_6)Os(\eta^6,\eta^6\text{-}[2_2](1,4)C_{16}H_{16})Ru(\eta^6,\eta^6\text{-}[2_2](1,4)C_{16}H_{16})Os(\eta^6\text{-}C_6H_6)][BF_4]_6$

Mark R.J. Elsegood and Derek A. Tocher *

Department of Chemistry, University College London, 20 Gordon Street, London WC1H 0AJ (U.K.)

(Received February 9th, 1990)

Abstract

When a solution of $[Ru(\eta^6\text{-}C_6H_6)(\eta^6\text{-}[2_2](1,4)C_{16}H_{16})][BF_4]_2$ and $[Os(\eta^6\text{-}C_6H_6((CH_3)_2CO)_3][BF_4]_2$ in a mixed $(CH_3)_2CO/CF_3CO_2H$ solvent is refluxed the paracyclophane ligand is transfered in part to the osmium ion. Pure samples of $[Os(\eta^6\text{-}C_6H_6)(\eta^6\text{-}[2_2](1,4)C_{16}H_{16})][BF_4]_2$ are obtained by refluxing a solution of $[Os(\eta^6\text{-}C_6H_6)((CH_3)_2CO)_3][BF_4]$ and paracyclophane in the mixed $(CH_3)_2CO/CF_3CO_2H$ solvent. This new osmium(II) compound has been characterised by NMR spectroscopy and X-ray crystallography. The reaction of $[Os(\eta^6\text{-}C_6H_6)((CH_3)_2\text{-}CO)_3][BF_4]_2$ with $[Ru(\eta^6\text{-}[2_2](1,4)C_{16}H_{16})_2][BF_4]_2$ in neat CF_3CO_2H yields the novel trinuclear heterometallic complex $[(\eta^6\text{-}C_6H_6)Os(\eta^6,\eta^6\text{-}[2_2](1,4)C_{16}H_{16})Ru(\eta^6,\eta^6\text{-}[2_2](1,4)C_{16}H_{16})Os(\eta^6\text{-}C_6H_6)][BF_4]_6$, which has been isolated and characterised by ^1H and ^{13}C NMR spectroscopy.

Introduction

Recently we reported [1] that reaction of $[Ru(\eta^6\text{-}[2_2](1,4)C_{16}H_{16})Cl_2]_2$ with a variety of donor ligands L ($L = NC_5H_5$, PPh_3, PMe_2Ph) in non-polar and polar solvents gave products of the types $[Ru(\eta^6\text{-}[2_2](1,4)C_{16}H_{16})Cl_2L]$ and $[Ru(\eta^6\text{-}[2_2](1,4)C_{16}H_{16})ClL_2]^+$, respectively. The mononuclear nature of these complexes was confirmed by single crystal X-ray diffraction studies on the representative compounds $[Ru(\eta^6\text{-}[2_2](1,4)C_{16}H_{16})Cl_2(PPh_3)]$ [2] and $[Ru(\eta^6[2_2](1,4)C_{16}H_{16})Cl\text{-}(NC_5H_5)_2][PF_6]$ [1]. Binuclear products are formed when $[Ru(\eta^6\text{-}[2_2](1,4)C_{16}\text{-}H_{16})Cl_2]_2$ reacts with freshly prepared NaOR in ROH (R=Me, Et), as we established by crystal structure determinations of $[Ru_2(\eta^6\text{-}[2_2](1,4)C_{16}H_{16})_2(OMe)_3]\text{-}[BPh_4]$ [2] and $[Ru_2(\eta^6\text{-}[2_2](1,4)C_{16}H_{16})_2(OEt)_3][PF_6]$ [3]. We now report the exten-

0022-328X/90/$03.50

sion of our studies to osmium(II) paracyclophane complexes, and to heterometallic species.

Results and discussion

The synthetic technique first described by Bennett [4] for the preparation of bis(η^6-arene)Ru(II) complexes is readily extended to (η^6-arene) (η^6-cyclophane)Ru(II) complexes [5]. Using a strictly analogous procedure we have prepared the osmium complex $[Os(\eta^6\text{-}C_6H_6)(\eta^6\text{-}[2_2](1,4)C_{16}H_{16})][BF_4]_2$. The ^1H NMR spectrum, recorded in CD_3NO_2, exhibits a singlet due to the benzene protons at δ 6.91, singlets at δ 6.54 and 7.11 ppm due to the protons of the coordinated and non-coordinated aromatic rings of the paracyclophane ligand, and an AA'BB' coupling pattern centred at δ 3.36 due to the ethylenic protons of the paracyclophane ligand [Fig. 1(a)]. Integration of the spectrum supports the proposed stoichiometry. When the ^1H NMR spectrum of this osmium compound is compared

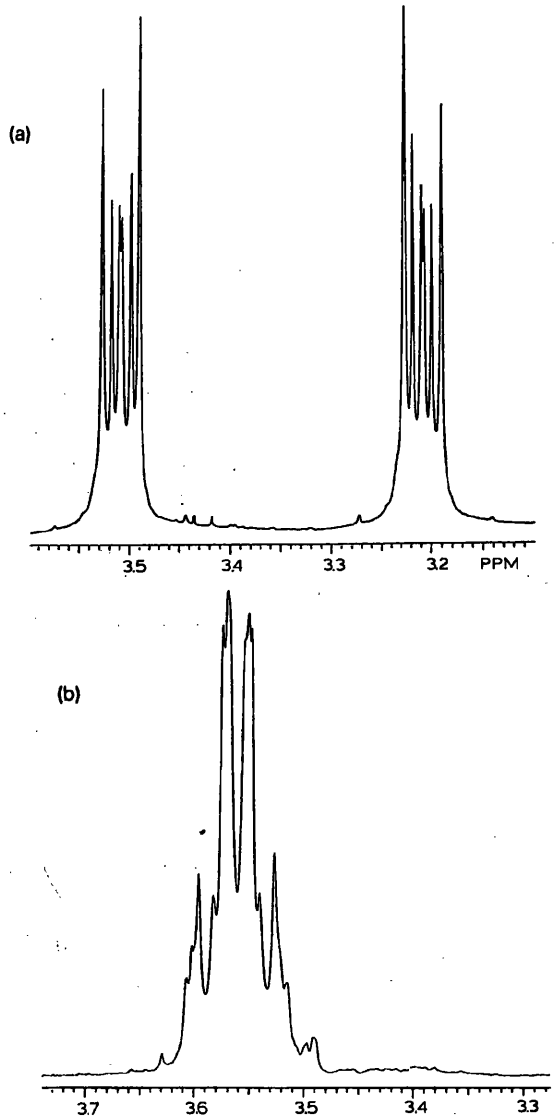

Fig. 1. ^1H NMR spectra, recorded in CD_3NO_2 at 400 MHz, of the ethylenic bridging groups of (a) $[Os(\eta^6\text{-}C_6H_6)(\eta^6\text{-}[2_2](1,4)C_{16}H_{16})][BF_4]_2$, and (b) $[(\eta^6\text{-}C_6H_6)Os(\eta^6,\eta^6\text{-}[2_2](1,4)C_{16}H_{16})Ru(\eta^6,\eta^6\text{-}[2_2](1,4)C_{16}H_{16})Os(\eta^6\text{-}C_6H_6)][BF_4]_6$.

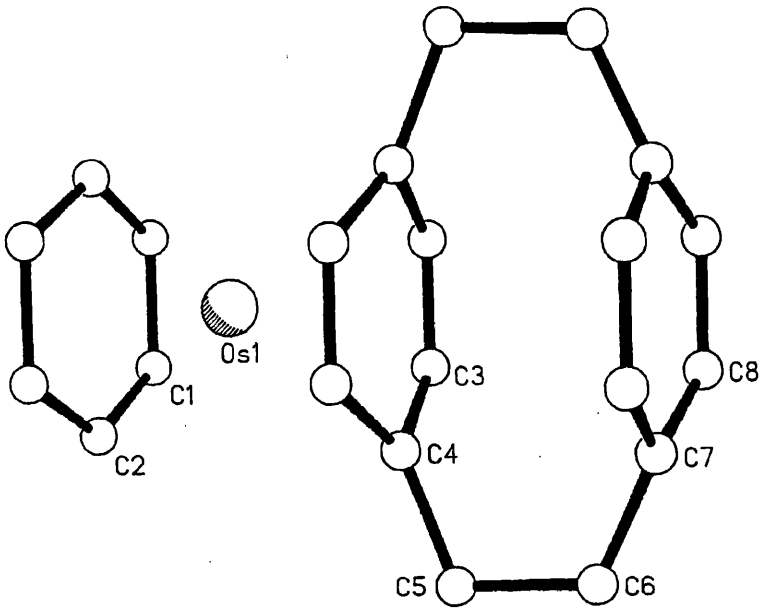

Fig. 2. Molecular structure of the cation $[Os(\eta^6\text{-}C_6H_6)(\eta^6\text{-}[2_2](1,4)C_{16}H_{16})]^{2+}$ showing the numbering scheme adopted. Selected averaged bond lengths (A): Os(1)–C(1) 2.22(2), Os(1)–C(2) 2.19(2), Os(1)–C(3) 2.20(2), Os(1)–C(4) 2.37(2), Os(1)–centroid of coordinated cyclophane ring 1.70, Os(1)–centroid of benzene ring 1.73, C(3)–C(4) 1.42(2), C(4)–C(5) 1.47(3), C(5)–C(6) 1.52(3), C(6)–C(7) 1.49(3), C(7)–C(8) 1.38(2), C(1)–C(1*) 1.36(5), C(3)–C(3*) 1.37(3), C(8)–C(8*) 1.39(3) (starred atoms generated by crystal symmetry).

with that of its ruthenium analogue the most noteworthy feature is the shifting of the signals due to the various aromatic protons to higher frequency [5], by ca 0.2 ppm. In contrast, when the ^{13}C NMR spectra of the two compounds are compared it is found that the signals from the ring carbon atoms appear, on average, at a chemical shift 7 ppm to lower frequency in the osmium compound.

Single crystals of the compound $[Os(\eta^6\text{-}C_6H_6)(\eta^6\text{-}[2_2](1,4)C_{16}H_{16})][BF_4]_2$ were obtained by slow evaporation of a dilute solution of the complex in acetonitrile, and the structure confirmed by X-ray diffraction. The cation is shown in Fig. 2. The osmium(II) ion is sandwiched between the benzene ring and one ring of the paracyclophane ligand in a similar fashion to reported structures of bis(η^6-arene)ruthenium(II) complexes [5,6]. For the reported (η^6-arene)osmium(II) structures [7–12] typical Os–C distances lie in the range 2.15–2.25 Å, while the corresponding metal–ring centroid distances average 1.68 Å. The corresponding values for this new structure are given in the figure caption, and are generally in agreement with previous data. The clear exception is the osmium to cyclophane bridgehead carbon distance Os(1)–C(4), 2.37(2) Å, which is significantly longer than the others. This is now a familiar and expected structural feature of paracyclophane. Both in the free ligand [13], and in its metal complexes, the aromatic rings are distorted into a shallow boat conformation by the electronic repulsions between the stacked rings. In the ruthenium(II) paracyclophane complexes which we studied previously [1–3] the ruthenium–bridgehead carbon distance fell in the range 2.27–2.38 Å. The distance between the aromatic decks of the cyclophane is 2.99 Å, which is less than the corresponding value for the free cyclophane, 3.09 Å. This reduction in inter-deck spacing, and by implication of the unfavourable electronic interactions, is often observed on coordination of a metal to the external face of the

paracyclophane ligand [1–3,5,14]. Crystal symmetry accounts for the apparently 0° torsion angle in the interdeck connectivity, C(4)–C(5)–C(6)–C(7). In other compounds this angle typically has a value of 3–11° [1–3,5]. Early crystal structure studies of paracyclophane also gave an apparent torsion angle of 0° [15,16]; however, a subsequent careful redetermination of the structure [13] identified a dynamic disorder that occurs by a twist of the aromatic rings and results in a torsion angle of ca 3°. We feel that a similar disorder must be present in our metal complex, but have been unable to refine an acceptable model owing to the presence of the heavy metal ion.

During synthetic studies on a variety of complexes containing the "(η^6-[2$_2$](1,4)$C_{16}H_{16}$)ruthenium(II)" sub-unit, Boekelheide et al. prepared triple-layered complexes of the type [(η^6-arene)Ru(η^6,η^6-[2$_2$](1,4)$C_{16}H_{16}$)Ru(η^6-arene)][BF_4]$_4$ [5,17]. It was our intention to prepare a mixed-metal analogue of this type of compound, namely [(η^6-C_6H_6)Ru(η^6,η^6-[2$_2$](1,4)$C_{16}H_{16}$)Os(η^6-C_6H_6)][BF_4]$_4$. To this end [Ru(η^6-C_6H_6)(η^6-[2$_2$](1,4)$C_{16}H_{16}$)][BF_4]$_2$ was treated with [Os(η^6-C_6H_6)-((CH_3)$_2$CO)$_3$][BF_4]$_2$ (1 : 1 mol ratio) in a mixture of (CH_3)$_2$CO/CF_3CO_2H for 30 minutes under reflux. Cooling followed by precipitation with diethyl ether gave a pale yellow powder. The ^{1}H NMR spectrum, recorded in d^6-DMSO, showed two sets of resonances, which could be attributed to the cations [Ru(η^6-C_6H_6)(η^6-[2$_2$](1,4)$C_{16}H_{16}$)]$^{2+}$ and [Os(η^6-C_6H_6)(η^6-[2$_2$](1,4)$C_{16}H_{16}$)]$^{2+}$. These compounds were present in solution in an approximate ratio of 1 : 3, and thus we conclude that under the experimental conditions employed in this reaction the paracyclophane ligand has been substantially transferred to the osmium(II) ion.

We also investigated the reaction between [Os(η^6-C_6H_6)((CH_3)$_2$CO)$_3$][BF_4]$_2$, generated from [Os(η^6-C_6H_6)Cl_2]$_2$ by addition of Ag[BF_4] in acetone, and the bisparacyclophane complex [Ru(η^6-[2$_2$](1,4)$C_{16}H_{16}$)$_2$][BF_4]$_2$ in trifluoroacetic acid. A two-fold excess of the osmium compound was employed, and the reaction time was kept to a minimum (10 minutes) to avoid decomposition of the product. The analysis of the off-white solid obtained corresponded closely with that expected for the heterotrimetallic complex [(η^6-C_6H_6)Os(η^6,η^6-[2$_2$](1,4)$C_{16}H_{16}$)Ru(η^6,η^6-[2$_2$]-(1,4)$C_{16}H_{16}$)Os(η^6-C_6H_6)][BF_4]$_6$. Compelling evidence supporting the proposed trinuclear, quadruplelayered structure comes from the ^{1}H and ^{13}C NMR spectra of the compound recorded in CD_3NO_2. In the ^{1}H NMR spectrum there are just three singlet resonances in the aromatic region: at δ 7.14 for the benzene protons, at δ 6.95 for the aromatic cyclophane protons on the rings adjacent to the osmium ions, and at δ 6.68 for the protons on the aromatic rings bound to the ruthenium ion. In the closely related trinuclear ruthenium complex [(η^6-C_6Me_6)Ru(η^6,η^6-[2$_2$](1,4)C_{16}-H_{16})Ru(η^6,η^6-[2$_2$](1,4)$C_{16}H_{16}$)Ru(η^6-C_6Me_6)][BF_4]$_6$ the aromatic protons of the cyclophane ligands resonate at δ 6.36 and 6.47 ppm. These differences in chemical shift are consistent with those described above for the monomeric complexes [M(η^6-C_6H_6)(η^6-[2$_2$](1,4)$C_{16}H_{16}$)][BF_4]$_2$.

The ethylenic protons now show a radically different second-order coupling pattern [Fig. 1(b)]. The chemical shifts of the two sets of signals from the methylenic protons are now closely similar. In addition these signals now appear at higher frequency than either of the signals from the complexes in which only one face of the paracyclophane ligand is bound to a metal. This dramatic change in coupling pattern and the enhanced second-order character of the spectrum provide compelling evidence indicating that each face of the cyclophane ligand is coordinated to a

different metal ion. The integration of the complete spectrum is consistent with the proposed stoichiometry.

We predict that seven resonances should be observed in the ^{13}C NMR spectrum of the heterometallic trinuclear cation. Two signals from aliphatic carbon atoms are observed at δ 33.3 and δ 32.9 ppm. The chemical shift difference between these is much smaller than that observed when only one face of the paracyclophane ligand is bound to a metal. Two signals from the non-bridgehead aromatic carbon atoms are observed, at δ 90.2 and 84.0 ppm, while two further signals, at δ 131.5 and 136.6 ppm, are assigned to the bridgehead carbon atoms. The resonance due to the benzene carbon atoms is observed at δ 89.6 ppm.

The significance of the results reported above lies in the obvious possibility of extension of this chemistry to the synthesis of heterometallo-organic polymers having one-dimensional properties.

Experimental

Microanalyses were carried out in the Chemistry Department of University College London. NMR spectra (^1H, ^{13}C) were obtained on a Varian VXR-400 spectrometer (chemical shifts quoted in ppm with positive values to high frequency of $SiMe_4$).

Materials

$[Ru(\eta^6\text{-}C_6H_6)Cl_2]_2$, $[Os(\eta^6\text{-}C_6H_6)Cl_2]_2$, $[Ru(\eta^6\text{-}C_6H_6)(\eta^6\text{-}[2_2](1,4)C_{16}H_{16})][BF_4]_2$ and $[Ru(\eta^6\text{-}[2_2](1,4)C_{16}H_{16})_2][BF_4]_2$ were prepared by published methods [4,5,18]. All other reagents were obtained from commercial suppliers.

All reactions were carried out in degassed solvents under nitrogen.

$[Os(\eta^6\text{-}C_6H_6)(\eta^6\text{-}[2_2](1,4)C_{16}H_{16})][BF_4]_2$

To a suspension of $[Os(\eta^6\text{-}C_6H_6)Cl_2]_2$ (0.42 g, 0.61 mmol) in acetone (10 cm^3) was added $Ag[BF_4]$ (0.55 g, 2.83 mmol). The AgCl was removed by filtration through celite. Paracyclophane (0.25 g, 1.20 mmol) and CF_3CO_2H (5 cm^3) were added to the yellow/orange filtrate and the mixture was refluxed for 30 minutes then allowed to cool, and diethyl ether (50 cm^3) was added. The pale yellow precipitate was filtered off, washed with acetone and diethyl ether, and dried in vacuum. Yield 0.44 g, 55%. (Found: C, 40.7; H, 3.5. Calc. for $C_{22}H_{22}B_2F_8Os$: C, 40.6; H, 3.4%). ^1H NMR (CD_3NO_2): δ 6.91 (s, C_6H_6), δ 6.54 (s, metallated C_6H_4), δ 7.11 (s, non-metallated C_6H_4), δ 3.36 (AA'BB', $-CH_2CH_2-$). ^{13}C NMR (CD_3NO_2): δ 87.2 (C_6H_6), δ 83.4 (metallated $C_2C_4H_4$), δ 133.0 (metallated $C_2C_4H_4$), δ 135.7 (non-metallated $C_2C_4H_4$), δ 141.1 (non-metallated $C_2C_4H_4$), δ 33.8 and 34.9 ($-CH_2CH_2$).

$[(\eta^6\text{-}C_6H_6)Os(\eta^6,\eta^6\text{-}[2_2](1,4)C_{16}H_{16})Ru(\eta^6,\eta^6\text{-}[2_2](1,4)C_{16}H_{16})Os(\eta^6\text{-}C_6H_6)][BF_4]_6$

To a suspension of $[Os(\eta^6\text{-}C_6H_6)Cl_2]_2$ (0.11 g, 0.17 mmol) in acetone (10 cm^3) was added $Ag[BF_4]$ (0.15 g, 0.77 mmol). The mixture was stirred at 20 °C for one hour and the AgCl then filtered off. The solvent was removed under vacuum to leave a residue of yellow $[Os(\eta^6\text{-}C_6H_6)((CH_3)_2CO)_3][BF_4]_2$, to which CF_3CO_2H (5 cm^3) and $[Ru(\eta^6\text{-}[2_2](1,4)C_{16}H_{16})_2][BF_4]_2$ (0.06 g, 0.09 mmol) were added. The mixture was refluxed for 10 minutes and then cooled to give a pale yellow

precipitate, which was filtered off, and identified as $[(\eta^6\text{-}C_6H_6)Os(\eta^6,\eta^6\text{-}[2_2](1,4)C_{16}H_{16})Ru(\eta^6,\eta^6\text{-}[2_2](1,4)C_{16}H_{16})Os(\eta^6\text{-}C_6H_6)][BF_4]_6$. Addition of diethyl ether (50 cm^3) to the reaction mixture gave a second crop of the precipitate which was filtered off, washed diethyl ether, and dried under vacuum. Combined yield 0.11 g, 0.07 mmol. (Found: C, 34.6; H, 2.8. Calc. for $C_{44}H_{44}B_6F_{24}Os_2Ru$: C, 33.5; H, 2.8%). ^1H NMR (CD_3NO_2): δ 7.14 (s, C_6H_6), δ 6.95 (s, OsC_6H_4), δ 6.68 (s, RuC_6H_4), δ 3.56 (A_2B_2, $-CH_2CH_2$). ^{13}C NMR (CD_3NO_2): δ 89.6 (C_6H_6), δ 84.0 and 90.2 ($C_2C_4H_4$), δ 131.5 and 136.6 ($C_2C_4H_4$), δ 33.3 and 32.9 ($-CH_2CH_2-$).

Crystal structure determination of $[Os(\eta^6\text{-}C_6H_6)(\eta^6\text{-}[2_2](1,4)C_{16}H_{16})][BF_4]_2$

Crystal data: $C_{22}H_{22}B_2F_8Os$, $M = 650.3$, orthorhombic, a 7.728(2), b 18.642(2), c 14.852(4) Å, V 2140(1) Å^3, D_c 2.02 g cm^{-3}, $Z = 4$, μ(Mo-K_α) 60.4 cm^{-1}, F(000) 1248, λ(Mo–K_α) 0.71073 Å, space group *Cmcm* from systematic absences.

A crystal of dimensions $0.80 \times 0.12 \times 0.02$ mm was used to collect 1050 unique reflections in the range $5° \leqslant 2\theta \leqslant 50°$, on a Nicolet R3m/V diffractometer equipped with a molybdenum X-ray tube and graphite monochromator.

The asymmetric unit contains one quarter of the cation and one half of a $[BF_4]^-$ anion. The position of the osmium atom was derived from a three-dimensional Patterson function. Least-squares refinement followed by difference-Fourier synthesis were used to locate the remaining non-hydrogen atoms. It was immediately apparent that each component of the structure was subject to disorder. The cation is disordered in two respects. Firstly the cyclophane ligand is disordered over two

Table 1

Atomic coordinates ($\times 10^4$) and equivalent isotropic displacement parameters (Å$^2 \times 10^3$)

	x	y	z	U_{eq} [a]
Os(1)	0	1282(1)	2500	33(1)
C(1)	956(16)	2203(6)	3336(9)	49(3)
C(2)	1811(29)	2180(10)	2500	52(5)
C(3)	883(20)	326(7)	3296(10)	28(3)
C(4)	1870(31)	234(12)	2500	36(5)
C(5)	3639(31)	−78(12)	2500	51(6)
C(6)	3502(36)	−887(14)	2500	67(7)
C(7)	1794(32)	−1215(12)	2500	40(5)
C(8)	871(24)	−1275(7)	3302(11)	37(3)
C(1A)	1480(54)	2231(20)	2921(29)	51(8)
C(2A)	0	2224(17)	3397(23)	19(7)
C(3A)	1552(19)	399(7)	2967(10)	31(3)
C(4A)	0	314(10)	3475(15)	33(4)
C(5A)	0	33(15)	4384(21)	66(7)
C(6A)	0	−787(11)	4388(16)	45(5)
C(7A)	0	−1133(12)	3451(15)	38(5)
C(8A)	1519(21)	−1202(8)	2980(11)	36(3)
B(1)	0	3605(14)	5391(14)	83(8)
F(1)	0	3603(13)	6284(14)	211(12)
F(2)	0	3496(32)	4570(29)	249(33)
F(3)	1541(31)	3447(23)	5139(18)	208(19)
F(2A)	0	2817(16)	5459(28)	173(19)
F(3A)	1128(41)	4134(16)	5307(26)	224(19)

[a] Equivalent isotropic U defined as one-third of the trace of the orthogonalized U_{ij} tensor.

positions related by a 90° rotation with the two sites having equal occupancy. The benzene ring is similarly disordered, though in this case one site is occupied 75% of the time, the alternative site 25% of the time. The $[BF_4]^-$ anion is located on the mirror plane at $(0, y, z)$. The boron atom and two fluorines lie in that plane. The anion is highly disordered. Attempts to refine chemically reasonable models based upon interpenetrating rigid tetrahedra were largely unsuccessful. When the atoms of the anion were allowed to refine freely a chemically unsatisfactory solution was obtained. This solution did however result in the best overall refinement, and more importantly, led to the greatest precision for the parameters describing the chemically more interesting cation. As there are no short contacts between cation and anions this imperfect result was accepted. The osmium, boron, and fluorine atoms were refined anisotropically. The hydrogen atoms were included in fixed positions with a common isotropic temperature factor (U 0.08 Å^2). At the end of refinement $R = 0.0380$ ($R_w = 0.0402$), based on the 928 unique, absorption-corrected data with $I \leqslant 1.5\sigma(I)$. The largest shift/esd was 0.02 and the largest peak in the final difference-Fourier synthesis was 1.1 e Å^{-3}, close to the metal atom. Crystallographic calculations used the SHELXTL PLUS program package [19]. Final fractional coordinates are given in Table 1. Tables of observed and calculated structure factors and a full list of positional and thermal parameters are available on request from the authors.

Acknowledgements

We thank Johnson Matthey plc for generous loans of ruthenium trichloride and the SERC for financial support (to MRJE) and for provision of the X-ray equipment.

References

1 M.R.J. Elsegood and D.A. Tocher, J. Organomet. Chem., 356 (1988) C29.
2 M.R.J. Elsegood and D.A. Tocher, unpublished results.
3 M.R.J. Elsegood and D.A. Tocher, Inorg. Chim. Acta, 161 (1989) 147.
4 M.A. Bennett and T.W. Matheson, J. Organomet. Chem., 175 (1979) 87.
5 R.T. Swann, A.W. Hanson and V. Boekelheide, J. Am. Chem. Soc., 108 (1986) 3324.
6 H. Werner, H. Kletzin and Ch. Burschka, J. Organomet. Chem., 276 (1984) 231.
7 J.A. Cabeza, A.J. Smith, H. Adams and P.M. Maitlis, J. Chem. Soc. Dalton Trans., (1986) 1155.
8 S.F. Watkins and F.R. Fronczek, Acta Cryst., B38 (1982) 270.
9 J.A. Cabeza, H. Adams and A.J. Smith, Inorg. Chim. Acta, 114 (1986) L17.
10 H. Werner, W. Knaup and M. Dziallas, Angew. Chem. Int. Ed. Engl., 26 (1987) 248.
11 M.A. Bennett, I.J. McMahon, S. Pelling, G.B. Robertson and W.A. Wickranasinghe, Organometallics, 4 (1985) 754.
12 R.O. Gould, C.L. Jones, T.A. Stephenson and D.A. Tocher, J. Organomet. Chem., 264 (1984) 365.
13 H. Hope, J. Bernstein and K.N. Trueblood, Acta Cryst., B28 (1972) 1733.
14 Y. Kai, N. Yasuoka and N. Kasai, Acta Cryst., B34 (1978) 2840.
15 C.J. Brown, J. Chem. Soc., (1953) 3265.
16 K. Lonsdale, J.J. Milledge and K.V.K. Rao, Proc. R. Soc., A255 (1960) 82.
17 E.D. Laganis, R.H. Voegeli, R.T. Swann, R.G. Finke, H. Hopf and V. Boekelheide, Organometallics, 1 (1982) 1415.
18 T. Arthur and T.A. Stephenson, J. Organomet. Chem., 208 (1981) 369.
19 G.M. Sheldrick, SHELXTL PLUS, An Integrated System for Refining and Displaying Crystal Structures from Diffraction Data, University of Gottingen, F.R.G., 1986.

The Synthesis of New Binuclear Paracyclophane Complexes of Ruthenium(II): Crystal Structure of $[Ru_2(\eta^6\text{-}C_{16}H_{16})_2(OEt)_3][PF_6]$

MARK R. J. ELSEGOOD and DEREK A. TOCHER*

Department of Chemistry, University College London, 20 Gordon Street, London WC1H 0AJ (U.K.)

(Received January 24, 1989)

Recently we reported [1] that reaction of $[Ru(\eta^6\text{-}C_{16}H_{16})Cl_2]_2$ with a variety of donor ligands L (L = pyridine, PPh_3, PMe_2Ph) gave rise to a range of products of the types $[Ru(\eta^6\text{-}C_{16}H_{16})Cl_2L]$ and $[Ru(\eta^6\text{-}C_{16}H_{16})ClL_2]^+$. The mononuclear nature of these products was confirmed by crystal structure determinations of the representative compounds $[Ru(\eta^6\text{-}C_{16}H_{16})Cl(C_5H_5N)_2][PF_6]$ [1] and $[Ru(\eta^6\text{-}C_{16}H_{16})Cl_2(PPh_3)]$ [2]. In this report we describe the synthesis and characterisation of some new binuclear compounds containing the '$Ru(\eta^6\text{-}C_{16}H_{16})$' moiety.

Results and Discussion

In recent years it has been shown that hydroxo-bridged arene–ruthenium complexes such as $[Ru_4(\eta^6\text{-}C_6H_6)_4(OH)_4(O)][BPh_4]_2\cdot 2Me_2CO$ and $[Ru_2(\eta^6\text{-}C_6Me_6)(OH)_3]Cl$ react with ROH (R = Me, Et) to form the binuclear cations $[Ru_2(\eta^6\text{-arene})_2(OR)_3]^+$ which have a confacial bioctahedral geometry with three alkoxo bridging ligands shared by the two metal ions [3, 4]. Alkoxide-bridged species of this type were also obtained when the dimers $[Ru(\eta^6\text{-arene})Cl_2]_2$ were treated with freshly prepared solutions of NaOR in ROH [3, 5]. We now report the results of our preliminary investigations into the reactions of the paracyclophane compound bis(η^6-[2$_2$](1,4)cyclophane)dichlorobis(μ-chloro)diruthenium with solutions of NaOR (R = Me, Et).

The reaction between $[Ru(\eta^6\text{-}C_{16}H_{16})Cl_2]_2$ and NaOMe in methanol proceeds smoothly to give a yellow solution from which an orange solid can be precipitated by addition of $Na[BPh_4]$. The infrared spectrum of this product contains no bands attributable to ν(Ru–Cl) but exhibits a strong ν(C–O) vibration at *c.* 1050 cm^{-1}. The presence of a $[BPh_4]^-$ counterion is confirmed by the presence of strong bands at 708, 722 and 734 cm^{-1}. The ^1H NMR spectrum in CD_2Cl_2 reveals three signals due to the coordinated cyclophane ligand. The coordinated and non-coordinated rings give rise to singlet resonances at δ 4.55 and 6.62 ppm, respectively, while the methylene protons appear as an AA'BB' signal centred at δ 2.87 ppm. The methoxide ligands appear as a singlet at δ4.22 ppm, while the protons of the $[BPh_4]^-$ anion give rise to multiplet signals at δ 6.91, 7.06 and 7.34 ppm. Integration of the spectrum is consistent with a $C_{16}H_{16}$:$[OMe]^-$:$[BPh_4]^-$ ratio of 2:3:1, suggesting the formulation $[Ru_2(\eta^6\text{-}C_{16}H_{16})_2(OMe)_3][BPh_4]$. Microanalytical data and conductivity measurements support this formulation. Similarly, the reaction of $[Ru(\eta^6\text{-}C_{16}H_{16})Cl_2]_2$ with NaOEt/K$[PF_6]$ in ethanol gives a product which is characterised by analytical and spectroscopic measurements as $[Ru_2(\eta^6\text{-}C_{16}H_{16})_2(OEt_3)][PF_6]$. The binuclear nature of the cationic products formed in these reactions has been confirmed by the X-ray structural analysis of the hexafluorophosphate salt.

Crystal data for $C_{38}H_{47}O_3F_6PRu_2$: $M = 934.9$, $a = 18.170(3)$, $b = 21.560(3)$, $c = 19.696(2)$ Å; $\beta = 105.54(1)°$, $V = 7431(2)$ Å^3, $Z = 8$; $D_{calc} = 1.61$ g cm^{-3}, $F(000) = 3648$, $\mu = 8.70$ cm^{-1}, monoclinic space group *C2/c*. Structure determination: a crystal of dimensions 0.52 × 0.25 × 0.06 mm was used to collect 6582 unique data in the range $5° < 2\theta < 50°$ on a Nicolet R3m/V diffractometer. The positions of the two ruthenium ions in the asymmetric unit were derived by direct methods and the remaining non-hydrogen atoms found by iterative application of least-squares refinement and difference-Fourier synthesis [6]. The final least-squares refinement included 454 parameters for 5054 ($I > 1.5\sigma(I)$) variables. The last cycle gave $R = 0.0641$, $R_w = 0.0693$ (weighting scheme $w^{-1} = \sigma^2(F) + 0.000596F^2$). The structure of the cation is presented in Fig. 1.

The cation has a confacial-bioctahedral geometry (see Fig. 1 and Table 1 for selected intramolecular distances and angles) with a Ru···Ru distance of 3.015(1) Å, which is similar to that found for the related cation $[Ru_2(\eta^6\text{-}C_6H_6)_2(OMe)_3]^+$, 3.005(2) Å [5], as well as for other triply bridged arene–ruthenium(II) compounds (cf. 3.283 Å in $[Ru_2(\eta^6\text{-}1,4\text{-}MeC_6H_4CHMe_2)_2Cl_3]^+$ [7], and 2.989(3) Å in $[Ru_2(\eta^6\text{-}C_6Me_3H_3)_2(OH)_3]^+$ [4]). The Ru–O distances lie in the range 2.055 to 2.084 Å and have an average value of 2.068(5) Å, which is indistinguishable from that of 2.060(8) Å observed in the compound $[Ru_2(\eta^6\text{-}C_6H_6)_2(OMe)_3][BPh_4]$ [5]. As with the other examples of paracyclophane complexes of ruthenium(II) which we have characterised, there is considerable variation in the Ru–C distances, with bonds to the carbon atoms attached to the ethylenic bridging functions being appreciably longer than those to the remaining arene carbon atoms (average values of 2.292(9) and 2.178(9) Å respectively). The resulting non-planarity of the aromatic rings is a well-

*Author to whom correspondence should be addressed.

0020-1693/89/$3.50

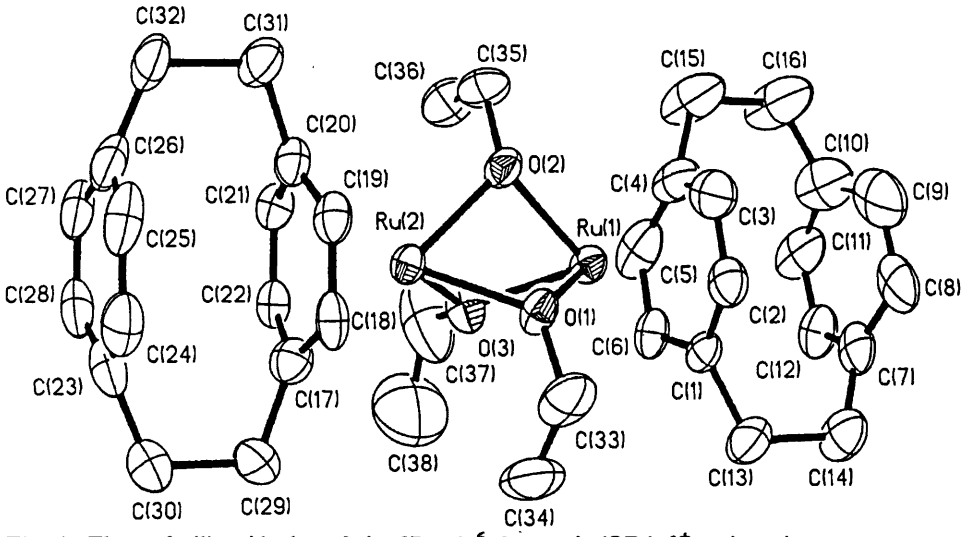

Fig. 1. Thermal ellipsoid plot of the $[Ru_2(\eta^6\text{-}C_{16}H_{16})_2(OEt)_3]^+$ cation. Atoms are represented by thermal vibration ellipsoids at the 50% level, and the atomic labelling scheme is defined.

TABLE 1. Selected bond lengths and angles for $[Ru_2(\eta^6\text{-}C_{16}H_{16})_2(OEt)_3][PF_6]$

Bond lengths (Å)			
Ru(1)–Ru(2)	3.015(1)	Ru(2)–O(1)	2.084(5)
Ru(1)–O(1)	2.058(5)	Ru(2)–O(2)	2.076(5)
Ru(1)–O(2)	2.081(5)	Ru(2)–O(3)	2.054(5)
Ru(1)–O(3)	2.055(5)	Ru(2)–C(17)	2.271(9)
Ru(1)–C(1)	2.269(7)	Ru(2)–C(18)	2.159(8)
Ru(1)–C(2)	2.155(9)	Ru(2)–C(19)	2.196(7)
Ru(1)–C(3)	2.175(10)	Ru(2)–C(20)	2.332(8)
Ru(1)–C(4)	2.298(9)	Ru(2)–C(21)	2.183(8)
Ru(1)–C(5)	2.177(9)	Ru(2)–C(22)	2.215(8)
Ru(1)–C(6)	2.167(8)		
Bond angles (°)			
Ru(1)–O(1)–Ru(2)	93.4(2)	O(1)–Ru(2)–O(2)	69.8(2)
Ru(1)–O(2)–Ru(2)	93.0(2)	O(1)–Ru(2)–O(3)	73.3(2)
Ru(1)–O(3)–Ru(2)	94.4(2)	O(2)–Ru(2)–O(3)	74.4(2)
O(1)–Ru(1)–O(2)	70.3(2)		
O(1)–Ru(1)–O(3)	73.8(2)		
O(2)–Ru(1)–O(3)	74.3(2)		

established feature in the chemistry of paracyclophane and its metal complexes [1, 2, 7–9]. The two coordinated cyclophane rings are staggered with respect to each other as might have been expected. However, one ring, C17–C18–C19–C20–C21–C22, is eclipsed with respect to the three oxygen sites. The ethoxide bridging ligands have not adopted the three-fold symmetry which might have been expected.

Further work on the synthesis and characterisation of other binuclear cyclophane–ruthenium(II) compounds is in progress [10]. These studies will be described in a future publication.

Acknowledgements

We thank Johnson Matthey plc for generous loans of ruthenium trichloride and the SERC for financial support (M.R.J.E.) and for provision of the X-ray equipment.

References

1 M. R. J. Elsegood and D. A. Tocher, *J. Organomet. Chem., 356* (1988) C29.
2 M. R. J. Elsegood and D. A. Tocher, unpublished results.
3 T. Arthur, D. R. Robertson, D. A. Tocher and T. A. Stephenson, *J. Organomet. Chem., 208* (1981) 389.
4 R. O. Gould, C. L. Jones, T. A. Stephenson and D. A. Tocher, *J. Organomet. Chem., 264* (1984) 365.
5 R. O. Gould, T. A. Stephenson and D. A. Tocher, *J. Organomet. Chem., 263* (1984) 375.
6 G. M. Sheldrick, *SHELXTL PLUS*, an integrated system

for refining and displaying crystal structures from diffraction data, University of Gottingen, Federal Republic of Germany, 1986.
7 R. T. Swann, A. W. Hanson and V. Boekelheide, *J. Am. Chem. Soc., 108* (1986) 3324.
8 Y. Kai, N. Yasuoka and N. Kasai, *Acta Crystallogr. Sect. B, 34* (1978) 2840.
9 H. Hope, J. Bernstein and K. N. Trueblood, *Acta Crystallogr. Sect. B, 28* (1972) 1733.
10 M. R. J. Elsegood and D. A. Tocher, unpublished results.